

**A METHODOLOGY FOR  
THE DYNAMIC ANALYSIS OF  
BRIDGE/ABUTMENT/BACKFILL  
SYSTEMS  
SUBJECTED TO  
TRAVELING SEISMIC WAVES**

March 1983

Prepared Under

**National Science Foundation  
Grant No. CEE-8007518**

**AGBABIAN ASSOCIATES**

250 North Nash Street

P.O. Box 956

El Segundo, CA 90245-0956



<b>REPORT DOCUMENTATION PAGE</b>	1. REPORT NO. R-8113-5470	2.	3. Recipient's Accession No. R-8113-5470
4. Title and Subtitle Bridge Response to Traveling Seismic Waves		5. Report Date	
7. Author(s) Dendrou, B.D., et al.		6.	
9. Performing Organization Name and Address Agbabian Associates 250 North Nash Street P.O. Box 956 El Segundo, CA 90245-0956		8. Performing Organization Rept. No.	
12. Sponsoring Organization Name and Address National Science Foundation Washington D.C. 20550		10. Project/Task/Work Unit No.	
15. Supplementary Notes		11. Contract(C) or Grant(G) No. (C) (G) CEE-8007518	
16. Abstract (Limit: 200 words)  This report describes an advanced methodology (BASSIN), for analyzing traveling seismic wave effects on the dynamic response of an arbitrarily-configured, elastic bridge system (comprised of a road deck, piers, abutments, backfill, etc.). A substructuring approach has been used to formulate BASSIN; in this, the bridge system is represented using a three-dimensional finite element model, and the underlying soil is depicted using a boundary element approach based on elastic half-space theory. Seismic excitations are induced by plane body waves or Raleigh waves with arbitrary direction of incidence, wavelength, and amplitude. BASSIN allows for a fully deformable interface between the bridge system and the underlying soil, and incorporates a special modal truncation procedure to account for higher mode response characteristics.		13. Type of Report & Period Covered Final Report 9/15/80 - 3/31/83	
17. Document Analysis a. Descriptors Bridges (Structures)      Earthquakes Dynamic Response        Seismic Waves Dynamics                  Vibration  b. Identifiers/Open-Ended Terms BASSIN  c. COSATI Field/Group		14.	
18. Availability Statement: Release Unlimited		19. Security Class (This Report) Unclassified	21. No. of Pages 251
		20. Security Class (This Page) Unclassified	22. Price





## ABSTRACT

This report describes a new and advanced methodology for analyzing the dynamic response of bridge systems subjected to traveling seismic waves. The methodology (named BASSIN) treats an arbitrarily-configured, elastic, bridge system (comprised of a road deck, piers, abutments, backfill, etc.), that rests on the surface of an elastic soil continuum. A substructuring approach has been used to formulate BASSIN; in this, the bridge system is represented using a three-dimensional finite element model, and the underlying soil is depicted using a boundary element approach based on elastic half-space theory. Seismic excitations are induced by plane body waves or Rayleigh waves with arbitrary direction of incidence, wavelength, and amplitude. BASSIN allows for a fully deformable interface between the bridge system and the underlying soil, and incorporates a special modal truncation procedure to account for higher mode response characteristics.





## ACKNOWLEDGEMENTS

This research project has been supported by a National Science Foundation grant to Agbabian Associates (Grant No. CEE-8007518). This support is gratefully acknowledged.

Principle contributor to this work was B. Dendrou, who carried out the bulk of the design and development of the BASSIN program described in this report. Significant contributions were also made by K.T. Dill, who supported the program development effort, and K.L. Merz, who developed the modal truncation approach described herein. Other AA contributors to the project were J.M. Brendt, R.W. Fellner, and L.C. Lee. S.D. Werner provided project management and research direction for this effort.







## TABLE OF CONTENTS

<u>Chapter</u>		<u>Page</u>
1	INTRODUCTION . . . . .	1-1
	1.1 Objective . . . . .	1-1
	1.2 Scope . . . . .	1-1
2	OVERVIEW OF METHODOLOGY. . . . .	2-1
	2.1 General Description . . . . .	2-1
	2.2 Assumptions . . . . .	2-3
	2.3 Significant Features. . . . .	2-4
3	BASSIN ANALYSIS PROCEDURE. . . . .	3-1
	3.1 Subprogram BASSIN1. . . . .	3-1
	3.2 Subprogram BASSIN2. . . . .	3-8
4	INCIDENT WAVE MOTIONS. . . . .	4-1
	4.1 Body Wave Excitations . . . . .	4-1
	4.2 Rayleigh Wave Excitations . . . . .	4-17
5	COMPUTATION OF GREEN'S FUNCTIONS FOR AN ELASTIC HALF-SPACE. . . . .	5-1
	5.1 Basic Definitions . . . . .	5-1
	5.2 Green's Functions for an Elastic Half-Space . . . . .	5-4
	5.3 Numerical Evaluation of Green's Functions for an Elastic Half-Space . . . . .	5-8
6	HALF-SPACE IMPEDANCE MATRIX AND DRIVING FORCE VECTORS. . . . .	6-1
	6.1 Impedance Matrix. . . . .	6-1
	6.2 Driving Forces. . . . .	6-16
7	DYNAMIC RESPONSE ANALYSIS FORMULATION. . . . .	7-1
	7.1 General Analysis Procedure. . . . .	7-1
	7.2 Analysis Procedure Including Modal Truncation . . . . .	7-7
	7.3 Illustrative Example. . . . .	7-15
	REFERENCES . . . . .	R-1
<u>Appendix</u>		
A	Input Description for BASSIN1. . . . .	A-1
B	Input Description for BASSIN2. . . . .	B-1
C	Sample Problem . . . . .	C-1





CHAPTER 1  
REPORT DESCRIPTION

1.1 OBJECTIVE

The objective of this report is to describe a new methodology (named BASSIN), that was developed by Agbabian Associates under NSF Grant No. CEE-8007518 for analyzing the effects of traveling seismic waves on the dynamic response of bridge/abutment/backfill systems.

1.2 SCOPE

The report contains a complete description of the BASSIN methodology, including its basic theory and the computer program input requirements and output results. To provide this information, the remainder of this report is divided into six chapters and three appendixes. Chapter 2 of the report contains an overview of BASSIN including its inherent assumptions and significant features, while Chapter 3 provides a summary of the BASSIN analysis procedure. Theoretical development pertaining to the computation of incident wave motions, Green's functions for an elastic half-space, half-space impedance matrices and driving force vectors, and the BASSIN dynamic analysis procedure are described in Chapters 4 through 7 respectively. Appendixes A and B contain input descriptions for the BASSIN1 and BASSIN2 subprograms that comprise the methodology, and Appendix C contains input and output from a sample analysis that was carried out as part of this research effort.





## CHAPTER 2

## OVERVIEW OF METHODOLOGY

2.1 GENERAL DESCRIPTION

The objective of the BASSIN methodology is to provide an advanced procedure for analyzing the dynamic response of bridge/abutment/backfill systems subjected to traveling seismic waves. BASSIN is a substantially updated version of a prior methodology, named CAST, that was developed at Agbabian Associates under previous National Science Foundation grants (Werner et al., 1977; Werner and Lee, 1980).

The BASSIN methodology has the following features (Fig. 2-1):

- It computes the three-dimensional dynamic response of an arbitrarily configured, elastic, bridge/abutment/backfill system.
- It assumes this system to be underlain by a soil continuum, represented herein as an elastic half-space.
- It represents seismic input motions as being harmonic and induced by planar P-, SV-, SH-, or Rayleigh waves with arbitrary wavelength, amplitudes, and directions of incidence.

The methodology uses a substructure approach in which the structure (which herein comprises the bridge, abutment, and backfill) is represented using a three-dimensional finite element model, and the underlying soil continuum is represented using a boundary element approach. The finite element model defines the stiffness matrix, mass matrix, and fixed-base modes for the structure. The boundary element approach characterizes the underlying soil medium using frequency-dependent impedance matrices and driving force vectors that also incorporate the

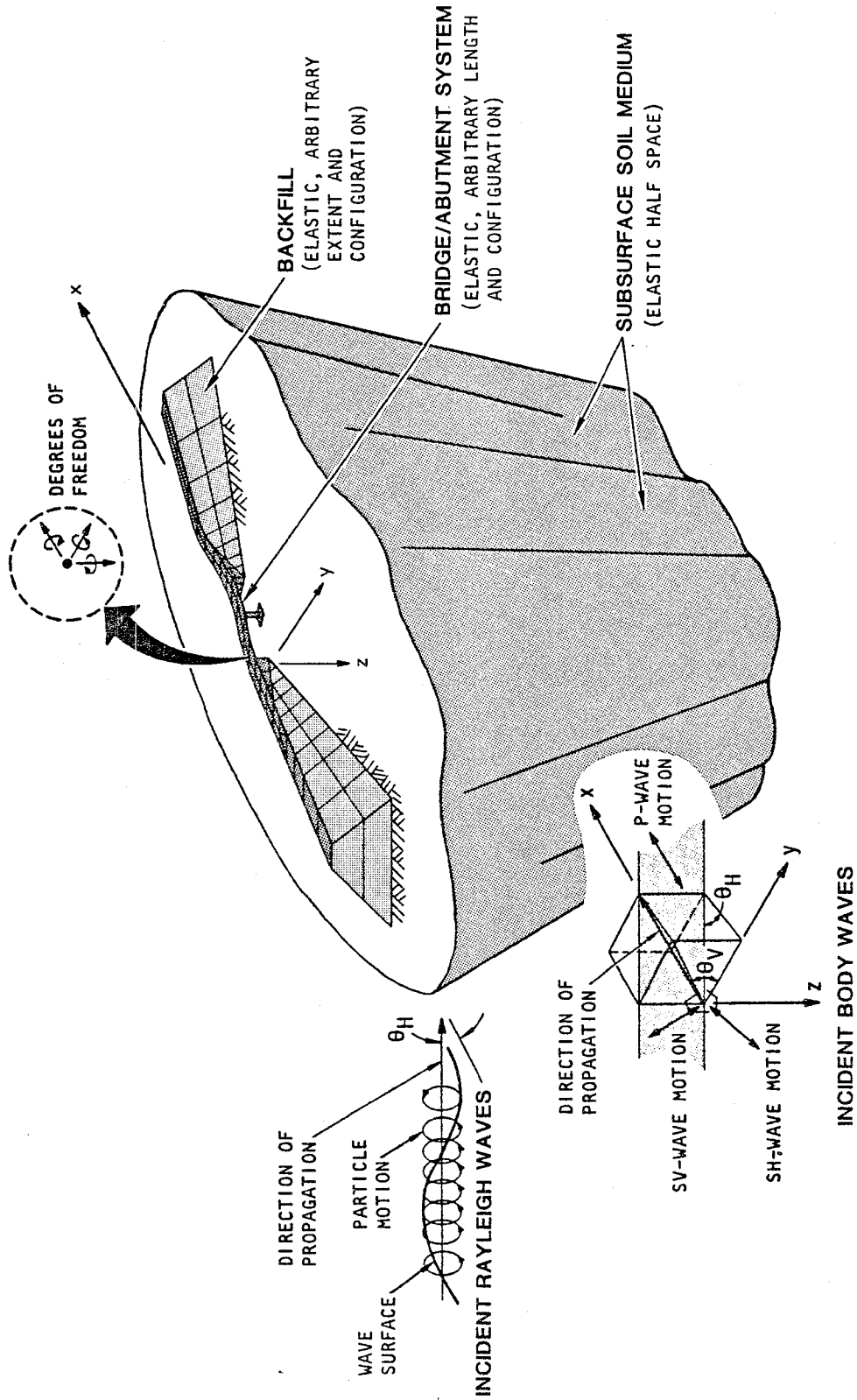


FIGURE 2-1. BRIDGE/SOIL CONFIGURATION CONSIDERED BY BASSIN METHODOLOGY



free-field wave motions. Compatibility and equilibrium requirements at the soil/structure interface are used to couple these substructures, and the steady-state response of the soil/structure system is then computed.

## 2.2 ASSUMPTIONS

### 2.2.1 STRUCTURE

The bridge/abutment/backfill structure is assumed to be three dimensional, linear elastic, and arbitrarily configured. It is represented by a general finite element model that comprises any combination of the several element types described in Section 3.1.2. Each node point in the model can have as many as six degrees of freedom depending on the particular element types used. The node point spacing and element sizes depend on the system geometry and the highest frequency of response pertinent to the calculations.

### 2.2.2 SOIL MEDIUM

The underlying soil medium is represented as an elastic half-space. Because of this, the BASSIN methodology cannot accommodate effects of soil layering, strain-dependent soil properties, etc., that may be important for actual structure sites. Nevertheless, the methodology in its present form is valuable for studying basic phenomena associated with traveling wave effects on the three-dimensional response of bridges, as well as other structural systems. Furthermore, because BASSIN is modular, procedures for representing the soil as a visco-elastic layered medium can be readily incorporated.

### 2.2.3 SOIL/STRUCTURE INTERFACE

The interface between the structure and the underlying soil medium is fully deformable. Hence, the soil/structure system



response in the vicinity of this interface is dependent on its geometry, mass, and stiffness, and is not constrained by assumptions of rigid interfaces, as per the prior methodologies of this type.

#### 2.2.4 INPUT MOTIONS

The input motions to BASSIN correspond to incident wave motions induced by planar, harmonic, P-, SV-, SH-, or Rayleigh waves. The angles of incidence, excitation frequencies, and complex amplitudes of these wave motions are arbitrary. BASSIN is structured so that Fast-Fourier Transform techniques can be readily incorporated at a later stage, to permit the representation of arbitrary transient excitations as the superposition of a series of the harmonic excitations now considered.

#### 2.3 SIGNIFICANT FEATURES

The BASSIN methodology has several significant features over and above our prior CAST methodology, which renders it an excellent analytical tool for assessing the dynamic response characteristics of bridge/abutment/backfill systems. These are:

- The interface between the structure and the underlying soil medium is now fully deformable, rather than rigid. Therefore BASSIN is applicable not only to bridge/abutment/backfill systems, but also to any other structure for which the deformability of the soil/structure interface is particularly important (e.g. earth dams). Furthermore, effects of shallow-embedded foundations can now be represented approximately, by using a finite element model of the soil medium, to the depth of the base of the foundation.
- The dynamic analysis procedure now incorporates a new modal truncation technique which greatly reduces the required number of modes for the structure, while maintaining excellent accuracy of the final dynamic analysis results.





- The BASSIN methodology has been programmed according to ANSI 66 Fortran standards, to facilitate installation on virtually any current computer system with a minimum of effort.
- The basic program is now modular; so that any future technical developments that further enhance particular aspects of the BASSIN methodology can be readily accommodated.





## CHAPTER 3

## BASSIN ANALYSIS PROCEDURE

The BASSIN analysis procedure is organized into two subprograms, named BASSIN1 and BASSIN2. The basic features of these subprograms, as indicated in Figure 3-1, are summarized in this chapter.

### 3.1 SUBPROGRAM BASSIN1

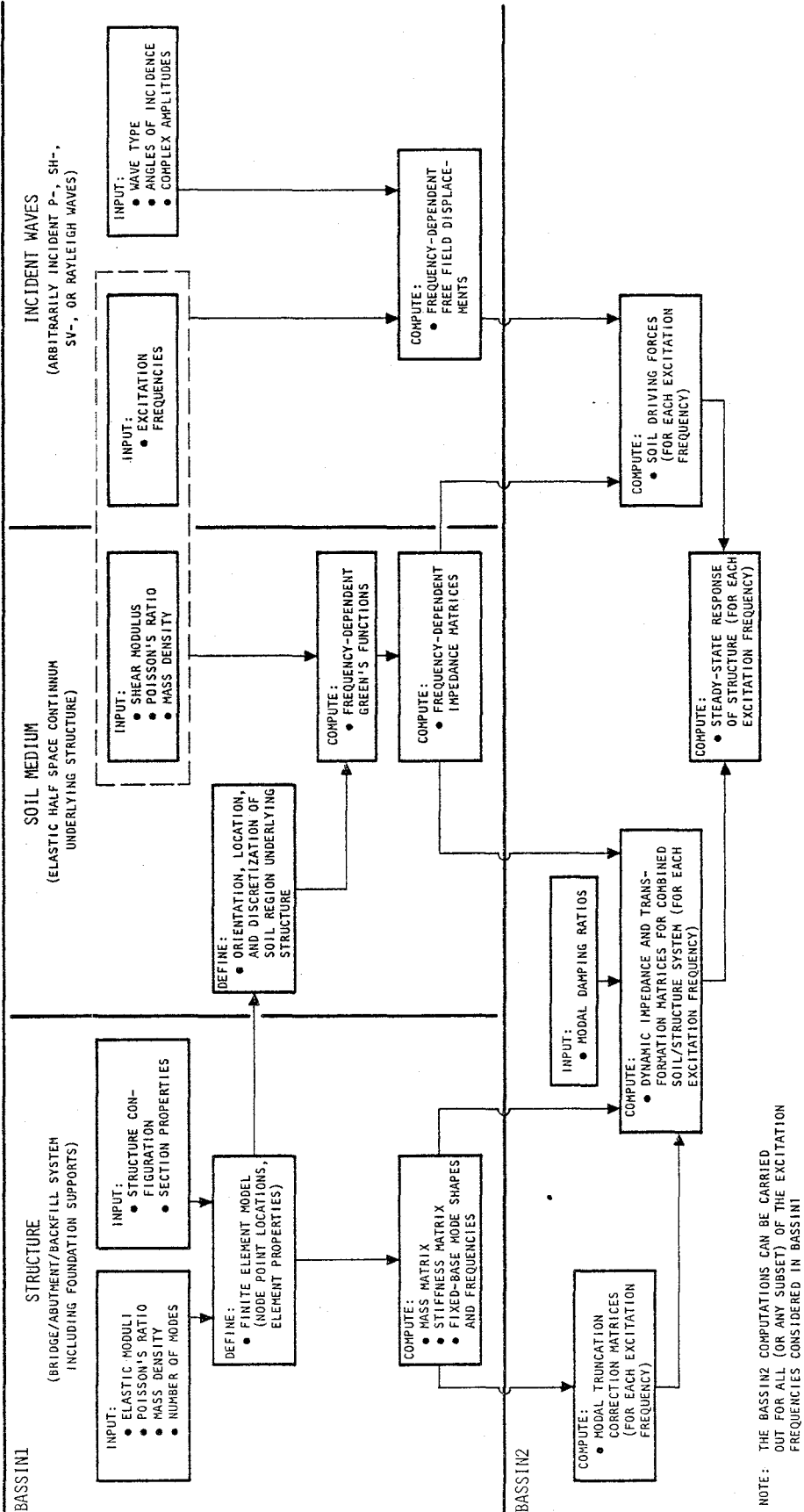
#### 3.1.1 SCOPE

The function of BASSIN1 is to perform computations required to characterize the structure, soil medium, and incident wave motions in the manner required for the subsequent dynamic response calculations in BASSIN2. To fulfill this function, BASSIN1 is comprised of three main operations. First, it reads all necessary input data for the dynamic analysis. Then it performs computations to define required characteristics of the structure (mass matrix, stiffness matrix, and normal modes), the soil (frequency-dependent Green's functions and impedance matrices), and the incident wave motions (ground surface displacements). Finally, it writes all of these quantities onto a data tape, for use as input into BASSIN2.

The BASSIN1 operations pertaining to the characterization of the bridge structure, soil medium, and incident wave motions are summarized in the remainder of this section. Further theoretical background pertaining to these operations is provided in Chapters 4 through 6.

#### 3.1.2 STRUCTURE

The input data required to represent the structure (i.e., the bridge, abutment, and backfill system) describe its geometry, material, properties, and modal parameters. As shown in Figure 3-1, these data are comprised of the following:



AA601

FIGURE 3-1. BASSIN ANALYSIS PROCEDURE

137



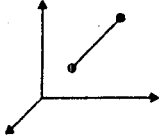


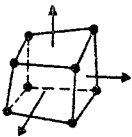
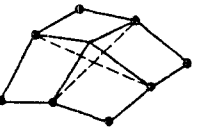

- Geometry. The configuration and section properties of the structure are represented from an appropriate combination of several finite element types built into the BASSIN1 element library. As shown in Figure 3-2, these include truss, beam, planar, brick, shell, and boundary (spring) elements. It is noted that BASSIN1's modular nature facilitates incorporation of additional or alternative element types into its element library, whenever appropriate.
- Material Properties. The specific material properties required for the structure vary according to element type, but are typically comprised of various elastic parameters and the mass density.
- Modal Parameters. The only modal parameter required for use in BASSIN1 is the number of modes to be considered in the analysis. This required number of modes should be relatively small\*, owing to the modal truncation feature in BASSIN which provides higher mode corrections using the lower mode parameters and the structure stiffness and inertial characteristics (see Chapt. 7).

Once the above input properties are provided, BASSIN1 proceeds to form the structure mass and stiffness matrices and to extract its fixed-base mode shapes and frequencies. The subspace iteration method described by Bathe and Wilson (1976) is used in BASSIN1 for the mode shape and frequency extraction.

---

\* As an approximate rule-of-thumb, we have found that the highest mode to be included should (1) have a natural frequency of at least 5 times greater than the highest excitation frequency of interest; and (2) be such that the lower modes included encompass the principal response directions for the structure due to the applied seismic excitations.



ELEMENT TYPE	DESCRIPTION	DEGREES OF FREEDOM PER NODE POINT	USE	FORCES OR STRESSES COMPUTED
<p>3-D TRUSS</p> 	<p>Straight, prismatic, elastic element; stiffness matrix computed from standard theory for truss members.</p>	<p>Three translations.</p>	<p>Represents one-dimensional members that transmit axial forces only.</p>	<p>Axial force.</p>
<p>3-D BEAM</p> 	<p>Straight, prismatic, elastic element; stiffness matrix computed from classical beam theory.</p>	<p>Three translations and three rotations.</p>	<p>Represents beams that transmit axial and shear forces, bending moments, and torsional moments.</p>	<p>Three forces and three moments at each end of element.</p>
<p>PLANE STRESS OR PLANE STRAIN</p> 	<p>Quadrilateral or triangular elastic element. Stiffness matrix formulation based on assumed parabolic variation of displacements within element.</p>	<p>Two in-plane translations.</p>	<p>Represents elastic continuum with known state of lateral constraint.</p>	<p>Normal and shear stresses at center of element.</p>
<p>3-D BRICK</p> 	<p>Eight-node, solid brick elastic element. Stiffness matrix formulation based on assumed cubic variation of displacements within element.</p>	<p>Three translations.</p>	<p>Represents any 3-D, elastic, isotropic continuum.</p>	<p>Six stress components at center of element and at center of each side.</p>
<p>SHELL</p> 	<p>Flat, elastic, quadrilateral or triangular element. Uses constant-strain triangle and LCCT9 element* to represent membrane and bending behavior, respectively.</p>	<p>Three translations and three rotations.</p>	<p>Models thin-shell or plate structures that transmit in-plane and out-of-plane forces and moments.</p>	<p>Three normal stresses and three moments at center of element.</p>
<p>BOUNDARY</p> 	<p>Elastic spring element.</p>	<p>One axial translation and one rotation about element axis.</p>	<p>Imposes displacement boundary conditions and defines support reactions.</p>	<p>Axial force and torsional moment.</p>

\*Linear Curvature Compatible Triangular flat-shell bending element developed by Clough and Felippa (1968)

FIGURE 3-2. STRUCTURE ELEMENT LIBRARY IN *BASSINI* (Bathé et al., 1974)



### 3.1.3 SOIL MEDIUM

To represent the soil medium, BASSIN1 employs input parameters that define its material properties as well as the geometry of its interface with the overlying structure. The material properties are defined in terms of the shear modulus, Poisson's ratio, and mass density of the elastic half-space. The interface geometry is represented by subdividing the interface region of the half-space surface into subregions of constant stress. The half-space node points from these interface subregions correspond on a one-to-one basis with the node points in the finite element interface representation within the structure model (Fig. 3-3). This facilitates the coupling of the finite element and half-space substructures in the subsequent dynamic response computations in BASSIN2.

Once the above input data are provided, BASSIN1 proceeds to compute frequency-dependent Green's functions for the elastic half-space. Then, these Green's functions are used to compute the impedance matrix for the half-space. As shown in Figure 3-4, the  $j$ th column of this impedance matrix corresponds to the reaction forces at each interface degree of freedom, as caused by a unit harmonic displacement applied at the  $j$ th degree of freedom with all other degrees of freedom fixed. Detailed formulation and description of the BASSIN1 procedures for computing the half-space Green's functions and impedance matrix are provided in Chapters 5 and 6 respectively.

### 3.1.4 INCIDENT WAVES

The BASSIN1 computations pertaining to the incident wave motions require input data in the form of the excitation frequencies, the wave types (P-, SV-, SH-, or Rayleigh waves), the angles of incidence (as previously defined in Fig. 2-1), and the complex amplitudes (real and imaginary parts) of the wave displacement (Fig. 3-1). Then, for each given excitation frequency, basic wave theory is used to compute the corresponding

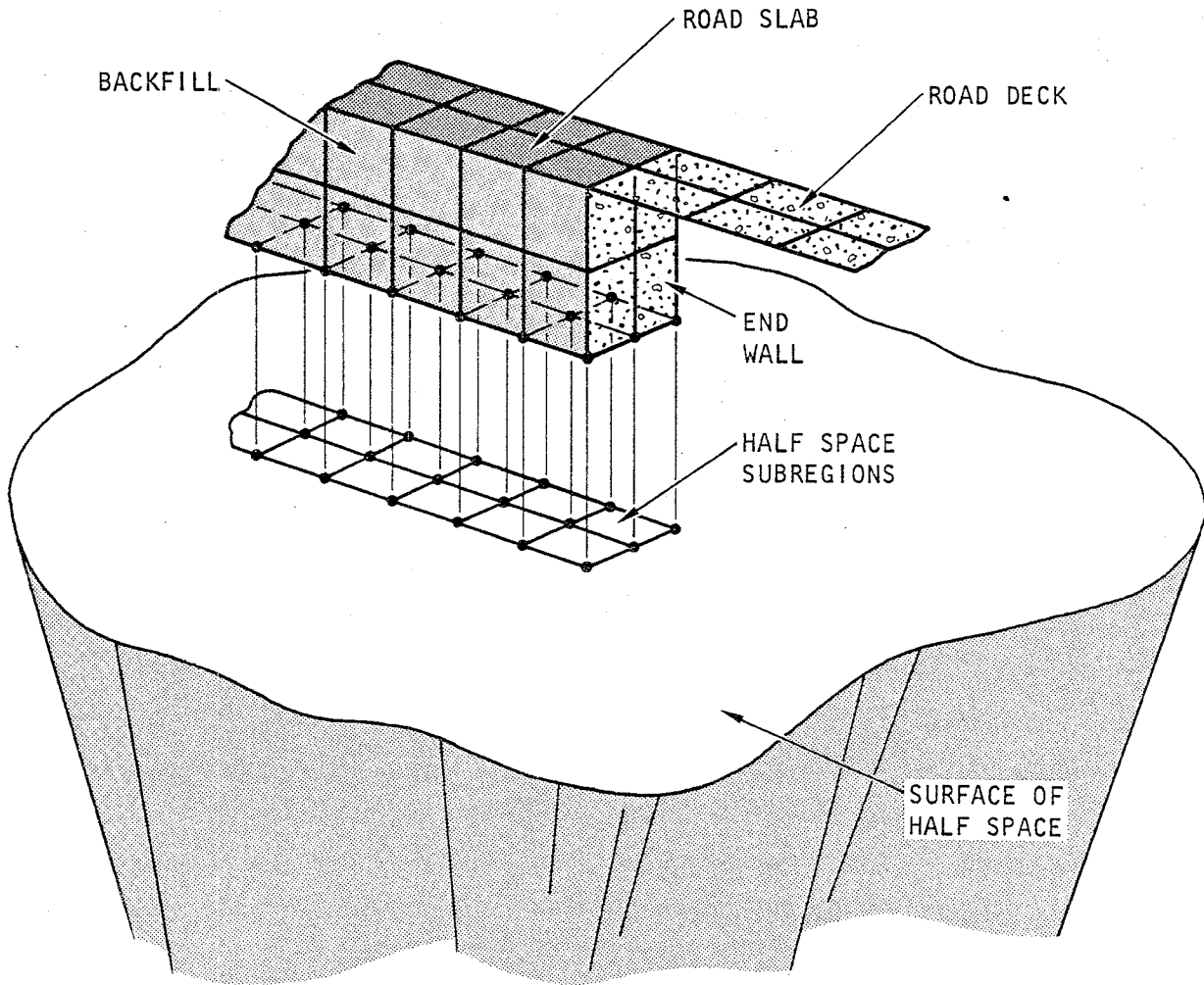


FIGURE 3-3. SOIL/STRUCTURE INTERFACE MODELING



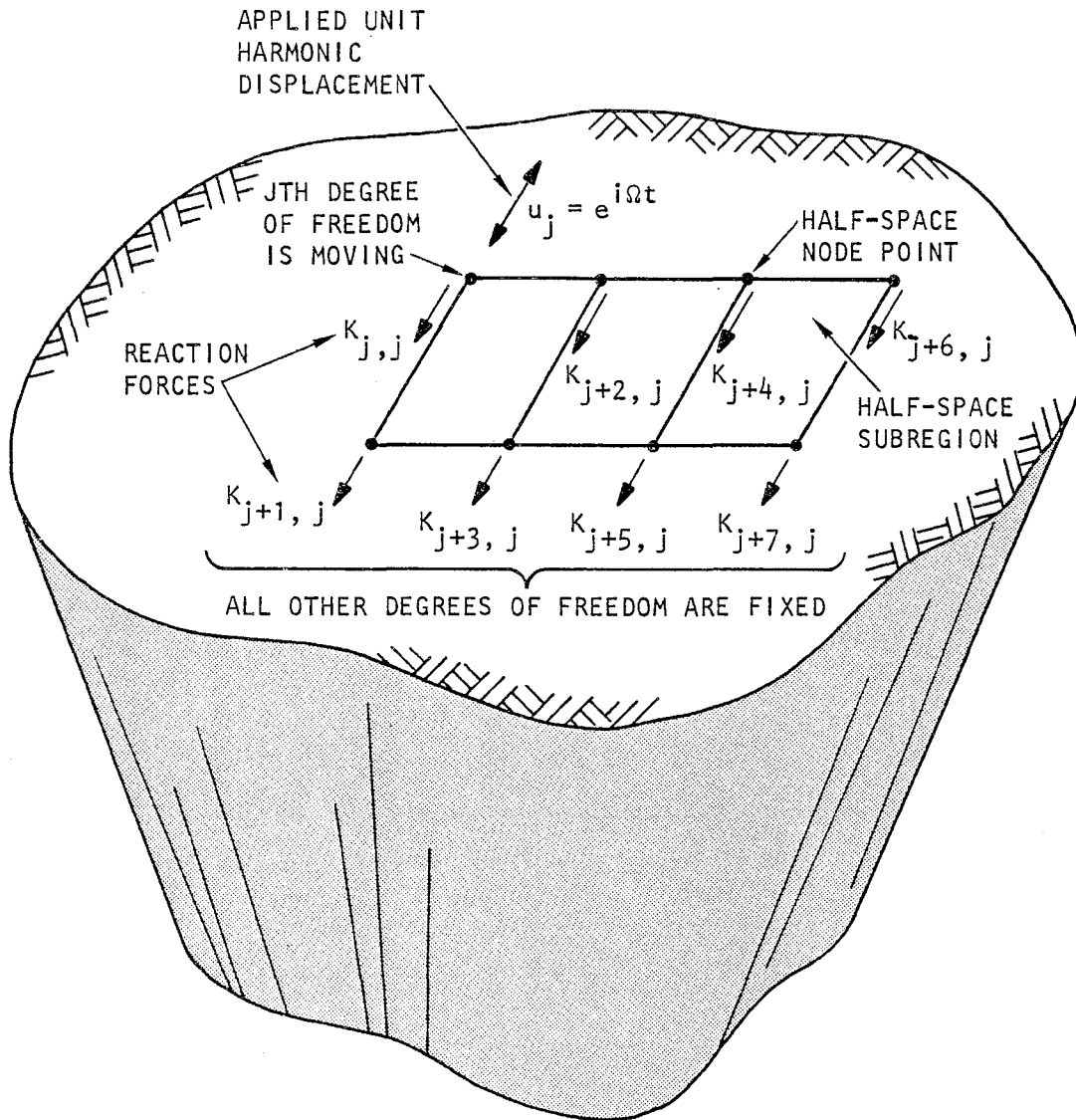


FIGURE 3-4. DEVELOPMENT OF Jth COLUMN OF HALF SPACE IMPEDENCE MATRIX (ONLY LONGITUDINAL FORCES SHOWN)



free-field displacements along the surface of the elastic half-space (Ewing et al., 1957). A formulation of the procedures for carrying out these computations is provided in Chapter 4.

### 3.2 SUBPROGRAM BASSIN2

#### 3.2.1 SCOPE

The main function of BASSIN2 is to carry out the dynamic response computations for the soil/structure system. To do this, BASSIN2 first reads a tape containing the various quantities computed in BASSIN1 for characterizing the soil medium and the structure, as well as cards containing the damping ratios for each structure mode. Then, the program proceeds to calculate (1) the half-space driving forces induced along the ground surface by the seismic waves; and (2) modal truncation correction matrices to account for higher mode effects. All of these results are implemented in the final computation of the steady-state response of the soil/structure system. Each of these calculation efforts is summarized in the remainder of this section.

#### 3.2.2 INCIDENT WAVE DRIVING FORCES

The free-field ground surface displacements and the half-space Green's functions, as computed in BASSIN1, are used in BASSIN2 to develop the corresponding driving forces applied along the structure/half-space interface. These driving forces act as applied loads in the subsequent dynamic response computations for the structure. They are obtained by fixing each degree of freedom within each half-space subregion, and then calculating the frequency-dependent reaction forces induced by the incident seismic waves (Fig. 3-5). Formulation of the procedure used in BASSIN2 to compute the driving forces is provided in Section 6.2 of Chapter 6.

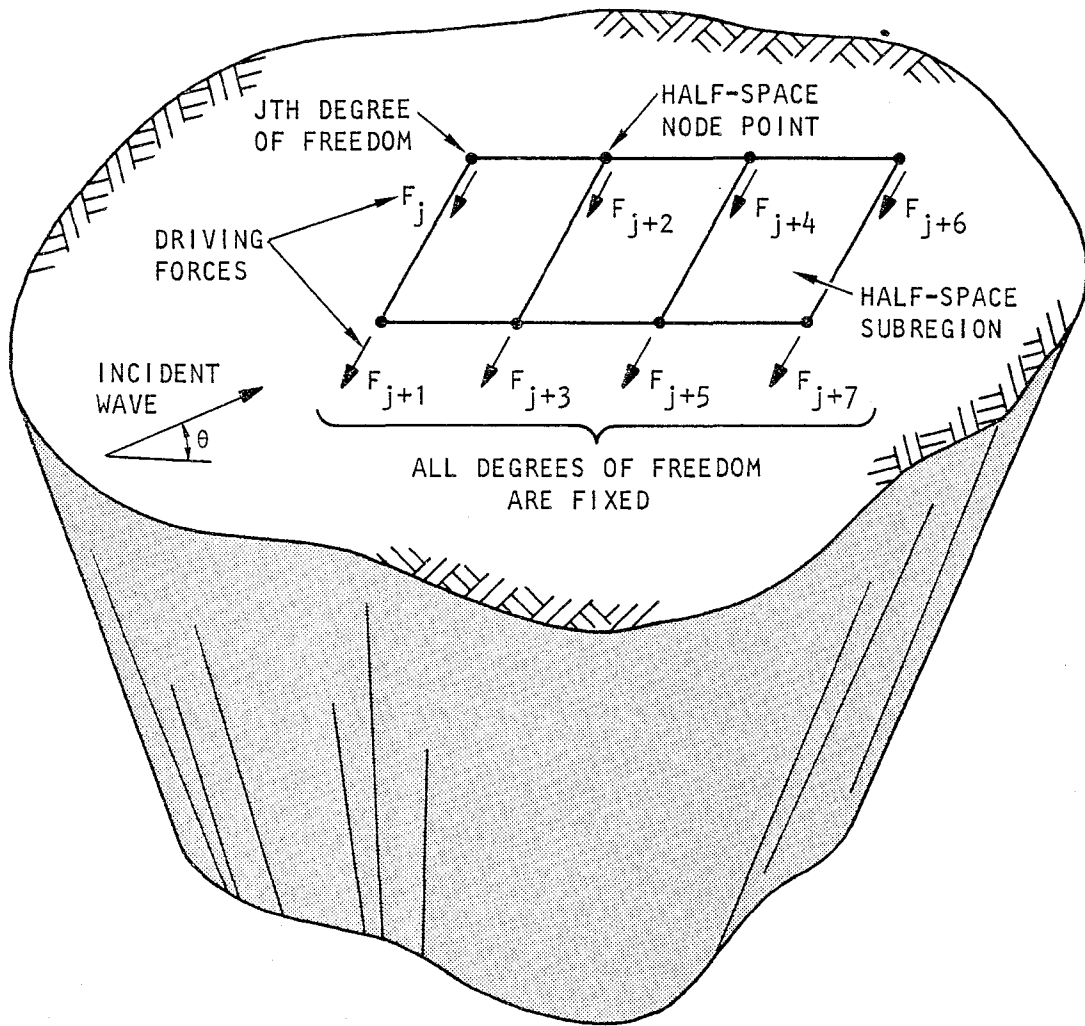


FIGURE 3-5. DEVELOPMENT OF INCIDENT WAVE DRIVING FORCES (ONLY LONGITUDINAL FORCES SHOWN)



### 3.2.3 MODAL TRUNCATION CORRECTION MATRICES

A unique feature of the BASSIN methodology is its use of a new modal truncation procedure, which substantially reduces the number of normal modes necessary to represent the structure response in an adequate manner. This approach involves the use of certain simplifications in the modal equations of steady-state motion that result for modes whose natural frequency is substantially higher than the excitation frequency. On this basis, the dynamic analysis can be carried out considering only a relatively few lower modes (herein termed "kept" modes). Effects of the higher mode contributions to the structure response are represented as correction matrices used in forming the overall structure/half-space impedance matrix and transformation matrix (see Sec. 3.2.4). These higher mode correction matrices are expressed in terms of the structure's stiffness matrix, mass matrix, and modal parameters for its kept modes. The formulation of these correction matrices is provided in Chapter 7.

### 3.2.4 DYNAMIC RESPONSE COMPUTATIONS

With the formation of the driving forces and the modal truncation correction matrices, as summarized in the preceding subsections, BASSIN2 proceeds with the computation of the frequency-dependent dynamic response of the structure. For each frequency, the first step in these computations is to characterize the structure/half-space system using the following matrices:

- A system impedance matrix used to compute the response of the structure at its degrees of freedom that lie along the interface with the half-space.
- A system transformation matrix that relates the structure response at its aboveground degrees of freedom to that along its interface with the half-space.

In both of these matrices, the structure is represented in terms of its stiffness and mass matrices, the modal characteristics



corresponding to its kept modes (i.e., mode shapes, frequencies, and damping ratios), and the modal truncation corrections for higher mode effects (Sec. 3.2.3). In addition, the system impedance matrix includes the effects of the impedance of the underlying half-space, which is coupled to the structure by imposing conditions of displacement compatibility and dynamic force equilibrium along the structure/half-space interface.

Once the development of these matrices is completed, the dynamic response of the structure along its interface with the half-space is computed as the product of the inverse of the system impedance matrix and the vector of driving forces. The resulting vector of structure/half-space interface displacements is then premultiplied by the system transformation matrix, in order to obtain the response of the aboveground portion of the structure. This computational procedure, as well as the formation of the system impedance and transformation matrices, is described further in Chapter 7.





## CHAPTER 4

## INCIDENT WAVE MOTIONS

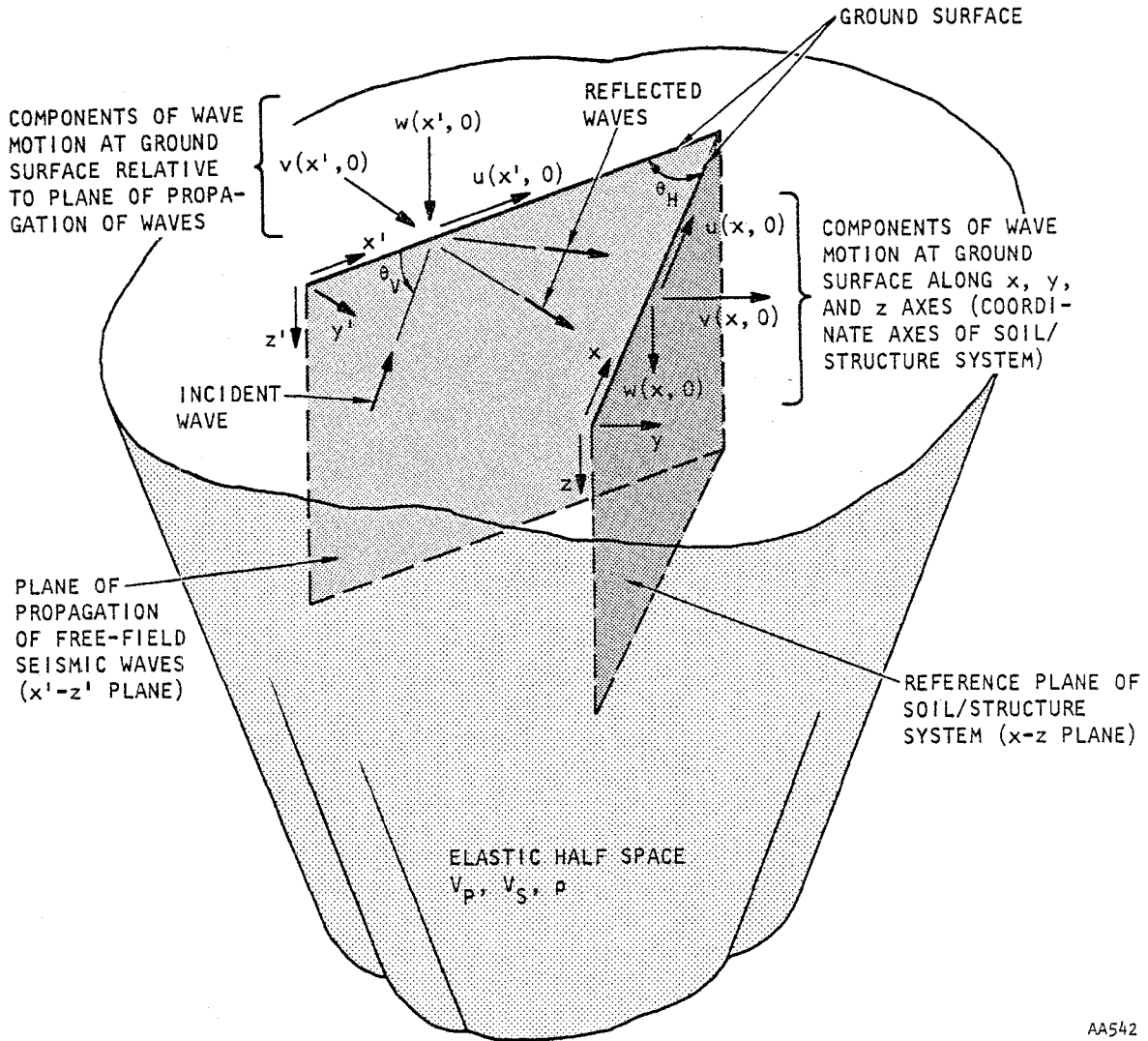
This chapter provides the basis for the BASSIN1 computation of free-field displacements induced along the surface of an elastic half-space by traveling seismic waves. As noted in Chapter 3, these displacements are subsequently used in BASSIN2 to compute driving forces (see Chapt. 6) which, in turn, serve as the basic seismic excitation from which the soil/structure system response is computed (see Chapt. 7). Displacements due to body waves and surface waves are treated separately in the two main sections that comprise this chapter.

#### 4.1 BODY WAVE EXCITATIONS

This derivation of the BASSIN1 expressions for free-field ground surface motions induced by arbitrarily incident plane body waves is divided into five main parts. The first four parts describe various aspects of the formulation for ground surface displacements relative to the  $x'-z'$  plane of propagation of the free-field seismic waves (Fig. 4-1); these are described for each of the three types of body waves in an elastic half-space: P-, SV-, and SH-waves. The final part of this section summarizes the transformation of these displacements to correspond to the  $x-z$  reference plane of the structure, which will be offset from the  $x'-z'$  plane, because of the horizontal angle of incidence  $\theta_H$ .

##### 4.1.1 GENERAL POTENTIAL FUNCTIONS

We first treat the case involving the propagation of a plane P- or SV-wave with a vertical angle of incidence  $\theta_V$ . Such waves cause displacements at any point in the  $x'-z'$  plane of the wave which, as shown by Ewing et al. (1957), can be defined as



AA542

FIGURE 4-1. RELATIVE ORIENTATIONS OF  $x'-z'$  PLANE OF PROPAGATION OF SEISMIC WAVES AND  $x-z$  REFERENCE PLANE OF SOIL/STRUCTURE SYSTEM





$$u(x', z') = \frac{\partial \phi}{\partial x'} - \frac{\partial \psi_2}{\partial z'} \quad (4-1)$$

$$w(x', z') = \frac{\partial \phi}{\partial z'} + \frac{\partial \psi_2}{\partial x'}$$

In this,  $u$  and  $w$  are the horizontal and vertical displacements,  $\phi$  and  $\psi$  are the potential functions that satisfy the wave equations

$$\nabla^2 \phi = \frac{1}{V_P^2} \frac{\partial^2 \phi}{\partial t^2} \quad (4-2)$$

$$\nabla^2 \psi = \frac{1}{V_S^2} \frac{\partial^2 \psi_2}{\partial t^2}$$

and  $V_P$  and  $V_S$  are the P-wave velocity and shear wave velocity respectively. The P-wave and SV-wave displacement components defined by Equation 4-1 can be considered separately from the SH-wave component, which represents a horizontal displacement oriented normal to the  $x'$ - $z'$  plane and caused by a pure distortion. This SH-displacement component,  $v$ , is defined in terms of its own potential functions  $\psi_1$  and  $\psi_3$  as

$$v(x', z') = \frac{\partial \psi_1}{\partial z'} - \frac{\partial \psi_3}{\partial x'} \quad (4-3)$$

Returning to the P-wave and SV-wave cases, it can be shown that  $\phi$  and  $\psi_2$  satisfy the wave equations if they are of the form

$$\begin{Bmatrix} \phi \\ \psi_2 \end{Bmatrix} = \begin{Bmatrix} f(z') \\ g(z') \end{Bmatrix} \exp \left[ i\Omega \left( t - \frac{x'}{c} \right) \right]$$

where  $\Omega$  is the excitation frequency and  $c$  is the apparent wave velocity of propagation along the ground surface. This results in the following expressions for  $\phi$  and  $\psi_2$

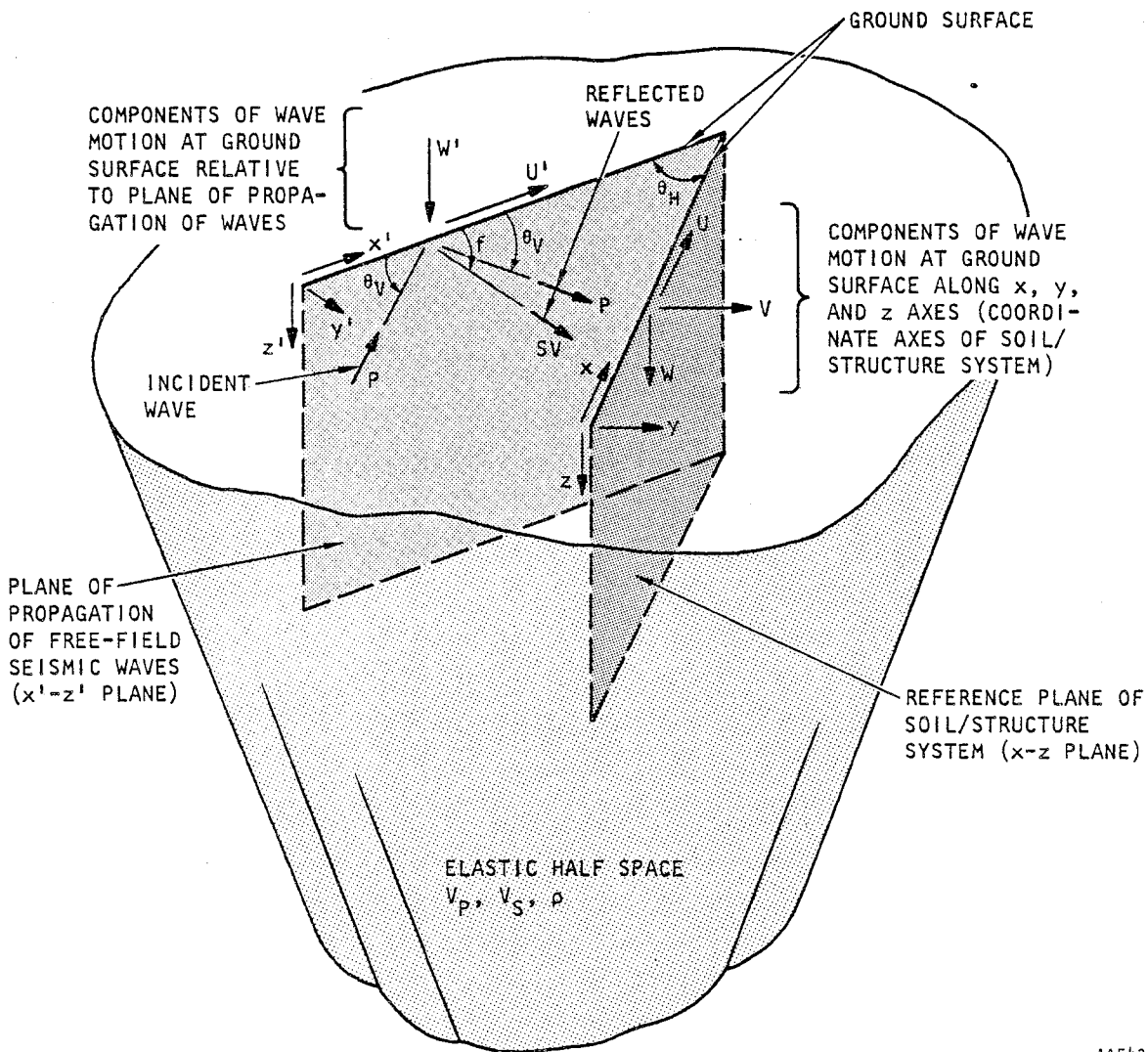
$$\begin{aligned} \phi = & A_1 \exp \left[ i\Omega \left( t - \frac{x'}{c} + \frac{z'}{c} \sqrt{\frac{c^2}{V_P^2} - 1} \right) \right] \\ & + A_2 \exp \left[ i\Omega \left( t - \frac{x'}{c} - \frac{z'}{c} \sqrt{\frac{c^2}{V_P^2} - 1} \right) \right] \end{aligned} \quad (4-4)$$

$$\begin{aligned} \psi_2 = & B_1 \exp \left[ i\Omega \left( t - \frac{x'}{c} + \frac{z'}{c} \sqrt{\frac{c^2}{V_S^2} - 1} \right) \right] \\ & + B_2 \exp \left[ i\Omega \left( t - \frac{x'}{c} - \frac{z'}{c} \sqrt{\frac{c^2}{V_S^2} - 1} \right) \right] \end{aligned} \quad (4-5)$$

In the above expressions, the terms involving the coefficients  $A_1$  and  $B_1$  represent the incident wave component of the displacement potential functions, and the terms involving  $A_2$  and  $B_2$  represent the reflected wave component. Each of these coefficients is unknown and is determined from the boundary conditions for P-waves and SV-waves at the ground surface. Furthermore, it is apparent from Equations 4-2, 4-4 and 4-5 that  $\phi$  is associated with P-wave propagation, and  $\psi_2$  is representative of SV-wave propagation.

#### 4.1.2 INCIDENT P-WAVES

The above potential functions  $\phi$  and  $\psi_2$  will now be used to treat the case of an incident P-wave propagating in the  $x'$ - $z'$  plane with an angle of vertical incidence  $\theta_V$ . This incident wave leads to reflected P- and SV-waves oriented at angles  $\theta_V$  and  $f$  respectively, relative to the ground surface (Fig. 4-2).



AA543

FIGURE 4-2. GROUND SURFACE DISPLACEMENTS AND REFLECTED WAVES DUE TO INCIDENT P-WAVE

The case of an incident P-wave and reflected P- and SV-waves requires setting  $B_1 = 0$  in Equation 4-5. Then, the remaining coefficients in Equations 4-4 and 4-5 are obtained through the use of the stress-strain and strain-displacement relationships for the half-space, and the requirement that the ground surface (defined by  $z'=0$ ) must be stress free. This leads to the following expressions for the ground surface displacements in the plane of propagation of the waves:

$$\begin{Bmatrix} u(x', 0) \\ w(x', 0) \end{Bmatrix} = \begin{Bmatrix} U' \\ W' \end{Bmatrix} \exp\left(i\Omega\left(t - \frac{x'}{c}\right)\right) \quad (4-6)$$

where  $U'$  and  $W'$  are the amplitudes of the ground surface displacements, and the prime (') superscript refers to the  $x'$ - $z'$  plane. These displacement amplitudes are defined as

$$\left. \begin{aligned} U' &= p \cos \theta_V [1 + R_{pp} - R_{ps} \tan f] \\ W' &= -p \sin \theta_V [1 - R_{pp} - R_{ps} \cot \theta_V] \end{aligned} \right\} \quad (4-7)$$

and

$$\begin{aligned} R_{pp} &= \frac{A_2}{A_1} = \frac{4 \tan \theta_V \tan f - (\tan^2 f - 1)^2}{D_p} \\ R_{ps} &= \frac{B_2}{A_1} = \frac{-4 \tan \theta_V (\tan^2 f - 1)}{D_p} \\ D_p &= 4 \tan \theta_V \tan f + (\tan^2 f - 1)^2 \\ \tan f &= \sqrt{\frac{2(1-v)}{1-2v} (1 + \tan^2 \theta_V) - 1} \end{aligned} \quad (4-8)$$



$\nu$  = Poisson's ratio of half-space

$p$  = Amplitude of incident P-wave

To supplement the above expressions, the following additional aspects of the P-wave-induced ground surface motions should be noted:

- When  $\theta_V = 90$  deg (vertically propagating P-wave),  $R_{ps} = 0$  and  $R_{pp} = -1$ . For this case, the incident P-wave is reflected as a P-wave, the horizontal displacement  $u(x', 0)$  vanishes, and the vertical displacement  $w(x', 0)$  has an amplitude of twice that of the incident wave.
- An alternative interrelationship between  $\theta_V$  and  $f$  is

$$\cos f = \frac{V_S}{V_P} \cos \theta_V \quad (4-9)$$

Since  $V_P > V_S$ , Equation 4-9 shows that  $f$  is always real; i.e., there is always a reflected SV-wave for all nonvanishing angles of incidence  $\theta_V$ . Therefore, the ground surface displacements induced by incident P-waves are always real and in-phase with one another. Only the amplitudes of  $U'$  and  $W'$  vary with  $\theta_V$ , as illustrated in Figure 4-3.

#### 4.1.3 INCIDENT SV-WAVES

We now consider the case of an incident SV-wave propagating in the  $x'-z'$  plane with an angle of vertical incidence  $\theta_V$ . This incident wave leads to reflected SV- and P-waves oriented at angles  $\theta_V$  and  $e$  respectively, relative to the ground surface (Fig. 4-4).

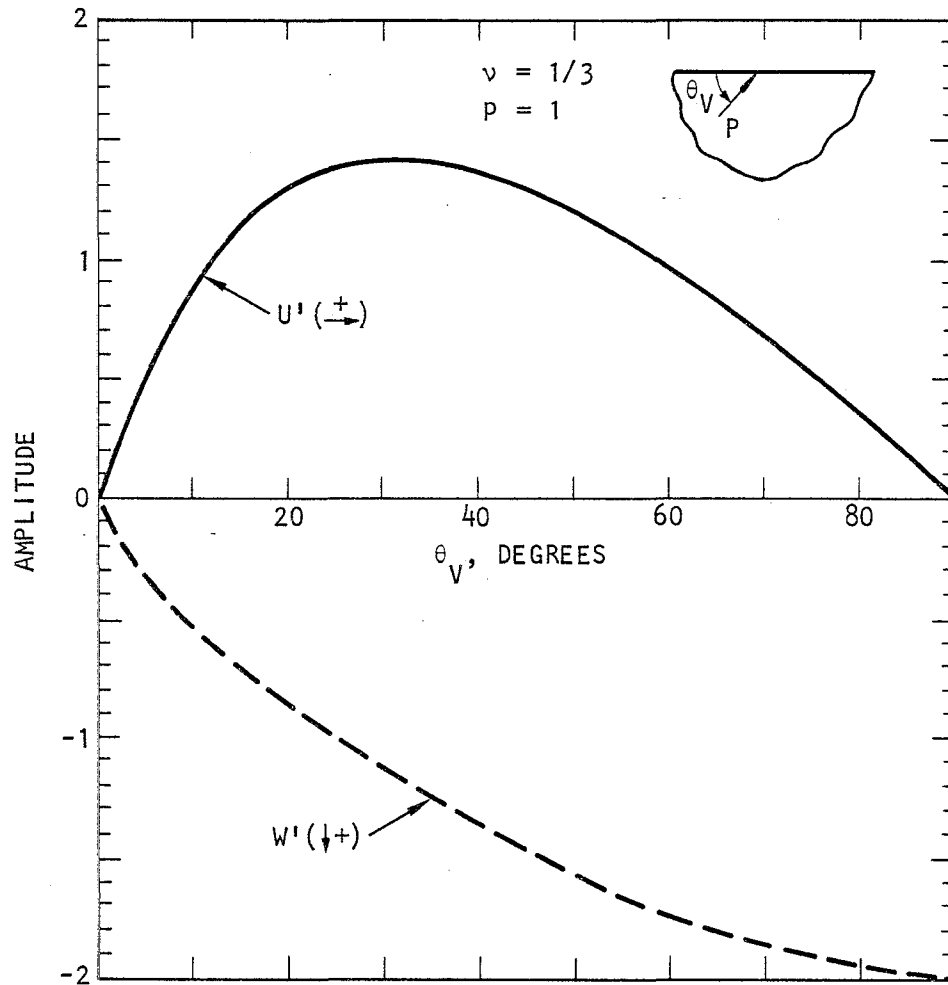


FIGURE 4-3. HORIZONTAL AND VERTICAL P-WAVE GROUND SURFACE DISPLACEMENT AMPLITUDES FOR POISSON'S RATIO = 1/3 (Werner and Lee, 1980)

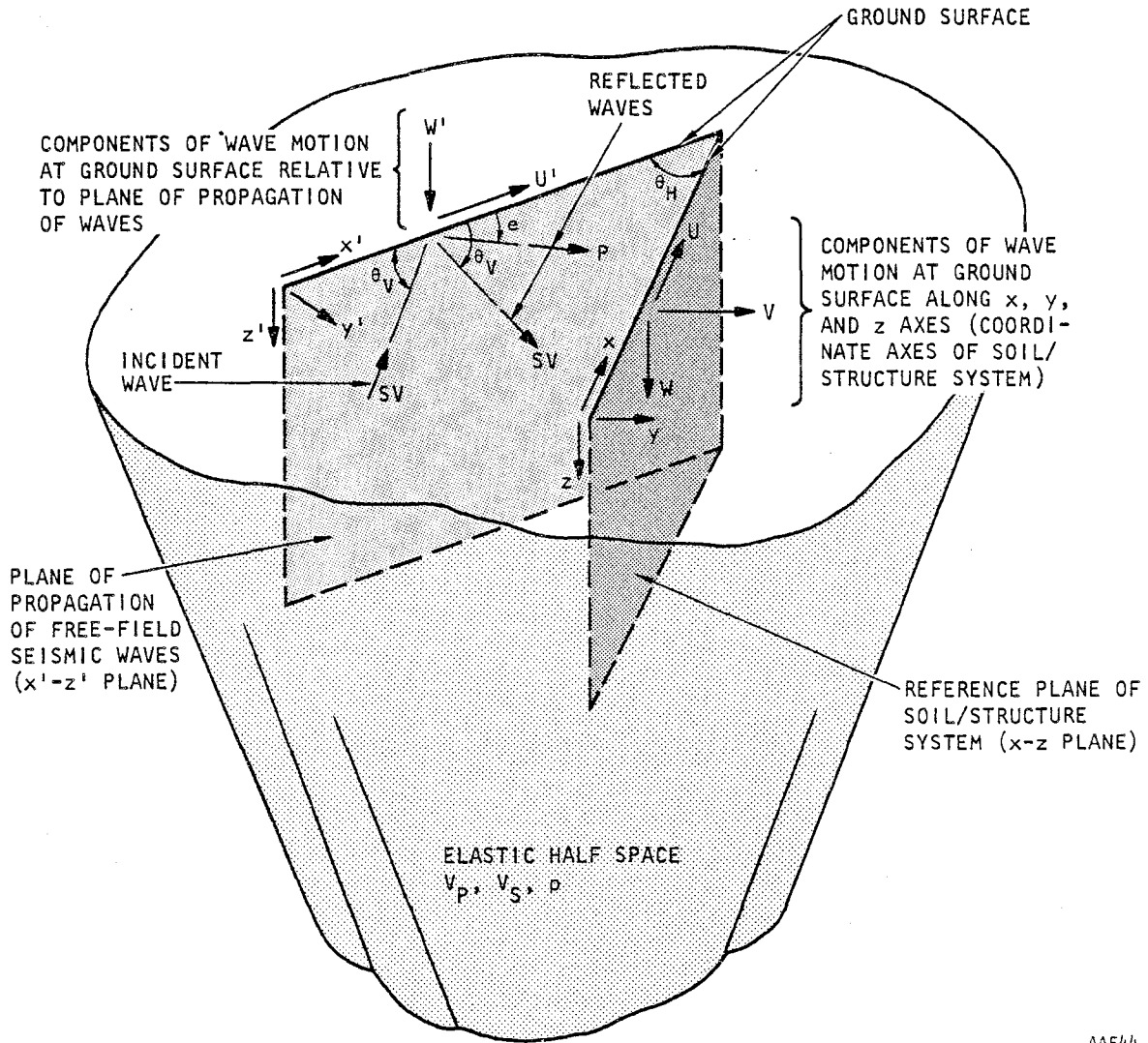


FIGURE 4-4. GROUND SURFACE DISPLACEMENTS AND REFLECTED WAVES DUE TO INCIDENT SV-WAVE



The case of an incident SV-wave and reflected SV- and P-waves requires setting  $A_1 = 0$  in Equation 4-4. Then, following procedures parallel to those previously outlined for incident P-waves, the requirements that the ground surface be stress free are used to determine an expression for the ground surface displacements  $u(x',0)$  and  $w(x',0)$ . This expression is identical in form to Equation 4-6 for the incident P-wave case, but with displacement amplitudes  $U'$  and  $W'$  now expressed as

$$\left. \begin{aligned} U' &= -s \sin \theta_V [1 - R_{ss} + R_{sp} \cot \theta_V] \\ W' &= -s \cos \theta_V [1 + R_{sp} \tan e + R_{ss}] \end{aligned} \right\} \quad (4-10)$$

where

$$\begin{aligned} R_{ss} &= \frac{B_2}{B_1} = \frac{4 \tan e \tan \theta_V - (\tan^2 \theta_V - 1)^2}{D_{SV}} \\ R_{sp} &= \frac{A_2}{A_1} = \frac{4 \tan \theta_V (\tan^2 \theta_V - 1)}{D_{SV}} \end{aligned} \quad (4-11)$$

$$D_{SV} = 4 \tan e \tan \theta_V + (\tan^2 \theta_V - 1)^2$$

$$\tan e = \sqrt{\frac{1 - 2\nu}{2(1 - \nu)} (1 + \tan^2 \theta_V) - 1}$$

$\nu$  = Poisson's ratio for half-space

$s$  = Amplitude of incident SV-wave

An important aspect of the ground-surface displacement field induced by incident SV-waves can be seen from the following alternative relationship between the angles  $\theta_V$  (for the





incident and reflected SV-waves) and  $e$  (for the reflected P-wave):

$$\cos e = \frac{V_P}{V_S} \cos \theta_V \quad (4-12)$$

Since  $V_P > V_S$ , Equation 4-12 indicates that no real value of  $e$  exists until  $\theta_V$  attains the value  $\theta_{cr}$ , where

$$\theta_{cr} = \cos^{-1} \frac{V_S}{V_P} \quad (4-13)$$

Therefore, for an incident SV-wave, there is no reflected P-wave when  $\theta_V < \theta_{cr}$ . Within this range, the angle  $e$  is imaginary and is computed as

$$\tan e = i \sqrt{1 - \frac{1 - 2\nu}{2(1 - \nu)} (1 + \tan^2 \theta_V)} \quad (4-14)$$

which, in turn, leads to a phase lag in the displacement field when  $\theta_V < \theta_{cr}$ . The value of  $\theta_{cr}$  depends on the Poisson's ratio for the half-space, as shown in Figure 4-5.

To further illustrate these aspects of incident SV-wave excitations, Figure 4-6 defines how the ground surface displacements are affected by  $\theta_V$  when  $\nu = 1/3$  and  $s = 1$ . For this case,  $\theta_{cr} = 60$  deg, and Figure 4-6 shows that when  $\theta_V > \theta_{cr}$ ,  $U'$  and  $W'$  are in phase, although their relative amplitudes still vary with  $\theta_V$ . However, when  $\theta_V < \theta_{cr}$ , the following types of free-field response take place:

1.  $\theta_V < 45$  deg. The free-field ground surface motions are elliptic retrograde, wherein the positive horizontal displacement vector,  $U'$ , trails the positive vertical displacement vector,  $W'$ , by 90 deg (where the positive vectors are defined in Fig. 4-4). The aspect ratio of this elliptic motion (i.e., the ratio of  $W'$  to  $U'$ ), varies with  $\theta_V$  within this range.

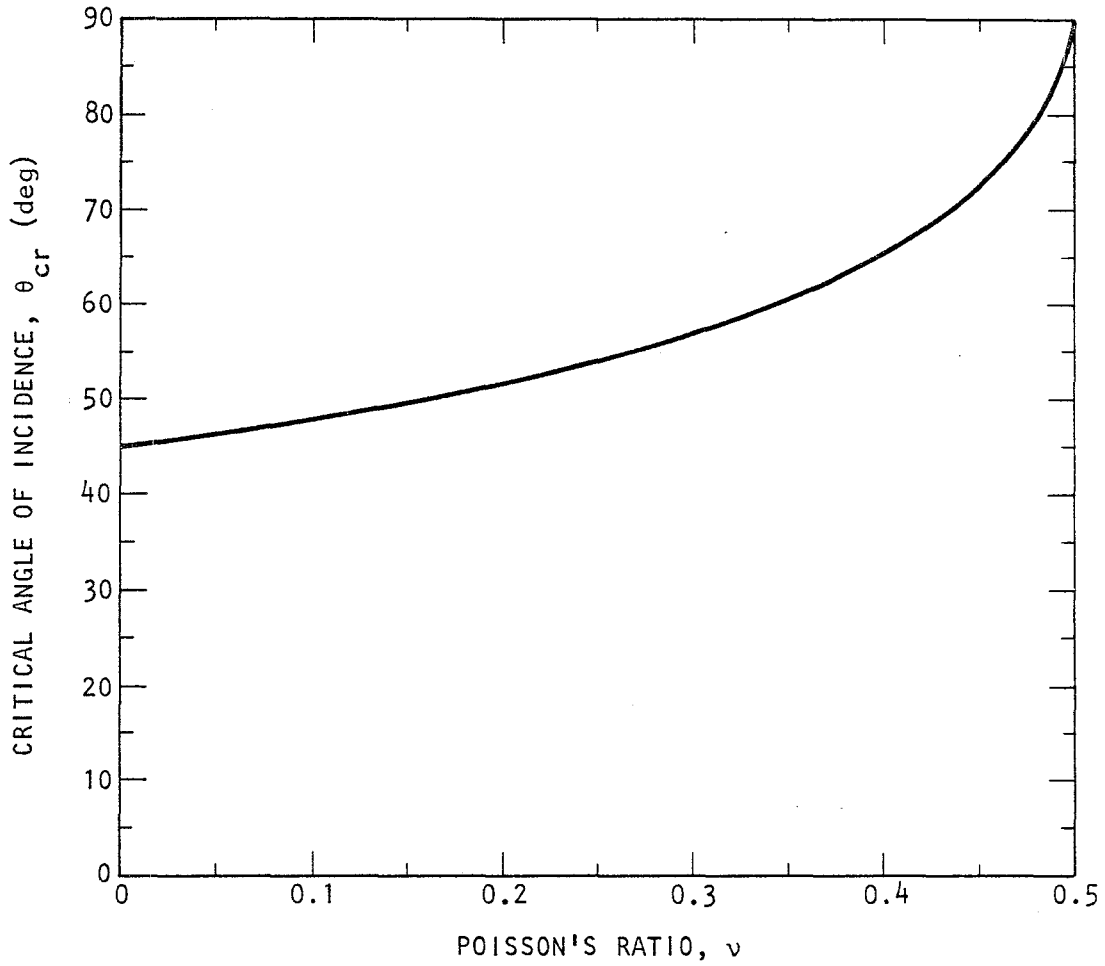
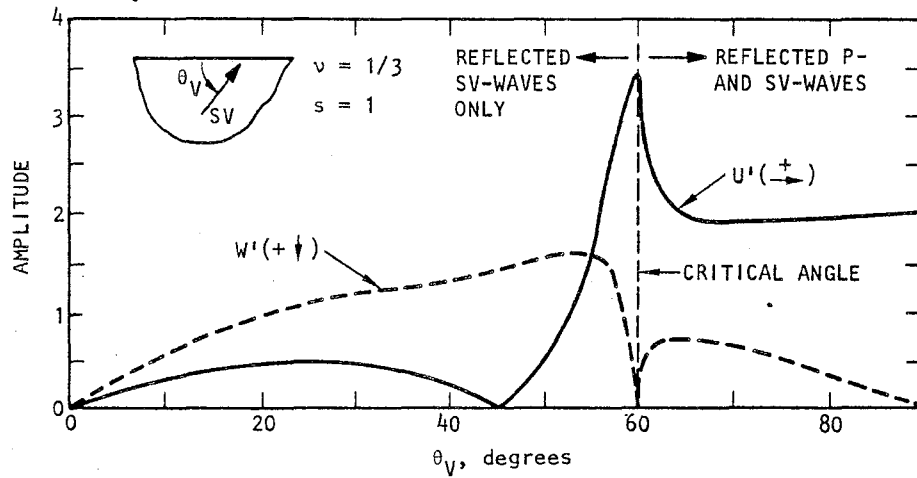
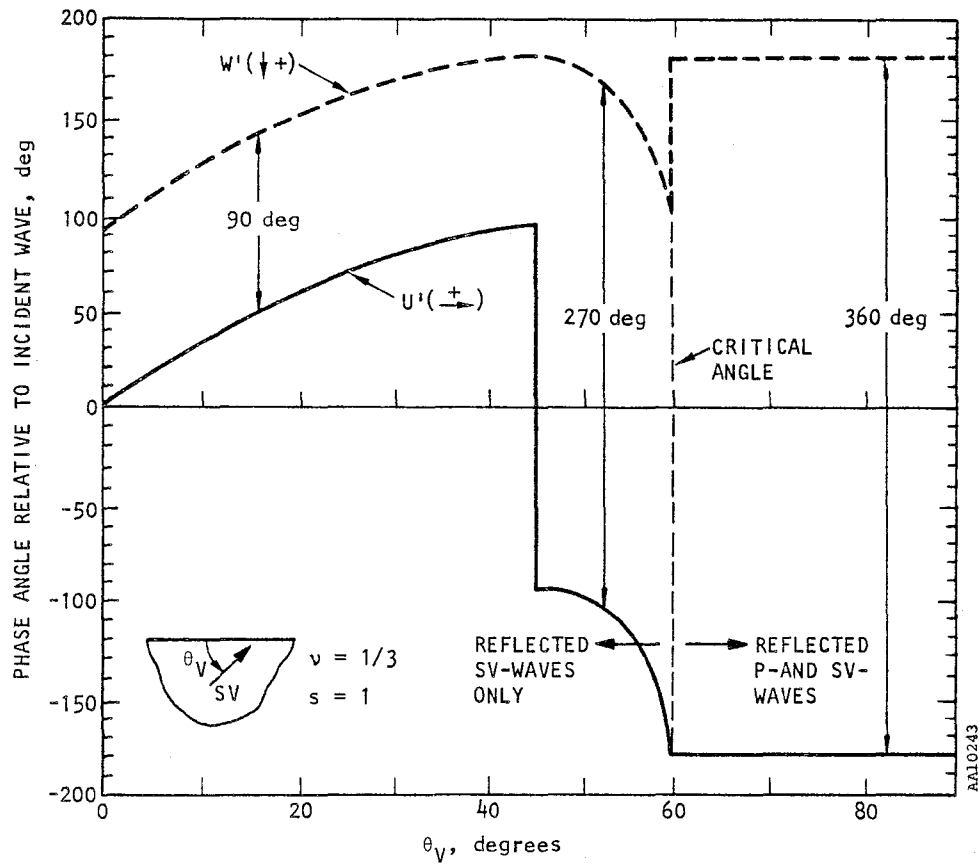


FIGURE 4-5. VARIATION OF CRITICAL ANGLE OF VERTICAL INCIDENCE WITH POISSON'S RATIO FOR INCIDENT SV-WAVE EXCITATION



(a) Amplitude



(b) Phase angle

FIGURE 4-6. HORIZONTAL AND VERTICAL FREE-FIELD SV-WAVE GROUND SURFACE DISPLACEMENTS FOR POISSON'S RATIO = 1/3 (Werner and Lee, 1980)



2. 45 deg <  $\theta_V$  < 60 deg. The free-field ground surface motions are elliptic prograde, wherein the positive vertical displacement vector,  $U'$ , is ahead of the positive vertical displacement vector,  $W'$ , by 90 deg. As for  $\theta_V < 45$  deg, the aspect ratio of this elliptic motion, varies with  $\theta_V$  within this range.

#### 4.1.4 INCIDENT SH-WAVES

For an incident SH-wave propagating in the  $x'$ - $z'$  plane, a derivation similar to that outlined above for the incident P-waves and SV-waves shows that all of the energy is reflected at the ground surface as an SH-wave (Fig. 4-7). Therefore, the resulting displacement field at the ground surface has an amplitude twice that of the wave amplitude, and is oriented horizontally and normal to the  $x'$ - $z'$  plane, i.e.

$$v(x', 0) = V' \exp\left(i\Omega\left(t - \frac{x'}{c}\right)\right) \quad (4-15)$$

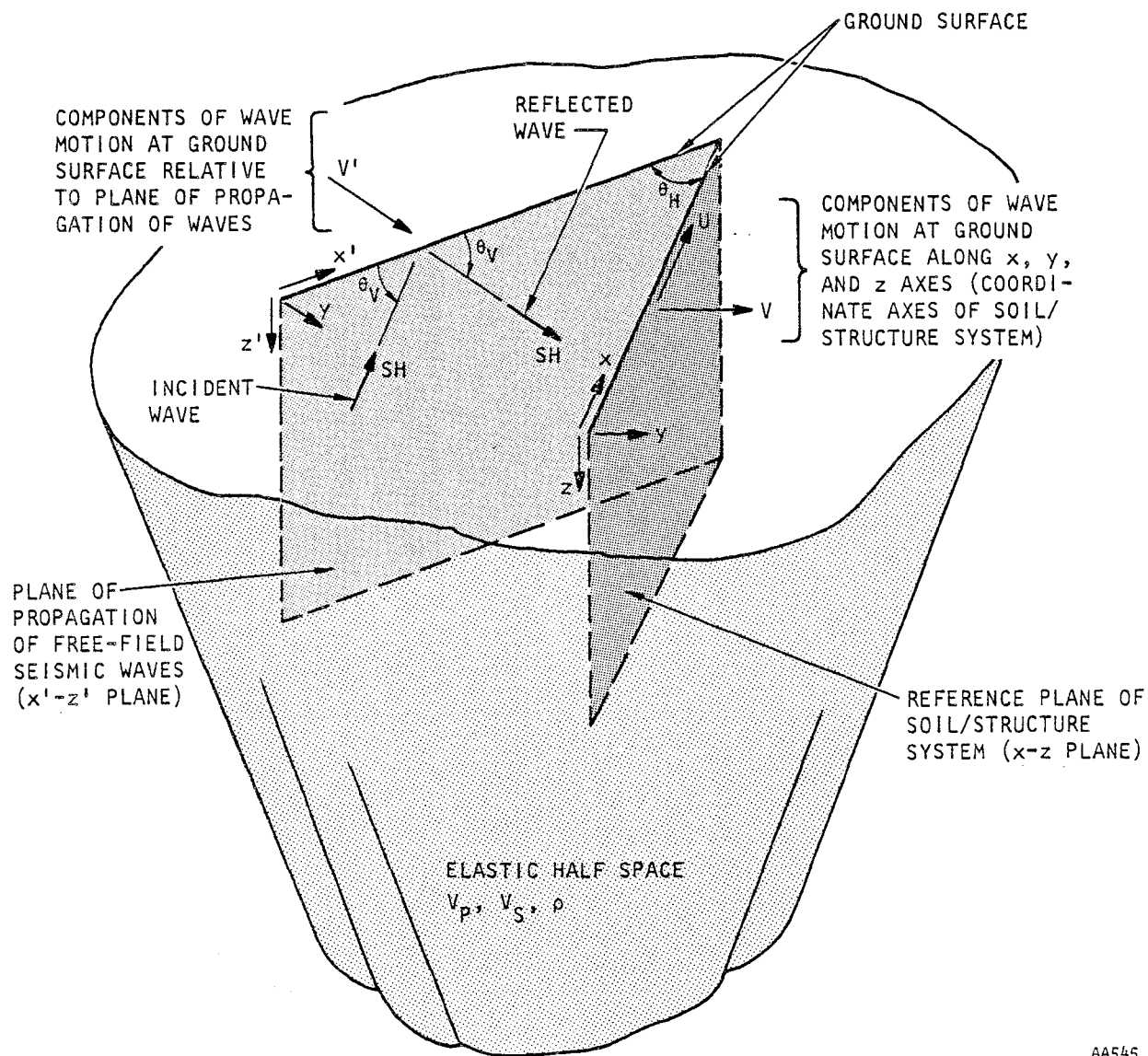
where

$$V' = 2s \quad (4-16)$$

and  $s$  is the amplitude of the incident SH-wave. Therefore, it is seen that, unlike the P-wave and SV-wave cases, the free-field ground surface displacement amplitudes induced by incident SH-waves are independent of  $\theta_V$ .

#### 4.1.5 TRANSFORMATION TO ACCOUNT FOR HORIZONTAL ANGLE OF INCIDENCE

The prior formulations define the free-field ground surface displacements induced by seismic body waves, relative to the  $x'$ - $z'$  plane of propagation of the waves. However, as previously noted, this plane will generally be offset relative to the reference plane of the structure (i.e., the  $x$ - $z$  plane) by a horizontal angle of incidence  $\theta_H$  (Fig. 4-1). To account for



AA545

FIGURE 4-7. GROUND SURFACE DISPLACEMENTS AND REFLECTED WAVES DUE TO INCIDENT SH-WAVE



this angular offset, the amplitudes of the ground surface displacements must be transformed as follows:

$$\begin{Bmatrix} U \\ V \\ W \end{Bmatrix} = \begin{bmatrix} \cos \theta_H & -\sin \theta_H & 0 \\ \sin \theta_H & \cos \theta_H & 0 \\ 0 & 0 & 1 \end{bmatrix} \begin{Bmatrix} U' \\ V' \\ W' \end{Bmatrix} \quad (4-17)$$

where  $U$ ,  $V'$ , and  $W'$  are the displacement amplitudes induced by the incident body waves with reference to the  $x'$ - $z'$  plane of free-field wave propagation, and  $U$ ,  $V$ , and  $W$  are the values of these displacement amplitudes transformed to correspond to the  $x$ - $z$  reference plane of the structure. The corresponding values of the ground surface displacement at each node point along the structure/half-space interface are then computed as

$$\{u_{ff}\} = \begin{Bmatrix} U \\ V \\ W \end{Bmatrix} \exp \left[ i\Omega \left( t - \frac{x}{c} \cos \theta_H - \frac{y}{c} \sin \theta_H \right) \right] \quad (4-18)$$

where  $c$  is the apparent wave velocity and  $\Omega$  is the excitation frequency.

At this point, all of the pertinent expressions used in BASSIN1 to compute the free-field ground surface displacements due to body wave excitations have been provided. The steps involved in these displacement computations are as follows:

1. Compute the displacement amplitudes with reference to the  $x'$ - $z'$  plane of propagation of the waves. These involve the use of Equations 4-7 and 4-8 for incident P-waves, Equations 4-10 and 4-11 for incident SV-waves, and Equation 4-16 for incident SH-waves.
2. Use Equations 4-17 and 4-18 to transform these displacement amplitudes to account for the horizontal angle of incidence  $\theta_H$  and to define the phased displacements at each interface node.



## 4.2 RAYLEIGH WAVE EXCITATIONS

To define the free-field ground surface displacements induced by a Rayleigh wave with angle of incidence  $\theta_H$ , one can follow steps similar to those previously described for body wave conditions. Therefore, as before, the first step in the definition of Rayleigh wave displacements is to define the following potential functions that satisfy the wave equations (Ewing et al., 1957).

$$\begin{aligned}\phi &= A \exp \left[ i\Omega \left( t - \frac{x'}{V_R} \pm \frac{z'}{V_R} \sqrt{\frac{V_R^2}{V_P^2} - 1} \right) \right] \\ \psi &= B \exp \left[ i\Omega \left( t - \frac{x'}{V_R} \pm \frac{z'}{V_R} \sqrt{\frac{V_R^2}{V_S^2} - 1} \right) \right]\end{aligned}\tag{4-19}$$

where  $V_R$  is the unknown Rayleigh wave velocity and  $\Omega$  is the excitation frequency. The constants A and B are determined from the requirements for a vanishing normal stress and shear stress at the ground surface. This results in the following set of two simultaneous equations in two unknowns.

$$\begin{bmatrix} \left( 2 - \frac{V_R^2}{V_S^2} \right) & \pm 2 \sqrt{\frac{V_R^2}{V_S^2} - 1} \\ \mp 2 \sqrt{\frac{V_R^2}{V_P^2} - 1} & \left( 2 - \frac{V_R^2}{V_S^2} \right) \end{bmatrix} \begin{Bmatrix} A \\ B \end{Bmatrix} = \begin{Bmatrix} 0 \\ 0 \end{Bmatrix}\tag{4-20}$$

In order for nontrivial solutions for A and B to exist from the above equations, the determinant of the coefficient matrix



must vanish. This results in the following expression for either the upper or lower set of signs:

$$\left(2 - \frac{v_R^2}{v_S^2}\right)^2 = 4 \sqrt{1 - \frac{v_R^2}{v_P^2}} \sqrt{1 - \frac{v_R^2}{v_S^2}}$$

which, in turn, leads to the following Rayleigh equation relating the longitudinal, shear, and Rayleigh wave velocities:

$$\left(\frac{v_R^2}{v_S^2}\right)^3 - 8 \left(\frac{v_R^2}{v_S^2}\right)^2 + \left[24 - 16 \left(\frac{v_S^2}{v_P^2}\right)\right] \left(\frac{v_R^2}{v_S^2}\right) - 16 \left[1 - \frac{v_S^2}{v_P^2}\right] = 0 \quad (4-21)$$

Equation 4-21, which is a cubic equation in  $v_R^2/v_S^2$ , must be solved using numerical procedures. Then, with the known value of  $v_R$ , Equation 4-20 can be used to obtain A and B, in which the sign is chosen so that the potential functions approach zero as  $z$  approaches  $\infty$ . This, in turn, defines the potential functions from which the ground surface displacements can be determined at any point within the  $x'-z'$  plane of wave propagation. These displacements are then transformed to correspond to the  $x-z$  reference plane of the structure, by accounting for the horizontal angle of incidence  $\theta_H$ .

All of the above steps lead to the following results for the ground surface displacements relative to the  $x-y-z$  coordinate system.





$$u(x, y, 0) = R_H \cos \theta_H \exp \left\{ i\Omega \left[ t - \left( \frac{x \cos \theta_H + y \sin \theta_H}{V_R} \right) \right] \right\}$$

$$v(x, y, 0) = R_H \cos \theta_H \exp \left\{ i\Omega \left[ t - \left( \frac{x \cos \theta_H + y \sin \theta_H}{V_R} \right) \right] \right\}$$

$$w(x, y, 0) = R_V \exp \left\{ i\Omega \left[ t - \left( \frac{x \cos \theta_H + y \sin \theta_H}{V_R} \right) \right] \right\}$$

(4-22)

where

- $u, v, w$  = Free-field ground surface displacements  
 $\Omega$  = Circular frequency of excitation  
 $V_R$  = Rayleigh wave velocity

and  $R_H$  and  $R_V$  are the amplitudes of the horizontal and vertical components of motion along the ground surface. These are obtained from the following expressions

$$R_H = i \left[ \frac{2 \sqrt{1 - \frac{V_R^2}{V_S^2}}}{\left(2 - \frac{V_R^2}{V_S^2}\right)} - \sqrt{1 - \frac{V_R^2}{V_S^2}} \right] A$$

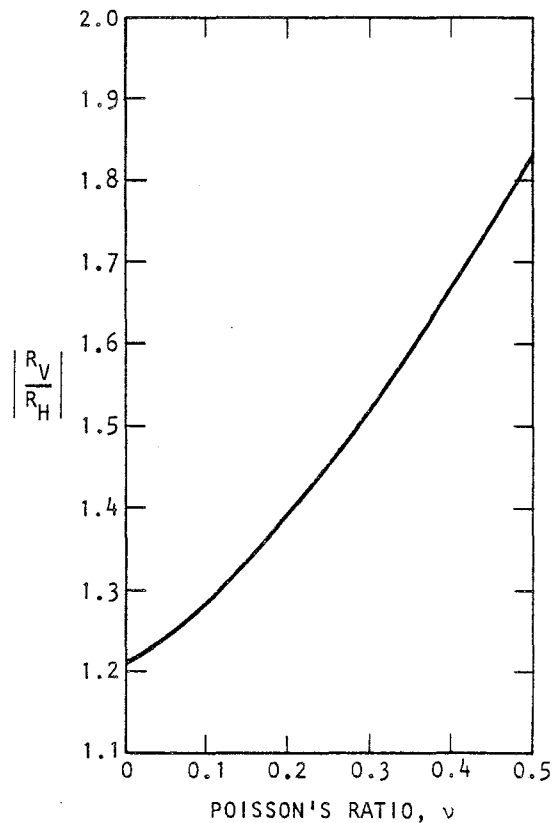
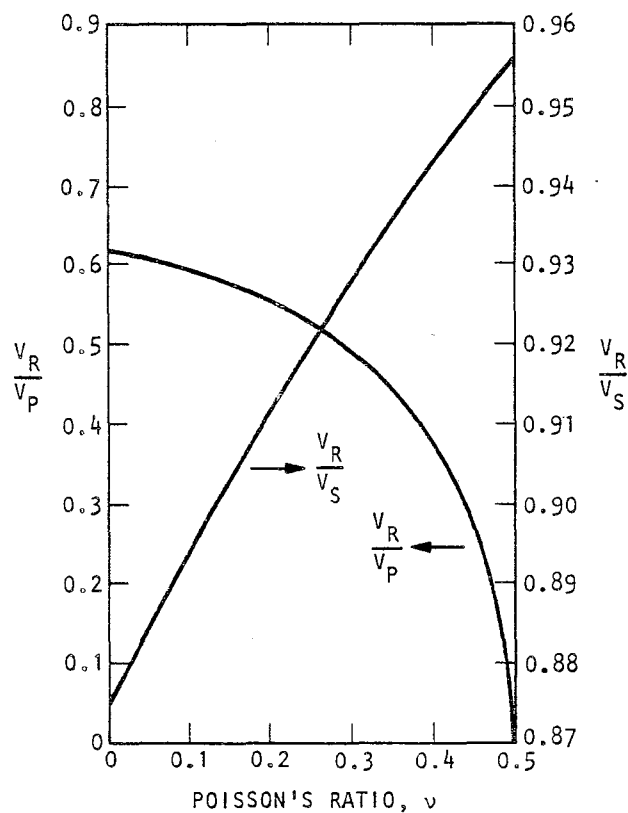
(4-23)

$$R_V = \left[ \frac{2 \sqrt{1 - \frac{V_R^2}{V_S^2}} \sqrt{1 - \frac{V_R^2}{V_P^2}}}{\left(2 - \frac{V_R^2}{V_S^2}\right)} - 1 \right] A$$



where  $A$  is a function of the wave number  $\Omega/V_R$ . By considering the limiting values of  $V_R/V_S$  and  $V_P/V_S$  for  $0 \leq v \leq 0.5$  (Fig. 4-8a), the quantity within the brackets in the above expression for  $R_H$  is seen to be always positive whereas, in the expression for  $R_V$ , the bracketed quantity is always negative. From this, it can be shown that the ground surface displacement induced by Rayleigh waves is always elliptic retrograde; furthermore, Equation 4-23 indicates that the aspect ratio of this elliptic path,  $|R_V/R_H|$ , is dependent on Poisson's ratio (see Fig. 4-8b). These features of the ground surface motion are illustrated in Figure 4-9 for the case of an elastic half-space with a Poisson's ratio of  $1/3$ ; for this case  $V_R = 0.9325 V_S$  and  $|R_V| = 1.565 |R_H|$ .

With this as background, the procedures followed in BASSIN1 for computing the free-field displacements induced by incident Rayleigh waves can now be summarized. The first step in this approach, given the elastic properties of the half-space, is to solve the cubic equation for  $V_R^2/V_S^2$  (Eq. 4-21). A Newton-Raphson iterative procedure is used in BASSIN1 for this purpose. Then, the amplitudes of the ground surface displacement amplitudes,  $R_H$  and  $R_V$ , are determined using Equation 4-23 for all excitation frequencies; these displacement amplitudes are presently normalized in BASSIN1 so that  $R_H = 1.0$ . The resulting values of  $R_H$  and  $R_V$  are substituted into Equation 4-22 to define the free-field displacements at each interface node point.

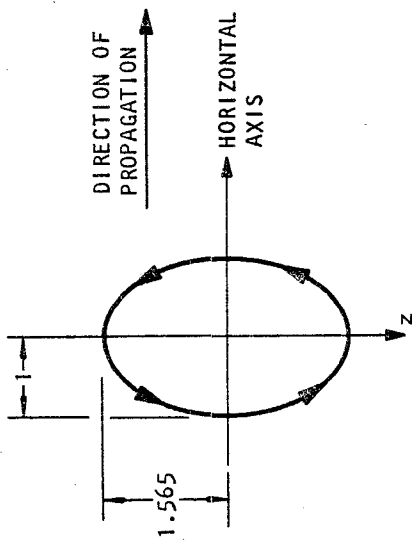


AA541

(a) Rayleigh wave velocity ratios (Kropoff, 1952)

(b) Ground surface displacement amplitude ratio

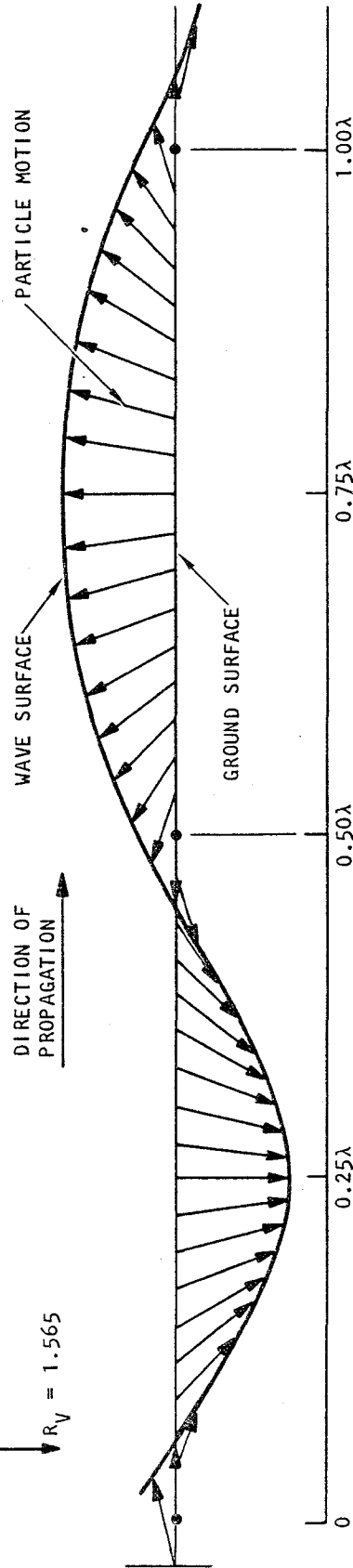
FIGURE 4-8. RAYLEIGH WAVE FREE-FIELD RESPONSE PARAMETERS



(a) Particle motion at a point

NOTE:  $\lambda$  = WAVELENGTH OF INCIDENT RAYLEIGH WAVE

$R_H = 1.0$   
 $R_V = 1.565$



AA9740

(b) Ground surface displacement profile at a particular time

FIGURE 4-9. RAYLEIGH WAVE MOTION AT SURFACE OF SOIL MEDIUM WITH POISSON'S RATIO = 1/3 (Werner and Lee, 1980)



## CHAPTER 5

COMPUTATION OF GREEN'S FUNCTIONS FOR  
AN ELASTIC HALF-SPACE

This chapter provides the mathematical formulation for the BASSIN1 computation of Green's functions for an elastic half-space (Lamb, 1904; Nakano, 1930). This formulation is similar to that used in our prior work in this area (Werner et al., 1977), and is included here for purposes of completeness. The use of these Green's functions to compute half-space impedance matrices and driving forces is described in Chapter 6.

This chapter is organized into three main sections. The first provides basic definitions pertaining to the Green's function matrix for any elastic continuum. The second section provides the analytical expressions of the Green's functions for an elastic half-space, while the final section outlines the numerical procedures used in the actual computation of these Green's functions in BASSIN1.

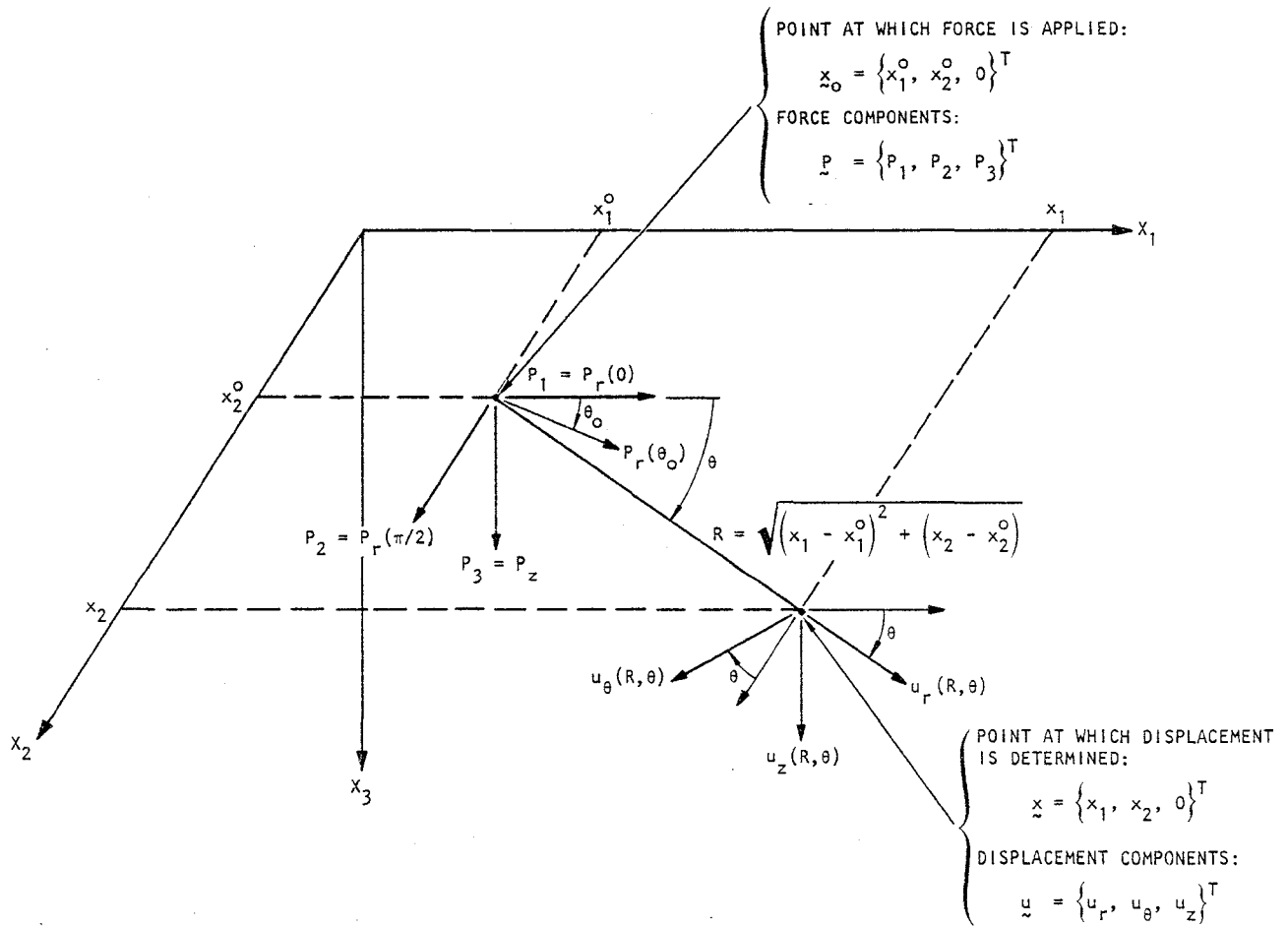
5.1 BASIC DEFINITIONS

Consider a harmonic force vector  $\{P\}$  with an excitation frequency  $\Omega$ , that is defined as

$$\{P\} = \begin{Bmatrix} P_1 \\ P_2 \\ P_3 \end{Bmatrix} e^{i\Omega t} = \underline{P} \quad (5-1)$$

and acts along the surface of a linear elastic soil medium (see Fig. 5-1). In Equation 5-1,  $P_1$ ,  $P_2$ , and  $P_3$  are the three components of force oriented along the coordinate axes at an arbitrary point on the surface defined by the vector  $\{x_o\}$ , where

$$\{x_o\} = \begin{Bmatrix} x_1^o \\ x_2^o \\ 0 \end{Bmatrix} = \underline{x}_o \quad (5-2)$$



AA8724

FIGURE 5-1. NOTATION FOR DEVELOPMENT OF GREEN'S FUNCTIONS FOR A LINEAR ELASTIC SOIL MEDIUM

and the coordinate axes are shown in Figure 5-1. The displacement vector  $\{u\}$  that results at another arbitrary point along the surface of the medium defined by  $\{x\}$ , where

$$\{x\} = \begin{Bmatrix} x_1 \\ x_2 \\ 0 \end{Bmatrix} = \underline{x} \quad (5-3)$$

is computed as

$$\{u(x)\} = \begin{Bmatrix} u_1 \\ u_2 \\ u_3 \end{Bmatrix} e^{i\Omega t} = [G(\Omega, \underline{x} - \underline{x}_0)] \{P(\underline{x}_0)\} \quad (5-4)$$

where  $u_1$ ,  $u_2$ , and  $u_3$  are the three components of displacement. The matrix  $[G(\Omega, \underline{x} - \underline{x}_0)]$  is termed the Green's function matrix and is of order  $3 \times 3$ , i.e.,

$$[G(\Omega, \underline{x} - \underline{x}_0)] = \begin{bmatrix} g_{11} & g_{12} & g_{13} \\ g_{21} & g_{22} & g_{23} \\ g_{31} & g_{32} & g_{33} \end{bmatrix} \quad (5-5)$$

In Equation 5-5,  $g_{\ell m}(\Omega, \underline{x} - \underline{x}_0)$  relates the  $\ell$ th component of the displacement at  $\underline{x}$ ,  $u_\ell$ , and the  $m$ th component of the force at  $\underline{x}_0$ ,  $P_m$ . Some properties of  $g_{\ell m}$  are that

$$g_{21} = g_{12} ; g_{13} = -g_{31} ; g_{23} = -g_{32} \quad (5-6)$$

Equations 5-5 and 5-6 indicate that  $[G(\Omega, \underline{x} - \underline{x}_0)]$  has only six independent matrix elements. However, as shown subsequently, these six components can be specified by just four functions if the point load is considered in polar coordinates, as shown in Figure 5-1. Therefore, in the remainder of this chapter, polar coordinates are employed.

For loads defined in polar coordinates, axis-symmetry and axis-asymmetry considerations require specification of only one



horizontal load,  $P_r(\theta_0)$ , in addition to the vertical load  $P_z$ ; i.e., all other horizontal loads can be represented by redefining the coordinate  $\theta$  (Fig. 5-1). Thus, without loss of generality, Equation 5-4 can be expressed in polar coordinates as

$$\begin{Bmatrix} u_r(R, \theta) \\ u_\theta(R, \theta) \\ u_z(R, \theta) \end{Bmatrix} = \frac{1}{\mu R} \begin{bmatrix} f_{rr} \cos(\theta - \theta_0) & f_{rz} \\ f_{\theta r} \sin(\theta - \theta_0) & f_{\theta z} \\ f_{zr} \cos(\theta - \theta_0) & f_{zz} \end{bmatrix} \begin{Bmatrix} P_r(\theta_0) \\ P_z \end{Bmatrix} \quad (5-7)$$

where

$\mu$  = Shear modulus of elastic medium

$$R = |\underline{x} - \underline{x}_0| = \sqrt{(x_1 - x_1^0)^2 + (x_2 - x_2^0)^2}$$

$$\theta = \arg(\underline{x} - \underline{x}_0) = \tan^{-1} \left( \frac{x_2 - x_2^0}{x_1 - x_1^0} \right)$$

Equation 5-7 holds for any linear elastic soil medium with an axis of symmetry about the z-axis. Therefore, a horizontally layered medium will also have Green's functions of the form indicated by Equation 5-7.

## 5.2 GREEN'S FUNCTIONS FOR AN ELASTIC HALF-SPACE

### 5.2.1 GREEN'S FUNCTIONS IN POLAR COORDINATES

Consider now an elastic half-space with Poisson's ratio  $\nu$ , shear modulus  $\mu$ , and shear wave velocity  $V_s$ . By rearranging the Green's functions (in polar coordinates) according to Equation 5-7, the functions  $f_{rr}$ ,  $f_{\theta r}$ ,  $f_{zr}$ ,  $f_{rz}$ ,  $f_{\theta z}$ , and  $f_{zz}$  are dependent only on a dimensionless frequency parameter,  $a_0$ , defined as

$$a_0 = \frac{\Omega R}{V_s} \quad (5-8)$$





The resulting formulas are as follows:

$$f_{rr}(a_o) = \frac{a_o}{4\pi} \left[ \int_0^\infty \frac{z \sqrt{z^2 - 1} \{J_2(a_o z) - J_0(a_o z)\}}{F(z)} dz + \int_0^\infty \frac{z}{\sqrt{z^2 - 1}} \{J_2(a_o z) + J_0(a_o z)\} dz \right] \quad (5-9)$$

$$f_{rz}(a_o) = \frac{a_o}{2\pi} \int_0^\infty \frac{z^2 \left[ (2z^2 - 1) - 2\sqrt{z^2 - n^2} \sqrt{z^2 - 1} \right] J_1(a_o z)}{F(z)} dz \quad (5-10)$$

$$f_{\theta r}(a_o) = \frac{a_o}{4\pi} \left[ \int_0^\infty \frac{z \sqrt{z^2 - 1} \{J_2(a_o z) + J_0(a_o z)\}}{F(z)} dz + \int_0^\infty \frac{z}{\sqrt{z^2 - 1}} \{J_2(a_o z) - J_0(a_o z)\} dz \right] \quad (5-11)$$

$$f_{\theta z}(a_o) = 0 \quad (5-12)$$

$$f_{zr}(a_o) = -f_{rz}(a_o) \quad (5-13)$$

$$f_{zz}(a_o) = -\frac{a_o}{2\pi} \int_0^\infty \frac{\sqrt{z^2 - n^2} z J_0(a_o z)}{F(z)} dz \quad (5-14)$$

where

$$F(z) = \text{Rayleigh determinant} \\ = (2z^2 - 1)^2 - 4z^2 \sqrt{(z^2 - n^2)(z^2 - 1)}$$

$$n = \frac{V_s}{V_p} = \sqrt{\frac{1 - 2\nu}{2(1 - \nu)}}$$



$V_s, V_p, \nu$  = S-wave velocity, P-wave velocity, and Poisson's ratio, respectively, of the elastic half-space

$J_0, J_1, J_2$  = Bessel functions of order 0, 1, and 2, respectively

In Equations 5-9 through 5-14 it is observed that  $f_{\theta z} = 0$  and  $f_{zr} = -f_{rz}$ ; therefore, the total number of functions needed to define the Green's function matrix [G] in Equation 5-7 is four. Furthermore, it is of interest for future reference to note the static limit of Equations 5-9 through 5-14, which corresponds to the limit of these expressions as  $a_0$  approaches zero. These are:

$$f_{rr}(a_0 = 0) = \frac{1}{2\pi} \quad (5-15)$$

$$f_{rz}(0) = \frac{-n^2}{4\pi(1 - n^2)} \quad (5-16)$$

$$f_{\theta r}(0) = -\frac{-1}{4\pi(1 - n^2)} \quad (5-17)$$

$$f_{\theta z}(0) = 0 \quad (5-18)$$

$$f_{zr}(0) = -f_{rz}(0) \quad (5-19)$$

$$f_{zz}(0) = \frac{1}{4\pi(1 - n^2)} \quad (5-20)$$

### 5.2.2 GREEN'S FUNCTIONS IN CARTESIAN COORDINATES

The relationship of the displacements  $\{u_1 \ u_2 \ u_3\}^T$  in Cartesian coordinates to those in polar coordinates  $\{u_r \ u_\theta \ u_z\}^T$  can be expressed as

$$\begin{Bmatrix} u_1(x) \\ u_2(x) \\ u_3(x) \end{Bmatrix} = \begin{bmatrix} \cos \theta & -\sin \theta & 0 \\ \sin \theta & \cos \theta & 0 \\ 0 & 0 & 1 \end{bmatrix} \begin{Bmatrix} u_r(x) \\ u_\theta(x) \\ u_z(x) \end{Bmatrix} \quad (5-21)$$



Thus, by noting from Figure 5-1 that

$$\begin{Bmatrix} P_1(x_0) \\ P_2(x_0) \\ P_3(x_0) \end{Bmatrix} = \begin{Bmatrix} P_r(0) \\ P_r(\pi/2) \\ P_z \end{Bmatrix} \quad (5-22)$$

one can relate  $\{u_r \ u_\theta \ u_z\}^T$  at  $\underline{x}$  to  $\{P_1 \ P_2 \ P_3\}^T$  at  $\underline{x}_0$  by combining Equations 5-7 and 5-22, i.e.,

$$\begin{Bmatrix} u_r(\underline{x}) \\ u_\theta(\underline{x}) \\ u_z(\underline{x}) \end{Bmatrix} = \frac{1}{\mu R} \begin{bmatrix} f_{rr} \cos \theta & f_{rr} \cos(\theta - \frac{\pi}{2}) & f_{rz} \\ f_{\theta r} \sin \theta & f_{\theta r} \sin(\theta - \frac{\pi}{2}) & f_{\theta z} \\ f_{zr} \cos \theta & f_{zr} \cos(\theta - \frac{\pi}{2}) & f_{zz} \end{bmatrix} \begin{Bmatrix} P_1(x_0) \\ P_2(x_0) \\ P_3(x_0) \end{Bmatrix} \quad (5-23)$$

By substituting Equation 5-23 into 5-21, the quantities  $g_{ij}$ , as defined in Equation 5-5, can be obtained as

$$\begin{bmatrix} g_{11} & g_{12} & g_{13} \\ g_{21} & g_{22} & g_{23} \\ g_{31} & g_{32} & g_{33} \end{bmatrix} = \frac{1}{\mu R} \begin{bmatrix} f_{rr}^2 c^2 - f_{\theta r}^2 s^2 & (f_{rr} + f_{\theta r})s \cdot c & f_{rz}c - f_{\theta z}s \\ (f_{rr} + f_{\theta r})s \cdot c & f_{rr}^2 s^2 - f_{\theta r}^2 c^2 & f_{rz}s + f_{\theta z}c \\ f_{zr}c & f_{zr}s & f_{zz} \end{bmatrix} \quad (5-24)$$

where  $c$  and  $s$  are shorthand notations for  $\cos \theta$  and  $\sin \theta$ , respectively. In the above expression, the relationships defined in Equation 5-6 between the off-diagonal  $g_{ij}$  elements are satisfied when Equations 5-12 and 5-13 are substituted into Equation 5-24. Furthermore, a simplified form of Equation 5-24 results if the expressions

$$\cos \theta = \frac{x_1 - x_1^0}{R} \quad (5-25)$$

$$\sin \theta = \frac{x_2 - x_2^0}{R} \quad (5-26)$$

are employed. This form is as follows:

$$g_{11} = \frac{1}{\mu R^3} \left\{ (x_1 - x_1^0)^2 f_{rr} - (x_2 - x_2^0)^2 f_{\theta r} \right\} \quad (5-27)$$

$$g_{12} = \frac{1}{\mu R^3} (x_1 - x_1^0) (x_2 - x_2^0) (f_{rr} + f_{\theta r}) \quad (5-28)$$

$$g_{13} = \frac{1}{\mu R^2} (x_1 - x_1^0) f_{rz} \quad (5-29)$$

$$g_{22} = \frac{1}{\mu R^3} \left\{ (x_2 - x_2^0)^2 f_{rr} - (x_1 - x_1^0) f_{\theta r} \right\} \quad (5-30)$$

$$g_{23} = \frac{1}{\mu R^2} (x_2 - x_2^0) f_{rz} \quad (5-31)$$

$$g_{33} = \frac{1}{\mu R} f_{zz} \quad (5-32)$$

With the above expressions, the values of  $g_{ij}$  can be calculated readily by interpolation if  $f_{rr}$ ,  $f_{\theta r}$ ,  $f_{rz}$ , and  $f_{zz}$  are tabulated as functions of  $a_0$  for a constant value of  $\nu$ .

### 5.3 NUMERICAL EVALUATION OF GREEN'S FUNCTIONS FOR AN ELASTIC HALF-SPACE

In BASSINI1, the parameters  $f_{rr}$ ,  $f_{rz}$ ,  $f_{\theta r}$ , and  $f_{zz}$ , which were originally defined in Equations 5-9, 5-10, 5-11, and 5-14, are numerically evaluated. The corresponding Green's functions are then provided using Equations 5-27 through 5-32.

The numerical evaluation of these parameters involves expressing them in the form:

$$f_{rr} = \frac{a_0}{4\pi} (I_5 - I_6 + I_3 + I_4) \quad (5-33)$$

$$f_{rz} = \frac{a_0}{2\pi} I_2 \quad (5-34)$$

$$f_{\theta r} = \frac{a_0}{4\pi} (I_5 + I_6 + I_3 - I_4) \quad (5-35)$$



$$f_{zz} = -\frac{a_0}{2\pi} I_1 \quad (5-36)$$

where

$$I_1 = \int_0^\infty \frac{z \sqrt{z^2 - n^2} J_0(a_0 z) dz}{F(z)} \quad (5-37)$$

$$I_2 = \int_0^\infty \frac{z^2 \left[ (2z^2 - 1) - 2 \sqrt{z^2 - n^2} \sqrt{z^2 - 1} \right] J_1(a_0 z) dz}{F(z)} \quad (5-38)$$

$$I_3 = \int_0^\infty \frac{z J_2(a_0 z) dz}{\sqrt{z^2 - 1}} \quad (5-39)$$

$$I_4 = \int_0^\infty \frac{z}{\sqrt{z^2 - 1}} J_0(a_0 z) dz \quad (5-40)$$

$$I_5 = \int_0^\infty \frac{z \sqrt{z^2 - 1} J_2(a_0 z) dz}{F(z)} \quad (5-41)$$

$$I_6 = \int_0^\infty \frac{z \sqrt{z^2 - 1} J_0(a_0 z) dz}{F(z)} \quad (5-42)$$

and

$F(z) =$  Rayleigh determinant

$$= (2z^2 - 1)^2 - 4z^2 \sqrt{(z^2 - n^2)(z^2 - 1)}$$

Therefore, it is seen that the determination of Green's functions for an elastic half-space essentially reduces to computing the functions  $I_1, I_2 \dots I_6$ . The paragraphs that follow describe how this is carried out.



It is relatively simple to define the integrals  $I_3$  and  $I_4$ . Using any standard set of integral tables, they can be expressed as follows:

$$I_3 = \frac{1}{a_0} \left\{ \left[ \frac{2 \sin a_0}{a_0} - \cos a_0 \right] + i \left[ \sin a_0 - \frac{2(1 - \cos a_0)}{a_0} \right] \right\} \quad (5-43)$$

$$I_4 = \frac{1}{a_0} \left[ \cos a_0 - i \sin a_0 \right] \quad (5-44)$$

In this, it is noted that  $I_3$  and  $I_4$  are both imaginary because, in Equations 5-39 and 5-40, the integrand  $z/\sqrt{z^2 - 1}$  is imaginary for  $0 < z < 1$ .

Unlike  $I_3$  and  $I_4$ , which correspond to the horizontal SH-waves generated by the source, the integrands of  $I_1$ ,  $I_2$ ,  $I_5$ , and  $I_6$  all contain the Rayleigh determinant  $F(z)$ . Because of the complexity of  $F(z)$ , these integrals must be evaluated numerically. Prior to the numerical integration, however, it is convenient to first transform the integrals by a contour integration path similar to that suggested by Ewing et al. (1957). This step is necessitated by the fact that  $F(z) = 0$  at  $z = s$ . Having this singularity at  $z = s$ , the conventional numerical integration scheme would fail; however, by using contour integration, the residue of this singularity contributes the Rayleigh waves with the wave speed  $V_R = V_s/s$ , where  $V_s$  is the shear wave velocity. This results in the following integrals:

$$I_1 = -\frac{2}{\pi} \int_0^{\infty} \frac{\tau \sqrt{\tau^2 + n^2} K_0(a_0 \tau) d\tau}{(2\tau^2 + 1)^2 - 4\tau^2 \sqrt{\tau^2 + 1} \sqrt{\tau^2 + n^2}} + i \left\{ -\pi H_0^{(2)}(a_0 s) \frac{s \sqrt{s^2 - n^2}}{F'(s)} \right\}$$



$$\begin{aligned}
 & + \int_0^n \frac{k \sqrt{n^2 - k^2} H_0^{(2)}(a_0 k) dk}{(2k^2 - 1)^2 + 4k^2 \sqrt{(1 - k^2)(n^2 - k^2)}} \\
 & + 4 \int_n^1 \frac{k^3 (k^2 - n^2) \sqrt{1 - k^2} H_0^{(2)}(a_0 k) dk}{(2k^2 - 1)^4 + 16k^4 (1 - k^2)(k^2 - n^2)} \left. \right\} \quad (5-45)
 \end{aligned}$$

where  $K_0(a_0 \tau)$  is the Kelvin function and  $H_0^{(2)}(a_0 k)$  is the Hankel function of the second kind, both of which are of zeroth order. Similarly,

$$\begin{aligned}
 I_2 = i \left\{ -\pi H_1^{(2)}(a_0 s) \frac{s^2 \left[ (2s^2 - 1) - 2\sqrt{(s^2 - n^2)(s^2 - 1)} \right]}{F'(s)} \right. \\
 \left. + 2 \int_n^1 \frac{k^2 (2k^2 - 1) \sqrt{(1 - k^2)(k^2 - n^2)} H_1^{(2)}(a_0 k) dk}{(2k^2 - 1)^4 + 16k^4 (1 - k^2)(k^2 - n^2)} \right\} \quad (5-46)
 \end{aligned}$$

where  $H_1^{(2)}(a_0 s)$  is the Hankel function of the second kind and of first order.

$$\begin{aligned}
 I_5 = & -4 \int_n^1 \frac{\tau^2 \sqrt{\tau^2 - n^2} (1 - \tau^2) J_2(a_0 \tau) d\tau}{(2\tau^2 - 1)^4 + 16\tau^4 (1 - \tau^2)(\tau^2 - n^2)} + 2 \int_0^{(s-1)} E(x) dx \\
 & + \int_{2s-1}^\infty \frac{\tau \sqrt{\tau^2 - 1} J_2(a_0 \tau) d\tau}{F(\tau)} + i \left\{ \int_0^n \frac{k \sqrt{1 - k^2} J_2(a_0 k) dk}{F(k)} \right. \\
 & + \int_n^1 \frac{k \sqrt{1 - k^2} (2k^2 - 1)^2 J_2(a_0 k) dk}{(2k^2 - 1)^4 + 16k^4 (1 - k^2)(k^2 - n^2)} \\
 & \left. - \frac{\pi s \sqrt{s^2 - 1} J_2(a_0 s)}{\frac{dF(k)}{dk} \Big|_{k=s}} \right\} \quad (5-47)
 \end{aligned}$$



where  $s$  is the root of the equation:

$$F(s) = (2s^2 - 1)^2 - 4s^2 \sqrt{(s^2 - n^2)(s^2 - 1)} = 0$$

and

$$E(x) = \frac{1}{2} \left[ \frac{(s+x) \sqrt{(s+x)^2 - 1} J_2(a_0(s+x))}{F(x)} + \frac{(s-x) \sqrt{(s-x)^2 - 1} J_2(a_0(s-x))}{F(-x)} \right]$$

$$I_6 = -\frac{2}{\pi} \int_0^\infty \frac{\tau \sqrt{\tau^2 + 1} K_0(a_0 \tau) d\tau}{(2\tau^2 + 1)^2 - 4\tau^2 \sqrt{(\tau^2 + 1)(\tau^2 + n^2)}}$$

$$+ i \left\{ -\pi H_0^{(2)}(a_0 s) \frac{s \sqrt{s^2 - 1}}{F'(s)} \right.$$

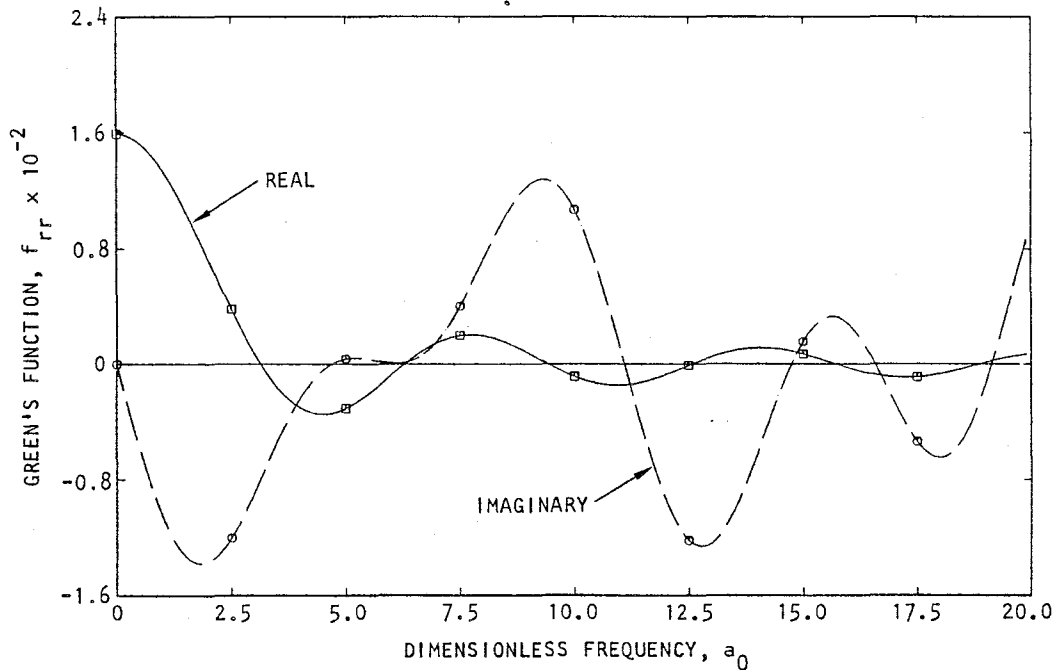
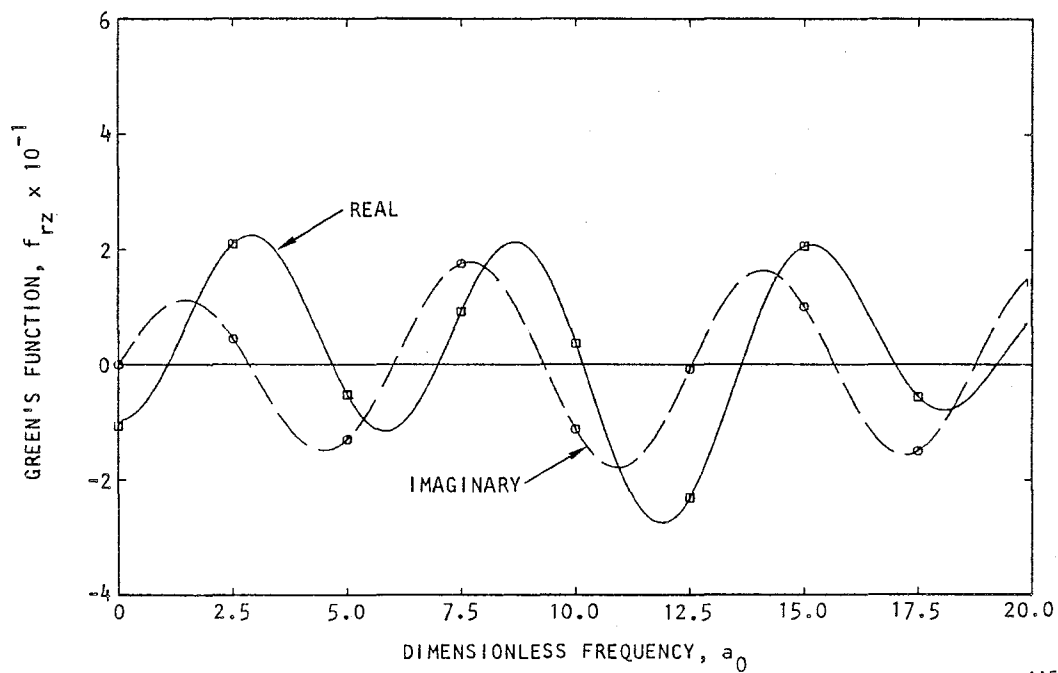
$$+ \int_0^n \frac{k \sqrt{1 - k^2} H_0^{(2)}(a_0 k) dk}{(2k^2 - 1)^2 + 4k^2 \sqrt{(1 - k^2)(n^2 - k^2)}}$$

$$\left. + \int_n^1 \frac{k \sqrt{1 - k^2} (2k^2 - 1)^2 H_0^{(2)}(a_0 k) dk}{(2k^2 - 1)^4 + 16k^4 (1 - k^2)(k^2 - n^2)} \right\}$$

(5-48)

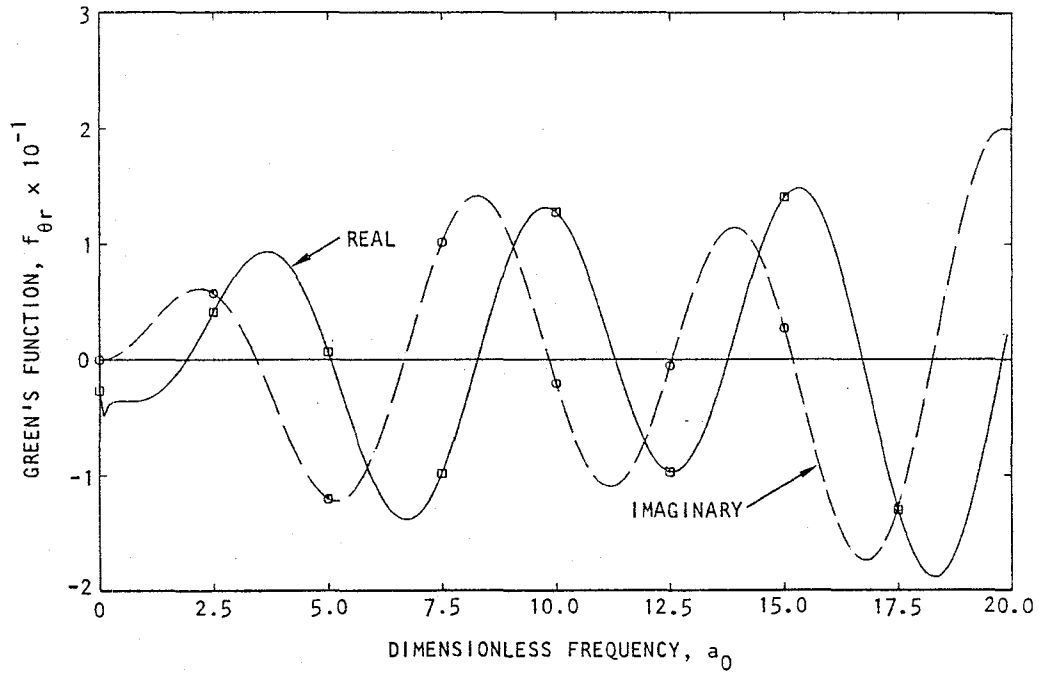
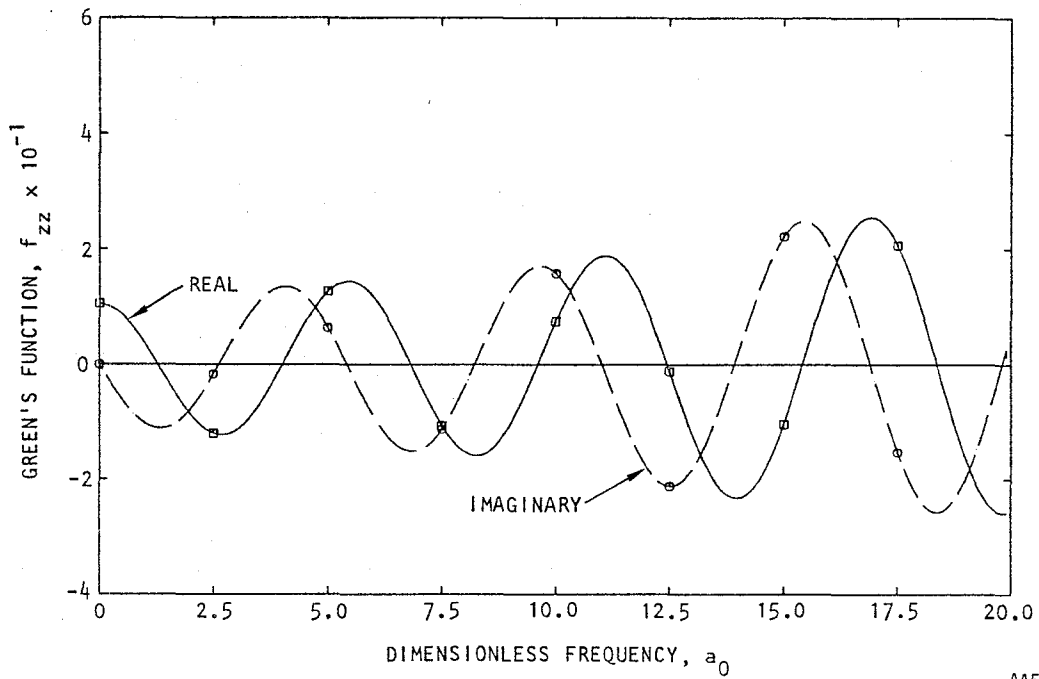
The significance of Equations 5-45 through 5-48 is that all singularities are now eliminated in the integrands for  $I_1$ ,  $I_2$ ,  $I_5$ , and  $I_6$ . Therefore, these integrals can be readily evaluated using standard numerical integration procedures. This numerical integration is carried out in BASSIN1 using Simpson's rule. Plots of the functions  $f_{rr}$ ,  $f_{rz}$ ,  $f_{\theta r}$ , and  $f_{zz}$  that result from the superposition of  $I_1 \dots I_6$  are provided in Figure 5-2.



(a)  $f_{rr}$  (Eq. 5-33)(b)  $f_{rz}$  (Eq. 5-34)

AA540

FIGURE 5-2. *BASSINI* COMPUTATIONS OF GREEN'S FUNCTIONS FOR ELASTIC HALF SPACE WITH POISSON'S RATIO = 1/3

(c)  $f_{\theta r}$  (Eq. 5-35)(d)  $f_{zz}$  (Eq. 5-36)

AA540

FIGURE 5-2. (CONCLUDED)



## CHAPTER 6

HALF-SPACE IMPEDANCE MATRIX AND  
DRIVING FORCE VECTORS

This chapter describes how the Green's functions for an elastic half-space (Chapt. 5) and the free-field ground surface motions induced by traveling seismic waves (Chapt. 4) are used in BASSIN1 to characterize the half-space and the seismic excitations in terms of a frequency-dependent impedance matrix and driving force vector. The approach described herein is valid for any number of arbitrarily shaped, deformable interfaces between the structure and the half-space. It is an extension of our earlier work in this area, which was carried out for rigid foundation conditions (Werner et al., 1977).

6.1 IMPEDANCE MATRIX

## 6.1.1 BASIC CONCEPTS AND ASSUMPTIONS

As noted in Chapter 5, the displacements at any point along the surface of a half-space,  $\{u(\underline{x}_i)\}$ , as induced by a harmonic force located at any other point,  $\{P(\underline{x}_j)\}e^{i\Omega t}$ , can be expressed as

$$\{u(\underline{x}_i)\} = [G(\Omega, \underline{x}_i - \underline{x}_j)]\{P(\underline{x}_j)\}e^{i\Omega t} \quad (6-1)$$

where

$\underline{x}_i, \underline{x}_j$  = Vectors of coordinates of computed displacement and applied force respectively

$\Omega$  = Excitation frequency

$[G(\Omega, \underline{x}_i - \underline{x}_j)]$  = 3 x 3 matrix of Green's functions, as formulated in Chapter 5



and  $\{u(\underline{x}_i)\}$  and  $\{P(\underline{x}_j)\}$  are each of order  $3 \times 1$ . By superimposing many such point loads within an area  $A$ , the displacement at  $\underline{x}$  can be expressed as

$$\{u(\underline{x}_i)\} = \iint_A [G(\Omega, \underline{x}_i - \underline{x}_j)] \{\sigma(\underline{x}_j)\} dS_j \quad (6-2)$$

where  $\{\sigma(\underline{x}_j)\}$  is a  $3 \times 1$  vector that denotes the contact stress state at  $\underline{x}_j$ .

To define the impedance matrix for an elastic half-space, it is necessary to numerically integrate the above integral equation. Following our prior approach for arbitrarily-shaped rigid interface conditions (Werner et al., 1977), BASSINI incorporates the following assumptions in order to simplify this numerical integration process (Fig. 6-1):

- The arbitrarily shaped interface can be partitioned into many small and regular (e.g., rectangular) subregions.
- The contact stress within each subregion is constant.

On this basis, the right side of Equation 6-2 becomes

$$\iint_A [G(\Omega, \underline{x}_i - \underline{x}_j)] \{\sigma(\underline{x}_j)\} dS_j = \sum_{j=1}^S [\phi(\underline{x}_i, \underline{x}_j)] \{\sigma_j\} \quad (6-3)$$

where the above summation is over the  $S$  subregions that comprise the structure/half-space interface and

$$[\phi(\underline{x}_i, \underline{x}_j)] = \left[ \iint_{A_j} G(\Omega, \underline{x}_i - \underline{x}_j) dS_j \right] \quad (6-4)$$

$\{\sigma_j\}$  =  $3 \times 1$  vector of constant stresses in the  $j$ th subregion

$A_j, \underline{x}_j$  = Area and coordinate of centroid, respectively, of the  $j$ th subregion

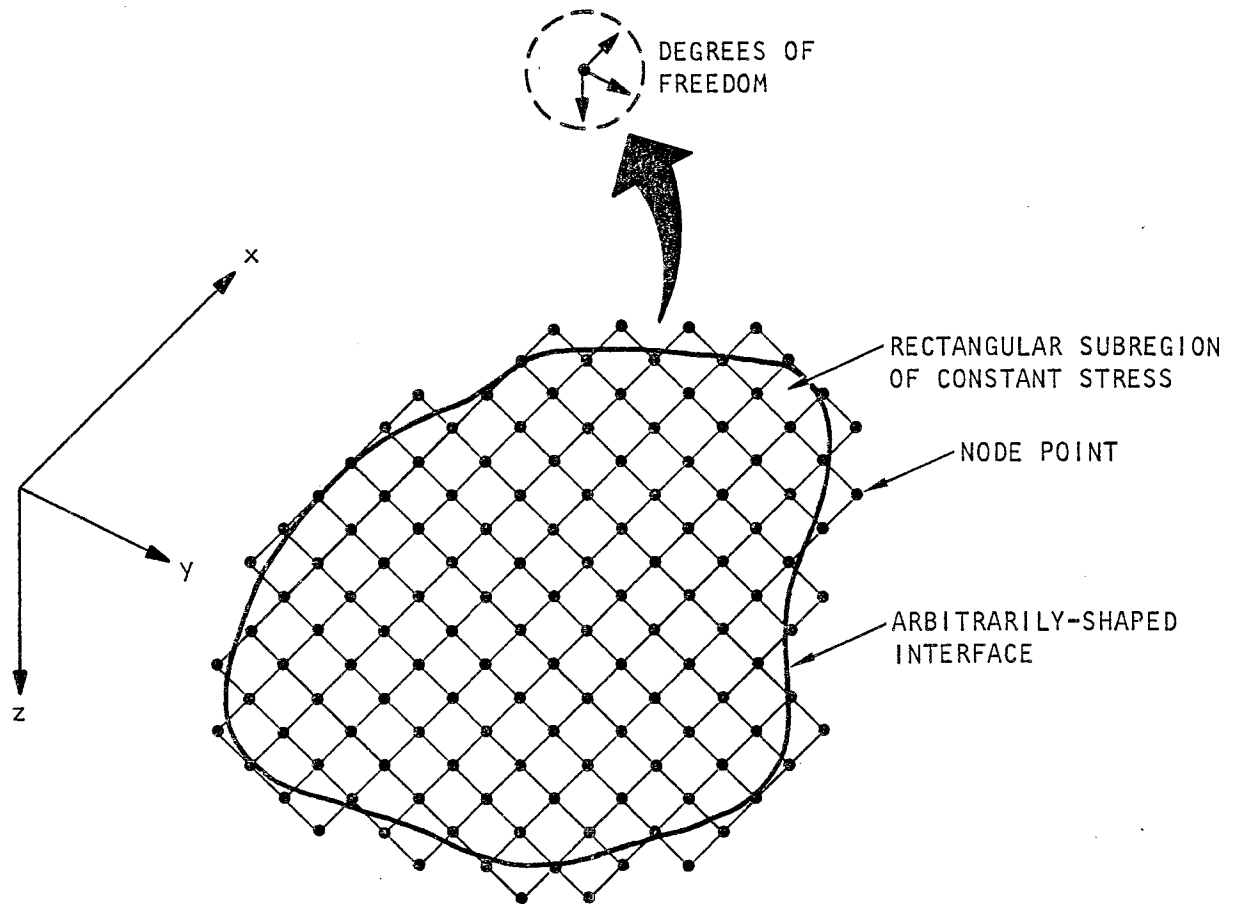


FIGURE 6-1. *BASSINI* REPRESENTATION OF STRUCTURE/HALF-SPACE INTERFACE



Substitution of Equations 6-3 and 6-4 into Equation 6-2 results in the following interrelationship between the displacements at any point along the surface of the half-space interface and the contact stress state within the interface

$$\{u(\underline{x})\} = \sum_{j=1}^S [\phi(\underline{x}_i, \underline{x}_j)] \{\sigma_j\} \quad (6-5)$$

Equation 6-5 is a basic building block for constructing the system impedance matrix. In its above general form, this expression is valid for either rigid or deformable structure/half-space interfaces.

#### 6.1.2 NUMERICAL PROCEDURE

##### 6.1.2.1 General Description

With the preceding subsection as background, we can now consider a deformable interface between the overlying structure and the half-space that is of arbitrary shape and is comprised of rectangular subregions (Fig. 6-1). In the treatment that follows, this interface need not be restricted to a single structure/half-space contact area; instead, the interface can be comprised of several separate contact areas that would exist for structures of extended length supported by multiple footings.

The major effort in this phase of BASSIN1 is directed toward computing the compliance matrix for the half-space interface region; this matrix is then inverted to obtain the impedance matrix. The computation of the compliance matrix is illustrated in Figure 6-2, which shows that the  $j$ th column of this matrix contains the displacements at each degree of freedom of the interface, as induced by a unit harmonic force applied to the  $j$ th degree of freedom. Basic features of the BASSIN1 computation of the compliance matrix are as follows:

- To facilitate coupling of the half-space and the overlying structure in the subsequent dynamic

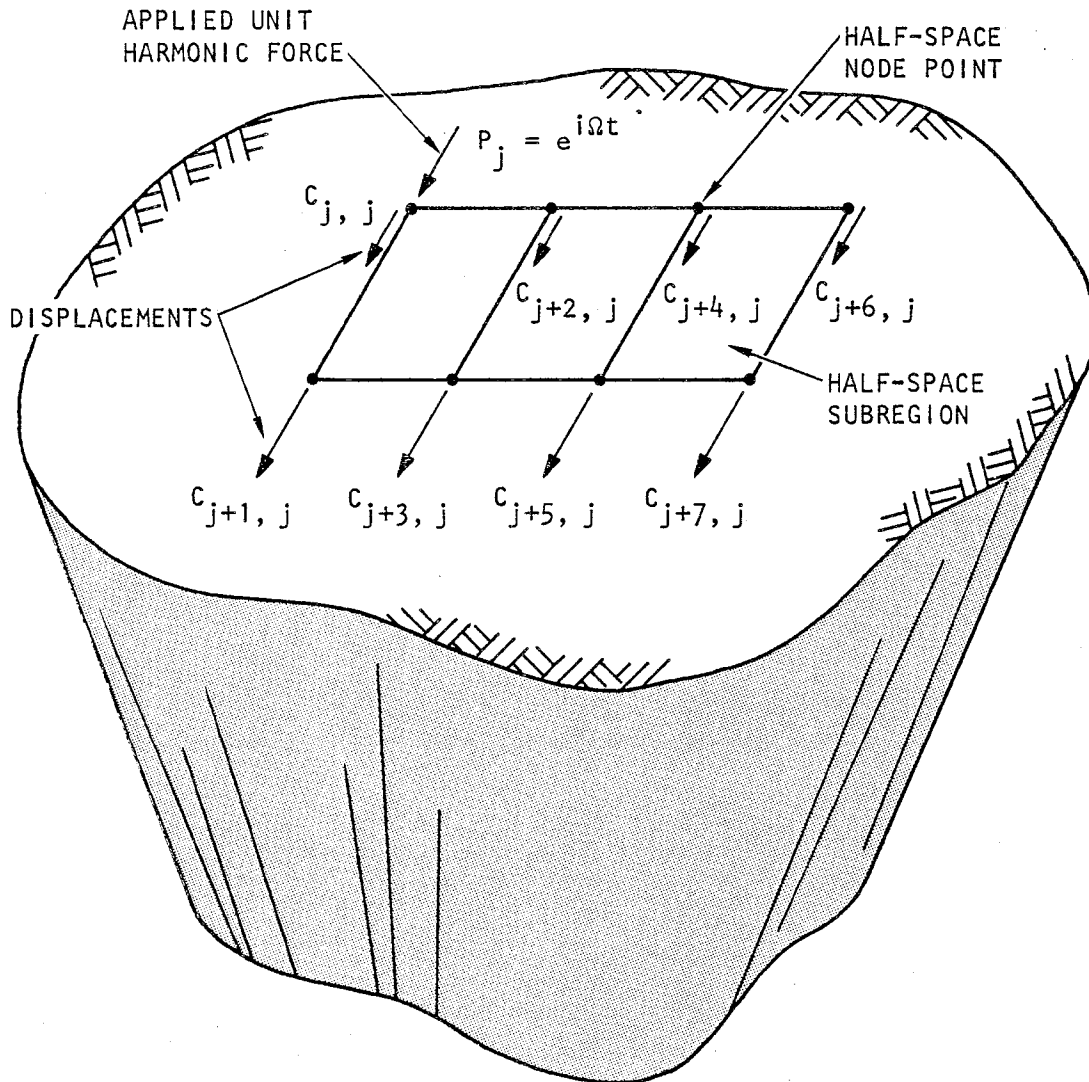


FIGURE 6-2. DEVELOPMENT OF JTH COLUMN OF HALF-SPACE COMPLIANCE MATRIX (Only longitudinal displacements shown)



analysis, the half-space compliance matrix is developed for degrees of freedom located at the corner node points of the subregions. As noted in Chapter 3, these subregion corner modes correspond on a one-to-one basis to the interface nodes from the finite element model of the overlying structure.

- In the computation of the compliance matrix, the unit force applied to the degree of freedom at each node point is replaced by a system of statically equivalent forces applied at the centroids of the immediately adjacent subregions. This system of equivalent forces is the basis for computing the node point displacements that comprise each column of the compliance matrix. The purpose of this approach is to avoid the numerical difficulties that would otherwise result when evaluating Green's functions for defining displacements at the point of application of the unit force (i.e., for  $x_i - x_j = 0$  in Eq. 6-4).
- Several methods of varying degrees of refinement are available for determining this system of statically equivalent subregion-centroid forces. In BASSIN1, a simple approach is used in which a constant stress state is assumed only for the subregions immediately adjacent to the node point location of the applied unit force; elsewhere, the subregion stresses are considered to vanish. This approach is described further in Subsection 6.1.2.2.

#### 6.1.2.2 FORMULATION

With this as background, the formulation of the expression for the  $j$ th column of the half-space compliance matrix is





initiated by applying the following harmonic force vector of excitation frequency  $\Omega$ :

$$\{P\} = \begin{pmatrix} 0 \\ 0 \\ \vdots \\ 1 \\ \vdots \\ 0 \end{pmatrix} e^{i\Omega t} \quad (6-6)$$

In Equation 6-7,  $\{P\}$  is a vector of order  $3N \times 1$ , where  $N$  is the total number of half-space nodes (with 3 degrees of freedom per node). Only the  $j$ th element of  $\{P\}$  is nonzero; this element has a value of unity.

The next step in the formulation process is to transform the node point force vector  $\{P\}$  to a set of statically equivalent forces acting at the centroids of the immediately adjacent subregions. As noted previously, this transformation is based on the assumption that the node point force induces a constant state of stress in these immediately adjacent subregions, and a vanishing state of stress elsewhere. Therefore, the nature of this transformation depends on whether the location of the unit force in  $\{P\}$  is at an interior node, an edge node, or a corner node of the half-space interface (Fig. 6-3). The transformation is expressed mathematically as

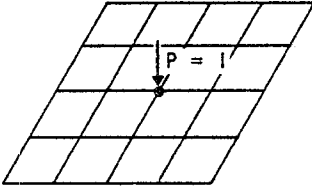
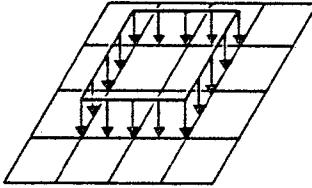
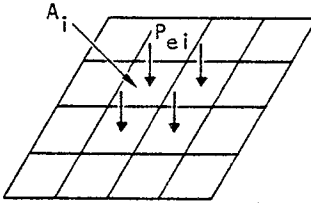
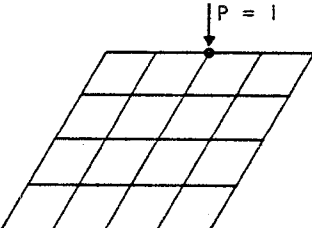
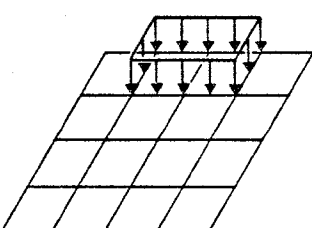
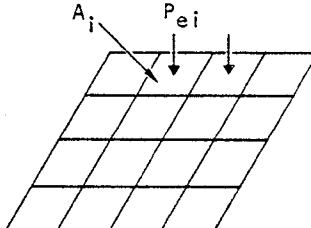
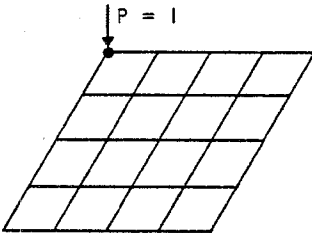
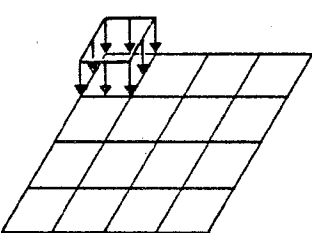
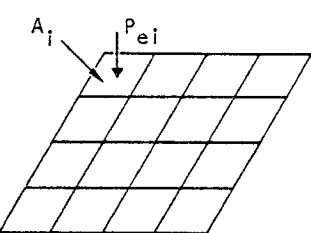
$$\{P_s\} = [T]\{P\} \quad (6-7)$$

where

$\{P_s\}$  =  $3S \times 1$  vector of forces located at the centroid of each of  $S$  subregions that comprise the half-space interface

$[T]$  = Transformation matrix, which is of order  $3S \times 3N$



LOCATION OF UNIT FORCE	NODAL FORCE	ASSUMED SUBREGION STRESS STATE	EQUIVALENT SUBREGION FORCES
AT INTERIOR NODE		 $(\sigma = P/\Sigma A)$	 $(P_{ei} = \sigma A_i)$
AT EDGE NODE		 $(\sigma = P/\Sigma A)$	 $(P_{ei} = \sigma A_i)$
AT CORNER NODE		 $(\sigma = P/\Sigma A)$	 $(P_{ei} = \sigma A_i)$

AA547

FIGURE 6-3. TRANSFORMATION OF NODAL FORCE TO EQUIVALENT SUB-REGION FORCE FOR COMPUTATION OF COMPLIANCE MATRIX



Equation 6-7 can also be expressed in terms of contact stress vectors for each subregion, as follows

$$\{\sigma_s\} = [A]_D^{-1}\{P_s\} = [A]_D^{-1}[T]\{P\} \quad (6-8)$$

where  $\{\sigma_s\}$  is a  $3S \times 1$  vector of contact stresses, and  $[A]_D$  is a diagonal matrix of order  $3S \times 3S$  containing the areas of each subregion, i.e.,

$$[A]_D = \begin{bmatrix} \underline{A}_1 & \underline{0} & \cdot & \cdot & \cdot & \underline{0} & \cdot & \cdot & \cdot & \underline{0} \\ \underline{0} & \underline{A}_2 & \cdot & \cdot & \cdot & \underline{0} & \cdot & \cdot & \cdot & \underline{0} \\ \cdot & \cdot & \cdot & \cdot & \cdot & \cdot & \cdot & \cdot & \cdot & \cdot \\ \cdot & \cdot & \cdot & \cdot & \cdot & \cdot & \cdot & \cdot & \cdot & \cdot \\ \cdot & \cdot & \cdot & \cdot & \cdot & \underline{A}_k & \cdot & \cdot & \cdot & \cdot \\ \cdot & \cdot & \cdot & \cdot & \cdot & \cdot & \cdot & \cdot & \cdot & \cdot \\ \cdot & \cdot & \cdot & \cdot & \cdot & \cdot & \cdot & \cdot & \cdot & \cdot \\ \cdot & \cdot & \cdot & \cdot & \cdot & \cdot & \cdot & \cdot & \cdot & \cdot \\ 0 & 0 & \cdot & \cdot & \cdot & 0 & \cdot & \cdot & \cdot & \underline{A}_S \end{bmatrix} \quad (6-9)$$

In Equation 6-9,  $\underline{A}_k$  is a diagonal matrix of order  $3 \times 3$  whose diagonal elements contain the area of the  $k$ th subregion, and  $\underline{0}$  is a null matrix of order  $3 \times 3$ .

Knowing the state of stress induced in the half-space by the load vector  $\{P\}$ , the resulting node point displacements induced by this stress field,  $\{u\}$ , can be expressed as the following expanded form of Equation 6-5:

$$\{u\} = [\Phi]\{\sigma_s\} \quad (6-10)$$



where  $\{u\}$  is of order  $3N \times 1$ , and

$$[\Phi] = \begin{bmatrix} \phi(x'_1, x_1) & \phi(x'_1, x_2) & \dots & \phi(x'_1, x_S) \\ \phi(x'_2, x_1) & \phi(x'_2, x_2) & \dots & \phi(x'_2, x_S) \\ \vdots & \vdots & \ddots & \vdots \\ \phi(x'_N, x_1) & \phi(x'_N, x_2) & \dots & \phi(x'_N, x_S) \end{bmatrix} \quad (6-11)$$

In Equation 6-11,  $\phi(x'_i, x_j)$  is a  $3 \times 3$  Green's function matrix which interrelates the  $3 \times 1$  displacement field at node  $i$  with the  $3 \times 1$  stress field at subregion  $j$ ; i.e., from Equation 6-4

$$\phi(x'_i, x_j) = \left[ \iint_{A_j} G(\Omega, x'_i - x_j) dS_j \right] \quad (6-12)$$

Substituting Equation 6-8 into Equation 6-10, the expression for the node point displacement field throughout the half-space interface, as induced by the node point force vector  $\{P\}$ , becomes

$$\{u\} = [\Phi][A]_D^{-1}[T]\{P\} \quad (6-13)$$

In view of the definition of  $\{P\}$  given in Equation 6-6,  $\{u\}$  represents the  $j$ th column of the compliance matrix. By applying the unit force in  $\{P\}$  at all node point degrees of freedom and repeating the above process, Equation 6-13 can be generalized to provide the following expression for the half-space compliance matrix  $[C_{HS}]$

$$[C_{HS}] = [\Phi][A]_D^{-1}[T] \quad (6-14)$$



The half-space impedance matrix,  $[K_{HS}]$ , is then obtained by inverting  $[C_{HS}]$ , i.e.,

$$[K_{HS}] = [C_{HS}]^{-1} \quad (6-15)$$

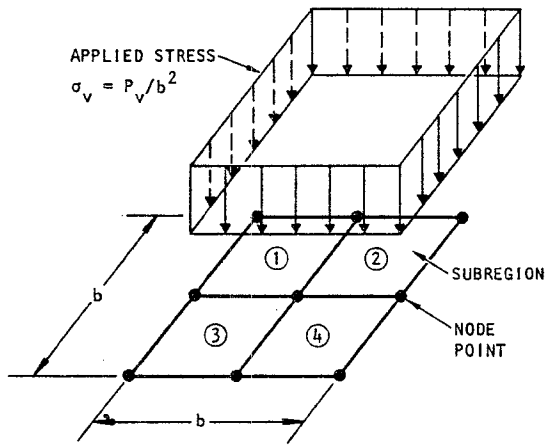
### 6.1.3 CORRELATION WITH RESULTS BY OTHERS

To provide verification of the BASSIN1 approach for computing the half-space compliance and impedance matrices, results from BASSIN1 have been compared with results from the prior analytical solutions of Thomson and Kobori (1963) and of Veletsos and Wei (1971). Both of these solutions treat the case of a rigid foundation on an elastic half-space; the Thomson-Kobori solutions address vertical compliance of a rectangular footing whereas the Veletsos-Wei solutions develop horizontal and rocking compliances for a circular footing.

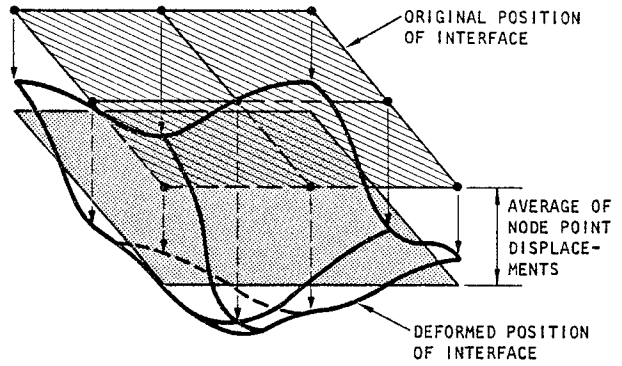
#### 6.1.3.1 Comparisons with Thomson-Kobori

The BASSIN1 comparisons with Thomson-Kobori were carried out for a rigid square footing resting on an elastic half-space with a Poisson's ratio of 1/4. The footing/half-space interface for this case was represented in BASSIN1 as a network of four square subregions that, to be consistent with the Thomson-Kobori assumptions, were subjected to a uniform vertical stress field (Fig. 6-4a). The resulting displacements computed by BASSIN1 at each subregion node point were arithmetically averaged for purposes of comparison with the Thomson-Kobori rigid foundation results (Fig. 6-4b).

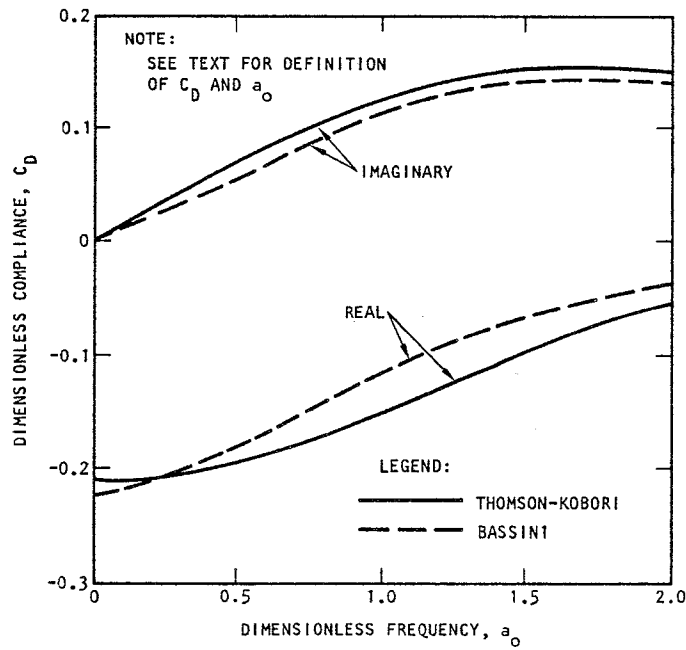
The results of these comparisons are provided in Figure 6-4c as plots of real and imaginary components of the dimensionless compliance,  $C_D$ , vs. dimensionless frequency,  $a_0$ , where



(a) Interface discretization and applied stresses



(b) BASSINI averaging of node point displacements



(c) Comparison of results (for Poisson's ratio = 1/4)

AA548

FIGURE 6-4. COMPARISON OF BASSINI AND THOMSON-KOBORI (1963) RESULTS



$$C_D = \frac{w\mu}{\sigma_v b} \quad a_o = \frac{\Omega b}{V_s}$$

and

$w$  = Vertical displacement

$\mu, V_s$  = Shear modulus and shear wave velocity respectively of elastic half-space

$\sigma_v$  = Applied vertical stress

$\Omega$  = Excitation frequency

$b$  = Length of a side of square footing

This figure shows that the average compliance obtained from BASSIN1 for this case compares quite well with the Thomson-Kobori compliance, over the entire range of dimensionless frequencies considered in these comparisons. The real component of the BASSIN1 compliance is seen to be within 25% of the real component from Thomson-Kobori, and the imaginary components from the two sets of results compare even more closely. The differences that do exist in these comparisons are primarily related to the approximations introduced by the arithmetic averaging of the BASSIN1 compliances in this example.

#### 6.1.3.2 Comparisons with Veletsos-Wei

In their analytical treatment of the dynamic response of a rigid circular footing on an elastic half-space, Veletsos and Wei treated the particular case of the coupled horizontal and rocking response of the footing when subjected to a harmonic horizontal force and moment. Their results were presented as frequency-dependent dynamic amplification factors, denoted below as  $f_{ij}$  ( $i, j=1, 2$ ), that related the dynamic values of the footing's horizontal displacement,  $u$ , and rotation,  $\alpha$ , to their uncoupled static values,  $u_{st}$  and  $\alpha_{st}$ , through the expression

$$\begin{Bmatrix} u \\ \alpha r_o \end{Bmatrix} = \begin{bmatrix} (f_{11} + ig_{11}) & (f_{12} + ig_{12}) \\ (f_{21} + ig_{21}) & (f_{22} + ig_{22}) \end{bmatrix} \begin{Bmatrix} u_{st} \\ \alpha_{st} r_o \end{Bmatrix} \quad (6-16)$$



where

$$u_{st} = \frac{2 - \nu}{8\mu r_o} P_{st}$$

$$\alpha_{st} = \frac{3(1 - \nu)}{8\mu r_o^3} M_{st}$$

and

$P_{st}$ ,  $M_{st}$  = Static horizontal force and moment, respectively

$\mu$ ,  $\nu$  = Shear modulus and Poisson's ratio respectively of the elastic half-space

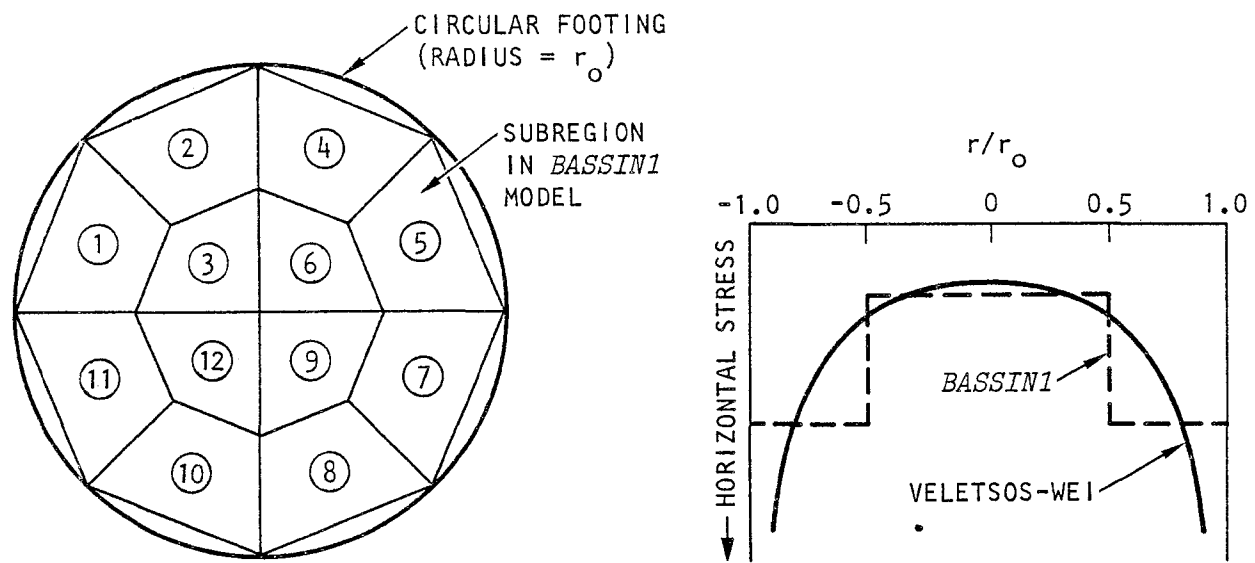
$r_o$  = Radius of circular footing

The particular quantities from Equation 6-16 that were compared between BASSIN1 and Veletsos-Wei were the dynamic amplification functions,  $f_{11}$  and  $g_{11}$ , that define the horizontal displacement due to an applied horizontal dynamic force. To carry out these comparisons, a special version of BASSIN1 was developed that incorporates nonrectangular quadrilateral subregions and excitations in the form of applied uniform stresses that could vary from one subregion to the next. On this basis, a 12-subregion model of the footing/half-space interface was developed (Fig. 6-5a), and this interface was subjected to a system of applied subregion stresses that approximated the theoretical contact stress distribution developed by Veletsos and Wei (Fig. 6-5b). The calculations were then carried out for an elastic half-space with a Poisson's ratio of 1/3.

The resulting comparisons between the BASSIN1 and Veletsos-Wei results are provided in Figure 6-5c as plots of  $f_{11}$  and  $g_{11}$  vs. a dimensionless frequency,  $a_o$ , defined as

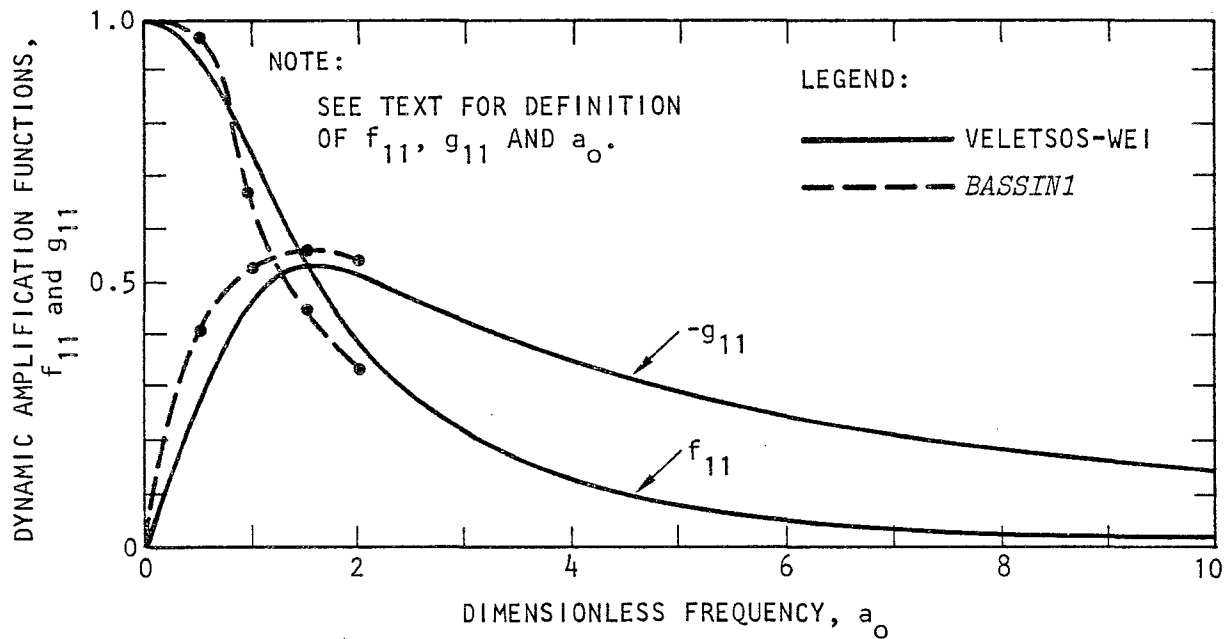
$$a_o = \frac{\Omega r_o}{V_s}$$





(a) Discretization of interface region

(b) Simulation of horizontal stress distribution



(c) Comparison of results (for Poisson's ratio = 1/3)

FIGURE 6-5. COMPARISON OF BASSINI AND VELETOSOS-WEI (1971) RESULTS



where  $\Omega$  is the excitation frequency,  $r_0$  is the radius of the footing, and  $V_s$  is the shear wave velocity of the elastic half-space. This figure shows that the two sets of results compare quite well over the range of dimensionless frequencies considered in these comparisons. Those differences that do exist in these comparisons can be attributed primarily to the coarse representation of the Veletsos-Wei stress distribution in the BASSIN1 model.

## 6.2 DRIVING FORCES

To compute the driving forces applied by the seismic waves at each degree of freedom at the various half-space node points, we first consider the various elements that contribute to the total displacement at each of these degrees of freedom. Following the approach of Luco et al., (1975), this can be expressed as

$$\{u_T\}e^{i\Omega t} = \{u_{ff}\}e^{i\Omega t} + \{u_0\}e^{i\Omega t} \quad (6-17)$$

where, for an excitation frequency  $\Omega$ ,  $\{u_T\}$  corresponds to the total displacement amplitude at each half-space degree of freedom,  $\{u_{ff}\}$  represents the displacement amplitudes at these degrees of freedom due to the seismic waves and in the absence of external forces (see Chapt. 3), and  $\{u_0\}$  depicts the displacement amplitudes at these degrees of freedom due to applied interaction forces in the absence of seismic wave excitations. Each of these vectors are of order  $(3N \times 1)$ , where  $N$  is the total number of half-space nodes.

Now, from Section 6-1, it is seen that

$$\{u_0\} = - [C_{HS}]\{P_0\} \quad (6-18)$$

where  $[C_{HS}]$  is the compliance matrix for the half-space and  $\{P_0\}$  is the vector of applied interaction forces. The substitution



of Equation 6-17 into Equation 6-16 results in the following expression (neglecting the  $e^{i\Omega t}$  terms)

$$\{u_T\} = \{u_{ff}\} - [C_{HS}]\{P_O\} \quad (6-19)$$

Equation 6-19 can be used directly to obtain the expression for the driving forces. To do this, we note that these driving forces are defined as the force applied by the seismic waves at each half space degree of freedom, when these degrees of freedom are fixed against motion under the action of these seismic waves (see Sec. 3.2.2). Therefore, we see that if

$$\{u_T\} = \{0\}$$

then

$$\{P_O\} = \{P_{DO}\} = \text{vector of driving forces}$$

and Equation 6-19 becomes

$$\{0\} = \{u_{ff}\} - [C_{HS}]\{P_{DO}\} \quad (6-20)$$

From this, the driving forces can be computed as

$$\{P_{DO}\} = [C_{HS}]^{-1}\{u_{ff}\} = [K_{HS}]\{u_{ff}\} \quad (6-21)$$

where  $[K_{HS}]$  is the impedance matrix for the half-space (see Sec. 6.1). Equation 6-21 is implemented in BASSIN2 to compute the driving force vector for use in the dynamic analysis of the soil/structure system (Chapt. 7).





## CHAPTER 7

## DYNAMIC RESPONSE ANALYSIS FORMULATION

This chapter describes the formulation of the procedure used in BASSIN to analyze the dynamic response of the bridge/abutment/backfill system. This formulation is provided in the first two of the three sections that comprise this chapter. In this, the first section contains the derivation of the general analysis procedure and the second section shows how this derivation is specialized to include modal truncation. An example application of the modal truncation procedure is contained in the final section of the chapter.

7.1 GENERAL ANALYSIS PROCEDURE

## 7.1.1 OVERALL SYSTEM OF EQUATIONS OF MOTION

The equations of motion of the structure (bridge/abutment/backfill) system can be expressed in partitioned matrix form as

$$\begin{bmatrix} \underline{\underline{M}}_{11} & \underline{\underline{0}} \\ \underline{\underline{0}} & \underline{\underline{M}}_{22} \end{bmatrix} \begin{Bmatrix} \ddot{\underline{\tilde{y}}}_1 \\ \ddot{\underline{\tilde{y}}}_2 \end{Bmatrix} + \begin{bmatrix} \underline{\underline{C}}_{11} & \underline{\underline{0}} \\ \underline{\underline{0}} & \underline{\underline{0}} \end{bmatrix} \begin{Bmatrix} \dot{\underline{\tilde{y}}}_1 \\ \dot{\underline{\tilde{y}}}_2 \end{Bmatrix} + \begin{bmatrix} \underline{\underline{K}}_{11} & \underline{\underline{K}}_{12} \\ \underline{\underline{K}}_{12}^T & \underline{\underline{K}}_{22} \end{bmatrix} \begin{Bmatrix} \underline{\tilde{y}}_1 \\ \underline{\tilde{y}}_2 \end{Bmatrix} = \begin{Bmatrix} \underline{\underline{0}} \\ \underline{\underline{P}}_2 \end{Bmatrix} \quad (7-1)$$

where the subscript "1" denotes all aboveground degrees of freedom (DOF's) of the structure and the subscript "2" denotes the structure DOF's along its interface with the half-space. Also in Equation 7-1, a term underlain by a double-dash denotes a matrix, whereas a term underlain by a tilde (~) denotes a vector. Finally, the quantities M, C, and K are the mass, damping, and stiffness matrices, respectively, and  $\underline{\underline{P}}_2$  is the vector of forces applied along the structure/half-space interface.



### 7.1.2 INTERRELATIONSHIP BETWEEN RESPONSES AT INTERFACE AND ABOVEGROUND DOF'S

The first phase of this formulation is directed toward deriving an interrelationship between  $\{y_1\}$  and  $\{y_2\}$ . The first step in this derivation is to express the aboveground response DOF's,  $\{y_1\}$ , as the superposition of a pseudostatic component  $\{y_{1s}\}$  and a dynamic component  $\{y_{1d}\}$ , i.e.,

$$\{y_1\} = \{y_{1s}\} + \{y_{1d}\} \quad (7-2)$$

where, from Clough and Penzien (1975),

$$\{y_{1s}\} = [R_s]\{y_2\} \quad (7-3)$$

in which

$$[R_s] = - [K_{11}]^{-1}[K_{12}] \quad (7-4)$$

Substituting Equations 7-2 through 7-4 into the upper set of partitioned equations in Equation 7-1, and neglecting the contributions of damping to the forcing function (Clough and Penzien, 1975), we obtain

$$[M_{11}]\{\ddot{y}_{1d}\} + [C_{11}]\{\dot{y}_{1d}\} + [K_{11}]\{y_{1d}\} = - [M_{11}][R_s]\{\ddot{y}_2\} \quad (7-5)$$

Next,  $\{y_{1d}\}$  is expanded into normal modes, i.e.,

$$\{y_{1d}\} = [\phi]\{\eta\} \quad (7-6)$$

where  $[\phi]$  is the matrix of eigenvectors, and  $\{\eta\}$  is the vector of modal response amplitudes. Substituting Equation 7-6 into



Equation 7-5 and making use of the following orthogonality relationships,

$$[\phi]^T [M_{11}] [\phi] = [I]_D$$

$$[\phi]^T [C_{11}] [\phi] = [2\omega_n \xi_n]_D \quad (7-7)$$

$$[\phi]^T [K_{11}] [\phi] = [\omega_n^2]_D$$

Equation 7-5 takes the form

$$[I]_D \ddot{\{\eta\}} + [2\omega_n \xi_n]_D \dot{\{\eta\}} + [\omega_n^2]_D \{\eta\} = - [\phi]^T [M_{11}] [R_s] \{\ddot{Y}_2\} \quad (7-8)$$

In Equations 7-7 and 7-8,  $\omega_n$  and  $\xi_n$  are the natural frequency and damping ratio, respectively, of the  $n$ th mode,  $[ ]_D$  denotes a diagonal matrix, and  $[I]_D$  corresponds to the unit diagonal matrix.

The next step in the derivation is to consider Equation 7-8 in the context of harmonic motion, i.e.,

$$\{Y_2\} = \{Y_{20}\} e^{i\Omega t} \quad (7-9)$$

$$\{\eta\} = \{\eta_0\} e^{i\Omega t}$$

where  $\Omega$  is the excitation frequency. Substituting Equation 7-9 into Equation 7-8 and rearranging terms, we obtain

$$\{\eta_0\} = \Omega^2 [S]_D^{-1} [\phi]^T [M_{11}] [R_s] \{Y_{20}\} \quad (7-10)$$



in which

$$[S]_D = - [\Omega^2]_D + i[2\Omega\omega_n\xi_n]_D + [\omega_n^2]_D \quad (7-11)$$

Furthermore, if we define

$$[\Gamma] = [\phi]^T [M_{11}] [R_s] \quad (7-12)$$

$$[R_d] = \Omega^2 [\phi] [S]_D^{-1} [\Gamma] \quad (7-13)$$

and make use of Equation 7-6, then

$$\{y_{1d}\} = [R_d] \{y_{20}\} e^{i\Omega t} \quad (7-14)$$

From this, substituting Equations 7-14 and 7-3 into Equation 7-2, we see that the response of the aboveground portion of the structure,  $\{y_1\}$ , is expressed in terms of its response along the half-space interface,  $\{y_2\}$ , through a transformation matrix,  $[T]$ , i.e.,

$$\{y_1\} = [T] \{y_2\} = [T] \{y_{20}\} e^{i\Omega t} \quad (7-15)$$

where

$$[T] = [R_s] + [R_d] \quad (7-16)$$

and  $[R_s]$  and  $[R_d]$  are defined in Equations 7-4 and 7-13 respectively.

### 7.1.3 DETERMINATION OF STRUCTURE RESPONSE AT INTERFACE DOF'S

The next phase of the derivation is to solve for the structure response at its interface with the half-space. To do





this, we consider the lower set of partitioned equations in Equation 7-1

$$[M_{22}]\{\ddot{y}_2\} + [K_{12}]^T\{y_1\} + [K_{22}]\{y_2\} = \{P_2\} \quad (7-17)$$

Substituting Equation 7-15 and considering harmonic motion, the above system of equations becomes

$$[K_{ST}]\{y_{20}\} = \{P_{20}\} \quad (7-18)$$

where

$$[K_{ST}] = -\Omega^2[M_{22}] + [K_{12}]^T[T] + [K_{22}] \quad (7-19)$$

and

$$\{P_2\} = \{P_{20}\}e^{i\Omega t} \quad (7-20)$$

In this,  $[K_{ST}]$  can be regarded as an effective impedance matrix for the structure.

Next,  $\{P_2\}$ , the vector of forces applied along the structure/half-space interface, can be expressed as the superposition of half-space driving forces and resisting forces, i.e.,

$$\{P_2\} = \{P_{20}\}e^{i\Omega t} = [\{P_{DO}\} + \{P_{RO}\}]e^{i\Omega t} \quad (7-21)$$

where

$P_{DO}$  = Vector of driving force amplitudes, as derived in Section 6.2 of Chapter 6

$P_{RO}$  = Vector of resisting force amplitudes =  $-[K_{HS}][y_{20}]$



and

$[K_{HS}]$  = Half-space impedance matrix, as derived in Section 6.1 of Chapter 6

The substitution of Equation 7-21 into Equation 7-18 assures that compatibility of displacements and dynamic equilibrium is maintained along the interface of the half-space and the structure. This results in the following expression:

$$[K_{ST} + K_{HS}]\{y_{20}\} = \{P_{DO}\} \quad (7-22)$$

from which  $\{y_{20}\}$  is obtained as

$$\{y_{20}\} = [K_{ST} + K_{HS}]^{-1}\{P_{DO}\} \quad (7-23)$$

where  $[K_{ST} + K_{HS}]$  is the combined structure/half-space impedance matrix.

#### 7.1.4 DETERMINATION OF STRUCTURE RESPONSE AT ABOVEGROUND DOF'S

Now that  $\{y_{20}\}$  is determined, the previously derived inter-relationship between  $\{y_1\}$  and  $\{y_2\}$  can serve to obtain  $\{y_1\}$ . Substituting Equation 7-23 into Equation 7-15, we see that

$$\{y_1\} = [T][K_{ST} + K_{HS}]^{-1}\{P_{DO}\}e^{i\Omega t} \quad (7-24)$$

or, substituting for  $[T]$

$$\{y_1\} = [R_s + R_d][K_{ST} + K_{HS}]^{-1}\{P_{DO}\}e^{i\Omega t} \quad (7-25)$$

where, once again,  $[R_s]$  and  $[R_d]$  are defined in Equations 7-4 and 7-13 respectively.



## 7.2 ANALYSIS PROCEDURE INCLUDING MODAL TRUNCATION

### 7.2.1 GENERAL DISCUSSION

The derivation of the dynamic analysis procedure including modal truncation closely follows that of the general analysis procedure provided in Section 7.1. The only differences are that

- The overall system of modal equations of motion are partitioned into separate equations for the "kept modes" (i.e., lower modes that will be retained in the analysis) and the "residual modes" (i.e., higher modes whose contributions will be approximated in this procedure).
- These residual mode effects are represented in this procedure as functions of the kept mode parameters. This is accomplished through the use of modal identities, together with certain simplifications that can be made in the equations of motion for modes with natural frequencies substantially greater than the excitation frequency.

It is noted that modal truncation approaches analogous to that presented in this section have been used in the analysis of piping systems on discrete supports subjected to multiple support excitations (e.g., Powell, 1979; AA, 1979). Herein this approach is extended to soil/structure systems subjected to traveling seismic waves, in which the soil/structure interface can be of extended length.

### 7.2.2 INTERRELATIONSHIP BETWEEN STRUCTURE RESPONSE AT INTERFACE AND ABOVEGROUND DOF'S

This subsection is directed toward developing an inter-relationship between  $\{y_1\}$  and  $\{y_2\}$  in a manner analogous to Equation 7-15 for the general case, except that now modal truncation effects are included. This development effort is based on the use of partitioned modal equations of motion and



certain modal identities, as described in the paragraphs that follow.

### 7.2.2.1 Partitioned Modal Equations of Motion

The previously derived modal equations for the general case were expressed in Equation 7-8 as

$$[I]_D \{\ddot{\eta}\} + [2\omega_n \xi_n]_D \{\dot{\eta}\} + [\omega_n^2]_D \{\eta\} = - [\Gamma] \{\ddot{y}_2\} \quad (7-26)$$

where, from Equation 7-12

$$\begin{aligned} [\Gamma] &= \text{Matrix of modal participation factors} \\ &= [\Phi]^T [M_{11}] [R_s] \end{aligned}$$

In Equation 7-26, the equation of motion for the  $j$ th mode can be written in scalar form as

$$\ddot{\eta}_j + 2\omega_j \xi_j \dot{\eta}_j + \omega_j^2 \eta_j = - \sum_{s=1}^{NI} \Gamma_{js} \ddot{y}_{2s} \quad (7-27)$$

where the index  $s$  ranges over the  $NI$  structure degrees of freedom along its interface with the half-space, and

$$\Gamma_{js} = - \frac{1}{\omega_j} \sum_{n=1}^{NA} \phi_{nj} (K_{12})_{ns} \quad (7-28)$$

where the index  $n$  ranges over the  $NA$  aboveground DOF's of the structure. For harmonic motion, Equation 7-27 takes the form

$$\left( -\Omega^2 + 2i\Omega\omega_j \xi_j + \omega_j^2 \right) \eta_{jo} e^{i\Omega t} = - \sum_{s=1}^{NI} \Gamma_{js} \ddot{y}_{2s} \quad (7-29)$$



in which

$$\eta_j = \eta_{j0} e^{i\Omega t} \quad \ddot{y}_{2s} = \ddot{y}_{2s0} e^{i\Omega t} = -\Omega^2 y_{2s0} e^{i\Omega t} \quad (7-30)$$

Now it is clear that for  $\omega_j^2 \gg \Omega^2$ , the term involving  $\omega_j^2$  will dominate the left side of Equation 7-29. Therefore, for these higher modes, the solution for  $\eta_{j0}$  is approximately its "static" response, i.e.,

$$\eta_{j0} = -\frac{1}{\omega_j^2} \sum_{s=1}^{NI} \Gamma_{js} \ddot{y}_{2s0} \quad (7-31)$$

Applying this concept to the general set of modal equations results in the following expression for the modal response amplitudes

$$\{\eta_j\} = -[\omega_j^2]_D^{-1} [\Gamma] \{\ddot{y}_2\} \quad (7-32)$$

For future reference, Equation 7-29 will be used subsequently in this derivation to define modal response amplitudes for the residual modes, since these higher modes satisfy the conditions of applicability of this equation, i.e., that  $\omega_j^2 \gg \Omega^2$ .

Now let us rewrite Equation 7-6 in terms of kept modes and residual modes, i.e.,

$$\{y_{1d}\} = [\phi] \{\eta\} = \begin{bmatrix} \phi_k & | & \phi_r \end{bmatrix} \begin{Bmatrix} \eta_k \\ \hline \eta_r \end{Bmatrix}$$

or

$$\{y_{1d}\} = [\phi_k] \{\eta_k\} + [\phi_r] \{\eta_r\} \quad (7-33)$$



in which the subscript "k" denotes kept modes and the subscript "r" represents residual modes. Substituting Equation 7-32 for  $\{\eta_r\}$ , we obtain

$$\{y_{1d}\} = [\phi_k]\{\eta_k\} - [\phi_r][\omega_r^2]_D^{-1}[\Gamma_r]\{\ddot{y}_2\} \quad (7-34)$$

where  $[\Gamma_r]$  is the matrix of modal participation factors for the residual modes, i.e.,

$$[\Gamma] = \begin{bmatrix} \Gamma_k \\ -\Gamma_r \end{bmatrix} = \begin{bmatrix} [\phi_k]^T [M_{11}] [R_s] \\ [\phi_r]^T [M_{11}] [R_s] \end{bmatrix} \quad (7-35)$$

The two subsections that follow will be directed toward defining the residual mode term on the right side of Equation 7-34 in terms of kept modes.

#### 7.2.2.2 Modal Identities

To express Equation 7-34 only in terms of kept mode quantities it is necessary to make use of certain modal identities. From the normal mode orthogonality relationships (Eqs. 7-7) and the previously stated definition of  $[\Gamma]$  (Eq. 7-12), it can be shown that

$$[\phi][\omega_n^2]_D^{-1}[\Gamma] = [K_{11}]^{-1}[M_{11}][R_s] \quad (7-36)$$

or, in terms of the eigenvector matrix

$$[\phi][\omega_n^2]_D^{-1}[\Gamma] = [K_{11}]^{-1}[M_{11}][\phi][\phi]^T[M_{11}][R_s] \quad (7-37)$$



In this, the left sides of the above equations can be expressed in terms of kept modes and residual modes as follows

$$[\phi][\omega_n^2]_D^{-1}[\Gamma] = [\phi_k][\omega_k^2]_D^{-1}[\Gamma_k] + [\phi_r][\omega_r^2]_D^{-1}[\Gamma_r] \quad (7-38)$$

By using Equations 7-12, 7-36 and 7-37, the residual mode term in the above expression becomes:

$$[\phi_r][\omega_r^2]_D^{-1}[\Gamma_r] = [K_{11}]^{-1}[M_{11}][R_s] - [\phi_k][\omega_k^2]_D^{-1}[\Gamma_k] \quad (7-39)$$

or, substituting for  $[\Gamma_k]$  from Equation 7-35

$$[\phi_r][\omega_r^2]_D^{-1}[\Gamma_r] = [K_{11}]^{-1}[M_{11}] \left[ [I]_D - [\phi_k][\phi_k]^T[M_{11}] \right] [R_s] \quad (7-40)$$

### 7.2.2.3 Final Development of $\{y_1\}$ vs. $\{y_2\}$ Interrelationship

To obtain the final form of the interrelationship between  $\{y_1\}$  and  $\{y_2\}$ , it remains to incorporate the above modal identities into Equation 7-34, express the resulting equation for the case of harmonic excitations, and then combine the resulting dynamic component of  $\{y_1\}$  with its pseudostatic component in accordance with Equation 7-2.

To begin this process, we substitute Equation 7-40 into Equation 7-34, in order to obtain

$$\{y_{1d}\} = [\phi_k]\{\eta_k\} - [K]_{11}^{-1}[M_{11}] \left[ [I]_D - [\phi_k][\phi_k]^T[M_{11}] \right] [R_s] \{\ddot{y}_2\} \quad (7-41)$$

Now, for the case of harmonic excitation

$$\{y_2\} = \{y_{20}\}e^{i\Omega t} \quad (7-42)$$

$$\{\eta_k\} = \{\eta_{k0}\}e^{i\Omega t}$$



which can be substituted into Equation 7-41 to obtain (by analogy to Eqs. 7-10 and 7-11 for the general case) the following expression for the modal response for the kept modes

$$\begin{aligned} \{\eta_{ko}\} &= \Omega^2 [S_k]_D^{-1} [\phi_k]^T [M_{11}] [R_s] \{y_{20}\} \\ &= \Omega^2 [S_k]_D^{-1} [\Gamma_k] \{y_{20}\} \end{aligned} \quad (7-43)$$

where

$$[S_k]_D = - [\Omega^2]_D + i[2\Omega\omega_k \xi_k]_D + [\omega_k]_D^2 \quad (7-44)$$

Therefore, substituting Equations 7-42 and 7-43 into Equation 7-41

$$\begin{aligned} \{y_{1d}\} &= \left[ [R_{dk}] \right. \\ &\quad \left. + \Omega^2 [K_{11}]^{-1} [M_{11}] [I]_D - [\phi_k] [\phi_k]^T [M_{11}] [R_s] \right] \{y_{20}\} e^{i\Omega t} \end{aligned} \quad (7-45)$$

where, by analogy with Equations 7-13 and 7-14 for the general case

$$[R_{dk}] = \Omega^2 [\phi_k] [S_k]_D [\Gamma_k] \quad (7-46)$$

Finally, substituting Equations 7-45 and 7-3 into Equation 7-2, the final interrelationship between  $\{y_1\}$  and  $\{y_2\}$  takes the form

$$\{y_1\} = [T_k] + [T_c] \{y_2\} = [T_k] + [T_c] \{y_{20}\} e^{i\Omega t} \quad (7-47)$$





where, by analogy with Equation 7-16 for the general case

$$[T_k] = [R_s] + [R_{dk}] \quad (7-48)$$

and

$$[T_c] = \Omega^2 [K_{11}]^{-1} [M_{11}] \left[ [I]_D - [\Phi_k] [\Phi_k]^T [M_{11}] \right] [R_s] \quad (7-49)$$

In this,  $[T_k]$  is identical to the transformation matrix between  $\{y_1\}$  and  $\{y_2\}$  for the general case (Eq. 7-16), except that now it is evaluated only for the kept modes. The quantity  $[T_c]$  is a correction matrix that accounts for the effects of higher (residual) modes that are truncated in this approach.

### 7.2.3 DETERMINATION OF STRUCTURE RESPONSE AT INTERFACE DOF'S

To determine  $\{y_2\}$ , the structure response along its interface with the underlying half-space, we proceed in a manner identical to that for the general case (Sec. 7.1.3). In this, Equation 7-47 is substituted into the lower set of partitioned equations in Equation 7-1 and conditions of harmonic excitation are imposed. This results in the following expression (which is analogous to Eq. 7-18 for the general case)

$$\left[ [K_{STk}] + [K_{STc}] \right] \{y_{20}\} = \{P_{20}\} \quad (7-50)$$

where

$$[K_{STk}] = -\Omega^2 [M_{22}] + [K_{12}]^T [T_k] + [K_{22}] \quad (7-51)$$

$$[K_{STc}] = [K_{12}]^T [T_c] \quad (7-52)$$



and

$$\{Y_2\} = \{Y_{20}\}e^{i\Omega t}$$

$$\{P_2\} = \{P_{20}\}e^{i\Omega t}$$

$[T_k]$ ,  $[T_c]$  = given by Equations 7-48 and 7-49 respectively.

In this,  $[K_{STk}]$  is an effective impedance matrix for the structure. Its form is identical to that for the general case, (Eq. 7-19), except that now it is evaluated only for the kept modes.  $[K_{STc}]$  is a correction matrix that accounts for the effects of the higher (residual) modes on this structure impedance matrix. It can be computed either from Equation 7-52 or from the following alternate expression:

$$[K_{STc}] = -\Omega^2 [R_s]^T [M_{11}] [R_s] + \Omega^2 [\Gamma_k]^T [\Gamma_k] \quad (7-53)$$

It now remains to express  $\{P_{20}\}$ , the vector of harmonic amplitudes of the structure/half-space interface forces in Equation 7-50, as the superposition of half-space driving forces and resisting forces. As in Equation 7-21 for the general case, this expression takes the form:

$$\{P_{20}\} = \{P_{DO}\} + \{P_{RO}\} \quad (7-54)$$

where

$\{P_{DO}\}$  = Vector of driving force amplitudes as derived in Section 6.2 of Chapter 6.

$\{P_{RO}\}$  = Vector of resisting force amplitudes =  $- [K_{HS}] \{Y_{20}\}$

$[K_{HS}]$  = Half-space impedance matrix, as derived in Section 6.1 of Chapter 6.



Substituting Equation 7-54 into Equation 7-50 and solving for  $\{y_{20}\}$  results in

$$\{y_{20}\} = \left[ [K_{STk}] + [K_{STc}] + [K_{HS}] \right]^{-1} \{P_{DO}\} \quad (7-55)$$

where  $[K_{STk}] + [K_{STc}] + [K_{HS}]$  is the combined structure/half-space impedance matrix including effects of modal truncation.

#### 7.2.4 DETERMINATION OF STRUCTURE RESPONSE AT ABOVEGROUND DOF'S

Now that  $\{y_{20}\}$  is determined, we again proceed in a manner analogous to that for the general case in order to obtain  $\{y_1\}$  (see Sec. 7.1.4). Substituting Equation 7-55 into the previously derived interrelationship between  $\{y_2\}$  and  $\{y_1\}$  (Eq. 7-47), we obtain

$$\{y_1\} = [T_k + T_c][K_{STk} + K_{STc} + K_{HS}]^{-1} \{P_{DO}\} e^{i\Omega t} \quad (7-56)$$

or, substituting for  $[T_k]$

$$\{y_1\} = [R_s + R_{dk} + T_c][K_{STk} + K_{STc} + K_{HS}]^{-1} \{P_{DO}\} e^{i\Omega t} \quad (7-57)$$

where  $[R_s]$  and  $[R_{dk}]$  are defined in Equations 7-4 and 7-46, and  $[T_c]$  is defined in Equation 7-49. Equations 7-56 and 7-57 are analogous to Equations 7-22 and 7-23 respectively for the general case.

### 7.3 ILLUSTRATIVE EXAMPLE

#### 7.3.1 SOIL/STRUCTURE SYSTEM

To demonstrate the effectiveness of the modal truncation approach described in the previous section, an illustrative example application of the approach is summarized. The soil/



structure system to which the approach is applied in this example is a free-standing bridge structure supported on rigid footings that, in turn, rest on the surface of an elastic half-space. The configuration and model of the bridge is shown in Figure 7-1 and the bridge/soil system properties are provided in Table 7-1. The first few fixed-base mode shapes for the bridge are shown in Figure 7-2.

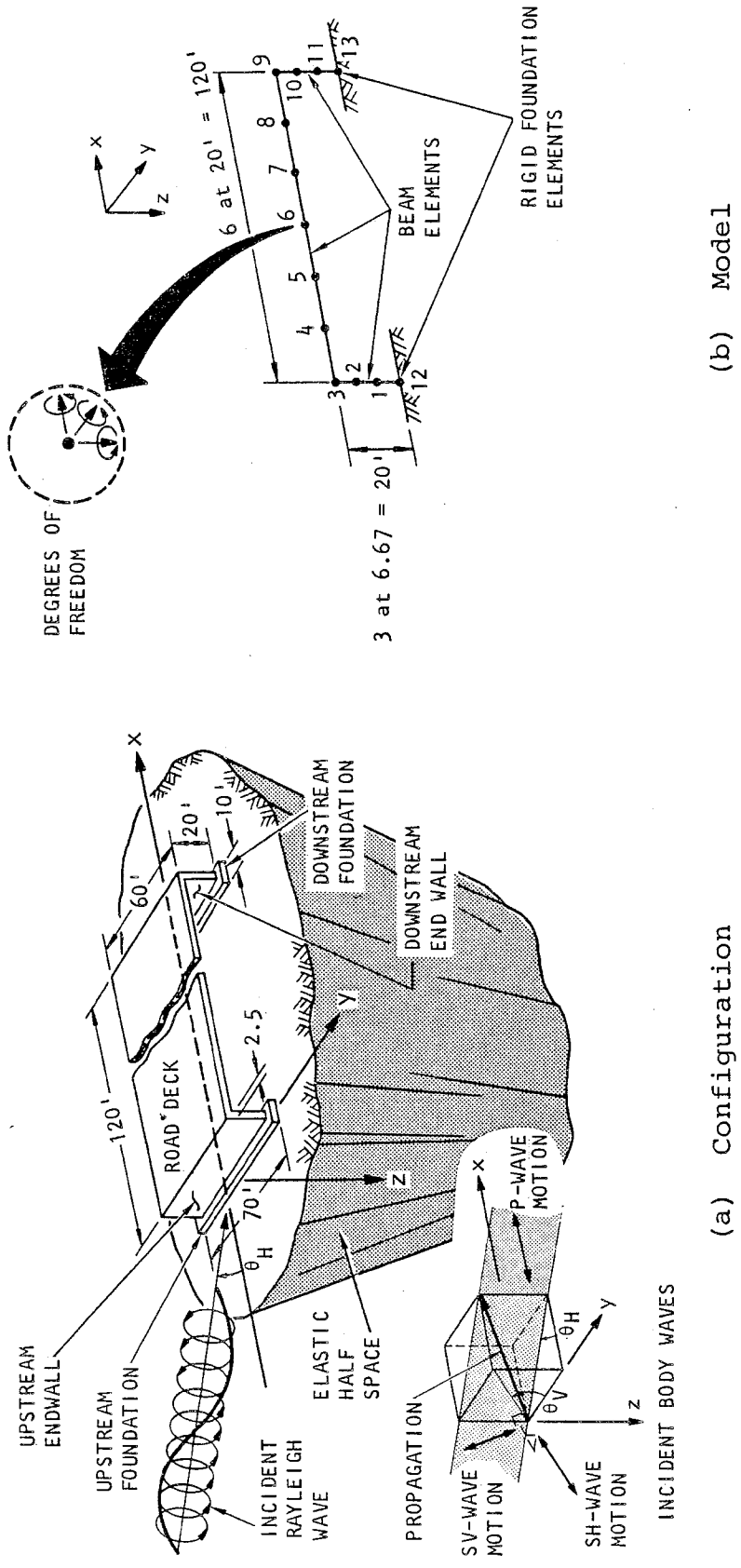
This bridge/soil system is identical to that considered in previous studies of traveling seismic wave effects on the response of bridges (Werner et al., 1977; Werner and Lee, 1980). In these prior studies, analyses carried out for a variety of wave types, wavelengths, and directions of incidence required the use of 29 modes to represent the structure, in order to obtain adequate convergence. The inclusion of this large number of modes was not only costly, but was also possibly prone to some uncertainty pertaining to the accuracy of the higher mode computations. Situations of this type are clearly ideal for application of modal truncation procedures of the type described in Section 7.2.

### 7.3.2 INCIDENT WAVE MOTIONS

Two cases involving seismic wave excitations are considered in this example. Case 1 corresponds to SV-waves with an excitation frequency of 8.8 Hz and a direction of incidence corresponding to  $\theta_H = 0$  deg and  $\theta_V = 45$  deg (see Fig. 7-1 for a definition of  $\theta_H$  and  $\theta_V$ ). Case 2 also corresponds to SV-waves with the same excitation frequency but with a direction of incidence of  $\theta_H = 45$  deg and  $\theta_V = 20$  deg. Case 1, as indicated above, represents conditions of relatively simple two-dimensional response whereas, in Case 2, the response will be three dimensional.

### 7.3.3 RESULTS

The results for each of the above cases are summarized in Tables 7-2 and 7-3. These tables provide amplitudes of response



(a) Configuration

(b) Model

FIGURE 7-1. BRIDGE CONFIGURATION AND MODEL  
(Werner et al, 1977)



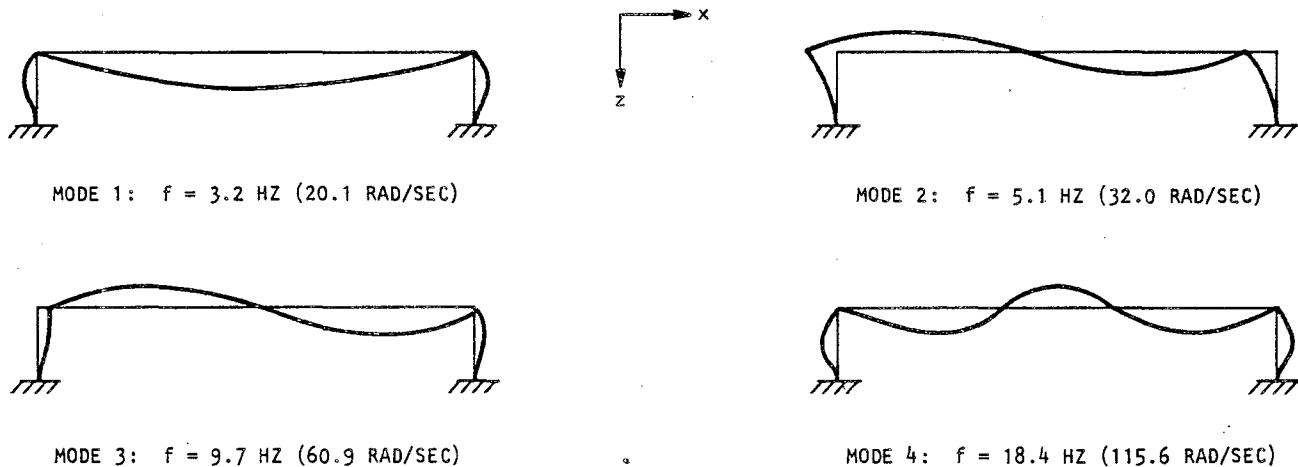
TABLE 7-1. BRIDGE/SOIL SYSTEM PROPERTIES  
(Werner et al., 1977)

Element	Section Properties				Material Properties		
	Cross Sectional Area, ft <sup>2</sup>	Moment of Inertia, ft <sup>4</sup>			Young's Modulus, psi	Unit Weight, pcf	Poisson's Ratio
		About Strong Axis	About Weak Axis	Torsion			
Road Deck	9.82 x 10	3.56 x 10 <sup>4</sup>	3.29 x 10 <sup>2</sup>	1.01 x 10 <sup>3</sup>	3.54 x 10 <sup>6</sup>	150	0.15
End Walls	1.48 x 10 <sup>2</sup>	4.28 x 10 <sup>4</sup>	7.69 x 10	3.08 x 10 <sup>2</sup>			

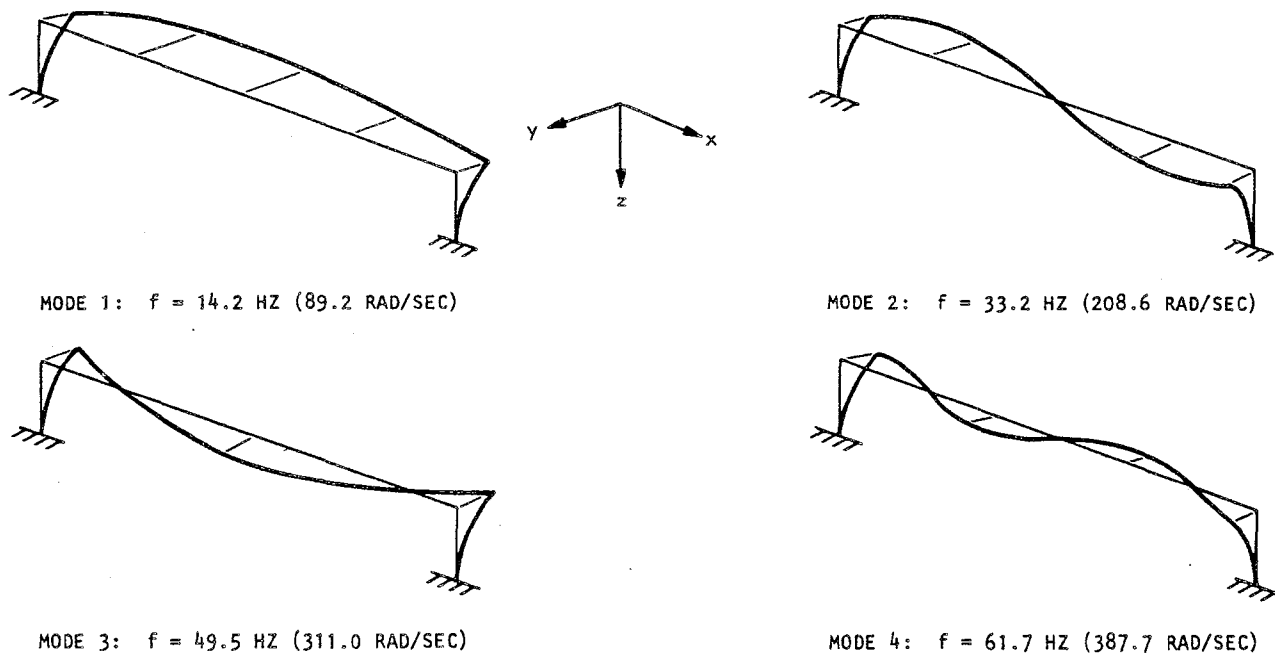
(a) Bridge

Unit weight	Poisson's Ratio	Shear Wave Velocity, fps	Other Wave Velocities, fps (for Poisson's Ratio = 1/3)	
			P-Wave Velocity	Rayleigh-Wave Velocity
110	0.33	500	1000	466.3

(b) Soil Medium



(a) In-plane modes (significant response in x-z plane)



AA8754

(b) Out-of-plane modes (significant response in y-direction)

FIGURE 7-2. FIXED-BASE MODE SHAPES AND FREQUENCIES OF BRIDGE (Werner et al., 1977)

TABLE 7-2. CASE 1 ANALYSIS RESULTS\*

Location	Number of Kept Modes	X-Displacement		Y-Displacement		Z-Displacement		X-Rotation		Y-Rotation		Z-Rotation	
		Uncor.	Cor.	Uncor.	Cor.	Uncor.	Cor.	Uncor.	Cor.	Uncor.	Cor.	Uncor.	Cor.
Upstream Foundation	4	1.0264 <sup>†</sup> (5.0%)	0.9775 (0%)	0	0	0.6905 (11.3%)	0.6216 (0.2%)	0	0	0.004946 (9.7%)	0.004511 (0%)	0	0
	6	1.0183 (4.2%)	0.9769 (0%)	0	0	0.6726 (8.4%)	0.6205 (0%)	0	0	0.004856 (7.7%)	0.004505 (0%)	0	0
	8	1.0181 (4.2%)	0.9769 (0%)	0	0	0.6729 (8.4%)	0.6205 (0%)	0	0	0.004854 (7.1%)	0.004505 (0%)	0	0
	29	0.9839 (0.7%)	0.9772 (*) <sup>†</sup>	0	0	0.6248 (0.7%)	0.6205 (*)	0	0	0.004537 (0.7%)	0.004507 (*)	0	0
Top of Upstream End Wall	4	0.5257 (19.0%)	0.4443 (0.6%)	0	0	0.7271 (10.9%)	0.6254 (-4.6%)	0	0	0.01817 (9.5%)	0.01592 (-4.0%)	0	0
	6	0.5109 (15.7%)	0.4438 (0.5%)	0	0	0.7088 (8.1%)	0.6268 (-4.4%)	0	0	0.01802 (8.6%)	0.01632 (-1.6%)	0	0
	8	0.5102 (15.5%)	0.4409 (0.2%)	0	0	0.7090 (8.1%)	0.6268 (-4.4%)	0	0	0.01802 (8.6%)	0.01632 (-1.6%)	0	0
	29	0.4455 (0.9%)	0.4416 (*)	0	0	0.6599 (0.6%)	0.6557 (*)	0	0	0.01671 (0.7%)	0.01659 (*)	0	0
Midspan of Road Deck	4	0.5670 (19.0%)	0.4858 (2.0%)	0	0	0.0253 (10.4%)	0.01764 (23.0%)	0	0	0.02629 (13.6%)	0.02375 (2.6%)	0	0
	6	0.5514 (15.7%)	0.4852 (1.8%)	0	0	0.0286 (24.8%)	0.02324 (1.4%)	0	0	0.02570 (11.0%)	0.02314 (0%)	0	0
	8	0.5514 (15.7%)	0.4852 (1.8%)	0	0	0.0291 (27.0%)	0.02245 (2.1%)	0	0	0.02570 (11.0%)	0.02314 (0%)	0	0
	29	0.4806 (0.9%)	0.4764 (*)	0	0	0.0235 (2.5%)	0.02292 (*)	0	0	0.02331 (0.7%)	0.02315 (*)	0	0
Top of Downstream End Wall	4	0.5460 (18.0%)	0.4599 (-0.6%)	0	0	0.7281 (15.3%)	0.6031 (-4.5%)	0	0	0.01813 (9.7%)	0.01580 (-4.4%)	0	0
	6	0.5311 (14.8%)	0.4588 (-0.8%)	0	0	0.7099 (12.4%)	0.6046 (-4.5%)	0	0	0.01801 (9.0%)	0.01628 (-1.5%)	0	0
	8	0.5319 (15.0%)	0.4618 (-0.2%)	0	0	0.7096 (12.4%)	0.6046 (-4.5%)	0	0	0.01801 (9.0%)	0.01628 (-1.5%)	0	0
	29	0.4667 (0.9%)	0.4627 (*)	0	0	0.6372 (0.9%)	0.6315 (*)	0	0	0.01664 (0.7%)	0.01652 (*)	0	0
Downstream Foundation	4	0.8330 (0.4%)	0.8290 (-0.1%)	0	0	0.6892 (16.1%)	0.5953 (0.3%)	0	0	0.01008 (7.3%)	0.00940 (0.1%)	0	0
	6	0.8287 (-0.1%)	0.8289 (-0.1%)	0	0	0.6711 (13.1%)	0.5939 (0.1%)	0	0	0.00999 (6.4%)	0.009395 (0%)	0	0
	8	0.8285 (-0.1%)	0.8289 (-0.1%)	0	0	0.6709 (13.1%)	0.5939 (0.1%)	0	0	0.00999 (6.4%)	0.009395 (0%)	0	0
	29	0.8329 (0.4%)	0.8296 (*)	0	0	0.5993 (1%)	0.5934 (*)	0	0	0.009450 (0.6%)	0.009393 (*)	0	0

Notes: \* Case 1 seismic excitations correspond to SV-waves with  $\theta_H = 0$  deg,  $\theta_V = 45$  deg, and excitation frequency = 8.8 Hz

<sup>†</sup>Numbers in parentheses correspond to percent errors (see text of Sec. 7.3.3 for discussion). Asterisk in parentheses (\*) denotes assumed correct quantities, which are basis for computation of percent errors for each group.

207 A



TABLE 7-3. CASE 2 ANALYSIS RESULTS\*

Location	Number of Kept Modes	X-Displacement		Y-Displacement		Z-Displacement		X-Rotation		Y-Rotation		Z-Rotation	
		Uncor.	Cor.	Uncor.	Cor.	Uncor.	Cor.	Uncor.	Cor.	Uncor.	Cor.	Uncor.	Cor.
Upstream Foundation	4	0.1075 (-1.5%) <sup>†</sup>	0.1089 (-0.2%)	0.1374 (-67.3%)	0.4046 (-3.6%)	0.1479 (7.2%)	0.1384 (0.3%)	0.002326 (-6.8%)	0.002539 (1.7%)	0.001028 (14.5%)	0.000899 (0.1%)	0.000876 (-0.6%)	0.000885 (0.5%)
	6	0.1075 (-1.5%)	0.1090 (-0.1%)	0.1374 (-67.3%)	0.4045 (-3.6%)	0.1460 (5.8%)	0.1381 (0.1%)	0.002326 (-6.8%)	0.002539 (1.7%)	0.001019 (13.5%)	0.000899 (0.1%)	0.000876 (-0.6%)	0.000885 (0.5%)
	8	0.1071 (-1.8%)	0.1090 (0.1%)	0.2247 (-46.5%)	0.4178 (-0.4%)	0.1461 (5.9%)	0.1381 (0.1%)	0.002761 (10.6%)	0.002503 (0.3%)	0.001012 (12.7%)	0.000899 (0.1%)	0.000898 (1.9%)	0.000882 (0.1%)
	29	0.1094 (0.2%)	0.1091 (*) <sup>†</sup>	0.4197 (0%)	0.4197 (*)	0.1388 (0.6%)	0.1380 (*)	0.002495 (0%)	0.002496 (*)	0.000907 (1.0%)	0.000898 (*)	0.000881 (0%)	0.000881 (*)
Top of Upstream End Wall	4	0.0712 (21.7%)	0.0606 (3.6%)	0.5590 (-26.6%)	0.6996 (-8.1%)	0.1536 (6.2%)	0.1406 (-2.8%)	0.002309 (-7.8%)	0.002483 (-0.8%)	0.002218 (14.5%)	0.001854 (-4.3%)	0.000953 (-14.5%)	0.001101 (-1.2%)
	6	0.0691 (18.1%)	0.0602 (2.9%)	0.5590 (-26.6%)	0.6997 (-8.1%)	0.1518 (5.0%)	0.1407 (-2.7%)	0.002309 (-7.8%)	0.002482 (-0.8%)	0.002211 (14.1%)	0.001937 (0%)	0.000953 (-14.5%)	0.001102 (-1.1%)
	8	0.0683 (16.8%)	0.0578 (-1.2%)	0.8458 (11.1%)	0.7362 (-3.3%)	0.1518 (5.0%)	0.1407 (-2.7%)	0.002764 (10.4%)	0.002491 (-0.5%)	0.002207 (13.9%)	0.001934 (-0.2%)	0.001317 (18.2%)	0.001060 (-4.8%)
	29	0.0590 (0.9%)	0.0585 (*)	0.7614 (0%)	0.7614 (*)	0.1454 (0.6%)	0.1446 (*)	0.002503 (0%)	0.002503 (*)	0.001957 (1.0%)	0.001938 (*)	0.001114 (0%)	0.001114 (*)
Midspan of Road Deck	4	0.0775 (19.8%)	0.0656 (1.4%)	0.1538 (43.5%)	0.1104 (3.0%)	0.0047 (-64.7%)	0.0054 (-59.4%)	0.000492 (-4.5%)	0.000515 (0%)	0.003529 (16.1%)	0.003094 (1.8%)	0.000895 (-20.7%)	0.000981 (-13.0%)
	6	0.0754 (16.5%)	0.0655 (1.2%)	0.1538 (43.5%)	0.1104 (3.0%)	0.00926 (-30.4%)	0.0139 (4.5%)	0.000492 (-4.5%)	0.000515 (0%)	0.003447 (13.4%)	0.003041 (0%)	0.000895 (-20.7%)	0.000981 (-13.0%)
	8	0.0754 (16.5%)	0.0655 (1.2%)	0.1538 (43.5%)	0.1104 (3.0%)	0.00881 (-33.8%)	0.0142 (6.8%)	0.000492 (-4.5%)	0.000515 (0%)	0.003447 (13.4%)	0.003041 (0%)	0.001326 (17.6%)	0.001114 (-1.2%)
	29	0.0653 (0.9%)	0.0647 (*)	0.1072 (0%)	0.1072 (*)	0.0127 (-4.5%)	0.0133 (*)	0.000515 (0%)	0.000515 (*)	0.003069 (1.0%)	0.003040 (*)	0.001128 (0%)	0.001128 (*)
Top of Downstream End Wall	4	0.0752 (17.0%)	0.0624 (-3.0%)	0.7354 (-12.4%)	0.7781 (-7.3%)	0.0420 (18.3%)	0.0341 (-3.9%)	0.002649 (11.3%)	0.002391 (0.5%)	0.002577 (11.6%)	0.002289 (-0.9%)	0.000827 (-20.6%)	0.001015 (-2.5%)
	6	0.0732 (13.8%)	0.0625 (-2.8%)	0.7354 (-12.4%)	0.7780 (-7.3%)	0.0390 (9.9%)	0.0344 (-3.1%)	0.002649 (11.3%)	0.002391 (0.5%)	0.002541 (10.0%)	0.002278 (-1.3%)	0.000827 (-20.6%)	0.001015 (-2.5%)
	8	0.0741 (15.2%)	0.0649 (0.9%)	1.0201 (21.5%)	0.8097 (-3.6%)	0.0390 (9.9%)	0.0344 (-3.1%)	0.002873 (20.7%)	0.002372 (-0.3%)	0.002545 (10.2%)	0.002281 (-1.2%)	0.001179 (13.3%)	0.000976 (-6.2%)
	29	0.0649 (0.9%)	0.0643 (*)	0.8397 (0%)	0.8397 (*)	0.0351 (-1.1%)	0.0355 (*)	0.002380 (0%)	0.002380 (*)	0.002329 (0.9%)	0.002309 (*)	0.001128 (8.4%)	0.001041 (*)
Downstream Foundation	4	0.1341 (8.8%)	0.1234 (0.2%)	0.1664 (-74.0%)	0.6332 (-0.9%)	0.0368 (8.6%)	0.0333 (-1.8%)	0.002650 (12.0%)	0.002426 (2.5%)	0.001045 (7.6%)	0.000973 (0.2%)	0.000807 (-2.9%)	0.000827 (-0.5%)
	6	0.1321 (7.2%)	0.1231 (0.1%)	0.1664 (-74.0%)	0.6331 (-0.9%)	0.0341 (8.6%)	0.0337 (-0.6%)	0.002650 (12.0%)	0.002426 (2.5%)	0.001028 (5.9%)	0.000970 (-0.1%)	0.000807 (-2.9%)	0.000827 (-0.5%)
	8	0.1331 (8.0%)	0.1232 (0%)	0.5038 (-21.2%)	0.6385 (-0.1%)	0.0341 (8.6%)	0.0337 (-0.6%)	0.002857 (20.7%)	0.002377 (0.4%)	0.001035 (6.6%)	0.000971 (0%)	0.000803 (-3.4%)	0.000830 (-0.1%)
	29	0.1246 (1.1%)	0.1232 (*)	0.6390 (0%)	0.6390 (*)	0.0333 (-1.8%)	0.0339 (*)	0.002367 (0%)	0.002367 (*)	0.000978 (0.7%)	0.000971 (*)	0.000831 (0%)	0.000831 (*)

Notes: \* Case 2 seismic excitations correspond to SV-waves with  $\theta_H = 45$  deg,  $\theta_V = 20$  deg, and excitation frequency = 8.8 Hz

<sup>†</sup> Numbers in parentheses correspond to percent errors (see text of Sec. 7.3.3 for discussion). Asterisk in parentheses (\*) denotes assumed correct quantities, which are basis for computation of percent errors for each group.



of the bridge at its upstream and downstream foundations, at the tops of its upstream and downstream end walls, and at the mid-span of its road deck. The results are developed in four sets of computations -- corresponding to 4, 6, 8, and 29 kept modes (see Table 7-4 for natural frequencies of the highest kept mode in each of these computations). At each location and for each assumed number of kept modes, the bridge response amplitudes were computed with and without the modal truncation corrections for higher mode effects. These results were compared to the response amplitudes corresponding to the condition of 29 kept modes and modal truncation corrections. The comparisons were depicted in terms of tabulated percent errors.

Results for the two-dimensional case (Case 1) demonstrate the effectiveness of the modal truncation procedure in accounting for higher mode effects under these conditions (Table 7-2). For example, in the analysis results involving only 6 kept modes, the modal truncation procedure is seen to reduce the percent error in the computed bridge response amplitudes to values that are typically well under 5%.

For the three-dimensional case (Case 2), the effectiveness of the modal truncation procedures is also clearly demonstrated (Table 7-3). In this case, the bridge response is much more complex, resulting in percent errors for both uncorrected and corrected conditions that are higher than for the two-dimensional situation. This suggests that the required number of kept modes will be larger for Case 2, although the modal truncation approach is quite effective even in this case. To illustrate, 6 kept modes result in percent errors of less than 13% and, if 8 kept modes are considered, the percent errors drop to values that are typically well under 4%.

#### 7.3.4 OVERALL TRENDS

The overall trends from these results demonstrate that, for this example, the modal truncation approach is quite effective in reducing the number of modes required to produce excellent



TABLE 7-4. NATURAL FREQUENCY OF HIGHEST KEPT  
MODE IN EACH COMPUTATION FOR  
ILLUSTRATIVE EXAMPLE

Kept Mode Number	Natural Frequency, Hz
4	14.2
6	28.8
8	36.0
29	288.8



results. In particular, for the two cases considered, 6 to 8 modes incorporating modal truncation corrections reproduced (with a very small error) the results obtained using 29 modes with no such corrections. The trends also illustrate that the required number of kept modes must be selected not only on the basis of natural frequencies\*, but also from consideration of the nature of the expected structure response to the incident wave motions. For example, if the structure response is expected to be predominantly transverse to the bridge span, (as would occur from SH-waves with  $\theta_H = 0$  deg for the bridge considered in this example) a sufficient number of transverse response modes should be included in the ensemble of kept modes for the analysis. Also, as illustrated by these Case 1 and Case 2 results, a larger number of kept modes will be required if the seismic excitations are expected to produce complex three-dimensional response, as opposed to much simpler in-plane response.

---

\*As noted in Section 7.2.2.1, the natural frequency of the highest kept mode should be markedly greater than the excitation frequency. Generally, we have found that if frequency is at least 5 times the excitation frequency, excellent results should be produced by this modal truncation approach.



## REFERENCES

- Agbabian Associates (AA). (1979) *A Comparison of Seismic Analysis Techniques for Piping Systems with Multisupport Input*, SAN/1011-123. El Segundo, CA: AA, Sep.
- Bathe, K.J. and Wilson, E.L. (1976) *Numerical Methods in Finite Element Analysis*. Englewood Cliffs, NJ: Prentice-Hall.
- Ewing, W.M.; Jardetsky, W.S.; and Press, F. (1957) *Elastic Waves in Layered Media*. New York: McGraw-Hill.
- Knopoff, L. (1952) "On Rayleigh Wave Velocities," *Bull. Seismol. Soc. Amer.*, 42:4, Oct, pp 307-308.
- Lamb, H. (1904) "On the Propagation of Tremors over the Surface of an Elastic Solid," *Philosophical Trans. Royal Soc. London, Ser. A*, 203, pp 1-42.
- Luco, J.E.; Wong, H.L.; and Trifunac, M.D. (1975) "A Note on the Dynamic Response of Rigid Embedded Foundations," *Intl. Jnl. Earthq. Eng. Struct. Dyn.*, 4:2, Oct-Dec, pp 119-128.
- Nakano, H. (1930) "Some Problems Concerning the Propagation of the Disturbances in and on Semi-Infinite Elastic Solid," *Geophysical Magazine*, Vol. 2, pp 189-348.
- Powell, G.H. (1979) "Missing Mass Correction in Modal Analysis of Piping Systems," *Trans. 5th Int. Conf. on Struct. Mech. in Reactor Technology*, Vol. K(6), Berlin, Aug, paper K10/3.
- Thomson, W.T. and Kobori, T. (1963) "Dynamic Compliance of Rectangular Foundations on an Elastic Half-Space," *Jnl. Applied Mech.*, ASME, Vol. 85, Dec, pp 579-584.
- Veletsos, A. S. and Wei, Y.T. (1971) "Lateral and Rocking Vibration of Footings," *Jnl. Soil Mech. and Found. Div.*, ASCE, 97:SM9, Sep, pp 1227-1248.
- Werner, S.D. and Lee, L.C. (1980) *Three-Dimensional Response of a Bridge Structure Subjected to Traveling Rayleigh Waves, S-V Waves, and P-Waves*, R-7911-5008. El Segundo, CA: Agbabian Assoc., May.
- Werner, S.D., et al. (1977) *Evaluation of the Effects of Traveling Seismic Waves on the Three-Dimensional Response of Structures*, R-7720-4514. El Segundo, CA: Agbabian Assoc., Oct.





APPENDIX A  
INPUT DESCRIPTION FOR BASSIN1

This appendix contains a description of the user-provided input data for the BASSIN1 subprogram, in accordance with the general description provided in Section 3.1 of Chapter 3. These data are contained in a total of 35 card groups, and can be provided to BASSIN1 in any consistent set of units.

The output from BASSIN1 is in the form of print, peripheral storage, and (optionally) plots. The peripheral storage is generated on FORTRAN Logical Unit 8, and is used as input to the BASSIN2 subprogram.

CARD GROUP 1:           PROBLEM TITLE  
 NO. OF CARDS:         VARIABLE\*  
 FORMAT:               IX,A1,12A6  
 ROUTINE:              BASSINI

COLUMNS	VARIABLE	ENTRY	NOTES
2	ISTAR	CARD GROUP TERMINATION FLAG;  = ^, CARD IS OPTIONAL, IGNORED, AND MAY BE USED FOR CONTROL DATA COMMENTS. ( ^ DENOTES A BLANK )  = *, CARD CONTAINS PROBLEM TITLE	
3-74	HEAD(1) THROUGH HEAD(12)	PROBLEM TITLE, 72 CHARACTERS MAXIMUM	(1)

GO TO CARD GROUP 2.

NOTES:

- (\*) THE COMMENT CAN BE SPECIFIED BY ANY NUMBER OF CARDS. HOWEVER, ONE CARD MUST BE INPUT WITH ISTAR = \* AND MUST BE THE LAST CARD OF THIS GROUP.
- (1) THIS INFORMATION IS INCLUDED IN ALL FORMS OF OUTPUT PROVIDED BY THE PROGRAM, AND SHOULD BE CENTERED IN THE FIELD PROVIDED.



CARD GROUP 2:  
 NO. OF CARDS:  
 FORMAT:  
 ROUTINE:

PROGRAM EXECUTION OPTIONS  
 VARIABLE\*  
 A4,3(6X,A4)  
 INOPTJ

R-8113-5470

COLUMNS	VARIABLE	ENTRY	NOTES
1-4	CRDOPT(1)	CALCULATION OPTION  = ELEM, STRUCTURE GEOMETRY, MATERIAL PROPERTIES AND LOADS.  = MODE, FIXED-BASE NORMAL MODES OF STRUCTURE.  = IMPE, HALF-SPACE IMPEDANCE MATRIX.  = FREE, HALF-SPACE FREE-FIELD DISPLACEMENTS.  = *GO^, PROCEED WITH EXECUTION. ( ^ DENOTES A BLANK )	(1)
11-14	CRDOPT(2)	FIRST CALCULATION SUBOPTION.	(1)
21-24	CRDOPT(3)	SECOND CALCULATION SUBOPTION.	(1)
31-34	CRDOPT(4)	THIRD CALCULATION SUBOPTION.	(1)

GO TO CARD GROUP 3.

NOTES:

(\*) THE EXECUTION OPTIONS MAY BE SPECIFIED IN ANY ORDER BY UP TO 5 CARDS. HOWEVER, ONE CARD MUST BE INPUT WITH CRDOPT(1) = \*GO^ AND MUST BE THE LAST CARD.

THE FOLLOWING ARE VALID OPTION COMBINATIONS:

ELEM	ELEM	ELEM	ELEM
*GO	MODE	MODE	MODE
	*GO	IMPE	IMPE
		*GO	FREE
			*GO

NOTES: (CONTINUED)

(1) THE FOLLOWING TABLE INDICATES VALID SUBOPTION COMBINATIONS:

CALCULATION		SUBOPTION		
OPTION	COMP	!	PLOT	
ELEM	X	!	X	
MODE	X	!	X	
IMPE	X	!		
FREE	X	!		

DEFINITION OF SUBOPTIONS:

= COMP, READ INPUT AND PERFORM RESPECTIVE CALCULATION.

COMP IS A NECESSARY SUBOPTION WHEN SAVING OR PLOTTING IS SPECIFIED.

= PLOT, PLOT RESULTS OF CALCULATION.

CARD GROUP 3:  
NO. OF CARDS:  
FORMAT:  
ROUTINE:

MASTER CONTROL INFORMATION  
1  
315  
BASSINI

R-8113-5470

COLUMNS	VARIABLE	ENTRY	NOTES
1-5	NNODE	NUMBER OF NODAL POINTS.	
6-10	NTYPEL	NUMBER OF ELEMENT TYPES.	
11-15	NFRQ	NUMBER OF MODES FOR EXTRACTION OF EIGEN PARAMETERS.	

IF A PLOT SUBOPTION HAS BEEN SPECIFIED GO TO CARD GROUP 4,  
OTHERWISE GO TO CARD GROUP 11.

CARD GROUP 4:  
NO. OF CARDS:  
FORMAT:  
ROUTINE:

PLOT SCALE CONTROL PARAMETERS  
1\*  
2F10.0  
INOPT

R-81113-5470

COLUMNS	VARIABLE	ENTRY	NOTES
1-10	SCALE	MAXIMUM PLOT WIDTH IN INCHES. DEFAULT = 8.	(1)
11-20	SMOD	FRACTION OF MAXIMUM PLOT WIDTH TO BE USED FOR THE MAXIMUM MODAL DEFORMATION OF A NODE. DEFAULT = 0.125.	

GO TO CARD GROUP 5.

NOTES:

- (\*) IF CRDOPT(2) IS NOT EQUAL TO PLOT, SKIP THIS CARD GROUP.
- (1) IF  $1.+2.*ABS(SMOD) > 28.0$ ,  $SCALE = 28./ (1.+2.*ABS(SMOD))$

CARD GROUP 5: TRUSS ELEMENT PLOT CONTROL PARAM\_ R-8113-5470  
 NO. OF CARDS: 1\*  
 FORMAT: 5x,215  
 ROUTINE: INOPT

COLUMNS	VARIABLE	ENTRY	NOTES
6-10	IEL(1,1)	BEGINNING TRUSS ELEMENT NUMBER TO BE PLOTTED.	(1)
11-15	IEL(2,1)	ENDING TRUSS ELEMENT NUMBER TO BE PLOTTED.	(1)

GO TO CARD GROUP 7.

NOTES:

- (\*) IF CRDOPT(2) IS NOT EQUAL TO PLOT, SKIP THIS CARD GROUP.
- (1) THE BEGINNING AND ENDING ELEMENT NUMBERS DEFINE A RANGE OF ELEMENTS TO BE PLOTTED.

CARD GROUP 6: BEAM ELEMENT PLOT CONTROL PARAMETER R-8113-5470  
NO. OF CARDS: 1\*  
FORMAT: SX,215  
ROUTINE: INOPT

COLUMNS	VARIABLE	ENTRY	NOTES
6-10	IEL(1,2)	BEGINNING BEAM ELEMENT NUMBER TO BE PLOTTED.	(1)
11-15	IEL(2,2)	ENDING BEAM ELEMENT NUMBER TO BE PLOTTED.	(1)

GO TO CARD GROUP 7.

NOTES:

- (\*) IF CRDOPT(2) IS NOT EQUAL TO PLOT, SKIP THIS CARD GROUP.
- (1) THE BEGINNING AND ENDING ELEMENT NUMBERS DEFINE A RANGE OF ELEMENTS TO BE PLOTTED.

CARD GROUP 7: PLANE ELEMENT PLOT CONTROL PARAM R-8113-5470  
 NO. OF CARDS: 1\*  
 FORMAT: 5X,2I5  
 ROUTINE: INOPT

COLUMNS	VARIABLE	ENTRY	NOTES
6-10	IEL(1,3)	BEGINNING PLANE ELEMENT NUMBER TO BE PLOTTED.	(1)
11-15	IEL(2,3)	ENDING PLANE ELEMENT NUMBER TO BE PLOTTED.	(1)

GO TO CARD GROUP 8.

NOTES:

- (\*) IF CRDOPT(2) IS NOT EQUAL TO PLOT, SKIP THIS CARD GROUP.
- (1) THE BEGINNING AND ENDING ELEMENT NUMBERS DEFINE A RANGE OF ELEMENTS TO BE PLOTTED.

CARD GROUP 8: BRICK ELEMENT PLOT CONTROL PARAM R-8113-5470  
NO. OF CARDS: 1\*  
FORMAT: 5X,215  
ROUTINE: INOPT

COLUMNS	VARIABLE	ENTRY	NOTES
6-10	IEL(1,4)	BEGINNING BRICK ELEMENT NUMBER TO BE PLOTTED.	(1)
11-15	IEL(2,4)	ENDING BRICK ELEMENT NUMBER TO BE PLOTTED.	(1)

GO TO CARD GROUP 9.

NOTES:

- (\*) IF CROOPT(2) IS NOT EQUAL TO PLOT, SKIP THIS CARD GROUP.
- (1) THE BEGINNING AND ENDING ELEMENT NUMBERS DEFINE A RANGE OF ELEMENTS TO BE PLOTTED.



CARD GROUP 9: SHELL ELEMENT PLOT CONTROL PARAM R-8113-5470  
NO. OF CARDS: 1\*  
FORMAT: 5X,215  
ROUTINE: INOPT

COLUMNS	VARIABLE	ENTRY	NOTES
6-10	IEL(1,5)	BEGINNING SHELL ELEMENT NUMBER TO BE PLOTTED.	(1)
11-15	IEL(2,5)	ENDING SHELL ELEMENT NUMBER TO BE PLOTTED.	(1)

GO TO CARD GROUP 10.

NOTES:

- (\*) IF CRDUPT(2) IS NOT EQUAL TO PLOT, SKIP THIS CARD GROUP.
- (1) THE BEGINNING AND ENDING ELEMENT NUMBERS DEFINE A RANGE OF ELEMENTS TO BE PLOTTED.

CARD GROUP 10: BOUNDARY ELEMENT PLOT CONTROL PA. R-8113-5470  
NO. OF CARDS: 1\*  
FORMAT: 5X,2I5  
ROUTINE: INOPT

COLUMNS	VARIABLE	ENTRY	NOTES
6-10	IEL(1,6)	BEGINNING BOUNDARY ELEMENT NUMBER TO BE PLOTTED.	(1)
11-15	IEL(2,6)	ENDING BOUNDARY ELEMENT NUMBER TO BE PLOTTED.	(1)

GO TO CARD GROUP 11.

NOTES:

(\*) IF CRDUPT(2) IS NOT EQUAL TO PLOT, SKIP THIS CARD GROUP.

(1) THE BEGINNING AND ENDING ELEMENT NUMBERS DEFINE A RANGE OF ELEMENTS TO BE PLOTTED.

CARD GROUP 11: NODAL CONTROL PARAMETERS  
 NO. OF CARDS: NNODE\*  
 FORMAT: 7I5,3F10.0,15  
 ROUTINE: NODATA

R-8113-5470

COLUMNS	VARIABLE	ENTRY	NOTES
1-5	N	NODE NUMBER.	
6-10	ID(N,1)	X-DIRECTION BOUNDARY CONDITION CODE. = 0, UNCONSTRAINED WITHIN THE STRUCTURE = 1, CONSTRAINED WITHIN THE STRUCTURE = 2, HALF-SPACE DEGREE-OF-FREEDOM	(1)
11-15	ID(N,2)	Y-DIRECTION BOUNDARY CONDITION CODE.	
16-20	ID(N,3)	Z-DIRECTION BOUNDARY CONDITION CODE.	
21-25	ID(N,4)	ROTATION ABOUT X-AXIS BOUNDARY CONDITION CODE.	
26-30	ID(N,5)	ROTATION ABOUT Y-AXIS BOUNDARY CONDITION CODE.	
31-35	ID(N,6)	ROTATION ABOUT Z-AXIS BOUNDARY CONDITION CODE.	
36-45	AX(N)	X-COORDINATE.	
46-55	AY(N)	Y-COORDINATE.	
56-65	AZ(N)	Z-COORDINATE.	
66-70	KN	INCREMENT TO BE ADDED TO THE PREVIOUS NODE NUMBER TO GENERATE A NEW NODE NUMBER IN THE SEQUENCE OF NODES ALONG A STRAIGHT LINE.	

GO TO CARD GROUP 12.

NOTES:

(\*) IF CROOPT(1) IS NOT EQUAL TO ELEM OR CROOPT(2) IS NOT EQUAL TO COMP, SKIP THIS CARD GROUP.

(1) IF A PARTICULAR DEGREE-OF-FREEDOM IS CONSTRAINED FOR A SERIES OF NODE CARDS, THIS MAY BE INDICATED BY A BOUNDARY CONDITION CODE OF -1 ON THE FIRST NODE CARD IN THE SERIES AND +1 ON THE LAST NODE CARD IN THE SERIES.

NODAL CONTROL PARAMETERS FOR A GIVEN NODE MAY BE SUPPLIED AND/OR GENERATED MORE THAN ONCE, IN WHICH CASE THE LATEST DATA OVERRIDES THE PREVIOUS ONES. THE INPUT IS TERMINATED BY READING THE DATA FOR THE LAST NODE IN THE SYSTEM.

CARD GROUP 12:  
NO. OF CARDS:  
FORMAT:  
ROUTINE:

TRUSS ELEMENT CONTROL PARAMETERS  
1\*  
315  
ELDATA

R-8113-5470

COLUMNS	VARIABLE	ENTRY	NOTES
1-5	NPAR(1)	ELEMENT TYPE.  = 1, TRUSS	
6-10	NPAR(2)	NUMBER OF TRUSS ELEMENTS.	
11-15	NPAR(3)	NUMBER OF MATERIAL PROPERTY SETS.	

GO TO CARD GROUP 13.

NOTES:

(\*) IF CRDOPT(1) IS NOT EQUAL TO ELEM OR CRDOPT(2) IS NOT EQUAL TO COMP OR TRUSS ELEMENTS ARE NOT EMPLOYED IN THE MODEL, SKIP THIS CARD GROUP.

CARD GROUP 13:  
NO. OF CARDS:  
FORMAT:  
ROUTINE:

TRUSS ELEMENT PROPERTIES  
NPAR(3)\*  
IS,4F10.0  
TRUSS

R-8113-5470

COLUMNS	VARIABLE	ENTRY	NOTES
1-5	N	MATERIAL PROPERTY SET NUMBER.	
6-15	E	MODULUS OF ELASTICITY. (FORCE/AREA)	
16-25	DEN	MASS DENSITY (MASS/VOLUME).	
26-35	AREA	CROSS-SECTIONAL AREA.	
36-45	WT	DISTRIBUTED WEIGHT (WEIGHT/LENGTH)	

GO TO CARD GROUP 14.

NOTES:

(\*) IF CROUPT(1) IS NOT EQUAL TO ELEM OR CROUPT(2) IS NOT EQUAL TO COMP OR TRUSS ELEMENTS ARE NOT EMPLOYED IN THE MODEL, SKIP THIS CARD GROUP.

CARD GROUP 14: TRUSS ELEMENT CONNECTIVITY PARAM. R-8113-5470  
 NO. OF CARDS: NPAR(2)\*  
 FORMAT: 4I5,45X,15  
 ROUTINE: TRUSS

COLUMNS	VARIABLE	ENTRY	NOTES
1-5	M	TRUSS ELEMENT NUMBER.	(1)
6-10	II	FIRST NODE NUMBER ASSOCIATED WITH THE M(TH) TRUSS ELEMENT.	
11-15	JJ	SECOND NODE NUMBER ASSOCIATED WITH THE M(TH) TRUSS ELEMENT.	
16-20	MTYP	MATERIAL PROPERTY SET NUMBER ASSOCIATED WITH THE M(TH) TRUSS ELEMENT.	
66-70	KK	FLAG FOR AUTOMATIC GENERATION OF TRUSS ELEMENT CONNECTIVITY PARAMETERS. DEFAULT = 1.	(1)

GO TO CARD GROUP 15.

NOTES:

(\*) IF CRDOPT(1) IS NOT EQUAL TO ELEM OR CRDOPT(2) IS NOT EQUAL TO COMP OR TRUSS ELEMENTS ARE NOT EMPLOYED IN THE MODEL, SKIP THIS CARD GROUP.

FEWER THAN NPAR(2) CARDS MAY BE INPUT BY MAKING USE OF KK AS DESCRIBED IN NOTE (1).

(1) M SHOULD BE SPECIFIED IN ASCENDING NUMERICAL ORDER. MISSING ELEMENTS ARE GENERATED BY ADDING KK TO THE NODE NUMBERS SPECIFIED ON THE PREVIOUS CARD AND USING THE MATERIAL AND TEMPERATURE CHANGE FROM THE PREVIOUS CARD.

FIGURE A-1 DESCRIBES THE COORDINATE SYSTEM AND DEGREES-OF-FREEDOM FOR THE TRUSS ELEMENT.

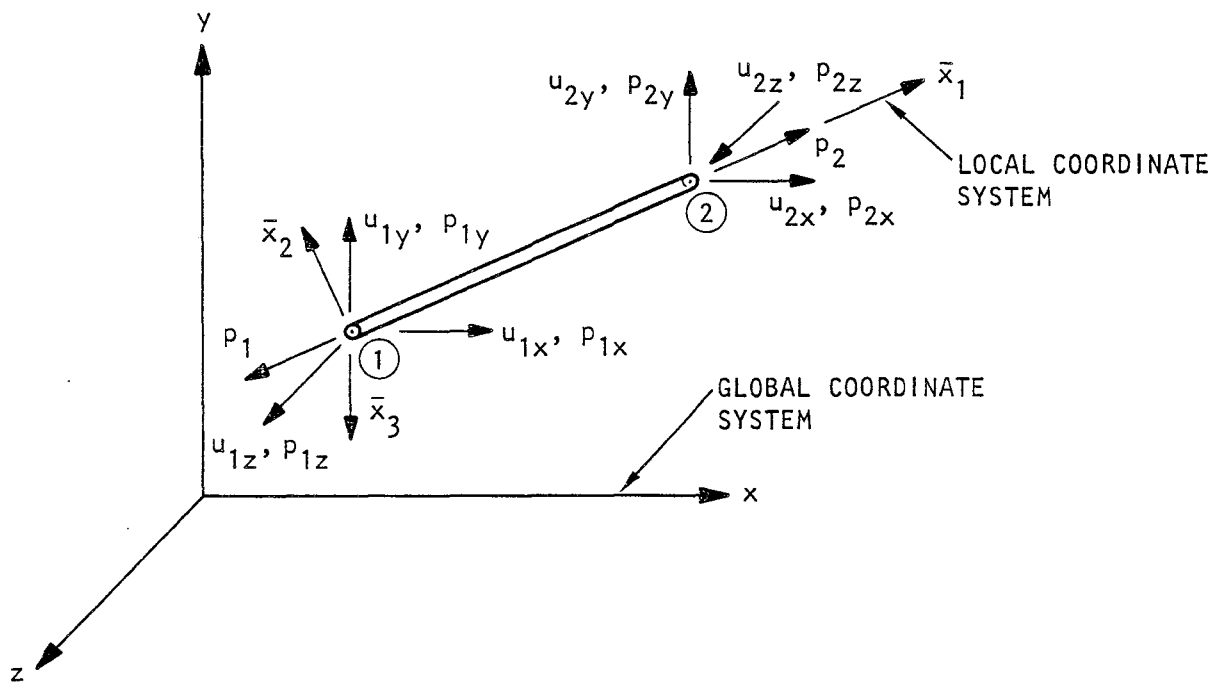


FIGURE A-1. THREE-DIMENSIONAL TRUSS ELEMENT

117<

CARD GROUP 15: BEAM ELEMENT CONTROL PARAMETERS  
 NU. OF CARDS: 1\*  
 FORMAT: 4I5  
 ROUTINE: ELDATA

COLUMNS	VARIABLE	ENTRY	NOTES
1-5	NPAR(1)	ELEMENT TYPE. = 2, BEAM	
6-10	NPAR(2)	NUMBER OF BEAM ELEMENTS.	
11-15	NPAR(3)	NUMBER OF GEOMETRY PROPERTY SETS.	
16-20	NPAR(4)	NUMBER OF MATERIAL PROPERTY SETS.	

GO TO CARD GROUP 16.

NOTES:

- (\*) IF CRDPT(1) IS NOT EQUAL TO ELEM OR CRDPT(2) IS NOT EQUAL TO COMP OR BEAM ELEMENTS ARE NOT EMPLOYED IN THE MODEL, SKIP THIS CARD GROUP.



CARD GROUP 16:  
NO. OF CARDS:  
FORMAT:  
ROUTINE:

BEAM ELEMENT MATERIAL PROPERTIES  
NPAR(4)  
15,3F10.0  
BEAM

R-8113-5470

COLUMNS	VARIABLE	ENTRY	NOTES
1-5	N	MATERIAL PROPERTY SET NUMBER.	
6-15	E	MODULUS OF ELASTICITY. (FORCE/AREA)	
16-25	G	POISSON'S RATIO.	
26-35	R0	MASS DENSITY (MASS/VOLUME).	

GO TO CARD GROUP 17.

NOTES:

- (\*) IF CROUPT(1) IS NOT EQUAL TO ELEM OR CROUPT(2) IS NOT EQUAL TO COMP OR BEAM ELEMENTS ARE NOT EMPLOYED IN THE MODEL, SKIP THIS CARD GROUP.

CARD GROUP 17:  
NO. OF CARDS:  
FORMAT:  
ROUTINE:

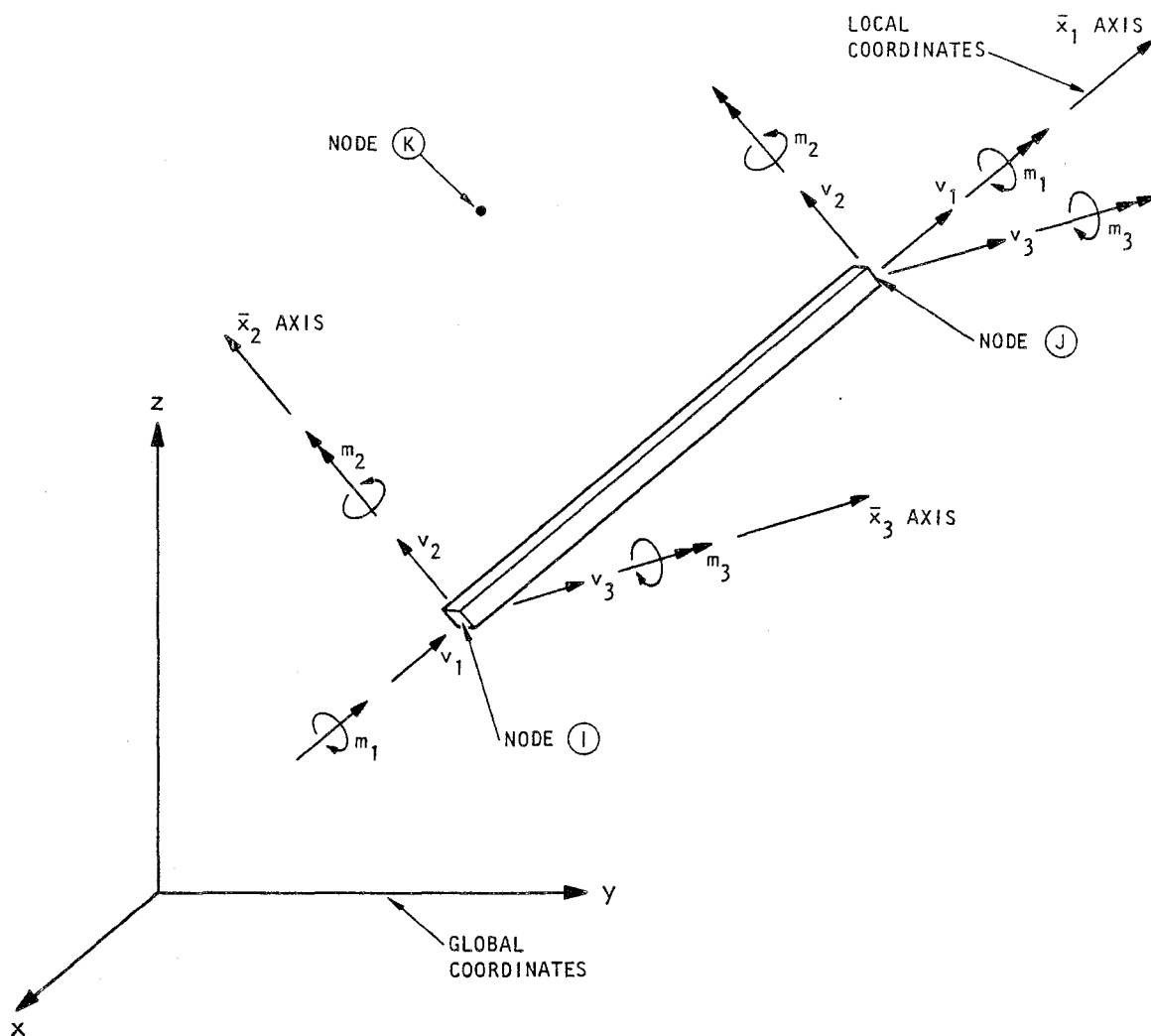
BEAM ELEMENT GEOMETRICAL PROPERTIES R-8113-5470  
NPAR(3)\*  
15,6F10.0  
BEAM

COLUMNS	VARIABLE	ENTRY	NOTES
1-5	N	GEOMETRICAL PROPERTY SET NUMBER.	
6-15	COPROP(1)	CROSS-SECTIONAL AREA.	
16-25	COPROP(2)	SHEAR AREA ASSOCIATED WITH SHEAR FORCES ALONG (1) THE LOCAL X2-AXIS.	
26-35	COPROP(3)	SHEAR AREA ASSOCIATED WITH SHEAR FORCES ALONG (1) THE LOCAL X3-AXIS.	
36-45	COPROP(4)	MOMENT OF INERTIA ABOUT THE LOCAL X1-AXIS.	(1)
46-55	COPROP(5)	MOMENT OF INERTIA ABOUT THE LOCAL X2 AXIS.	(1)
56-65	COPROP(6)	MOMENT OF INERTIA ABOUT THE LOCAL X3 AXIS.	(1)

GO TO CARD GROUP 18.

NOTES:

- (\*) IF CRDOPT(1) IS NOT EQUAL TO ELEM OR CRDOPT(2) IS NOT EQUAL TO COMP OR BEAM ELEMENTS ARE NOT EMPLOYED IN THE MODEL, SKIP THIS CARD GROUP.
- (1) THE ORIENTATION OF THE LOCAL AXES FOR THE BEAM ELEMENT ARE GIVEN IN FIGURE A-2.



## Notes:

- Node I defines the origin of the local coordinate system for the beam.
- Nodes I and J define the  $\bar{x}_1$  axis along the length of the beam.
- Node K can be any point in the  $\bar{x}_1$ - $\bar{x}_2$  plane; i.e., Nodes I, J, and K together define the orientation of this plane.
- The  $\bar{x}_3$  axis is normal to the  $\bar{x}_1$  and  $\bar{x}_2$  axes so as to form a right-handed system.

AA546

FIGURE A-2. BEAM ELEMENT

121

CARD GROUP 18: BEAM ELEMENT CONNECTIVITY PARAMETER R-8113-5470  
 NO. OF CARDS: NPAR(2)\*  
 FORMAT: 6I5,20X,2I6,I8  
 ROUTINE: BEAM

COLUMNS	VARIABLE	ENTRY	NOTES
1-5	INEL	BEAM ELEMENT NUMBER.	(1)
6-10	IN1	NODE I NUMBER ASSOCIATED WITH THE INEL(TH) BEAM ELEMENT.	(2)
11-15	IN2	NODE J NUMBER ASSOCIATED WITH THE INEL(TH) BEAM ELEMENT.	(2)
16-20	INK	NODE K NUMBER ASSOCIATED WITH THE INEL(TH) BEAM ELEMENT.	(2)
21-25	IMAT	MATERIAL PROPERTY SET NUMBER ASSOCIATED WITH THE INEL(TH) BEAM ELEMENT.	
26-30	IMEL	GEOMETRY PROPERTY SET NUMBER ASSOCIATED WITH THE INEL(TH) BEAM ELEMENT.	
51-56	INELKI	END RELEASE CODE AT NODE I.	(3)
57-62	INELKJ	END RELEASE CODE AT NODE J.	(3)
63-70	INC	FLAG FOR AUTOMATIC GENERATION OF BEAM ELEMENT CONNECTIVITY PARAMETERS. DEFAULT = 1.	(1)

GO TO CARD GROUP 19.

NOTES:

(\*) IF CRDOPT(1) IS NOT EQUAL TO ELEM OR CRDOPT(2) IS NOT EQUAL TO COMP OR BEAM ELEMENTS ARE NOT EMPLOYED IN THE MODEL, SKIP THIS CARD GROUP.

FEWER THAN NPAR(2) CARDS MAY BE INPUT BY MAKING USE OF INC AS DESCRIBED IN NOTE (1).

(1) INEL SHOULD BE SPECIFIED IN ASCENDING NUMERICAL ORDER.

MISSING ELEMENTS ARE GENERATED BY ADDING INC TO THE NODE NUMBERS SPECIFIED ON THE PREVIOUS CARD AND USING THE MATERIAL PROPERTY, GEOMETRY PROPERTY, AND FIXED-END FORCE SET NUMBERS, AND END-RELEASE CODES FROM THE PREVIOUS CARD.

(2) FIGURE A-2 DESCRIBES THE NODE NUMBERING FOR BEAM ELEMENTS.

## NOTES: (CONTINUED)

- (3) THE END RELEASE CODE AT EACH NODE IS A SIX DIGIT NUMBER OF 1'S AND 0'S. THE DIGITS CORRESPOND TO  $V_1$ ,  $V_2$ ,  $V_3$ ,  $M_1$ ,  $M_2$  AND  $M_3$ , RESPECTIVELY; WHERE, A 1 SPECIFIES THAT THE CORRESPONDING FORCE OR MOMENT COMPONENT IS ZERO. THIS ALLOWS FOR THE SPECIFICATION OF HINGES AND ROLLERS. FIGURE A-2 DEFINES THE POSITIVE DIRECTIONS OF THESE END FORCES AND MOMENTS.

CARD GROUP 19: PLANE STRESS AND PLANE STRAIN ELEM R-8113-5470  
 CONTROL PARAMETERS  
 NO. OF CARDS: 1\*  
 FORMAT: 415  
 ROUTINE: ELDATA

COLUMNS	VARIABLE	ENTRY	NOTES
1-5	NPAR(1)	ELEMENT TYPE. = 3, PLANAR	
6-10	NPAR(2)	NUMBER OF PLANAR ELEMENTS.	
11-15	NPAR(3)	NUMBER OF MATERIAL PROPERTY SETS.	
21-25	NPAR(4)	IDENTIFICATION FLAG FOR LOCAL X1X2-PLANE. = 0, XY-PLANE. = 1, OTHERWISE.	(1)

GO TO CARD GROUP 20.

NOTES:

- (\*) IF CRDOPT(1) IS NOT EQUAL TO ELEM OR CRDOPT(2) IS NOT EQUAL TO COMP OR PLANAR ELEMENTS ARE NOT EMPLOYED IN THE MODEL, SKIP THIS CARD GROUP.
- (1) THE LOCAL X1-AXIS OF A PLANAR ELEMENT IS ASSUMED TO LINE ALONG THE GLOBAL X-AXIS. A NPAR(4) OF "1" SPECIFIES THAT THE LOCAL X1-AXIS LIES ALONG THE IJ SIDE OF THE ELEMENT AND THE LOCAL X2-AXIS IS PERPENDICULAR TO IT AND IN THE PLANE OF THE ELEMENT. SEE FIGURE A-5.

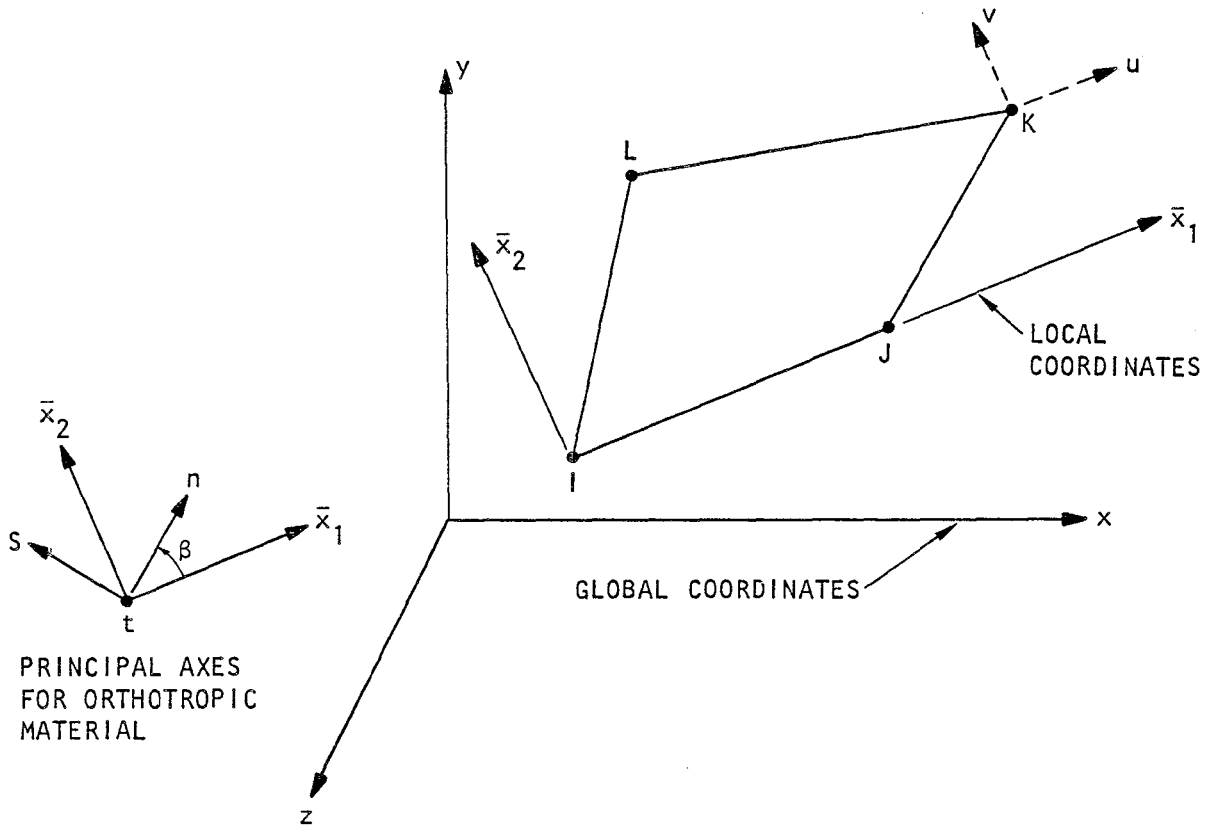


FIGURE A-3. PLANE STRESS AND PLANE STRAIN ELEMENT

CARD GROUP 20: PLANE STRESS AND PLANE STRAIN ELEMENTS  
 MATERIAL PROPERTIES  
 NO. OF CARDS: 2\*NPARK(3)\*  
 FORMAT: IS,3F10.0/7F10.0  
 ROUTINE: PLANE

CARD 1

-----

COLUMNS	VARIABLE	ENTRY	NOTES
1-5	MAT	MATERIAL PROPERTY SET NUMBER.	
6-15	WT	WEIGHT DENSITY (FORCE/VOLUME).	
16-25	RO	MASS DENSITY (WEIGHT/VOLUME).	
26-35	WANG	MATERIAL PRINCIPAL N-AXIS ORIENTATION MEASURED CONTOUR-CLOCKWISE FROM THE LOCAL X1-AXIS (DEGREES).	(1)

CARD 2

-----

1-10	E(2)	MODULUS OF ELASTICITY ALONG THE PRINCIPAL N-AXIS. (FORCE/AREA)	
11-20	E(3)	MODULUS OF ELASTICITY ALONG THE PRINCIPAL S-AXIS. (FORCE/AREA)	
21-30	E(4)	MODULUS OF ELASTICITY ALONG THE PRINCIPAL T-AXIS. (FORCE/AREA)	(2)
31-40	E(5)	POISSON'S RATIO OF THE PRINCIPAL N-AXIS STRAIN DUE TO UNIT STRAIN ALONG THE PRIN- CIPAL S-AXIS.	
41-50	E(6)	POISSON'S RATIO OF THE PRINCIPAL N-AXIS STRAIN DUE TO UNIT STRAIN ALONG THE PRIN- CIPAL T-AXIS.	(2)
51-60	E(7)	POISSON'S RATIO OF THE PRINCIPAL S-AXIS STRAIN DUE TO UNIT STRAIN ALONG THE PRIN- CIPAL T-AXIS.	(2)
61-70	E(8)	SHEAR MODULUS IN THE PRINCIPAL NS-PLANE. (FORCE/AREA)	

GO TO CARD GROUP 21.

NOTES:

- (\*) IF CRDPT(1) IS NOT EQUAL TO ELEM OR CRDPT(2) IS NOT EQUAL TO  
 COMP OR PLANE ELEMENTS ARE NOT EMPLOYED IN THE MODEL, SKIP THIS  
 CARD GROUP. THIS GROUP MUST BE REPEATED NPAR(3) TIMES.



## NOTES: (CONTINUED)

- (1) THE N, S, AND T AXES ARE THE PRINCIPAL AXES FOR THE ORTHOTROPIC MATERIAL. SEE FIGURE A-3.
- (2) PLANE STRESS IS CHARACTERIZED BY SETTING:  
 $E(4) = E(6) = E(7) = E(11) = 0.$   
THE VALUE OF  $E(8)$  SHOULD NOT BE 0.

CARD GROUP 21: PLANE STRESS AND PLANE STRAIN ELEMENT R-8113-5470  
CONNECTIVITY PARAMETERS  
NO. OF CARDS: NPAR(2)\*  
FORMAT: 6I5,F10.0,25X,I5  
ROUTINE: PLANE

COLUMNS	VARIABLE	ENTRY	NOTES
1-5	MM	PLANAR ELEMENT NUMBER.	(1)
6-10	IY(1)	NODE I NUMBER ASSOCIATED WITH THE MM(TH) PLANAR ELEMENT.	(2)
11-15	IY(2)	NODE J NUMBER ASSOCIATED WITH THE MM(TH) PLANAR ELEMENT.	(2)
16-20	IY(3)	NODE K NUMBER ASSOCIATED WITH THE MM(TH) PLANAR ELEMENT.	(2)
21-25	IY(4)	NODE L NUMBER ASSOCIATED WITH THE MM(TH) PLANAR ELEMENT. = IY(3) OR 0, TRIANGULAR ELEMENT.	(2)
26-30	IY(5)	MATERIAL PROPERTY SET NUMBER ASSOCIATED WITH THE MM(TH) PLANAR ELEMENT.	
31-40	TH	ELEMENT THICKNESS. = 0, PLANE STRAIN.	
66-70	INCL	FLAG FOR AUTOMATIC GENERATION OF PLANAR ELEMENT CONNECTIVITY PARAMETERS. DEFAULT = 1.	(1)

GO TO CARD GROUP 22.

NOTES:

(\*) IF CROOPT(1) IS NOT EQUAL TO ELEM OR CROOPT(2) IS NOT EQUAL TO COMP OR PLANE ELEMENTS ARE NOT EMPLOYED IN THE MODEL, SKIP THIS CARD GROUP.

FEWER THAN NPAR(2) CARDS MAY BE INPUT BY MAKING USE OF INCL AS DESCRIBED IN NOTE (1).

(1) MM SHOULD BE SPECIFIED IN ASCENDING NUMERICAL ORDER.

MISSING ELEMENTS ARE GENERATED BY ADDING INCL TO THE NODE NUMBERS SPECIFIED ON THE PREVIOUS CARD AND USING THE MATERIAL PROPERTY SET NUMBER AND THE ELEMENT THICKNESS FROM THE PREVIOUS CARD.

(2) A RIGHT-HAND COORDINATE SYSTEM DICTATES THAT NODES I, J, K AND L MUST BE SEQUENTIALLY POSITIONED IN A COUNTER-CLOCKWISE MANNER AROUND THE ELEMENT, WHEN THE LOCAL X1X2-PLANE LIES ON THE GLOBAL XY-PLANE. SEE FIGURE A-3.

CARD GROUP 22: BRICK ELEMENT CONTROL PARAMETERS  
 NO. OF CARDS: 1\*  
 FORMAT: 315  
 ROUTINE: ELDATA

COLUMNS	VARIABLE	ENTRY	NOTES
1-5	NPAR(1)	ELEMENT TYPE. = 4, THREE-DIMENSIONAL SOLID 8 NODE BRICK	
6-10	NPAR(2)	NUMBER OF BRICK ELEMENTS.	
11-15	NPAR(3)	NUMBER OF MATERIAL PROPERTY SETS.	

GO TO CARD GROUP 23.

NOTES:

- (\*) IF CRDOPT(1) IS NOT EQUAL TO ELEM OR CRDOPT(2) IS NOT EQUAL TO COMP OR BRICK ELEMENTS ARE NOT EMPLOYED IN THE MODEL, SKIP THIS CARD GROUP.

CARD GROUP 23:  
NO. OF CARDS:  
FORMAT:  
ROUTINE:

BRICK ELEMENT MATERIAL PROPERTIES R-8113-5470  
NPAR(3)\*  
15,3F10.0  
BRICK

COLUMNS	VARIABLE	ENTRY	NOTES
1-5	N	MATERIAL PROPERTY SET NUMBER.	
6-15	EE	MODULUS OF ELASTICITY. (FORCE/AREA)	
16-25	ENU	POISSON'S RATIO.	
26-35	RHO	WEIGHT DENSITY (WEIGHT/VOLUME).	

GO TO CARD GROUP 24.

NOTES:

(\*) IF CRDOPT(1) IS NOT EQUAL TO ELEM OR CRDOPT(2) IS NOT EQUAL TO COMP OR BRICK ELEMENTS ARE NOT EMPLOYED IN THE MODEL, SKIP THIS CARD GROUP.

CARD GROUP 24:  
NO. OF CARDS:  
FORMAT:  
ROUTINE:

BRICK ELEMENT CONNECTIVITY PARAMETER  
NPAR(2)\*  
1215  
BRICK

R-8113-5470

COLUMNS	VARIABLE	ENTRY	NOTES
1-5	INEL	BRICK ELEMENT NUMBER.	(1)
6-10	INP(1)	FIRST NODE NUMBER ASSOCIATED WITH THE INEL(TH) BRICK ELEMENT.	(2)
11-15	INP(2)	SECOND NODE NUMBER ASSOCIATED WITH THE INEL(TH) BRICK ELEMENT.	(2)
16-20	INP(3)	THIRD NODE NUMBER ASSOCIATED WITH THE INEL(TH) BRICK ELEMENT.	(2)
21-25	INP(4)	FOURTH NODE NUMBER ASSOCIATED WITH THE INEL(TH) BRICK ELEMENT.	(2)
26-30	INP(5)	FIFTH NODE NUMBER ASSOCIATED WITH THE INEL(TH) BRICK ELEMENT.	(2)
31-35	INP(6)	SIXTH NODE NUMBER ASSOCIATED WITH THE INEL(TH) BRICK ELEMENT.	(2)
36-40	INP(7)	SEVENTH NODE NUMBER ASSOCIATED WITH THE INEL(TH) BRICK ELEMENT.	(2)
41-45	INP(8)	EIGHTH NODE NUMBER ASSOCIATED WITH THE INEL(TH) BRICK ELEMENT.	(2)
46-50	ININT	ORDER OF INTEGRATION.  = 2, RECTANGULAR SHAPED ELEMENT = 3, SKEWED SHAPED ELEMENT = 4, EXTREMELY DISTORTED SHAPED ELEMENT	(3)
51-55	IMAT	MATERIAL PROPERTY SET NUMBER ASSOCIATED WITH THE INEL(TH) BRICK ELEMENT.	
56-60	IINC	FLAG FOR AUTOMATIC GENERATION OF BRICK ELEMENT CONNECTIVITY PARAMETERS.	(1)

GO TO CARD GROUP 25.

NOTES:

(\*) IF CRDPT(1) IS NOT EQUAL TO ELEM OR CRDPT(2) IS NOT EQUAL TO COMP OR BRICK ELEMENTS ARE NOT EMPLOYED IN THE MODEL, SKIP THIS CARD GROUP.

FEWER THAN NPAR(2) CARDS MAY BE INPUT BY MAKING USE OF IINC AS DESCRIBED IN NOTE (1).

## NOTES: (CONTINUED)

- (1) INEL SHOULD BE SPECIFIED IN ASCENDING NUMERICAL ORDER.

MISSING ELEMENTS ARE GENERATED BY ADDING IINC TO THE NODE NUMBERS SPECIFIED ON THE PREVIOUS CARD AND USING THE ORDER OF INTEGRATION AND MATERIAL PROPERTY SET NUMBER FROM THE PREVIOUS CARD.

- (2) FIGURE A-4 SHOWS NODE NUMBERING AND DEGREES-OF-FREEDOM FOR BRICK ELEMENTS.

- (3) COMPUTATION TIME FOR ELEMENTS STIFFNESS INCREASES WITH THE CUBE OF THE INTEGRATION ORDER. THEREFORE, THE SMALLEST POSSIBLE ORDER OF INTEGRATION SHOULD BE USED, AND RECTANGULAR ELEMENTS SHOULD BE EMPLOYED AS MUCH AS POSSIBLE.

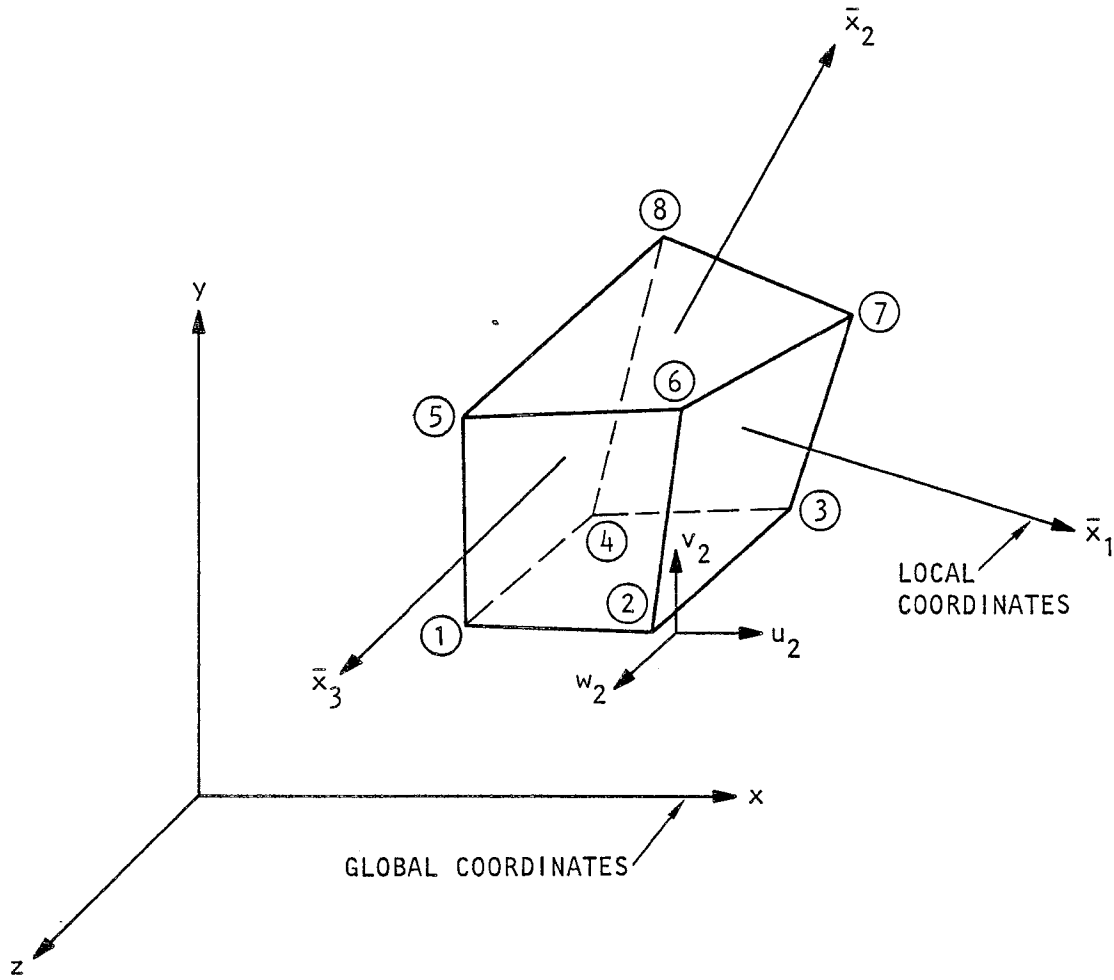


FIGURE A-4. THREE-DIMENSIONAL BRICK ELEMENT

CARD GROUP 25:  
NO. OF CARDS:  
FORMAT:  
ROUTINE:

SHELL ELEMENT CONTROL PARAMETERS  
1\*  
315  
ELDATA

R-8113-5470

COLUMNS	VARIABLE	ENTRY	NOTES
1-5	NPAR(1)	ELEMENT TYPE.  = 5, SHELL	
6-10	NPAR(2)	NUMBER OF SHELL ELEMENTS.	
11-15	NPAR(3)	NUMBER OF MATERIAL PROPERTY SETS.	

GO TO CARD GROUP 26.

NOTES:

- (\*) IF CRDPT(1) IS NOT EQUAL TO ELEM OR CRDPT(2) IS NOT EQUAL TO COMP OR SHELL ELEMENTS ARE NOT EMPLOYED IN THE MODEL, SKIP THIS CARD GROUP.



CARD GROUP 26: SHELL ELEMENT MATERIAL PROPERTIES  
 NO. OF CARDS: 2\*NPARK(3)\*  
 FORMAT: I10,7F10.0  
 ROUTINE: SHELL

CARD 1  
 -----

COLUMNS	VARIABLE	ENTRY	NOTES
1-10	J	MATERIAL PROPERTY SET NUMBER.	
11-20	C(1)	MASS DENSITY (MASS/VOLUME).	
21-30	C(2)	EFFECTIVE MODULUS OF ELASTICITY ALONG THE LOCAL X1-AXIS DUE TO A UNIT STRAIN ALONG THE LOCAL X1-AXIS, IE. $E / (1 - (\text{POIS})^{**2})$ .	(1)
31-40	C(3)	EFFECTIVE MODULUS OF ELASTICITY ALONG THE LOCAL X1-AXIS DUE TO A UNIT STRAIN ALONG THE LOCAL X2-AXIS, IE. $C(2) * \text{POIS}$ .	(1)
41-50	C(4)	EFFECTIVE MODULUS OF ELASTICITY ALONG THE LOCAL X1-AXIS DUE TO A UNIT STRAIN ALONG THE LOCAL X3-AXIS, IE. ZERO.	(1)
51-60	C(5)	EFFECTIVE MODULUS OF ELASTICITY ALONG THE LOCAL X2-AXIS DUE TO A UNIT STRAIN ALONG THE LOCAL X2-AXIS, IE. C(2).	(1)
61-70	C(6)	EFFECTIVE MODULUS OF ELASTICITY ALONG THE LOCAL X2-AXIS DUE TO A UNIT STRAIN ALONG THE LOCAL X3-AXIS, IE. ZERO.	(1)
71-80	C(7)	SHEAR MODULUS OF ELASTICITY, IE. $E / (2 * (1 + \text{POIS}))$	(1)

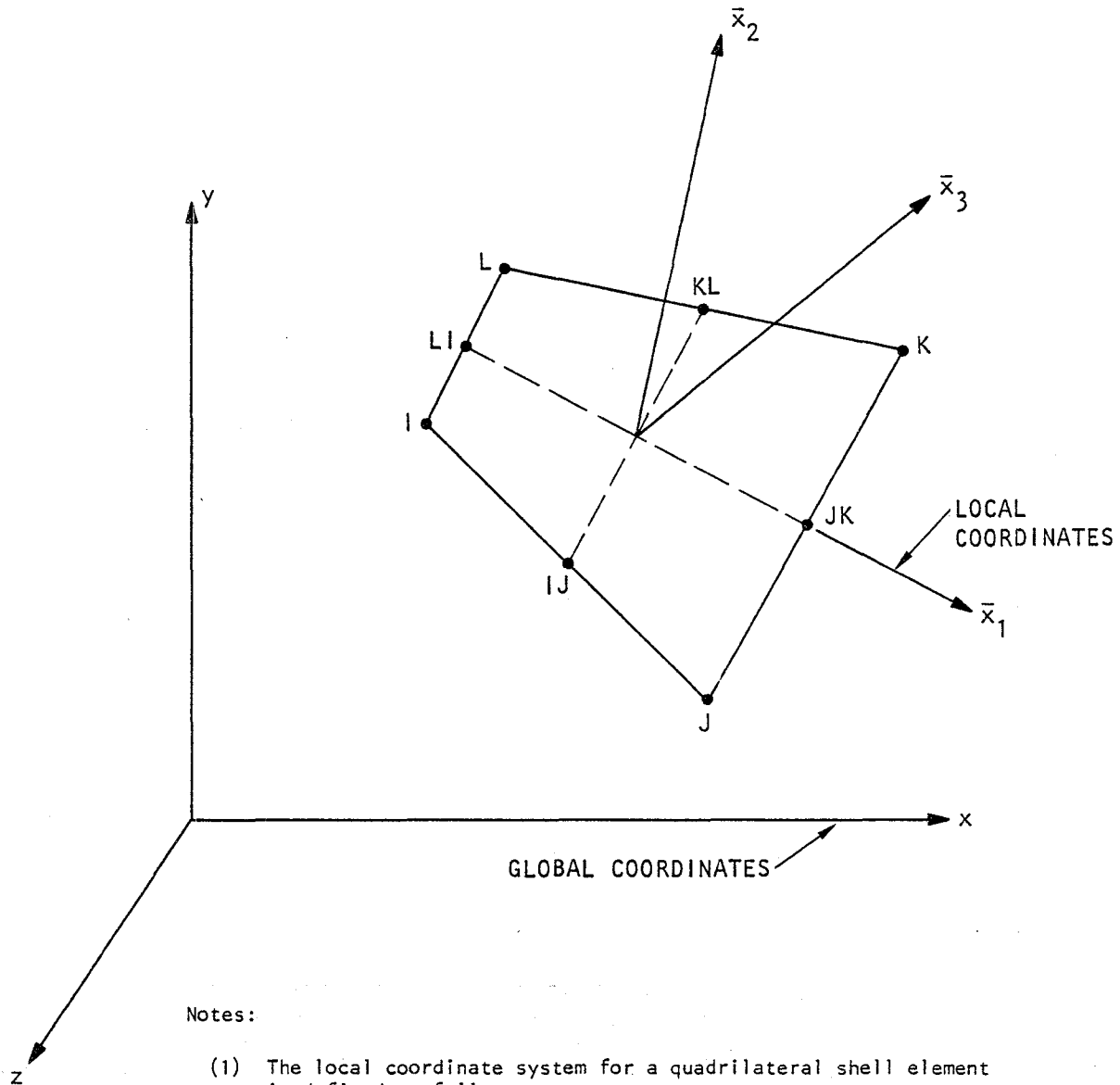
GO TO CARD GROUP 27.

NOTES:

(\*) IF CRDOPT(1) IS NOT EQUAL TO ELEM OR CRDOPT(2) IS NOT EQUAL TO COMP OR SHELL ELEMENTS ARE NOT EMPLOYED IN THE MODEL, SKIP THIS CARD GROUP.

(1) E ==> YOUNG'S MODULUS.  
 POIS ==> POISSON'S RATIO.

FIGURE A-5 SHOWS THE COORDINATE SYSTEM FOR SHELL ELEMENTS.



## Notes:

- (1) The local coordinate system for a quadrilateral shell element is defined as follows:

$\bar{x}_1$  — Specified by LI-JK, where LI and JK are midpoints of sides L-I and J-K.

$\bar{x}_3$  — Normal to  $\bar{x}_1$  and to the line joining midpoints IJ and KL.

$\bar{x}_2$  — Normal to  $\bar{x}_1$  and  $\bar{x}_3$  to complete the right-handed system.

- (2) For a triangular shell element, Nodes I and L share the same position, and the  $\bar{x}_1$ ,  $\bar{x}_2$  and  $\bar{x}_3$  axes are otherwise defined similarly as for a quadrilateral element.

FIGURE A-5. SHELL ELEMENT

CARD GROUP 27: SHELL ELEMENT CONNECTIVITY PARAMETER R-8113-5470  
 NO. OF CARDS: NPAR(2)\*  
 FORMAT: 8I5,F10.0  
 ROUTINE: SHELL

COLUMNS	VARIABLE	ENTRY	NOTES
1-5	MM	SHELL ELEMENT NUMBER.	(1)
6-10	IY(1)	NODE I NUMBER ASSOCIATED WITH THE MM(TH) SHELL ELEMENT.	(2)
11-15	IY(2)	NODE J NUMBER ASSOCIATED WITH THE MM(TH) SHELL ELEMENT.	(2)
16-20	IY(3)	NODE K NUMBER ASSOCIATED WITH THE MM(TH) SHELL ELEMENT.	(2)
21-25	IY(4)	NODE L NUMBER ASSOCIATED WITH THE MM(TH) SHELL ELEMENT. DEFAULT = TRIANGULAR ELEMENT.	(2)
26-30	IY(5)	NODE U NUMBER ASSOCIATED WITH THE MM(TH) SHELL ELEMENT. DEFAULT => CALCULATION OF MID-NODE PROPERTIES FROM AVERAGE OF CORNER NODES.	(2)
31-35	IY(6)	MATERIAL PROPERTY SET NUMBER ASSOCIATED THE MM(TH) SHELL ELEMENT.	
36-40	IY(7)	FLAG FOR AUTOMATIC GENERATION OF SHELL ELEMENT CONNECTIVITY PARAMETERS.	(1)
41-50	ELY(1)	ELEMENT THICKNESS.	

GO TO CARD GROUP 28.

NOTES:

(\*) IF CRDOPT(1) IS NOT EQUAL TO ELEM OR CRDOPT(2) IS NOT EQUAL TO COMP OR SHELL ELEMENTS ARE NOT EMPLOYED IN THE MODEL, SKIP THIS CARD GROUP.

FEWER THAN NPAR(2) CARDS MAY BE INPUT BY MAKING USE OF IY(7) AS DESCRIBED IN NOTE (1).

(1) MM SHOULD BE SPECIFIED IN ASCENDING NUMERICAL ORDER.

MISSING ELEMENTS ARE GENERATED BY ADDING IY(7) TO THE NODE NUMBERS SPECIFIED ON THE PREVIOUS CARD AND USING THE MATERIAL PROPERTY SET NUMBER AND THE ELEMENT THICKNESS FROM THE PREVIOUS CARD.

(2) A RIGHT-HAND COORDINATE SYSTEM DICTATES THAT NODES I, J, K AND L MUST BE SEQUENTIALLY POSITIONED IN A COUNTER-CLOCKWISE MANNER AROUND THE ELEMENT. SEE FIGURE A-5.

CARD GROUP 28:

BOUNDARY (SPRING) ELEMENT CONTROL  
PARAMETERS

R-8113-5470

NO. OF CARDS:

1\*

FORMAT:

IS

ROUTINE:

ELDATA

COLUMNS	VARIABLE	ENTRY	NOTES
1-5	NPAR(1)	ELEMENT TYPE. = 6, BOUNDARY ELEMENT.	
6-10	NPAR(2)	NUMBER OF BOUNDARY ELEMENTS.	

GO TO CARD GROUP 29.

NOTES:

(\*) IF CRDOPT(1) IS NOT EQUAL TO ELEM OR CRDOPT(2) IS NOT EQUAL TO  
COMP OR BOUNDARY ELEMENTS ARE NOT EMPLOYED IN THE MODEL, SKIP  
THIS CARD GROUP.

CARD GROUP 29:                   BOUNDARY ELEMENT CONNECTIVITY PARA   R-8113-5470  
 NO. OF CARDS:               NPAR(2)\*  
 FORMAT:                    815,2F10.0  
 ROUTINE:                    BDCUN

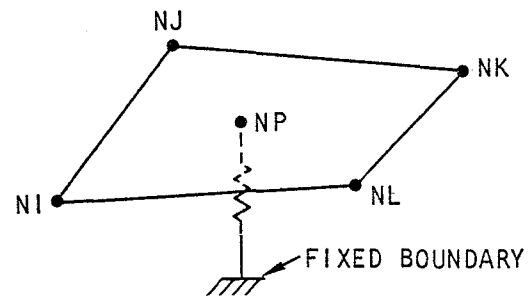
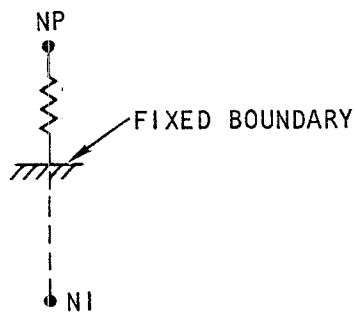
COLUMNS	VARIABLE	ENTRY	NOTES
1-5	NP	ATTACHMENT NODE NUMBER ASSOCIATED WITH THE BOUNDARY ELEMENT.	(1)
6-10	NI	NODE I NUMBER ASSOCIATED WITH THE BOUNDARY ELEMENT.	(1)
11-15	NJ	NODE J NUMBER ASSOCIATED WITH THE BOUNDARY ELEMENT.	(1)
16-20	NK	NODE K NUMBER ASSOCIATED WITH THE BOUNDARY ELEMENT.	(1)
21-25	NL	NODE L NUMBER ASSOCIATED WITH THE BOUNDARY ELEMENT.	(1)
25-30	KD	DISPLACEMENT INDICATOR. = 0, UNCONSTRAINED ( NO SPRING ). = 1, CONSTRAINED.	
31-35	KR	ROTATION INDICATOR. = 0, UNCONSTRAINED ( NO SPRING ). = 1, CONSTRAINED.	
36-40	KN	FLAG FOR AUTOMATIC GENERATION OF BOUNDARY ELEMENT CONNECTIVITY PARAMETERS.	
41-50	SD	SPECIFIED NORMAL DISPLACEMENT.	
51-60	SR	SPECIFIED ROTATION ABOUT THE NORMAL.	

GO TO CARD GROUP 30.

NOTES:

(\*) IF CRDPT(1) IS NOT EQUAL TO ELEM OR CRDPT(2) IS NOT EQUAL TO CUMP OR BOUNDARY ELEMENTS ARE NOT EMPLOYED IN THE MODEL, SKIP THIS CARD GROUP.

(1) SEE FIGURE A-6.



(a) Element with orientation defined by Nodes NP and NI

(b) Element normal to plane defined by Nodes NI, NJ, NK and NL

FIGURE A-6. ALTERNATIVE DEFINITIONS OF ONE-DIMENSIONAL BOUNDARY ELEMENT

CARD GROUP 30:

IMPEDANCE HALF-SPACE  
CONTROL PARAMETERS

R-8113-5470

NO. OF CARDS:

2\*

FORMAT:

215/3F10.0

ROUTINE:

BASSIN1

CARD 1

COLUMNS	VARIABLE	ENTRY	NOTES
1-5	NELINT	NUMBER OF HALF-SPACE SUBREGIONS.	
6-10	NFREQ	NUMBER OF EXCITATION FREQUENCIES.	

CARD 2

1-10	GNU	SHEAR MODULUS OF THE HALF-SPACE. ( FORCE / AREA )	
11-20	RHO	MASS DENSITY OF THE HALF-SPACE. ( WEIGHT * TIME**2 / DISTANCE**4 )	
21-30	POISSN	POISSON RATIO OF THE HALF-SPACE.	(1)

GO TO CARD GROUP 31.

NOTES:

(\*) IF CRDOPT(1) IS NOT EQUAL TO IMPE OR CRDOPT(2) IS NOT EQUAL TO COMP, SKIP THIS CARD GROUP.

(1)  $0.1 < \text{POISSN} < 0.4$ .

141<

CARD GROUP 31: IMPEDANCE HALF-SPACE  
 CONNECTIVITY PARAMETERS  
 NO. OF CARDS: NELINT\*  
 FORMAT: SIS  
 ROUTINE: FIMPD

COLUMNS	VARIABLE	ENTRY	NOTES
1-5	NLL	HALF-SPACE SUBREGION NUMBER.	
6-10	NE(1)	NODE I NUMBER ASSOCIATED WITH THE NLL(TH) HALF-SPACE SUBREGION.	(1)
11-15	NE(2)	NODE J NUMBER ASSOCIATED WITH THE NLL(TH) HALF-SPACE SUBREGION.	(1)
16-20	NE(3)	NODE K NUMBER ASSOCIATED WITH THE NLL(TH) HALF-SPACE SUBREGION.	(1)
21-25	NE(4)	NODE L NUMBER ASSOCIATED WITH THE NLL(TH) HALF-SPACE SUBREGION.	(1)

GO TO CARD GROUP 32.

NOTES:

- (\*) IF CRDOPT(1) IS NOT EQUAL TO IMPE OR CRDOPT(2) IS NOT EQUAL TO COMP, SKIP THIS CARD GROUP.
- (1) A RIGHT-HAND COORDINATE SYSTEM DICTATES THAT NODE I, J, K AND L MUST BE SEQUENTIALLY POSITIONED IN A COUNTER-CLOCKWISE MANNER AROUND THE SUBREGION.



CARD GROUP 32: IMPEDANCE HALF-SPACE  
EXCITATION PARAMETERS  
NO. OF CARDS: NFRFN\*  
FORMAT: F10.0  
ROUTINE: FIMPD

COLUMNS	VARIABLE	ENTRY	NOTES
1-10	A0	EXCITATION FREQUENCY (HERTZ)	

GO TO CARD GROUP 33.

NOTES:

(\* ) IF CRDOPT(1) IS NOT EQUAL TO IMPE OR CRDOPT(2) IS NOT EQUAL TO  
COMP, SKIP THIS CARD GROUP.

CARD GROUP 33: FREE-FIELD DISPLACEMENT  
CONTROL PARAMETERS  
NO. OF CARDS: 1\*  
FORMAT: 215  
ROUTINE: BASSINI

COLUMNS	VARIABLE	ENTRY	NOTES
1-5	LWTYP	WAVE TYPE INDICATOR.  = 0, RAYLEIGH WAVE. = 1, P-WAVE. = 2, SH-WAVE. = 3, SV-WAVE.	
6-10	NCASE	NUMBER OF WAVE PROPAGATION DIRECTIONS AS DEFINED BY THETA(H) AND THETA(V).	

IF LWTYP IS EQUAL TO ZERO GO TO CARD GROUP 35,  
OTHERWISE, GO TO CARD GROUP 34.

NOTES:

- (\*) IF CRDPT(1) IS NOT EQUAL TO FREE OR CRDPT(2) IS NOT EQUAL TO  
COMP, SKIP THIS CARD GROUP.

CARD GROUP 34: FREE-FIELD DISPLACEMENT  
 BODY WAVE PROPERTIES  
 NO. OF CARDS: NCASE\*  
 FORMAT: BF10.0  
 ROUTINE: FRWAVE

COLUMNS	VARIABLE	ENTRY	NOTES
1-10	TV	THE VERTICAL ANGLE OF INCIDENCE MEASURED RELATIVE TO THE GLOBAL XY-PLANE. (DEGREES)	
11-20	TH	THE HORIZONTAL ANGLE OF INCIDENCE MEASURED RELATIVE TO THE GLOBAL XZ-PLANE. (DEGREES)	
21-30	REAL(WA(1))	REAL COMPONENT OF PWAVE AMPLITUDE.	
31-40	IMAG(WA(1))	IMAGINARY COMPONENT OF PWAVE AMPLITUDE.	
41-50	REAL(WA(2))	REAL COMPONENT OF SHWAVE AMPLITUDE.	
51-60	IMAG(WA(2))	IMAGINARY COMPONENT OF SHWAVE AMPLITUDE.	
61-70	REAL(WA(3))	REAL COMPONENT OF SVWAVE AMPLITUDE.	
71-80	IMAG(WA(3))	IMAGINARY COMPONENT OF SVWAVE AMPLITUDE.	

TERMINATE PROGRAM EXECUTION.

NOTES:

- (\*) IF CRDOPT(1) IS NOT EQUAL TO FREE OR CRDOPT(2) IS NOT EQUAL TO  
 COMP OR LWTYP = 0, SKIP THIS CARD GROUP.

CARD GROUP 35:

FREE-FIELD DISPLACEMENT  
RAYLEIGH SURFACE WAVE PROPERTIES  
NCASE\*  
3F10.0  
FRWAVE

R-8113-5470

NO. OF CARDS:

FORMAT:

ROUTINE:

COLUMNS	VARIABLE	ENTRY	NOTES
1-10	TH	THE HORIZONTAL ANGLE OF INCIDENCE RELATIVE TO THE GLOBAL XZ-PLANE. (DEGREES)	
11-20	REAL(WA)	REAL COMPONENT OF RAYLEIGH WAVE AMPLITUDE.	
21-30	IMAG(WA)	IMAGINARY COMPONENT OF RAYLEIGH WAVE AMPLITUDE.	

TERMINATE PROGRAM EXECUTION.

NOTES:

(\*) IF CRDOPT(1) IS NOT EQUAL TO FREE OR CRDOPT(2) IS NOT EQUAL TO COMP OR LWTYP IS NOT EQUAL TO 0, SKIP THIS CARD GROUP.



APPENDIX B  
INPUT DESCRIPTION FOR BASSIN2

This appendix contains a description of the user-provided input data for the BASSIN2 subprogram, in accordance with the general description provided in Section 3.2 of Chapter 3. These data are contained in a total of 6 card groups, and should be provided in units that are consistent with those used for the BASSIN1 input. It is noted that, in addition to these card groups, peripheral storage generated by BASSIN1 must be input to BASSIN2 through FORTRAN Logical Unit 8. Output from BASSIN2 is in the form of print and (optionally) plots.

CARD GROUP 1:  
ND. OF CARDS:  
FORMAT:  
ROUTINE:

PROBLEM TITLE  
VARIABLE\*  
1X,A1,12A6  
BASSIN2

R-8113-5470

COLUMNS	VARIABLE	ENTRY	NOTES
2	ISTAR	CARD GROUP TERMINATION FLAG;  = ^, CARD IS OPTIONAL, IGNORED, AND MAY BE USED FOR CONTROL DATA COMMENTS. ( ^ DENOTES A BLANK )  = *, CARD CONTAINS PROBLEM TITLE	
3-74	HEAD(1) THROUGH HEAD(12)	PROBLEM TITLE, 72 CHARACTER MAXIMUM.	(1)

GO TO CARD GROUP 2.

NOTES:

- (\*) THE COMMENT CAN BE SPECIFIED BY ANY NUMBER OF CARDS. HOWEVER, ONE CARD MUST BE INPUT WITH ISTAR = \* AND MUST BE THE LAST CARD OF THIS GROUP.
- (1) THIS INFORMATION IS INCLUDED IN ALL FORMS OF OUTPUT PROVIDED BY THE PROGRAM, AND SHOULD BE CENTERED IN THE FIELD PROVIDED.

CARD GROUP 2:  
NO. OF CARDS:  
FORMAT:  
ROUTINE:

PLOT CONTROL PARAMETERS  
1  
IS  
DYNINT

R-8113-5470

COLUMNS	VARIABLE	ENTRY	NOTES
1-5	NPLOT	NUMBER OF PLOT FRAMES	

IF NPLOT IS SET TO ZERO, GO TO CARD GROUP 4.  
OTHERWISE, GO TO CARD GROUP 3.

CARD GROUP 3:  
NO. OF CARDS:  
FORMAT:  
ROUTINE:

PLOT FRAME PARAMETERS  
NPLUT  
I5,4X,A1,4X,A1  
DYNINT

R-8113-5470

COLUMNS	VARIABLE	ENTRY	NOTES
1-5	IPLUT(1)	NODAL POINT ORDINAL.	
10	IPLUT(2)	DIRECTION INDICATOR. = X, IN THE X DIRECTION. = Y, IN THE Y DIRECTION. = Z, IN THE Z DIRECTION.	
15	IPLUT(3)	COMPONENT INDICATOR. = A, AMPLITUDE. = P, PHASE.	

GO TO CARD GROUP 4.



CARD GROUP 4:  
NO. OF CARDS:  
FORMAT:  
ROUTINE:

MODAL TRUNCATION CONTROL PARAMETER R-8113-5470  
1  
IS  
DYNINI

COLUMNS	VARIABLE	ENTRY	NOTES
1-5	NTRUNC	MODAL TRUNCATION INDICATOR. = 0, MODAL TRUNCATION IS NOT EMPLOYED. = 1, MODAL TRUNCATION IS EMPLOYED.	

GO TO CARD GROUP 5.

CARD GROUP 5: DAMPING RATIOS  
 NO. OF CARDS: (NTRQ-1)/8+1\*  
 FORMAT: 8F10.0  
 ROUTINE: DYNINT

R-8113-5470

COLUMNS	VARIABLE	ENTRY	NO. E
1-10	DAMP(1)	DAMPING RATIO FOR MODE 1.	
11-20	DAMP(2)	DAMPING RATIO FOR MODE 2.	
:	:	:	
:	:	:	
71-80	DAMP(8)	DAMPING RATIO FOR MODE 8.	

NEXT CARD(S)--IF NECESSARY

1-10	DAMP(9)	DAMPING RATIO FOR MODE 9.	(1)
:	:	:	
---	DAMP(NTRQ)	DAMPING RATIO FOR MODE NTRQ.	

GO TO CARD GROUP 6.

NOTES:

- (\*) THE VALUE OF NTRQ IS SPECIFIED IN CARD GROUP 3 OF THE BASSINI INPUT.
- (1) IF NTRQ > 8, THE SECOND AND SUBSEQUENT CARDS, IF REQUIRED, USE THE SAME FORMAT 8F10.0.

CARD GROUP 6:  
NO. OF CARDS:  
FORMAT:  
ROUTINE:

FREQUENCY PARAMETERS  
NFREQ\*  
F10.0  
DYNINT

R-8113-5470

COLUMNS	VARIABLE	ENTRY	NOTES
1-10	ETA	EXCITATION FREQUENCY (HERTZ)	

TERMINATE PROGRAM EXECUTION.

NOTES:

(\* ) THE VALUE OF NFREQ IS SPECIFIED IN CARD GROUP 30 OF THE BASSINI INPUT.





APPENDIX C  
SAMPLE PROBLEM

To illustrate the application of the BASSIN methodology, a sample analysis of a single-span bridge is provided in this appendix. The bridge, shown in Figure C-1, has a span length of 36 m (118 ft), a width of 12 m (39.4 ft), and a clear height of 6 m (19.7 ft). The abutment/backfill system extends for a length of 24 m (78.7 ft) beyond each end of the bridge.

The model of this bridge contains 68 node points that are associated with various element types to represent the different parts of the bridge. These element types and the corresponding thicknesses and material properties for each type are given in Table C-1. The seismic excitations for the example are induced by SH-waves that propagate parallel to the bridge span and are horizontally incident (i.e.,  $\theta_H = \theta_V = 0$  deg). The amplitude of these SH-waves is 2.0, and a total of 9 excitation frequencies, that range from 0.07 Hz to 2.28 Hz are considered in these computations.

This sample problem is presented in the following parts: (1) input data for BASSIN1; (2) printed output from BASSIN1; (3) mode shape plots from BASSIN1; (4) input data for BASSIN2; (5) printed output from BASSIN2; and (6) frequency dependent response plots from BASSIN2. It is noted that the results contained in this output are not necessarily representative of a complete analysis of the bridge, since a much larger number of excitation frequencies would ordinarily be considered in such an analysis. This sample problem is, however, of sufficient extent to familiarize the reader with the nature of the required input and the resulting output from the BASSIN1 and BASSIN2 programs.

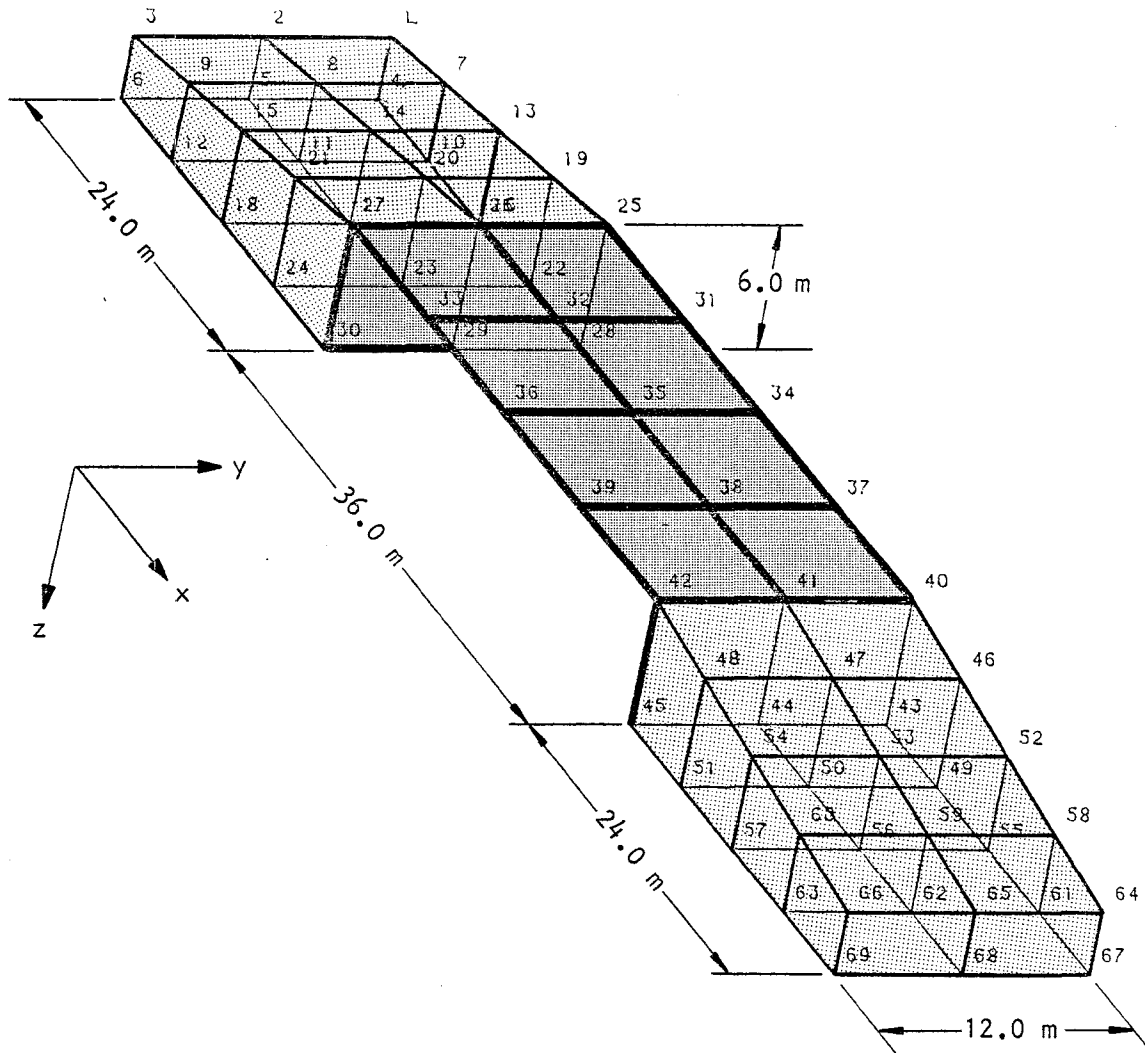


FIGURE C-1. BRIDGE CONFIGURATION FOR SAMPLE PROBLEM

TABLE C-1  
BRIDGE MODEL FOR SAMPLE PROBLEM

Bridge Region		Model Characteristics						
		Geometric Properties			Material Properties			
Type of Element	Number of Elements	Thickness	Young's Modulus	Poisson's Ratio	Weight Density			
Shell	8	1.0 m (3.30 ft)	$20.34 \times 10^8 \frac{\text{kg}}{\text{m}^2}$ ( $2.89 \times 10^6$ psi)	0.15	$2338.0 \frac{\text{kg}}{\text{m}^3}$ (146.0 lb/ft <sup>3</sup> )			
Plane Stress	20	0.3 m (0.98 ft)						
Brick	16	Variable	$1.86 \times 10^7 \frac{\text{kg}}{\text{m}^2}$ ( $2.64 \times 10^4$ psi)	0.33	$1500.0 \frac{\text{kg}}{\text{m}^3}$ (93.6 lb/ft <sup>3</sup> )			
Underlying Soil Material	Elastic Half-Space							







INPUT DATA FOR BASSIN1





GROUP	CARD	*****1*****2*****3*****4*****5*****6*****7*****8*****9	COLUMN	*****0					
11	51	44	2	2	2	60.00	0.00	0.00	0.00
11	52	45	2	2	2	60.00	0.00	0.00	0.00
11	53	46				66.00	12.00	-5.25	-5.25
11	54	47				66.00	6.00	-5.25	-5.25
11	55	48				66.00	0.00	-5.25	-5.25
11	56	49	2	2	2	66.00	12.00	0.00	0.00
11	57	50	2	2	2	66.00	6.00	0.00	0.00
11	58	51	2	2	2	66.00	0.00	0.00	0.00
11	59	52				72.00	12.00	-4.50	-4.50
11	60	53				72.00	6.00	-4.50	-4.50
11	61	54				72.00	0.00	-4.50	-4.50
11	62	55	2	2	2	72.00	12.00	0.00	0.00
11	63	56	2	2	2	72.00	6.00	0.00	0.00
11	64	57	2	2	2	72.00	0.00	0.00	0.00
11	65	58				78.00	12.00	-3.75	-3.75
11	66	59				78.00	6.00	-3.75	-3.75
11	67	60				78.00	0.00	-3.75	-3.75
11	68	61	2	2	2	78.00	12.00	0.00	0.00
11	69	62	2	2	2	78.00	6.00	0.00	0.00
11	70	63	2	2	2	78.00	0.00	0.00	0.00
11	71	64				84.00	12.00	-3.00	-3.00
11	72	65				84.00	6.00	-3.00	-3.00
11	73	66				84.00	0.00	-3.00	-3.00
11	74	67	2	2	2	84.00	12.00	0.00	0.00
11	75	68	2	2	2	84.00	6.00	0.00	0.00
11	76	69	2	2	2	84.00	0.00	0.00	0.00
11	77	70	2	2	2	84.00	12.00	0.00	0.00
19	77	5	20	1	1	84.00	6.00	0.00	0.00
20	78	1	2358.0	238.2		84.00	0.00	0.00	0.00
20	79	20.34E+8	20.34E+8			84.00	0.00	0.00	0.00
21	80	1	1	4	10	84.00	0.00	0.00	0.00
21	81	2	7	10	16	84.00	0.00	0.00	0.00
21	82	3	13	16	22	84.00	0.00	0.00	0.00
21	83	4	19	22	28	84.00	0.00	0.00	0.00
21	84	5	25	28	29	84.00	0.00	0.00	0.00
21	85	6	26	29	30	84.00	0.00	0.00	0.00
21	86	7	27	30	24	84.00	0.00	0.00	0.00
21	87	8	21	24	18	84.00	0.00	0.00	0.00
21	88	9	15	18	12	84.00	0.00	0.00	0.00
21	89	10	9	12	6	84.00	0.00	0.00	0.00
21	90	11	40	43	49	84.00	0.00	0.00	0.00
21	91	12	46	49	55	84.00	0.00	0.00	0.00
21	92	13	52	55	61	84.00	0.00	0.00	0.00
21	93	14	58	61	67	84.00	0.00	0.00	0.00
21	94	15	40	43	44	84.00	0.00	0.00	0.00
21	95	16	41	44	45	84.00	0.00	0.00	0.00
21	96	17	66	69	63	84.00	0.00	0.00	0.00
21	97	18	60	63	57	84.00	0.00	0.00	0.00
21	98	19	54	57	51	84.00	0.00	0.00	0.00
21	99	20	44	51	45	84.00	0.00	0.00	0.00
22	100	4	16	1		84.00	0.00	0.00	0.00

8.84E+8

GROUP	CARD	*****1*****2*****3*****4*****5*****6*****7*****8*****9	*****0.3333	*****1.5E+3	COLUMN	*****1	*****2	*****3	*****4	*****5	*****6	*****7	*****8	*****9
23	101	1	1.055E+7	0	3333	1	5	11	8	2	4	10	7	1
24	102	1	5	11	8	2	4	10	7	1	5	11	8	2
24	103	2	6	12	9	3	5	11	8	2	4	10	7	1
24	104	3	11	17	14	8	10	16	13	7	2	1	1	1
24	105	4	12	18	15	9	11	17	14	8	2	1	1	1
24	106	5	17	23	20	14	16	22	19	13	7	2	1	1
24	107	6	18	24	21	15	17	23	20	14	8	2	1	1
24	108	7	23	29	26	20	22	28	25	19	13	7	2	1
24	109	8	24	30	27	21	23	29	26	20	14	8	2	1
24	110	9	44	50	47	41	43	49	46	40	34	31	27	23
24	111	10	45	51	48	42	44	50	47	41	35	32	28	24
24	112	11	50	56	53	47	49	55	52	46	40	34	31	27
24	113	12	51	57	54	48	50	56	53	47	41	35	32	28
24	114	13	56	62	59	53	55	61	58	52	46	40	34	31
24	115	14	57	63	60	54	56	62	59	53	47	41	35	32
24	116	15	62	68	65	59	61	67	64	58	52	46	40	34
24	117	16	63	69	66	60	62	68	65	59	53	47	41	35
25	118	5	0	1	238.20	20.01E+8	3.12E+8	0.04E+8	20.01E+8	1.0	1.0	1.0	1.0	1.0
26	119	1	26	32	31	25	0	1	1	1	1	1	1	1
27	121	1	26	32	31	25	0	1	1	1	1	1	1	1
27	122	2	27	33	32	26	0	1	1	1	1	1	1	1
27	123	3	32	35	34	31	0	1	1	1	1	1	1	1
27	124	4	33	36	35	32	0	1	1	1	1	1	1	1
27	125	5	35	38	37	34	0	1	1	1	1	1	1	1
27	126	6	36	39	38	35	0	1	1	1	1	1	1	1
27	127	7	38	41	40	37	0	1	1	1	1	1	1	1
27	128	8	39	42	41	38	0	1	1	1	1	1	1	1
30	129	16	9	1	238.20	20.01E+8	3.12E+8	0.04E+8	20.01E+8	1.0	1.0	1.0	1.0	1.0
30	130	6.957+6	1.528E+2	0.3333										
31	131	1	4	5	11	10								
31	132	2	5	6	12	11								
31	133	3	10	11	17	16								
31	134	4	11	12	18	17								
31	135	5	16	17	23	22								
31	136	6	17	18	24	23								
31	137	7	22	23	29	28								
31	138	8	23	24	30	29								
31	139	9	43	44	50	49								
31	140	10	44	45	51	50								
31	141	11	49	50	56	55								
31	142	12	50	51	57	56								
31	143	13	55	56	62	61								
31	144	14	56	57	63	62								
31	145	15	61	62	68	67								
31	146	16	62	63	69	68								
32	147	0.07161972												
32	148	0.14323945												
32	149	0.21526762												
32	150	0.28488735												

GROUP	CARD	*****1*****2*****3*****4*****5*****6*****7*****8*****9	COLUMN
32	151	0.55650707	0.0
32	152	0.428126d0	0.0
32	153	0.57136625	0.0
32	154	1.13954939	0.0
32	155	2.27409d79	0.0
33	156	c	0.0
34	157	0.0	0.0



PRINTED OUTPUT FROM BASSIN1







5-D MODES OF BRIDGE/ADJUTMENT SYSTEM  
BASIS: REV. 1.01  
18 MAR 1983

5-D MODES OF BRIDGE/ADJUTMENT SYSTEM

\*\*\*\*\*

NUMBER OF NODAL POINTS = 69  
NUMBER OF ELEMENT TYPES = 3  
NUMBER OF LOAD CASES = 0  
NUMBER OF FREQUENCIES = 10  
NU. OF STARTING EIGENVAL= 1  
NU. OF FINAL EIGENVALUE = 10

-----

INPUT DATA AT EACH NODE

\*\*\*\*\*

DEFINITION OF BOUNDARY CONDITION CODE

FREE DEGREE OF FREEDOM = 0  
 CONSTRAINED DEGREE OF FREEDOM = 1  
 DEGREE OF FREEDOM AT INTERFACE = 2

NODE NUMBER	BOUNDARY CONDITION CODES							NODAL POINT COORDINATES		
	X	Y	Z	XX	YY	ZZ	X	Y	Z	
1	0	0	0	1	1	1	0.000	12.000	-3.000	
2	0	0	0	1	1	1	0.000	6.000	-3.000	
3	0	0	0	1	1	1	0.000	0.000	-3.000	
4	2	2	2	1	1	1	0.000	12.000	0.000	
5	2	2	2	1	1	1	0.000	6.000	0.000	
6	2	2	2	1	1	1	0.000	0.000	0.000	
7	0	0	0	1	1	1	6.000	12.000	-3.750	
8	0	0	0	1	1	1	6.000	6.000	-3.750	
9	0	0	0	1	1	1	6.000	0.000	0.000	
10	2	2	2	1	1	1	6.000	12.000	0.000	
11	2	2	2	1	1	1	6.000	6.000	0.000	
12	2	2	2	1	1	1	6.000	0.000	0.000	
13	0	0	0	1	1	1	12.000	12.000	-4.500	
14	0	0	0	1	1	1	12.000	6.000	-4.500	
15	0	0	0	1	1	1	12.000	0.000	-4.500	
16	2	2	2	1	1	1	12.000	12.000	0.000	
17	2	2	2	1	1	1	12.000	6.000	0.000	
18	2	2	2	1	1	1	12.000	0.000	0.000	
19	0	0	0	1	1	1	18.000	12.000	-5.250	
20	0	0	0	1	1	1	18.000	6.000	-5.250	
21	0	0	0	1	1	1	18.000	0.000	-5.250	
22	2	2	2	1	1	1	18.000	12.000	0.000	
23	2	2	2	1	1	1	18.000	6.000	0.000	
24	2	2	2	1	1	1	18.000	0.000	0.000	
25	0	0	0	1	0	1	24.000	12.000	-6.000	
26	0	0	0	1	0	1	24.000	6.000	-6.000	
27	0	0	0	1	0	1	24.000	0.000	-6.000	
28	2	2	2	1	1	1	24.000	12.000	0.000	
29	2	2	2	1	1	1	24.000	6.000	0.000	
30	2	2	2	1	1	1	24.000	0.000	0.000	
31	0	0	0	1	0	1	33.000	12.000	-6.000	
32	0	0	0	1	0	1	33.000	6.000	-6.000	
33	0	0	0	1	0	1	33.000	0.000	-6.000	
34	0	0	0	1	0	1	42.000	12.000	-6.000	
35	0	0	0	1	0	1	42.000	6.000	-6.000	
36	0	0	0	1	0	1	42.000	0.000	-6.000	
37	0	0	0	1	0	1	51.000	12.000	-6.000	
38	0	0	0	1	0	1	51.000	6.000	-6.000	
39	0	0	0	1	0	1	51.000	0.000	-6.000	
40	0	0	0	1	0	1	60.000	12.000	-6.000	
41	0	0	0	1	0	1	60.000	6.000	-6.000	
42	0	0	0	1	0	1	60.000	0.000	-6.000	
43	2	2	2	1	1	1	60.000	12.000	0.000	

44	2	2	2	2	1	1	1	60,000	6,000	0,000	0,000
45	2	0	0	0	1	1	1	60,000	0,000	0,000	0,000
46	0	0	0	0	1	1	1	66,000	12,000	-5,250	-5,250
47	0	0	0	0	1	1	1	66,000	6,000	0,000	0,000
48	0	0	0	0	1	1	1	66,000	0,000	-5,250	-5,250
49	2	2	2	2	1	1	1	66,000	12,000	0,000	0,000
50	2	2	2	2	1	1	1	66,000	6,000	0,000	0,000
51	2	2	2	2	1	1	1	66,000	0,000	0,000	0,000
52	0	0	0	0	1	1	1	72,000	12,000	-4,500	-4,500
53	0	0	0	0	1	1	1	72,000	6,000	-4,500	-4,500
54	0	0	0	0	1	1	1	72,000	0,000	-4,500	-4,500
55	2	2	2	2	1	1	1	72,000	12,000	0,000	0,000
56	2	2	2	2	1	1	1	72,000	6,000	0,000	0,000
57	2	2	2	2	1	1	1	72,000	0,000	0,000	0,000
58	0	0	0	0	1	1	1	78,000	12,000	-3,750	-3,750
59	0	0	0	0	1	1	1	78,000	6,000	-3,750	-3,750
60	0	0	0	0	1	1	1	78,000	0,000	0,000	0,000
61	2	2	2	2	1	1	1	78,000	12,000	0,000	0,000
62	2	2	2	2	1	1	1	78,000	6,000	0,000	0,000
63	2	2	2	2	1	1	1	78,000	0,000	0,000	0,000
64	0	0	0	0	1	1	1	84,000	12,000	-3,000	-3,000
65	0	0	0	0	1	1	1	84,000	6,000	-3,000	-3,000
66	0	0	0	0	1	1	1	84,000	0,000	0,000	0,000
67	2	2	2	2	1	1	1	84,000	12,000	0,000	0,000
68	2	2	2	2	1	1	1	84,000	6,000	0,000	0,000
69	2	2	2	2	1	1	1	84,000	0,000	0,000	0,000

## INPUT DATA FOR PLATE STRESS/ STRAIN ELEMENTS

NUMBER OF ELEMENTS = 20  
 \*\*\*\*\*

ELEMENT	I	J	K	L	MATERIAL	THICKNESS
1	1	4	10	7	1	0.3000
2	7	10	16	13	1	0.3000
3	13	16	22	19	1	0.3000
4	19	22	28	25	1	0.3000
5	25	28	29	26	1	0.3000
6	26	29	30	27	1	0.3000
7	27	30	24	21	1	0.3000
8	21	24	18	15	1	0.3000
9	15	18	12	9	1	0.3000
10	9	12	6	3	1	0.3000
11	40	43	49	46	1	0.3000
12	46	49	55	52	1	0.3000
13	52	55	61	58	1	0.3000
14	58	61	67	64	1	0.3000
15	40	43	44	41	1	0.3000
16	41	44	45	42	1	0.3000
17	66	69	63	60	1	0.3000
18	60	63	57	54	1	0.3000
19	54	57	51	48	1	0.3000
20	48	51	45	42	1	0.3000

INPUT DATA FOR 8-NODE 3-DIM. ELEMENTS

NUMBER OF ELEMENTS = 16

\*\*\*\*\*

ELEMENT NUMBER	1	2	3	4	5	6	7	8	INTEGRATION ORDER	MATERIAL NO.
1	5	11	8	2	4	10	7	1	2	1
2	6	12	9	3	5	11	8	2	2	1
3	11	17	14	8	10	16	13	7	2	1
4	12	18	15	9	11	17	14	8	2	1
5	17	23	20	14	16	22	19	13	2	1
6	18	24	21	15	17	23	20	14	2	1
7	23	29	26	20	22	28	25	19	2	1
8	24	30	27	21	23	29	26	20	2	1
9	44	50	47	41	43	49	46	40	2	1
10	45	51	48	42	44	50	47	41	2	1
11	50	56	53	47	49	55	52	46	2	1
12	51	57	54	48	50	56	53	47	2	1
13	56	62	59	53	55	61	58	52	2	1
14	57	63	60	54	56	62	59	53	2	1
15	62	68	65	59	61	67	64	58	2	1
16	63	69	66	60	62	68	65	59	2	1

INPUT DATA FOR THIN ELASTIC SHELL ELEMENTS

NUMBER OF ELEMENTS = 8  
\*\*\*\*\*

ELEMENT NUMBER	NODAL POINT NUMBERS						MATERIAL TYPE	THICKNESS
	I	J	K	L	O	0		
1	26	32	31	25	0	0	1	1.0000
2	27	33	32	26	0	0	1	1.0000
3	32	35	34	31	0	0	1	1.0000
4	33	36	35	32	0	0	1	1.0000
5	35	38	37	34	0	0	1	1.0000
6	36	39	38	35	0	0	1	1.0000
7	38	41	40	37	0	0	1	1.0000
8	39	42	41	38	0	0	1	1.0000

PLANE STRESS OR PLANE STRAIN ELEMENTS

\*\*\*\*\*

ELEMENT TYPE 3  
 NUMBER OF ELEMENTS 20  
 NUMBER OF DIFF. MATERIALS 1

\*\*\*\*\*

MATERIAL NUMBER 1

WGT. DENSITY = 0.2358E+04  
 MASS DENSITY = 0.2362E+03  
 ANGLE BETA = 0.0

ELEMENT DATA

ELEMENT	I	J	K	L	MATERIAL	THICKNESS	BAND
1	1	4	10	7	1	0.300	12
2	7	10	16	13	1	0.300	12
3	13	16	22	19	1	0.300	12
4	19	22	28	25	1	0.300	12
5	25	28	29	26	1	0.300	7
6	26	29	30	27	1	0.300	7
7	27	30	24	21	1	0.300	14
8	21	24	18	15	1	0.300	12
9	15	18	12	9	1	0.300	12
10	9	12	6	3	1	0.300	12
11	40	43	49	46	1	0.300	15
12	46	49	55	52	1	0.300	12
13	52	55	61	58	1	0.300	12
14	58	61	67	64	1	0.300	12
15	40	43	44	41	1	0.300	7
16	41	44	45	42	1	0.300	7
17	66	69	63	60	1	0.300	12
18	60	63	57	54	1	0.300	12
19	54	57	51	48	1	0.300	12
20	48	51	45	42	1	0.300	15



8-NODE THREE DIM. ELEMENTS

\*\*\*\*\*  
 NUMBER OF ELEMENTS 16  
 \*\*\*\*\*  
 NUMBER OF MATERIALS 1  
 \*\*\*\*\*  
 NUMBER OF LOAD TYPES 0  
 \*\*\*\*\*

MATERIAL NUMBER 1  
 MODULUS OF ELASTICITY =0.1055E+08  
 POISSON S RATIO =-0.3333E+00  
 MASS DENSITY =0.1500E+04

ELEMENT DATA

ELEMENT NUMBER	1	2	3	4	5	6	7	8	INTEGRATION ORDER	MATERIAL NO.	BARD
1	5	11	8	2	4	10	7	1	2	1	15
2	6	12	9	3	5	11	8	2	2	1	15
3	11	17	14	8	10	16	13	7	2	1	15
4	12	18	15	9	11	17	14	8	2	1	15
5	17	23	20	14	16	22	19	13	2	1	15
6	18	24	21	15	17	23	20	14	2	1	15
7	23	29	26	20	22	28	25	19	2	1	16
8	24	30	27	21	23	29	26	20	2	1	17
9	44	50	47	41	43	49	46	40	2	1	18
10	45	51	48	42	44	50	47	41	2	1	17
11	50	56	53	47	49	55	52	46	2	1	15
12	51	57	54	48	50	56	53	47	2	1	15
13	56	62	59	53	55	61	58	52	2	1	15
14	57	63	60	54	56	62	59	53	2	1	15
15	62	68	65	59	61	67	64	58	2	1	15
16	63	69	66	60	62	68	65	59	2	1	15

THIN SHELL ELEMENTS  
 \*\*\*\*\*  
 ELEMENT TYPE 6  
 \*\*\*\*\*  
 NUMBER OF ELEMENTS 8  
 \*\*\*\*\*  
 NUMBER OF MATERIALS 1  
 \*\*\*\*\*

SHELL ELEMENT DATA

ELEMENT NUMBER	NODAL POINT NUMBERS								MATERIAL TYPE	THICKNESS	BAND
	I	J	K	L	U						
1	26	32	31	25	0				1	1.0000	20
2	27	33	32	26	0				1	1.0000	20
3	32	35	34	31	0				1	1.0000	20
4	33	36	35	32	0				1	1.0000	20
5	35	38	37	34	0				1	1.0000	20
6	36	39	38	35	0				1	1.0000	20
7	38	41	40	37	0				1	1.0000	20
8	39	42	41	38	0				1	1.0000	20

TOTAL NUMBER OF D.O.F.s = 132  
BANDWIDTH = 20  
FOR SHELL ELEMENT NUMBER = 1  
NUMBER OF BLOCKS = 1  
NUMBER OF EQUATIONS IN A BLOCK = 132  
\*\*\*\*\*

SUCCESSFULL COMPUTATION OF STIFFNESS MATRIX

DIMENSIONS OF SUBMATRIX K(SS) = 132 X 20  
DIMENSIONS OF SUBMATRIX K(FF) = 90 X 20  
DIMENSIONS OF SUBMATRIX K(SF) = 90 X 132

\*\*\*\*\*

SUCCESSFULL COMPUTATION OF MASS MATRIX

DIMENSIONS OF SUBMATRIX M(SS) = 132  
DIMENSIONS OF SUBMATRIX M(FF) = 90

\*\*\*\*\*

\*\*\*\*\*  
EVALUATION OF EIGENVALUE PROBLEM  
\*\*\*\*\*

EXTRACTION OF 10 FREQUENCIES WITH MAX. OF 12 ITERATIONS

\*\*\*\*\*

NUMBER OF TRIAL VECTORS SELECTED ARE 18

\*\*\*\*\*

TOTAL ITERATIONS = 12

\*\*\*\*\*  
NUMBER OF COMPUTED EIGENVALUES = 10  
\*\*\*\*\*

MODE NUMBER	FREQUENCIES IN RAD/SEC	FREQUENCIES IN HERTZ	PERIODS IN SEC
1	6.541	1.041	0.961
2	26.693	4.248	0.235
3	60.430	9.618	0.104
4	70.834	11.274	0.089
5	82.977	13.206	0.076
6	131.246	20.888	0.048
7	132.626	21.108	0.047
8	143.576	22.851	0.044
9	154.436	24.579	0.041
10	163.232	25.982	0.038

COMPUTED MODE SHAPES

\*\*\*\*\*

MODE NUMBER = 1  
 FREQUENCY(HZ) = 1.041

MODE	X	Y	Z	XX	YY	ZZ
1	-0.135E-08	-0.995E-09	0.191E-08	0.00E+00	0.00E+00	0.00E+00
2	-0.254E-08	-0.111E-18	0.139E-07	0.00E+00	0.00E+00	0.00E+00
3	-0.135E-08	0.995E-09	0.191E-08	0.00E+00	0.00E+00	0.00E+00
4	0.000E+00	0.000E+00	0.000E+00	0.00E+00	0.00E+00	0.00E+00
5	0.000E+00	0.000E+00	0.000E+00	0.00E+00	0.00E+00	0.00E+00
6	0.000E+00	0.000E+00	0.000E+00	0.00E+00	0.00E+00	0.00E+00
7	0.372E-08	-0.384E-08	-0.544E-08	0.00E+00	0.00E+00	0.00E+00
8	-0.634E-08	0.601E-19	-0.302E-07	0.00E+00	0.00E+00	0.00E+00
9	0.372E-08	0.384E-08	-0.544E-08	0.00E+00	0.00E+00	0.00E+00
10	0.000E+00	0.000E+00	0.000E+00	0.00E+00	0.00E+00	0.00E+00
11	0.000E+00	0.000E+00	0.000E+00	0.00E+00	0.00E+00	0.00E+00
12	0.000E+00	0.000E+00	0.000E+00	0.00E+00	0.00E+00	0.00E+00
13	0.254E-07	-0.643E-07	0.172E-07	0.00E+00	0.00E+00	0.00E+00
14	0.124E-06	0.124E-18	0.153E-06	0.00E+00	0.00E+00	0.00E+00
15	0.254E-07	0.643E-07	0.172E-07	0.00E+00	0.00E+00	0.00E+00
16	0.000E+00	0.000E+00	0.000E+00	0.00E+00	0.00E+00	0.00E+00
17	0.000E+00	0.000E+00	0.000E+00	0.00E+00	0.00E+00	0.00E+00
18	0.000E+00	0.000E+00	0.000E+00	0.00E+00	0.00E+00	0.00E+00
19	0.247E-06	0.388E-06	-0.262E-06	0.00E+00	0.00E+00	0.00E+00
20	-0.348E-06	0.807E-19	-0.724E-06	0.00E+00	0.00E+00	0.00E+00
21	0.247E-06	-0.388E-06	-0.262E-06	0.00E+00	0.00E+00	0.00E+00

22	0.000E+00	0.000E+00	0.000E+00	0.000E+00	0.00E+00	0.00E+00	0.00E+00	0.00E+00
23	0.000E+00	0.000E+00	0.000E+00	0.000E+00	0.00E+00	0.00E+00	0.00E+00	0.00E+00
24	0.000E+00	0.000E+00	0.000E+00	0.000E+00	0.00E+00	0.00E+00	0.00E+00	0.00E+00
25	0.415E-06	0.792E-07	0.252E-05	0.00E+00	-0.39E-03	0.00E+00	0.00E+00	0.00E+00
26	0.267E-06	-0.108E-17	0.429E-05	0.00E+00	-0.39E-03	0.00E+00	0.00E+00	0.00E+00
27	0.415E-06	-0.782E-07	0.252E-05	0.00E+00	-0.39E-03	0.00E+00	0.00E+00	0.00E+00
28	0.000E+00	0.000E+00	0.000E+00	0.000E+00	0.00E+00	0.00E+00	0.00E+00	0.00E+00
29	0.000E+00	0.000E+00	0.000E+00	0.000E+00	0.00E+00	0.00E+00	0.00E+00	0.00E+00
30	0.000E+00	0.000E+00	0.000E+00	0.000E+00	0.00E+00	0.00E+00	0.00E+00	0.00E+00
31	0.170E-06	-0.902E-09	0.312E-02	0.00E+00	-0.28E-03	0.00E+00	0.00E+00	0.00E+00
32	0.164E-06	-0.976E-18	0.312E-02	0.00E+00	-0.28E-03	0.00E+00	0.00E+00	0.00E+00
33	0.170E-06	0.902E-09	0.312E-02	0.00E+00	-0.28E-03	0.00E+00	0.00E+00	0.00E+00
34	0.196E-18	0.189E-07	0.441E-02	0.00E+00	0.35E-16	0.00E+00	0.00E+00	0.00E+00
35	0.557E-18	-0.432E-18	0.441E-02	0.00E+00	0.34E-16	0.00E+00	0.00E+00	0.00E+00
36	0.888E-18	-0.189E-07	0.441E-02	0.00E+00	0.34E-16	0.00E+00	0.00E+00	0.00E+00
37	-0.170E-06	-0.902E-09	0.312E-02	0.00E+00	0.28E-03	0.00E+00	0.00E+00	0.00E+00
38	-0.164E-06	0.685E-19	0.312E-02	0.00E+00	0.28E-03	0.00E+00	0.00E+00	0.00E+00
39	-0.170E-06	0.902E-09	0.312E-02	0.00E+00	0.28E-03	0.00E+00	0.00E+00	0.00E+00
40	-0.415E-06	0.782E-07	0.252E-05	0.00E+00	0.39E-03	0.00E+00	0.00E+00	0.00E+00
41	-0.267E-06	0.121E-18	0.429E-05	0.00E+00	0.39E-03	0.00E+00	0.00E+00	0.00E+00
42	-0.415E-06	-0.782E-07	0.252E-05	0.00E+00	0.39E-03	0.00E+00	0.00E+00	0.00E+00
43	0.000E+00	0.000E+00	0.000E+00	0.000E+00	0.00E+00	0.00E+00	0.00E+00	0.00E+00
44	0.000E+00	0.000E+00	0.000E+00	0.000E+00	0.00E+00	0.00E+00	0.00E+00	0.00E+00
45	0.000E+00	0.000E+00	0.000E+00	0.000E+00	0.00E+00	0.00E+00	0.00E+00	0.00E+00
46	-0.247E-06	0.388E-06	-0.262E-06	0.00E+00	0.00E+00	0.00E+00	0.00E+00	0.00E+00
47	0.348E-06	0.216E-18	-0.724E-06	0.00E+00	0.00E+00	0.00E+00	0.00E+00	0.00E+00
48	-0.247E-06	-0.388E-06	-0.262E-06	0.00E+00	0.00E+00	0.00E+00	0.00E+00	0.00E+00
49	0.000E+00	0.000E+00	0.000E+00	0.000E+00	0.00E+00	0.00E+00	0.00E+00	0.00E+00
50	0.000E+00	0.000E+00	0.000E+00	0.000E+00	0.00E+00	0.00E+00	0.00E+00	0.00E+00
51	0.000E+00	0.000E+00	0.000E+00	0.000E+00	0.00E+00	0.00E+00	0.00E+00	0.00E+00
52	-0.254E-07	-0.643E-07	0.172E-07	0.00E+00	0.00E+00	0.00E+00	0.00E+00	0.00E+00



53	-0.124E+06	0.092E-19	0.155E-06	0.00E+00	0.00E+00	0.00E+00	0.00E+00
54	-0.254E-07	0.643E-07	0.172E-07	0.00E+00	0.00E+00	0.00E+00	0.00E+00
55	0.000E+00	0.000E+00	0.000E+00	0.00E+00	0.00E+00	0.00E+00	0.00E+00
56	0.000E+00	0.000E+00	0.000E+00	0.00E+00	0.00E+00	0.00E+00	0.00E+00
57	0.000E+00	0.000E+00	0.000E+00	0.00E+00	0.00E+00	0.00E+00	0.00E+00
58	-0.572E-08	-0.584E-08	-0.544E-08	0.00E+00	0.00E+00	0.00E+00	0.00E+00
59	0.634E-08	0.562E-19	-0.302E-07	0.00E+00	0.00E+00	0.00E+00	0.00E+00
60	-0.372E-08	0.384E-08	-0.544E-08	0.00E+00	0.00E+00	0.00E+00	0.00E+00
61	0.000E+00	0.000E+00	0.000E+00	0.00E+00	0.00E+00	0.00E+00	0.00E+00
62	0.000E+00	0.000E+00	0.000E+00	0.00E+00	0.00E+00	0.00E+00	0.00E+00
63	0.000E+00	0.000E+00	0.000E+00	0.00E+00	0.00E+00	0.00E+00	0.00E+00
64	0.135E-08	-0.995E-09	0.191E-08	0.00E+00	0.00E+00	0.00E+00	0.00E+00
65	0.254E-08	-0.958E-19	0.139E-07	0.00E+00	0.00E+00	0.00E+00	0.00E+00
66	0.135E-08	0.995E-09	0.191E-08	0.00E+00	0.00E+00	0.00E+00	0.00E+00
67	0.000E+00	0.000E+00	0.000E+00	0.00E+00	0.00E+00	0.00E+00	0.00E+00
68	0.000E+00	0.000E+00	0.000E+00	0.00E+00	0.00E+00	0.00E+00	0.00E+00
69	0.000E+00	0.000E+00	0.000E+00	0.00E+00	0.00E+00	0.00E+00	0.00E+00

MODE NUMBER = 2

FREQUENCY (HZ) = 4.248

NODE	X	Y	Z	XX	YY	ZZ
1	0.119E-07	0.716E-08	-0.151E-07	0.00E+00	0.00E+00	0.00E+00
2	0.200E-07	0.176E-19	-0.997E-07	0.00E+00	0.00E+00	0.00E+00
3	0.119E-07	-0.716E-08	-0.151E-07	0.00E+00	0.00E+00	0.00E+00
4	0.000E+00	0.000E+00	0.000E+00	0.00E+00	0.00E+00	0.00E+00
5	0.000E+00	0.000E+00	0.000E+00	0.00E+00	0.00E+00	0.00E+00
6	0.000E+00	0.000E+00	0.000E+00	0.00E+00	0.00E+00	0.00E+00
7	-0.561E-07	0.619E-07	0.525E-07	0.00E+00	0.00E+00	0.00E+00

8	0.243E-07	-0.967E-20	0.208E-06	0.00E+00	0.00E+00	0.00E+00	0.00E+00
9	-0.561E-07	-0.619E-07	0.523E-07	0.00E+00	0.00E+00	0.00E+00	0.00E+00
10	0.000E+00	0.000E+00	0.000E+00	0.00E+00	0.00E+00	0.00E+00	0.00E+00
11	0.000E+00	0.000E+00	0.000E+00	0.00E+00	0.00E+00	0.00E+00	0.00E+00
12	0.000E+00	0.000E+00	0.000E+00	0.00E+00	0.00E+00	0.00E+00	0.00E+00
13	-0.521E-06	0.895E-06	-0.395E-07	0.00E+00	0.00E+00	0.00E+00	0.00E+00
14	-0.134E-05	0.194E-19	-0.114E-05	0.00E+00	0.00E+00	0.00E+00	0.00E+00
15	-0.521E-06	-0.895E-06	-0.395E-07	0.00E+00	0.00E+00	0.00E+00	0.00E+00
16	0.000E+00	0.000E+00	0.000E+00	0.00E+00	0.00E+00	0.00E+00	0.00E+00
17	0.000E+00	0.000E+00	0.000E+00	0.00E+00	0.00E+00	0.00E+00	0.00E+00
18	0.000E+00	0.000E+00	0.000E+00	0.00E+00	0.00E+00	0.00E+00	0.00E+00
19	-0.384E-05	-0.626E-06	0.261E-05	0.00E+00	0.00E+00	0.00E+00	0.00E+00
20	-0.564E-06	-0.349E-19	0.469E-05	0.00E+00	0.00E+00	0.00E+00	0.00E+00
21	-0.384E-05	0.626E-06	0.261E-05	0.00E+00	0.00E+00	0.00E+00	0.00E+00
22	0.000E+00	0.000E+00	0.000E+00	0.00E+00	0.00E+00	0.00E+00	0.00E+00
23	0.000E+00	0.000E+00	0.000E+00	0.00E+00	0.00E+00	0.00E+00	0.00E+00
24	0.000E+00	0.000E+00	0.000E+00	0.00E+00	0.00E+00	0.00E+00	0.00E+00
25	-0.109E-04	-0.299E-06	-0.189E-04	0.00E+00	0.00E+00	0.79E-03	0.00E+00
26	-0.111E-04	0.415E-18	-0.302E-04	0.00E+00	0.00E+00	0.78E-03	0.00E+00
27	-0.109E-04	0.299E-06	-0.189E-04	0.00E+00	0.00E+00	0.79E-03	0.00E+00
28	0.000E+00	0.000E+00	0.000E+00	0.00E+00	0.00E+00	0.00E+00	0.00E+00
29	0.000E+00	0.000E+00	0.000E+00	0.00E+00	0.00E+00	0.00E+00	0.00E+00
30	0.000E+00	0.000E+00	0.000E+00	0.00E+00	0.00E+00	0.00E+00	0.00E+00
31	-0.111E-04	0.159E-07	-0.441E-02	0.00E+00	0.00E+00	-0.13E-05	0.00E+00
32	-0.110E-04	-0.891E-19	-0.441E-02	0.00E+00	0.00E+00	-0.15E-05	0.00E+00
33	-0.111E-04	-0.159E-07	-0.441E-02	0.00E+00	0.00E+00	-0.13E-05	0.00E+00
34	-0.111E-04	-0.751E-18	-0.405E-16	0.00E+00	0.00E+00	-0.79E-03	0.00E+00
35	-0.111E-04	-0.716E-18	-0.179E-17	0.00E+00	0.00E+00	-0.79E-03	0.00E+00
36	-0.111E-04	-0.719E-18	0.255E-16	0.00E+00	0.00E+00	-0.79E-03	0.00E+00
37	-0.111E-04	-0.159E-07	0.441E-02	0.00E+00	0.00E+00	-0.15E-05	0.00E+00
38	-0.110E-04	-0.170E-17	0.441E-02	0.00E+00	0.00E+00	-0.15E-05	0.00E+00
39	-0.111E-04	0.159E-07	0.441E-02	0.00E+00	0.00E+00	-0.15E-05	0.00E+00

40	-0.109E-04	0.299E-06	0.189E-04	0.00E+00	0.79E-03	0.00E+00
41	-0.111E-04	-0.321E-17	0.502E-04	0.00E+00	0.78E-03	0.00E+00
42	-0.109E-04	-0.299E-06	0.189E-04	0.00E+00	0.79E-03	0.00E+00
43	0.000E+00	0.000E+00	0.000E+00	0.00E+00	0.00E+00	0.00E+00
44	0.000E+00	0.000E+00	0.000E+00	0.00E+00	0.00E+00	0.00E+00
45	0.000E+00	0.000E+00	0.000E+00	0.00E+00	0.00E+00	0.00E+00
46	-0.384E-05	0.826E-06	-0.261E-05	0.00E+00	0.00E+00	0.00E+00
47	-0.568E-06	-0.344E-18	-0.469E-05	0.00E+00	0.00E+00	0.00E+00
48	-0.384E-05	-0.826E-06	-0.261E-05	0.00E+00	0.00E+00	0.00E+00
49	0.000E+00	0.000E+00	0.000E+00	0.00E+00	0.00E+00	0.00E+00
50	0.000E+00	0.000E+00	0.000E+00	0.00E+00	0.00E+00	0.00E+00
51	0.000E+00	0.000E+00	0.000E+00	0.00E+00	0.00E+00	0.00E+00
52	-0.521E-06	-0.895E-06	0.395E-07	0.00E+00	0.00E+00	0.00E+00
53	-0.134E-05	-0.205E-18	0.114E-05	0.00E+00	0.00E+00	0.00E+00
54	-0.521E-06	0.895E-06	0.395E-07	0.00E+00	0.00E+00	0.00E+00
55	0.000E+00	0.000E+00	0.000E+00	0.00E+00	0.00E+00	0.00E+00
56	0.000E+00	0.000E+00	0.000E+00	0.00E+00	0.00E+00	0.00E+00
57	0.000E+00	0.000E+00	0.000E+00	0.00E+00	0.00E+00	0.00E+00
58	-0.561E-07	-0.619E-07	-0.523E-07	0.00E+00	0.00E+00	0.00E+00
59	0.245E-07	0.349E-19	-0.208E-06	0.00E+00	0.00E+00	0.00E+00
60	-0.561E-07	0.619E-07	-0.523E-07	0.00E+00	0.00E+00	0.00E+00
61	0.000E+00	0.000E+00	0.000E+00	0.00E+00	0.00E+00	0.00E+00
62	0.000E+00	0.000E+00	0.000E+00	0.00E+00	0.00E+00	0.00E+00
63	0.000E+00	0.000E+00	0.000E+00	0.00E+00	0.00E+00	0.00E+00
64	0.119E-07	-0.716E-08	0.151E-07	0.00E+00	0.00E+00	0.00E+00
65	0.200E-07	-0.277E-19	0.997E-07	0.00E+00	0.00E+00	0.00E+00
66	0.119E-07	0.716E-08	0.151E-07	0.00E+00	0.00E+00	0.00E+00
67	0.000E+00	0.000E+00	0.000E+00	0.00E+00	0.00E+00	0.00E+00
68	0.000E+00	0.000E+00	0.000E+00	0.00E+00	0.00E+00	0.00E+00
69	0.000E+00	0.000E+00	0.000E+00	0.00E+00	0.00E+00	0.00E+00

MODE NUMBER = 3  
FREQUENCY (HZ) = 9.010

MODE	X	Y	Z	XX	YY	ZZ
1	0.214E-07	0.117E-07	-0.298E-07	0.00E+00	0.00E+00	0.00E+00
2	0.417E-07	0.290E-19	-0.220E-06	0.00E+00	0.00E+00	0.00E+00
3	0.214E-07	-0.117E-07	-0.298E-07	0.00E+00	0.00E+00	0.00E+00
4	0.000E+00	0.000E+00	0.000E+00	0.00E+00	0.00E+00	0.00E+00
5	0.000E+00	0.000E+00	0.000E+00	0.00E+00	0.00E+00	0.00E+00
6	0.000E+00	0.000E+00	0.000E+00	0.00E+00	0.00E+00	0.00E+00
7	-0.592E-07	0.566E-07	0.849E-07	0.00E+00	0.00E+00	0.00E+00
8	0.122E-06	0.184E-19	0.477E-06	0.00E+00	0.00E+00	0.00E+00
9	-0.592E-07	-0.566E-07	0.849E-07	0.00E+00	0.00E+00	0.00E+00
10	0.000E+00	0.000E+00	0.000E+00	0.00E+00	0.00E+00	0.00E+00
11	0.000E+00	0.000E+00	0.000E+00	0.00E+00	0.00E+00	0.00E+00
12	0.000E+00	0.000E+00	0.000E+00	0.00E+00	0.00E+00	0.00E+00
13	-0.402E-06	0.123E-05	-0.256E-06	0.00E+00	0.00E+00	0.00E+00
14	-0.207E-05	-0.139E-18	-0.238E-05	0.00E+00	0.00E+00	0.00E+00
15	-0.402E-06	-0.123E-05	-0.256E-06	0.00E+00	0.00E+00	0.00E+00
16	0.000E+00	0.000E+00	0.000E+00	0.00E+00	0.00E+00	0.00E+00
17	0.000E+00	0.000E+00	0.000E+00	0.00E+00	0.00E+00	0.00E+00
18	0.000E+00	0.000E+00	0.000E+00	0.00E+00	0.00E+00	0.00E+00
19	-0.383E-05	-0.658E-05	0.399E-05	0.00E+00	0.00E+00	0.00E+00
20	0.521E-05	-0.241E-18	0.111E-04	0.00E+00	0.00E+00	0.00E+00
21	-0.383E-05	0.658E-05	0.399E-05	0.00E+00	0.00E+00	0.00E+00
22	0.000E+00	0.000E+00	0.000E+00	0.00E+00	0.00E+00	0.00E+00
23	0.000E+00	0.000E+00	0.000E+00	0.00E+00	0.00E+00	0.00E+00
24	0.000E+00	0.000E+00	0.000E+00	0.00E+00	0.00E+00	0.00E+00
25	-0.651E-05	-0.117E-05	-0.389E-04	0.00E+00	0.98E-03	0.00E+00

26	-0.429E-05	-0.572E-17	-0.656E-04	0.00E+00	0.97E-05	0.00E+00
27	-0.651E-05	0.117E-05	-0.580E-04	0.00E+00	0.98E-05	0.00E+00
28	0.000E+00	0.000E+00	0.000E+00	0.00E+00	0.00E+00	0.00E+00
29	0.000E+00	0.000E+00	0.000E+00	0.00E+00	0.00E+00	0.00E+00
30	0.000E+00	0.000E+00	0.000E+00	0.00E+00	0.00E+00	0.00E+00
31	-0.274E-05	-0.124E-08	-0.512E-02	0.00E+00	-0.70E-05	0.00E+00
32	-0.266E-05	-0.789E-17	-0.512E-02	0.00E+00	-0.70E-05	0.00E+00
33	-0.274E-05	0.124E-08	-0.512E-02	0.00E+00	-0.70E-05	0.00E+00
34	-0.821E-17	-0.306E-06	0.441E-02	0.00E+00	-0.65E-15	0.00E+00
35	-0.749E-17	-0.919E-17	0.441E-02	0.00E+00	-0.61E-15	0.00E+00
36	-0.676E-17	0.506E-06	0.441E-02	0.00E+00	-0.58E-15	0.00E+00
37	0.274E-05	-0.124E-08	-0.512E-02	0.00E+00	0.70E-05	0.00E+00
38	0.266E-05	-0.582E-17	-0.512E-02	0.00E+00	0.70E-05	0.00E+00
39	0.274E-05	0.124E-08	-0.512E-02	0.00E+00	0.70E-05	0.00E+00
40	0.651E-05	-0.117E-05	-0.580E-04	0.00E+00	-0.98E-05	0.00E+00
41	0.429E-05	0.846E-18	-0.656E-04	0.00E+00	-0.97E-05	0.00E+00
42	0.651E-05	0.117E-05	-0.580E-04	0.00E+00	-0.98E-05	0.00E+00
43	0.000E+00	0.000E+00	0.000E+00	0.00E+00	0.00E+00	0.00E+00
44	0.000E+00	0.000E+00	0.000E+00	0.00E+00	0.00E+00	0.00E+00
45	0.000E+00	0.000E+00	0.000E+00	0.00E+00	0.00E+00	0.00E+00
46	0.383E-05	-0.658E-05	0.399E-05	0.00E+00	0.00E+00	0.00E+00
47	-0.521E-05	0.447E-18	0.111E-04	0.00E+00	0.00E+00	0.00E+00
48	0.383E-05	0.658E-05	0.399E-05	0.00E+00	0.00E+00	0.00E+00
49	0.000E+00	0.000E+00	0.000E+00	0.00E+00	0.00E+00	0.00E+00
50	0.000E+00	0.000E+00	0.000E+00	0.00E+00	0.00E+00	0.00E+00
51	0.000E+00	0.000E+00	0.000E+00	0.00E+00	0.00E+00	0.00E+00
52	0.402E-06	0.125E-05	-0.256E-06	0.00E+00	0.00E+00	0.00E+00
53	0.207E-05	0.234E-18	-0.238E-05	0.00E+00	0.00E+00	0.00E+00
54	0.402E-06	-0.125E-05	-0.256E-06	0.00E+00	0.00E+00	0.00E+00
55	0.000E+00	0.000E+00	0.000E+00	0.00E+00	0.00E+00	0.00E+00
56	0.000E+00	0.000E+00	0.000E+00	0.00E+00	0.00E+00	0.00E+00
57	0.000E+00	0.000E+00	0.000E+00	0.00E+00	0.00E+00	0.00E+00

58	0.592E-07	0.566E-07	0.849E-07	0.00E+00	0.00E+00	0.00E+00	0.00E+00	0.00E+00
59	-0.122E-06	-0.407E-19	0.477E-06	0.00E+00	0.00E+00	0.00E+00	0.00E+00	0.00E+00
60	0.592E-07	-0.566E-07	0.849E-07	0.00E+00	0.00E+00	0.00E+00	0.00E+00	0.00E+00
61	0.000E+00	0.000E+00	0.000E+00	0.00E+00	0.00E+00	0.00E+00	0.00E+00	0.00E+00
62	0.000E+00	0.000E+00	0.000E+00	0.00E+00	0.00E+00	0.00E+00	0.00E+00	0.00E+00
63	0.000E+00	0.000E+00	0.000E+00	0.00E+00	0.00E+00	0.00E+00	0.00E+00	0.00E+00
64	-0.214E-07	0.117E-07	-0.298E-07	0.00E+00	0.00E+00	0.00E+00	0.00E+00	0.00E+00
65	-0.417E-07	0.659E-19	-0.220E-06	0.00E+00	0.00E+00	0.00E+00	0.00E+00	0.00E+00
66	-0.214E-07	-0.117E-07	-0.298E-07	0.00E+00	0.00E+00	0.00E+00	0.00E+00	0.00E+00
67	0.000E+00	0.000E+00	0.000E+00	0.00E+00	0.00E+00	0.00E+00	0.00E+00	0.00E+00
68	0.000E+00	0.000E+00	0.000E+00	0.00E+00	0.00E+00	0.00E+00	0.00E+00	0.00E+00
69	0.000E+00	0.000E+00	0.000E+00	0.00E+00	0.00E+00	0.00E+00	0.00E+00	0.00E+00

MODE NUMBER = 4

FREQUENCY (HZ) = 11.274

----- X Y Z XX YY ZZ -----

1	0.205E-06	-0.233E-05	0.173E-08	0.00E+00	0.00E+00	0.00E+00	0.00E+00	0.00E+00
2	-0.923E-11	0.213E-05	0.290E-11	0.00E+00	0.00E+00	0.00E+00	0.00E+00	0.00E+00
3	-0.205E-06	-0.233E-05	-0.173E-08	0.00E+00	0.00E+00	0.00E+00	0.00E+00	0.00E+00
4	0.000E+00	0.000E+00	0.000E+00	0.00E+00	0.00E+00	0.00E+00	0.00E+00	0.00E+00
5	0.000E+00	0.000E+00	0.000E+00	0.00E+00	0.00E+00	0.00E+00	0.00E+00	0.00E+00
6	0.000E+00	0.000E+00	0.000E+00	0.00E+00	0.00E+00	0.00E+00	0.00E+00	0.00E+00
7	-0.245E-05	0.409E-05	0.717E-06	0.00E+00	0.00E+00	0.00E+00	0.00E+00	0.00E+00
8	-0.249E-11	-0.748E-05	-0.940E-12	0.00E+00	0.00E+00	0.00E+00	0.00E+00	0.00E+00
9	0.243E-05	0.409E-05	-0.717E-06	0.00E+00	0.00E+00	0.00E+00	0.00E+00	0.00E+00
10	0.000E+00	0.000E+00	0.000E+00	0.00E+00	0.00E+00	0.00E+00	0.00E+00	0.00E+00
11	0.000E+00	0.000E+00	0.000E+00	0.00E+00	0.00E+00	0.00E+00	0.00E+00	0.00E+00
12	0.000E+00	0.000E+00	0.000E+00	0.00E+00	0.00E+00	0.00E+00	0.00E+00	0.00E+00

13	-0.315E-04	-0.199E-04	0.669E-05	0.00E+00	0.00E+00	0.00E+00	0.00E+00
14	0.123E-10	-0.915E-05	-0.299E-12	0.00E+00	0.00E+00	0.00E+00	0.00E+00
15	0.315E-04	-0.199E-04	-0.669E-05	0.00E+00	0.00E+00	0.00E+00	0.00E+00
16	0.000E+00	0.000E+00	0.000E+00	0.00E+00	0.00E+00	0.00E+00	0.00E+00
17	0.000E+00	0.000E+00	0.000E+00	0.00E+00	0.00E+00	0.00E+00	0.00E+00
18	0.000E+00	0.000E+00	0.000E+00	0.00E+00	0.00E+00	0.00E+00	0.00E+00
19	-0.202E-05	0.189E-03	0.572E-04	0.00E+00	0.00E+00	0.00E+00	0.00E+00
20	0.167E-11	-0.114E-04	0.229E-11	0.00E+00	0.00E+00	0.00E+00	0.00E+00
21	0.202E-05	0.189E-03	-0.572E-04	0.00E+00	0.00E+00	0.00E+00	0.00E+00
22	0.000E+00	0.000E+00	0.000E+00	0.00E+00	0.00E+00	0.00E+00	0.00E+00
23	0.000E+00	0.000E+00	0.000E+00	0.00E+00	0.00E+00	0.00E+00	0.00E+00
24	0.000E+00	0.000E+00	0.000E+00	0.00E+00	0.00E+00	0.00E+00	0.00E+00
25	-0.810E-03	0.147E-02	0.205E-03	0.00E+00	0.45E-04	0.00E+00	0.00E+00
26	0.162E-12	0.147E-02	0.954E-12	0.00E+00	0.46E-12	0.00E+00	0.00E+00
27	0.810E-03	0.147E-02	-0.205E-03	0.00E+00	-0.45E-04	0.00E+00	0.00E+00
28	0.000E+00	0.000E+00	0.000E+00	0.00E+00	0.00E+00	0.00E+00	0.00E+00
29	0.000E+00	0.000E+00	0.000E+00	0.00E+00	0.00E+00	0.00E+00	0.00E+00
30	0.000E+00	0.000E+00	0.000E+00	0.00E+00	0.00E+00	0.00E+00	0.00E+00
31	-0.693E-05	0.514E-02	0.219E-04	0.00E+00	0.52E-05	0.00E+00	0.00E+00
32	0.431E-12	0.317E-02	0.590E-11	0.00E+00	0.36E-13	0.00E+00	0.00E+00
33	0.693E-05	0.314E-02	-0.219E-04	0.00E+00	-0.52E-05	0.00E+00	0.00E+00
34	0.487E-12	0.387E-02	0.505E-05	0.00E+00	0.24E-12	0.00E+00	0.00E+00
35	0.488E-12	0.591E-02	0.131E-14	0.00E+00	-0.27E-12	0.00E+00	0.00E+00
36	0.487E-12	0.387E-02	-0.505E-05	0.00E+00	0.24E-12	0.00E+00	0.00E+00
37	0.693E-05	0.514E-02	0.219E-04	0.00E+00	-0.52E-05	0.00E+00	0.00E+00
38	0.431E-12	0.317E-02	-0.590E-11	0.00E+00	0.36E-13	0.00E+00	0.00E+00
39	-0.693E-05	0.314E-02	-0.219E-04	0.00E+00	0.52E-05	0.00E+00	0.00E+00
40	0.810E-03	0.147E-02	0.205E-03	0.00E+00	-0.45E-04	0.00E+00	0.00E+00
41	0.162E-12	0.147E-02	-0.954E-12	0.00E+00	0.46E-12	0.00E+00	0.00E+00
42	-0.810E-03	0.147E-02	-0.205E-03	0.00E+00	0.45E-04	0.00E+00	0.00E+00
43	0.000E+00	0.000E+00	0.000E+00	0.00E+00	0.00E+00	0.00E+00	0.00E+00





1	-0.850E-06	-0.296E-06	0.625E-06	0.00E+00	0.00E+00	0.00E+00	0.00E+00
2	0.790E-07	0.447E-11	0.755E-06	0.00E+00	0.00E+00	0.00E+00	0.00E+00
3	-0.850E-06	0.296E-06	0.625E-06	0.00E+00	0.00E+00	0.00E+00	0.00E+00
4	0.000E+00	0.000E+00	0.000E+00	0.00E+00	0.00E+00	0.00E+00	0.00E+00
5	0.000E+00	0.000E+00	0.000E+00	0.00E+00	0.00E+00	0.00E+00	0.00E+00
6	0.000E+00	0.000E+00	0.000E+00	0.00E+00	0.00E+00	0.00E+00	0.00E+00
7	0.976E-05	-0.756E-05	-0.465E-05	0.00E+00	0.00E+00	0.00E+00	0.00E+00
8	0.330E-05	-0.304E-12	0.107E-05	0.00E+00	0.00E+00	0.00E+00	0.00E+00
9	0.976E-05	0.756E-05	-0.465E-05	0.00E+00	0.00E+00	0.00E+00	0.00E+00
10	0.000E+00	0.000E+00	0.000E+00	0.00E+00	0.00E+00	0.00E+00	0.00E+00
11	0.000E+00	0.000E+00	0.000E+00	0.00E+00	0.00E+00	0.00E+00	0.00E+00
12	0.000E+00	0.000E+00	0.000E+00	0.00E+00	0.00E+00	0.00E+00	0.00E+00
13	0.115E-03	-0.149E-03	-0.265E-04	0.00E+00	0.00E+00	0.00E+00	0.00E+00
14	0.129E-03	-0.206E-10	0.210E-04	0.00E+00	0.00E+00	0.00E+00	0.00E+00
15	0.113E-03	0.149E-03	-0.265E-04	0.00E+00	0.00E+00	0.00E+00	0.00E+00
16	0.000E+00	0.000E+00	0.000E+00	0.00E+00	0.00E+00	0.00E+00	0.00E+00
17	0.000E+00	0.000E+00	0.000E+00	0.00E+00	0.00E+00	0.00E+00	0.00E+00
18	0.000E+00	0.000E+00	0.000E+00	0.00E+00	0.00E+00	0.00E+00	0.00E+00
19	0.687E-03	-0.759E-03	-0.261E-03	0.00E+00	0.00E+00	0.00E+00	0.00E+00
20	0.971E-03	-0.456E-10	0.101E-03	0.00E+00	0.00E+00	0.00E+00	0.00E+00
21	0.687E-03	0.759E-03	-0.261E-03	0.00E+00	0.00E+00	0.00E+00	0.00E+00
22	0.000E+00	0.000E+00	0.000E+00	0.00E+00	0.00E+00	0.00E+00	0.00E+00
23	0.000E+00	0.000E+00	0.000E+00	0.00E+00	0.00E+00	0.00E+00	0.00E+00
24	0.000E+00	0.000E+00	0.000E+00	0.00E+00	0.00E+00	0.00E+00	0.00E+00
25	0.254E-02	-0.702E-04	0.477E-03	0.00E+00	0.00E+00	0.95E-04	0.00E+00
26	0.295E-02	-0.578E-11	0.116E-03	0.00E+00	0.00E+00	-0.25E-05	0.00E+00
27	0.254E-02	0.702E-04	0.477E-03	0.00E+00	0.00E+00	0.95E-04	0.00E+00
28	0.000E+00	0.000E+00	0.000E+00	0.00E+00	0.00E+00	0.00E+00	0.00E+00
29	0.000E+00	0.000E+00	0.000E+00	0.00E+00	0.00E+00	0.00E+00	0.00E+00
30	0.000E+00	0.000E+00	0.000E+00	0.00E+00	0.00E+00	0.00E+00	0.00E+00

31	0.305E-02	0.176E-04	0.248E-05	0.00E+00	0.20E-04	0.00E+00
32	0.305E-02	0.984E-14	-0.368E-04	0.00E+00	0.13E-04	0.00E+00
33	0.305E-02	-0.176E-04	0.248E-05	0.00E+00	0.20E-04	0.00E+00
34	0.315E-02	0.287E-11	0.848E-12	0.00E+00	-0.13E-04	0.00E+00
35	0.314E-02	0.302E-11	0.139E-17	0.00E+00	-0.13E-04	0.00E+00
36	0.315E-02	0.287E-11	-0.848E-12	0.00E+00	-0.13E-04	0.00E+00
37	0.305E-02	-0.176E-04	-0.248E-05	0.00E+00	0.20E-04	0.00E+00
38	0.305E-02	0.980E-14	0.368E-04	0.00E+00	0.13E-04	0.00E+00
39	0.305E-02	0.176E-04	-0.248E-05	0.00E+00	0.20E-04	0.00E+00
40	0.254E-02	0.702E-04	-0.477E-03	0.00E+00	0.95E-04	0.00E+00
41	0.295E-02	-0.578E-11	-0.116E-03	0.00E+00	-0.25E-05	0.00E+00
42	0.254E-02	-0.702E-04	-0.477E-03	0.00E+00	0.95E-04	0.00E+00
43	0.000E+00	0.000E+00	0.000E+00	0.00E+00	0.00E+00	0.00E+00
44	0.000E+00	0.000E+00	0.000E+00	0.00E+00	0.00E+00	0.00E+00
45	0.000E+00	0.000E+00	0.000E+00	0.00E+00	0.00E+00	0.00E+00
46	0.687E-03	0.759E-03	0.261E-03	0.00E+00	0.00E+00	0.00E+00
47	0.971E-03	-0.456E-10	-0.101E-03	0.00E+00	0.00E+00	0.00E+00
48	0.687E-03	-0.759E-03	0.261E-03	0.00E+00	0.00E+00	0.00E+00
49	0.000E+00	0.000E+00	0.000E+00	0.00E+00	0.00E+00	0.00E+00
50	0.000E+00	0.000E+00	0.000E+00	0.00E+00	0.00E+00	0.00E+00
51	0.000E+00	0.000E+00	0.000E+00	0.00E+00	0.00E+00	0.00E+00
52	0.113E-03	0.149E-03	0.265E-04	0.00E+00	0.00E+00	0.00E+00
53	0.129E-03	-0.206E-10	-0.210E-04	0.00E+00	0.00E+00	0.00E+00
54	0.113E-03	-0.149E-03	0.265E-04	0.00E+00	0.00E+00	0.00E+00
55	0.000E+00	0.000E+00	0.000E+00	0.00E+00	0.00E+00	0.00E+00
56	0.000E+00	0.000E+00	0.000E+00	0.00E+00	0.00E+00	0.00E+00
57	0.000E+00	0.000E+00	0.000E+00	0.00E+00	0.00E+00	0.00E+00
58	0.976E-05	0.756E-05	0.465E-05	0.00E+00	0.00E+00	0.00E+00
59	0.530E-05	-0.304E-12	-0.107E-05	0.00E+00	0.00E+00	0.00E+00
60	0.976E-05	-0.756E-05	0.465E-05	0.00E+00	0.00E+00	0.00E+00
61	0.000E+00	0.000E+00	0.000E+00	0.00E+00	0.00E+00	0.00E+00

62	0.000E+00	0.000E+00	0.000E+00	0.000E+00	0.00E+00	0.00E+00	0.00E+00	0.00E+00
63	0.000E+00	0.000E+00	0.000E+00	0.000E+00	0.00E+00	0.00E+00	0.00E+00	0.00E+00
64	-0.850E-06	0.296E-06	-0.625E-06	0.00E+00	0.00E+00	0.00E+00	0.00E+00	0.00E+00
65	0.790E-07	0.447E-11	-0.755E-06	0.00E+00	0.00E+00	0.00E+00	0.00E+00	0.00E+00
66	-0.850E-06	-0.296E-06	-0.625E-06	0.00E+00	0.00E+00	0.00E+00	0.00E+00	0.00E+00
67	0.000E+00	0.000E+00	0.000E+00	0.000E+00	0.00E+00	0.00E+00	0.00E+00	0.00E+00
68	0.000E+00	0.000E+00	0.000E+00	0.000E+00	0.00E+00	0.00E+00	0.00E+00	0.00E+00
69	0.000E+00	0.000E+00	0.000E+00	0.000E+00	0.00E+00	0.00E+00	0.00E+00	0.00E+00

MODE NUMBER = 6  
 FREQUENCY(HZ) = 20.888

----- X Y Z -----  
 ----- XX YY ZZ -----  
 -----

1	0.658E-07	-0.305E-04	-0.190E-05	0.00E+00	0.00E+00	0.00E+00	0.00E+00	0.00E+00
2	0.243E-16	-0.802E-05	-0.575E-17	0.00E+00	0.00E+00	0.00E+00	0.00E+00	0.00E+00
3	-0.658E-07	-0.305E-04	0.190E-05	0.00E+00	0.00E+00	0.00E+00	0.00E+00	0.00E+00
4	0.000E+00	0.000E+00	0.000E+00	0.00E+00	0.00E+00	0.00E+00	0.00E+00	0.00E+00
5	0.000E+00	0.000E+00	0.000E+00	0.00E+00	0.00E+00	0.00E+00	0.00E+00	0.00E+00
6	0.000E+00	0.000E+00	0.000E+00	0.00E+00	0.00E+00	0.00E+00	0.00E+00	0.00E+00
7	-0.461E-06	0.128E-04	0.582E-05	0.00E+00	0.00E+00	0.00E+00	0.00E+00	0.00E+00
8	-0.225E-16	0.285E-04	0.934E-18	0.00E+00	0.00E+00	0.00E+00	0.00E+00	0.00E+00
9	0.461E-06	0.128E-04	-0.582E-05	0.00E+00	0.00E+00	0.00E+00	0.00E+00	0.00E+00
10	0.000E+00	0.000E+00	0.000E+00	0.00E+00	0.00E+00	0.00E+00	0.00E+00	0.00E+00
11	0.000E+00	0.000E+00	0.000E+00	0.00E+00	0.00E+00	0.00E+00	0.00E+00	0.00E+00
12	0.000E+00	0.000E+00	0.000E+00	0.00E+00	0.00E+00	0.00E+00	0.00E+00	0.00E+00
13	-0.521E-04	-0.595E-04	-0.672E-05	0.00E+00	0.00E+00	0.00E+00	0.00E+00	0.00E+00
14	0.117E-16	-0.239E-05	-0.525E-17	0.00E+00	0.00E+00	0.00E+00	0.00E+00	0.00E+00
15	0.521E-04	-0.595E-04	0.672E-05	0.00E+00	0.00E+00	0.00E+00	0.00E+00	0.00E+00
16	0.000E+00	0.000E+00	0.000E+00	0.00E+00	0.00E+00	0.00E+00	0.00E+00	0.00E+00

17	0.000E+00	0.000E+00	0.000E+00	0.000E+00	0.000E+00	0.000E+00	0.000E+00	0.000E+00	0.000E+00
18	0.000E+00	0.000E+00	0.000E+00	0.000E+00	0.000E+00	0.000E+00	0.000E+00	0.000E+00	0.000E+00
19	-0.258E-03	-0.164E-02	0.117E-03	0.000E+00	0.000E+00	0.000E+00	0.000E+00	0.000E+00	0.000E+00
20	0.501E-16	-0.986E-03	0.476E-17	0.000E+00	0.000E+00	0.000E+00	0.000E+00	0.000E+00	0.000E+00
21	0.258E-03	-0.164E-02	-0.117E-03	0.000E+00	0.000E+00	0.000E+00	0.000E+00	0.000E+00	0.000E+00
22	0.000E+00	0.000E+00	0.000E+00	0.000E+00	0.000E+00	0.000E+00	0.000E+00	0.000E+00	0.000E+00
23	0.000E+00	0.000E+00	0.000E+00	0.000E+00	0.000E+00	0.000E+00	0.000E+00	0.000E+00	0.000E+00
24	0.000E+00	0.000E+00	0.000E+00	0.000E+00	0.000E+00	0.000E+00	0.000E+00	0.000E+00	0.000E+00
25	-0.861E-03	-0.573E-02	-0.118E-02	0.000E+00	0.000E+00	0.000E+00	-0.24E-03	0.000E+00	0.000E+00
26	-0.291E-16	-0.372E-02	-0.131E-16	0.000E+00	0.000E+00	0.000E+00	0.31E-15	0.000E+00	0.000E+00
27	0.861E-03	-0.573E-02	0.118E-02	0.000E+00	0.000E+00	0.000E+00	0.24E-03	0.000E+00	0.000E+00
28	0.000E+00	0.000E+00	0.000E+00	0.000E+00	0.000E+00	0.000E+00	0.000E+00	0.000E+00	0.000E+00
29	0.000E+00	0.000E+00	0.000E+00	0.000E+00	0.000E+00	0.000E+00	0.000E+00	0.000E+00	0.000E+00
30	0.000E+00	0.000E+00	0.000E+00	0.000E+00	0.000E+00	0.000E+00	0.000E+00	0.000E+00	0.000E+00
31	-0.134E-02	-0.269E-02	-0.570E-03	0.000E+00	0.000E+00	0.000E+00	-0.19E-04	0.000E+00	0.000E+00
32	0.804E-17	-0.273E-02	-0.176E-14	0.000E+00	0.000E+00	0.000E+00	0.27E-17	0.000E+00	0.000E+00
33	0.134E-02	-0.269E-02	0.570E-03	0.000E+00	0.000E+00	0.000E+00	0.19E-04	0.000E+00	0.000E+00
34	-0.176E-02	-0.223E-15	0.657E-15	0.000E+00	0.000E+00	0.000E+00	-0.26E-04	0.000E+00	0.000E+00
35	0.448E-16	-0.226E-15	-0.139E-16	0.000E+00	0.000E+00	0.000E+00	-0.51E-15	0.000E+00	0.000E+00
36	0.176E-02	-0.204E-15	-0.651E-15	0.000E+00	0.000E+00	0.000E+00	0.26E-04	0.000E+00	0.000E+00
37	-0.134E-02	0.269E-02	0.570E-03	0.000E+00	0.000E+00	0.000E+00	-0.19E-04	0.000E+00	0.000E+00
38	0.696E-16	0.273E-02	0.174E-14	0.000E+00	0.000E+00	0.000E+00	0.65E-18	0.000E+00	0.000E+00
39	0.134E-02	0.269E-02	-0.570E-03	0.000E+00	0.000E+00	0.000E+00	0.19E-04	0.000E+00	0.000E+00
40	-0.861E-03	0.573E-02	0.118E-02	0.000E+00	0.000E+00	0.000E+00	-0.24E-03	0.000E+00	0.000E+00
41	0.666E-16	0.572E-02	0.285E-17	0.000E+00	0.000E+00	0.000E+00	0.30E-15	0.000E+00	0.000E+00
42	0.661E-03	0.573E-02	-0.118E-02	0.000E+00	0.000E+00	0.000E+00	0.24E-03	0.000E+00	0.000E+00
43	0.000E+00	0.000E+00	0.000E+00	0.000E+00	0.000E+00	0.000E+00	0.000E+00	0.000E+00	0.000E+00
44	0.000E+00	0.000E+00	0.000E+00	0.000E+00	0.000E+00	0.000E+00	0.000E+00	0.000E+00	0.000E+00
45	0.000E+00	0.000E+00	0.000E+00	0.000E+00	0.000E+00	0.000E+00	0.000E+00	0.000E+00	0.000E+00
46	-0.258E-03	0.164E-02	-0.117E-03	0.000E+00	0.000E+00	0.000E+00	0.000E+00	0.000E+00	0.000E+00
47	0.998E-17	0.986E-03	-0.143E-17	0.000E+00	0.000E+00	0.000E+00	0.000E+00	0.000E+00	0.000E+00
48	0.258E-03	0.164E-02	0.117E-03	0.000E+00	0.000E+00	0.000E+00	0.000E+00	0.000E+00	0.000E+00





55	0.511E+00	0.415E+04	0.238E-13	0.00E+00	-0.29E+08	0.00E+00
56	0.509E+00	0.595E+04	0.021E+02	0.00E+00	0.21E+08	0.00E+00
57	0.536E+04	0.712E+05	-0.492E-02	0.00E+00	-0.14E+03	0.00E+00
58	0.450E+00	0.795E+05	-0.519E-07	0.00E+00	0.35E+09	0.00E+00
59	-0.536E+04	0.712E+05	0.442E-02	0.00E+00	0.14E-03	0.00E+00
60	0.486E+04	-0.662E+04	-0.112E-03	0.00E+00	-0.16E+03	0.00E+00
61	0.165E+00	-0.652E+04	-0.891E-08	0.00E+00	0.41E+08	0.00E+00
62	-0.486E+04	-0.562E+04	0.112E+05	0.00E+00	0.18E-03	0.00E+00
63	0.000E+00	0.000E+00	0.000E+00	0.00E+00	0.00E+00	0.00E+00
64	0.000E+00	0.000E+00	0.000E+00	0.00E+00	0.00E+00	0.00E+00
65	0.000E+00	0.000E+00	0.000E+00	0.00E+00	0.00E+00	0.00E+00
66	0.000E+00	0.000E+00	0.000E+00	0.00E+00	0.00E+00	0.00E+00
67	0.191E+04	-0.509E+04	0.129E-04	0.00E+00	0.00E+00	0.00E+00
68	0.172E+07	-0.260E+04	-0.245E-07	0.00E+00	0.00E+00	0.00E+00
69	-0.191E+04	-0.502E+04	-0.129E-04	0.00E+00	0.00E+00	0.00E+00
70	0.000E+00	0.000E+00	0.000E+00	0.00E+00	0.00E+00	0.00E+00
71	0.000E+00	0.000E+00	0.000E+00	0.00E+00	0.00E+00	0.00E+00
72	0.244E+05	0.665E+05	-0.402E-06	0.00E+00	0.00E+00	0.00E+00
73	0.131E+06	-0.927E+05	0.316E-08	0.00E+00	0.00E+00	0.00E+00
74	-0.244E+05	0.672E+05	0.401E-06	0.00E+00	0.00E+00	0.00E+00
75	0.000E+00	0.000E+00	0.000E+00	0.00E+00	0.00E+00	0.00E+00
76	0.000E+00	0.000E+00	0.000E+00	0.00E+00	0.00E+00	0.00E+00
77	0.000E+00	0.000E+00	0.000E+00	0.00E+00	0.00E+00	0.00E+00
78	0.149E+06	-0.409E+05	0.229E-05	0.00E+00	0.00E+00	0.00E+00
79	-0.515E+07	0.178E+05	0.100E-07	0.00E+00	0.00E+00	0.00E+00
80	-0.150E+06	-0.485E+05	-0.217E-06	0.00E+00	0.00E+00	0.00E+00
81	0.000E+00	0.000E+00	0.000E+00	0.00E+00	0.00E+00	0.00E+00
82	0.000E+00	0.000E+00	0.000E+00	0.00E+00	0.00E+00	0.00E+00
83	0.000E+00	0.000E+00	0.000E+00	0.00E+00	0.00E+00	0.00E+00
84	-0.515E+07	0.241E+05	-0.894E-07	0.00E+00	0.00E+00	0.00E+00
85	-0.988E+07	-0.155E+05	-0.510E-07	0.00E+00	0.00E+00	0.00E+00
86	0.591E+07	0.507E+05	0.771E-07	0.00E+00	0.00E+00	0.00E+00

67 0.000E+00 0.000E+00 0.000E+00 0.000E+00 0.000E+00 0.000E+00 0.000E+00 0.000E+00  
 68 0.000E+00 0.000E+00 0.000E+00 0.000E+00 0.000E+00 0.000E+00 0.000E+00 0.000E+00  
 69 0.000E+00 0.000E+00 0.000E+00 0.000E+00 0.000E+00 0.000E+00 0.000E+00 0.000E+00

MODE NUMBER = 8

FREQUENCY (HZ) = 22.851

NODE	X	Y	Z	XX	YY	ZZ
1	-0.370E-06	-0.471E-04	-0.682E-06	0.00E+00	0.00E+00	0.00E+00
2	0.194E-16	0.712E-05	-0.439E-17	0.00E+00	0.00E+00	0.00E+00
3	0.570E-06	-0.471E-04	0.682E-06	0.00E+00	0.00E+00	0.00E+00
4	0.000E+00	0.000E+00	0.000E+00	0.00E+00	0.00E+00	0.00E+00
5	0.000E+00	0.000E+00	0.000E+00	0.00E+00	0.00E+00	0.00E+00
6	0.000E+00	0.000E+00	0.000E+00	0.00E+00	0.00E+00	0.00E+00
7	0.616E-06	0.506E-04	0.964E-06	0.00E+00	0.00E+00	0.00E+00
8	-0.186E-16	0.231E-05	0.171E-18	0.00E+00	0.00E+00	0.00E+00
9	-0.616E-06	0.506E-04	-0.964E-06	0.00E+00	0.00E+00	0.00E+00
10	0.000E+00	0.000E+00	0.000E+00	0.00E+00	0.00E+00	0.00E+00
11	0.000E+00	0.000E+00	0.000E+00	0.00E+00	0.00E+00	0.00E+00
12	0.000E+00	0.000E+00	0.000E+00	0.00E+00	0.00E+00	0.00E+00
13	-0.170E-05	-0.705E-04	-0.180E-05	0.00E+00	0.00E+00	0.00E+00
14	0.145E-16	-0.584E-04	-0.166E-17	0.00E+00	0.00E+00	0.00E+00
15	0.170E-05	-0.705E-04	0.180E-05	0.00E+00	0.00E+00	0.00E+00
16	0.000E+00	0.000E+00	0.000E+00	0.00E+00	0.00E+00	0.00E+00
17	0.000E+00	0.000E+00	0.000E+00	0.00E+00	0.00E+00	0.00E+00
18	0.000E+00	0.000E+00	0.000E+00	0.00E+00	0.00E+00	0.00E+00
19	-0.955E-05	-0.352E-03	-0.968E-05	0.00E+00	0.00E+00	0.00E+00
20	0.260E-16	-0.183E-03	-0.577E-17	0.00E+00	0.00E+00	0.00E+00
21	0.955E-05	-0.352E-03	0.968E-05	0.00E+00	0.00E+00	0.00E+00



22	0.000E+00	0.000E+00	0.000E+00	0.000E+00	0.00E+00	0.00E+00	0.00E+00	0.00E+00
23	0.000E+00	0.000E+00	0.000E+00	0.000E+00	0.00E+00	0.00E+00	0.00E+00	0.00E+00
24	0.000E+00	0.000E+00	0.000E+00	0.000E+00	0.00E+00	0.00E+00	0.00E+00	0.00E+00
25	-0.526E-04	-0.328E-03	0.240E-04	0.00E+00	0.00E+00	-0.29E-05	0.00E+00	0.00E+00
26	-0.589E-17	-0.531E-03	0.396E-16	0.00E+00	0.00E+00	-0.31E-15	0.00E+00	0.00E+00
27	0.526E-04	-0.528E-03	-0.240E-04	0.00E+00	0.00E+00	0.29E-03	0.00E+00	0.00E+00
28	0.000E+00	0.000E+00	0.000E+00	0.000E+00	0.00E+00	0.00E+00	0.00E+00	0.00E+00
29	0.000E+00	0.000E+00	0.000E+00	0.000E+00	0.00E+00	0.00E+00	0.00E+00	0.00E+00
30	0.000E+00	0.000E+00	0.000E+00	0.000E+00	0.00E+00	0.00E+00	0.00E+00	0.00E+00
31	-0.119E-03	-0.268E-03	0.621E-02	0.00E+00	0.00E+00	0.39E-06	0.00E+00	0.00E+00
32	-0.275E-17	-0.272E-03	0.106E-14	0.00E+00	0.00E+00	0.20E-15	0.00E+00	0.00E+00
33	0.119E-03	-0.268E-03	-0.621E-02	0.00E+00	0.00E+00	-0.39E-06	0.00E+00	0.00E+00
34	-0.173E-03	0.244E-16	0.122E-14	0.00E+00	0.00E+00	0.29E-03	0.00E+00	0.00E+00
35	0.864E-18	0.244E-16	-0.155E-14	0.00E+00	0.00E+00	-0.54E-17	0.00E+00	0.00E+00
36	0.173E-03	0.252E-16	-0.401E-14	0.00E+00	0.00E+00	-0.29E-03	0.00E+00	0.00E+00
37	-0.119E-03	0.268E-03	-0.621E-02	0.00E+00	0.00E+00	0.39E-06	0.00E+00	0.00E+00
38	0.349E-17	0.272E-03	0.996E-15	0.00E+00	0.00E+00	-0.20E-15	0.00E+00	0.00E+00
39	0.119E-03	0.268E-03	0.621E-02	0.00E+00	0.00E+00	-0.39E-06	0.00E+00	0.00E+00
40	-0.526E-04	0.528E-03	-0.240E-04	0.00E+00	0.00E+00	-0.29E-03	0.00E+00	0.00E+00
41	0.487E-17	0.331E-03	0.265E-16	0.00E+00	0.00E+00	0.35E-15	0.00E+00	0.00E+00
42	0.526E-04	0.328E-03	0.240E-04	0.00E+00	0.00E+00	0.29E-03	0.00E+00	0.00E+00
43	0.000E+00	0.000E+00	0.000E+00	0.000E+00	0.00E+00	0.00E+00	0.00E+00	0.00E+00
44	0.000E+00	0.000E+00	0.000E+00	0.000E+00	0.00E+00	0.00E+00	0.00E+00	0.00E+00
45	0.000E+00	0.000E+00	0.000E+00	0.000E+00	0.00E+00	0.00E+00	0.00E+00	0.00E+00
46	-0.955E-05	0.552E-03	0.968E-05	0.00E+00	0.00E+00	0.00E+00	0.00E+00	0.00E+00
47	-0.271E-16	0.183E-03	-0.172E-17	0.00E+00	0.00E+00	0.00E+00	0.00E+00	0.00E+00
48	0.955E-05	0.552E-03	-0.968E-05	0.00E+00	0.00E+00	0.00E+00	0.00E+00	0.00E+00
49	0.000E+00	0.000E+00	0.000E+00	0.000E+00	0.00E+00	0.00E+00	0.00E+00	0.00E+00
50	0.000E+00	0.000E+00	0.000E+00	0.000E+00	0.00E+00	0.00E+00	0.00E+00	0.00E+00
51	0.000E+00	0.000E+00	0.000E+00	0.000E+00	0.00E+00	0.00E+00	0.00E+00	0.00E+00
52	-0.170E-05	0.705E-04	0.180E-05	0.00E+00	0.00E+00	0.00E+00	0.00E+00	0.00E+00

53	-0.155E-16	0.500E-04	-0.187E-17	0.00E+00	0.00E+00	0.00E+00	0.00E+00
54	0.170E-05	0.705E-04	-0.180E-05	0.00E+00	0.00E+00	0.00E+00	0.00E+00
55	0.000E+00	0.000E+00	0.000E+00	0.00E+00	0.00E+00	0.00E+00	0.00E+00
56	0.000E+00	0.000E+00	0.000E+00	0.00E+00	0.00E+00	0.00E+00	0.00E+00
57	0.000E+00	0.000E+00	0.000E+00	0.00E+00	0.00E+00	0.00E+00	0.00E+00
58	0.616E-06	-0.506E-04	-0.964E-06	0.00E+00	0.00E+00	0.00E+00	0.00E+00
59	0.179E-16	-0.231E-05	0.226E-18	0.00E+00	0.00E+00	0.00E+00	0.00E+00
60	-0.616E-06	-0.506E-04	0.964E-06	0.00E+00	0.00E+00	0.00E+00	0.00E+00
61	0.000E+00	0.000E+00	0.000E+00	0.00E+00	0.00E+00	0.00E+00	0.00E+00
62	0.000E+00	0.000E+00	0.000E+00	0.00E+00	0.00E+00	0.00E+00	0.00E+00
63	0.000E+00	0.000E+00	0.000E+00	0.00E+00	0.00E+00	0.00E+00	0.00E+00
64	-0.570E-06	0.471E-04	0.682E-06	0.00E+00	0.00E+00	0.00E+00	0.00E+00
65	-0.187E-16	-0.712E-05	-0.418E-17	0.00E+00	0.00E+00	0.00E+00	0.00E+00
66	0.570E-06	0.471E-04	-0.682E-06	0.00E+00	0.00E+00	0.00E+00	0.00E+00
67	0.000E+00	0.000E+00	0.000E+00	0.00E+00	0.00E+00	0.00E+00	0.00E+00
68	0.000E+00	0.000E+00	0.000E+00	0.00E+00	0.00E+00	0.00E+00	0.00E+00
69	0.000E+00	0.000E+00	0.000E+00	0.00E+00	0.00E+00	0.00E+00	0.00E+00

MODE NUMBER = 9

FREQUENCY (HZ) = 24.579

NODE	X	Y	Z	XX	YY	ZZ
1	-0.285E-06	-0.368E-04	-0.140E-06	0.00E+00	0.00E+00	0.00E+00
2	0.320E-05	0.879E-05	-0.100E-05	0.00E+00	0.00E+00	0.00E+00
3	0.524E-07	-0.156E-04	-0.922E-07	0.00E+00	0.00E+00	0.00E+00
4	0.000E+00	0.000E+00	0.000E+00	0.00E+00	0.00E+00	0.00E+00
5	0.000E+00	0.000E+00	0.000E+00	0.00E+00	0.00E+00	0.00E+00
6	0.000E+00	0.000E+00	0.000E+00	0.00E+00	0.00E+00	0.00E+00
7	0.113E-06	0.485E-04	0.186E-06	0.00E+00	0.00E+00	0.00E+00

8	0.955E-06	-0.913E-05	0.521E-06	0.00E+00	0.00E+00	0.00E+00	0.00E+00
9	-0.854E-07	0.245E-04	0.207E-06	0.00E+00	0.00E+00	0.00E+00	0.00E+00
10	0.000E+00	0.000E+00	0.000E+00	0.00E+00	0.00E+00	0.00E+00	0.00E+00
11	0.000E+00	0.000E+00	0.000E+00	0.00E+00	0.00E+00	0.00E+00	0.00E+00
12	0.000E+00	0.000E+00	0.000E+00	0.00E+00	0.00E+00	0.00E+00	0.00E+00
13	0.583E-05	-0.551E-04	-0.141E-06	0.00E+00	0.00E+00	0.00E+00	0.00E+00
14	-0.414E-05	0.259E-04	0.944E-07	0.00E+00	0.00E+00	0.00E+00	0.00E+00
15	-0.350E-05	-0.514E-04	0.881E-07	0.00E+00	0.00E+00	0.00E+00	0.00E+00
16	0.000E+00	0.000E+00	0.000E+00	0.00E+00	0.00E+00	0.00E+00	0.00E+00
17	0.000E+00	0.000E+00	0.000E+00	0.00E+00	0.00E+00	0.00E+00	0.00E+00
18	0.000E+00	0.000E+00	0.000E+00	0.00E+00	0.00E+00	0.00E+00	0.00E+00
19	0.304E-04	0.206E-03	-0.151E-04	0.00E+00	0.00E+00	0.00E+00	0.00E+00
20	-0.466E-06	0.915E-04	-0.781E-06	0.00E+00	0.00E+00	0.00E+00	0.00E+00
21	-0.306E-04	0.226E-03	0.145E-04	0.00E+00	0.00E+00	0.00E+00	0.00E+00
22	0.000E+00	0.000E+00	0.000E+00	0.00E+00	0.00E+00	0.00E+00	0.00E+00
23	0.000E+00	0.000E+00	0.000E+00	0.00E+00	0.00E+00	0.00E+00	0.00E+00
24	0.000E+00	0.000E+00	0.000E+00	0.00E+00	0.00E+00	0.00E+00	0.00E+00
25	0.810E-04	0.123E-03	0.148E-03	0.00E+00	0.00E+00	-0.19E-03	0.00E+00
26	-0.494E-07	0.119E-03	-0.235E-06	0.00E+00	0.00E+00	-0.10E-06	0.00E+00
27	-0.812E-04	0.122E-03	-0.148E-03	0.00E+00	0.00E+00	0.19E-03	0.00E+00
28	0.000E+00	0.000E+00	0.000E+00	0.00E+00	0.00E+00	0.00E+00	0.00E+00
29	0.000E+00	0.000E+00	0.000E+00	0.00E+00	0.00E+00	0.00E+00	0.00E+00
30	0.000E+00	0.000E+00	0.000E+00	0.00E+00	0.00E+00	0.00E+00	0.00E+00
31	0.591E-04	-0.121E-05	0.439E-02	0.00E+00	0.00E+00	0.16E-03	0.00E+00
32	-0.138E-06	-0.277E-05	-0.124E-05	0.00E+00	0.00E+00	-0.95E-08	0.00E+00
33	-0.594E-04	-0.121E-05	-0.439E-02	0.00E+00	0.00E+00	-0.16E-03	0.00E+00
34	-0.156E-06	-0.609E-04	-0.626E-02	0.00E+00	0.00E+00	-0.49E-07	0.00E+00
35	-0.157E-06	-0.643E-04	-0.780E-12	0.00E+00	0.00E+00	0.59E-07	0.00E+00
36	-0.156E-06	-0.609E-04	0.626E-02	0.00E+00	0.00E+00	-0.49E-07	0.00E+00
37	-0.594E-04	-0.121E-05	0.439E-02	0.00E+00	0.00E+00	-0.16E-03	0.00E+00
38	-0.138E-06	-0.277E-05	0.124E-05	0.00E+00	0.00E+00	-0.95E-08	0.00E+00
39	0.591E-04	-0.121E-05	-0.439E-02	0.00E+00	0.00E+00	0.16E-03	0.00E+00

40	-0.612E-04	0.122F-03	0.148E-03	0.00E+00	0.19E-03	0.00E+00
41	-0.494E-07	0.119E-03	0.235E-06	0.00E+00	-0.10E-06	0.00E+00
42	0.610E-04	0.123E-03	-0.148E-03	0.00E+00	-0.19E-03	0.00E+00
43	0.000E+00	0.000E+00	0.000E+00	0.00E+00	0.00E+00	0.00E+00
44	0.000E+00	0.000E+00	0.000E+00	0.00E+00	0.00E+00	0.00E+00
45	0.000E+00	0.000E+00	0.000E+00	0.00E+00	0.00E+00	0.00E+00
46	-0.306E-04	0.226E-03	-0.143E-04	0.00E+00	0.00E+00	0.00E+00
47	-0.467E-06	0.915E-04	0.780E-06	0.00E+00	0.00E+00	0.00E+00
48	0.304E-04	0.206E-03	0.151E-04	0.00E+00	0.00E+00	0.00E+00
49	0.000E+00	0.000E+00	0.000E+00	0.00E+00	0.00E+00	0.00E+00
50	0.000E+00	0.000E+00	0.000E+00	0.00E+00	0.00E+00	0.00E+00
51	0.000E+00	0.000E+00	0.000E+00	0.00E+00	0.00E+00	0.00E+00
52	-0.590E-05	-0.514E-04	-0.881E-07	0.00E+00	0.00E+00	0.00E+00
53	-0.414E-05	0.259E-04	-0.945E-07	0.00E+00	0.00E+00	0.00E+00
54	0.583E-05	-0.551E-04	0.141E-06	0.00E+00	0.00E+00	0.00E+00
55	0.000E+00	0.000E+00	0.000E+00	0.00E+00	0.00E+00	0.00E+00
56	0.000E+00	0.000E+00	0.000E+00	0.00E+00	0.00E+00	0.00E+00
57	0.000E+00	0.000E+00	0.000E+00	0.00E+00	0.00E+00	0.00E+00
58	-0.834E-07	0.245E-04	-0.207E-06	0.00E+00	0.00E+00	0.00E+00
59	0.955E-06	-0.913E-05	-0.321E-06	0.00E+00	0.00E+00	0.00E+00
60	0.113E-06	0.485E-04	-0.186E-06	0.00E+00	0.00E+00	0.00E+00
61	0.000E+00	0.000E+00	0.000E+00	0.00E+00	0.00E+00	0.00E+00
62	0.000E+00	0.000E+00	0.000E+00	0.00E+00	0.00E+00	0.00E+00
63	0.000E+00	0.000E+00	0.000E+00	0.00E+00	0.00E+00	0.00E+00
64	0.324E-07	-0.156E-04	0.922E-07	0.00E+00	0.00E+00	0.00E+00
65	0.320E-05	0.079E-05	0.100E-05	0.00E+00	0.00E+00	0.00E+00
66	-0.285E-06	-0.368E-04	0.140E-06	0.00E+00	0.00E+00	0.00E+00
67	0.000E+00	0.000E+00	0.000E+00	0.00E+00	0.00E+00	0.00E+00
68	0.000E+00	0.000E+00	0.000E+00	0.00E+00	0.00E+00	0.00E+00
69	0.000E+00	0.000E+00	0.000E+00	0.00E+00	0.00E+00	0.00E+00

MODE NUMBER = 10  
 FREQUENCY(HZ) = 23.982

MODE	X	Y	Z	XX	YY	ZZ
1	0.678E+04	0.402E-02	0.248E-04	0.00E+00	0.00E+00	0.00E+00
2	-0.177E-02	0.201E-08	0.442E-03	0.00E+00	0.00E+00	0.00E+00
3	0.678E+04	-0.402E-02	0.248E-04	0.00E+00	0.00E+00	0.00E+00
4	0.000E+00	0.000E+00	0.000E+00	0.00E+00	0.00E+00	0.00E+00
5	0.000E+00	0.000E+00	0.000E+00	0.00E+00	0.00E+00	0.00E+00
6	0.000E+00	0.000E+00	0.000E+00	0.00E+00	0.00E+00	0.00E+00
7	-0.215E-04	-0.692E-02	-0.861E-04	0.00E+00	0.00E+00	0.00E+00
8	0.116E-02	-0.165E-08	-0.762E-04	0.00E+00	0.00E+00	0.00E+00
9	-0.215E-04	0.692E-02	-0.861E-04	0.00E+00	0.00E+00	0.00E+00
10	0.000E+00	0.000E+00	0.000E+00	0.00E+00	0.00E+00	0.00E+00
11	0.000E+00	0.000E+00	0.000E+00	0.00E+00	0.00E+00	0.00E+00
12	0.000E+00	0.000E+00	0.000E+00	0.00E+00	0.00E+00	0.00E+00
13	0.625E-05	0.105E-01	0.185E-03	0.00E+00	0.00E+00	0.00E+00
14	-0.490E-03	0.132E-08	0.187E-03	0.00E+00	0.00E+00	0.00E+00
15	0.625E-05	-0.105E-01	0.185E-03	0.00E+00	0.00E+00	0.00E+00
16	0.000E+00	0.000E+00	0.000E+00	0.00E+00	0.00E+00	0.00E+00
17	0.000E+00	0.000E+00	0.000E+00	0.00E+00	0.00E+00	0.00E+00
18	0.000E+00	0.000E+00	0.000E+00	0.00E+00	0.00E+00	0.00E+00
19	-0.206E-04	-0.747E-02	-0.146E-03	0.00E+00	0.00E+00	0.00E+00
20	-0.214E-02	0.805E-08	-0.111E-03	0.00E+00	0.00E+00	0.00E+00
21	-0.206E-04	0.747E-02	-0.146E-03	0.00E+00	0.00E+00	0.00E+00
22	0.000E+00	0.000E+00	0.000E+00	0.00E+00	0.00E+00	0.00E+00
23	0.000E+00	0.000E+00	0.000E+00	0.00E+00	0.00E+00	0.00E+00
24	0.000E+00	0.000E+00	0.000E+00	0.00E+00	0.00E+00	0.00E+00
25	0.418E-04	0.124E-04	-0.495E-04	0.00E+00	-0.79E-05	0.00E+00

26	0.929E-04	0.115E-08	-0.496E-04	0.00E+00	-0.80E-05	0.00E+00
27	0.418E-04	-0.123E-04	-0.493E-04	0.00E+00	-0.79E-05	0.00E+00
28	0.000E+00	0.000E+00	0.000E+00	0.00E+00	0.00E+00	0.00E+00
29	0.000E+00	0.000E+00	0.000E+00	0.00E+00	0.00E+00	0.00E+00
30	0.000E+00	0.000E+00	0.000E+00	0.00E+00	0.00E+00	0.00E+00
31	0.395E-04	0.735E-05	0.181E-05	0.00E+00	-0.19E-05	0.00E+00
32	0.359E-04	-0.356E-10	0.645E-06	0.00E+00	-0.19E-05	0.00E+00
33	0.395E-04	-0.735E-05	0.181E-05	0.00E+00	-0.19E-05	0.00E+00
34	0.221E-10	0.269E-05	-0.162E-05	0.00E+00	-0.24E-11	0.00E+00
35	0.226E-10	-0.624E-09	-0.146E-05	0.00E+00	0.10E-11	0.00E+00
36	0.221E-10	-0.269E-05	-0.162E-05	0.00E+00	-0.24E-11	0.00E+00
37	-0.395E-04	0.735E-05	0.181E-05	0.00E+00	0.19E-05	0.00E+00
38	-0.359E-04	-0.356E-10	0.645E-06	0.00E+00	0.19E-05	0.00E+00
39	-0.395E-04	-0.735E-05	0.181E-05	0.00E+00	0.19E-05	0.00E+00
40	-0.418E-04	0.124E-04	-0.493E-04	0.00E+00	0.79E-05	0.00E+00
41	-0.929E-04	0.115E-08	-0.496E-04	0.00E+00	0.80E-05	0.00E+00
42	-0.418E-04	-0.123E-04	-0.493E-04	0.00E+00	0.79E-05	0.00E+00
43	0.000E+00	0.000E+00	0.000E+00	0.00E+00	0.00E+00	0.00E+00
44	0.000E+00	0.000E+00	0.000E+00	0.00E+00	0.00E+00	0.00E+00
45	0.000E+00	0.000E+00	0.000E+00	0.00E+00	0.00E+00	0.00E+00
46	0.206E-04	-0.747E-02	-0.146E-03	0.00E+00	0.00E+00	0.00E+00
47	0.214E-02	0.805E-08	-0.111E-03	0.00E+00	0.00E+00	0.00E+00
48	0.206E-04	0.747E-02	-0.146E-03	0.00E+00	0.00E+00	0.00E+00
49	0.000E+00	0.000E+00	0.000E+00	0.00E+00	0.00E+00	0.00E+00
50	0.000E+00	0.000E+00	0.000E+00	0.00E+00	0.00E+00	0.00E+00
51	0.000E+00	0.000E+00	0.000E+00	0.00E+00	0.00E+00	0.00E+00
52	-0.625E-05	0.105E-01	0.185E-03	0.00E+00	0.00E+00	0.00E+00
53	0.490E-03	0.132E-08	0.187E-03	0.00E+00	0.00E+00	0.00E+00
54	-0.625E-05	-0.105E-01	0.185E-03	0.00E+00	0.00E+00	0.00E+00
55	0.000E+00	0.000E+00	0.000E+00	0.00E+00	0.00E+00	0.00E+00
56	0.000E+00	0.000E+00	0.000E+00	0.00E+00	0.00E+00	0.00E+00
57	0.000E+00	0.000E+00	0.000E+00	0.00E+00	0.00E+00	0.00E+00

58	0.215E-04	-0.692E-02	-0.861E-04	0.00E+00	0.00E+00	0.00E+00	0.00E+00
59	-0.116E-02	-0.165E-08	-0.762E-04	0.00E+00	0.00E+00	0.00E+00	0.00E+00
60	0.215E-04	0.692E-02	-0.861E-04	0.00E+00	0.00E+00	0.00E+00	0.00E+00
61	0.000E+00	0.000E+00	0.000E+00	0.00E+00	0.00E+00	0.00E+00	0.00E+00
62	0.000E+00	0.000E+00	0.000E+00	0.00E+00	0.00E+00	0.00E+00	0.00E+00
63	0.000E+00	0.000E+00	0.000E+00	0.00E+00	0.00E+00	0.00E+00	0.00E+00
64	-0.678E-04	0.402E-02	0.248E-04	0.00E+00	0.00E+00	0.00E+00	0.00E+00
65	0.177E-02	0.201E-08	0.442E-03	0.00E+00	0.00E+00	0.00E+00	0.00E+00
66	-0.678E-04	-0.402E-02	0.248E-04	0.00E+00	0.00E+00	0.00E+00	0.00E+00
67	0.000E+00	0.000E+00	0.000E+00	0.00E+00	0.00E+00	0.00E+00	0.00E+00
68	0.000E+00	0.000E+00	0.000E+00	0.00E+00	0.00E+00	0.00E+00	0.00E+00
69	0.000E+00	0.000E+00	0.000E+00	0.00E+00	0.00E+00	0.00E+00	0.00E+00

## EVALUATION OF HALF SPACE IMPEDANCE

\*\*\*\*\*

SHEAR MODULUS = 6.95700E+06

MASS DENSITY = 1.52800E+02

POISSON RATIO = 3.53300E-01

-----

SHEAR WAVE VELOCITY 2.1338E+02

NUMBER OF INTERFACE NODES 30

-----

NUMBER OF FREQUENCIES 9

-----

ELEMENT	I	J	K	L	AREA
1	4	5	11	10	3.6000E+01
2	5	6	12	11	3.6000E+01
3	10	11	17	16	3.6000E+01
4	11	12	18	17	3.6000E+01
5	16	17	23	22	3.6000E+01
6	17	18	24	23	3.6000E+01
7	22	23	29	28	3.6000E+01
8	23	24	30	29	3.6000E+01
9	43	44	50	49	3.6000E+01
10	44	45	51	50	3.6000E+01
11	49	50	56	55	3.6000E+01
12	50	51	57	56	3.6000E+01
13	55	56	62	61	3.6000E+01
14	56	57	63	62	3.6000E+01
15	61	62	68	67	3.6000E+01
16	62	63	69	68	3.6000E+01



EXCITATION  
1 FREQUENCY (HZ)  
1 7.1620E-02  
2 1.4524E-01  
3 2.1327E-01  
4 2.8489E-01  
5 3.5651E-01  
6 4.2815E-01  
7 5.7137E-01  
8 1.1395E+00  
9 2.2791E+00

EVALUATION OF FREE-FIELD DISPLACEMENTS DUE TO INCIDENT SH-WAVE

\*\*\*\*\*

----- INCIDENT AMPLITUDE -----

INCIDENT ANGLE (DEGREES)		LONGITUDINAL		TRANSVERSE		VERTICAL	
VERTICAL	HORIZONTAL	REAL	IMAGINARY	REAL	IMAGINARY	REAL	IMAGINARY
0.0000E+00	0.0000E+00	0.0000E+00	0.0000E+00	2.0000E+00	0.0000E+00	0.0000E+00	0.0000E+00

----- FREE-FIELD DISPLACEMENT AT EXCITATION FREQUENCY 0.0716 (HZ) -----

NODE NO.	COORDINATE			X			Y			Z		
	X	Y	Z	MAGNITUDE	PHASE (DEG)	PHASE (DEG)	MAGNITUDE	PHASE (DEG)	MAGNITUDE	PHASE (DEG)	PHASE (DEG)	
4	0.0000E+00	1.2000E+01	0.0000E+00	0.0000E+00	0.0000E+00	0.0000E+00	4.0000E+00	0.0000E+00	0.0000E+00	0.0000E+00	0.0000E+00	
5	0.0000E+00	6.0000E+00	0.0000E+00	0.0000E+00	0.0000E+00	0.0000E+00	4.0000E+00	0.0000E+00	0.0000E+00	0.0000E+00	0.0000E+00	
6	0.0000E+00	0.0000E+00	0.0000E+00	0.0000E+00	0.0000E+00	0.0000E+00	4.0000E+00	0.0000E+00	0.0000E+00	0.0000E+00	0.0000E+00	
10	6.0000E+00	1.2000E+01	0.0000E+00	0.0000E+00	0.0000E+00	0.0000E+00	4.0000E+00	-7.2500E-01	0.0000E+00	0.0000E+00	0.0000E+00	
11	6.0000E+00	6.0000E+00	0.0000E+00	0.0000E+00	0.0000E+00	0.0000E+00	4.0000E+00	-7.2500E-01	0.0000E+00	0.0000E+00	0.0000E+00	
12	6.0000E+00	0.0000E+00	0.0000E+00	0.0000E+00	0.0000E+00	0.0000E+00	4.0000E+00	-7.2500E-01	0.0000E+00	0.0000E+00	0.0000E+00	
16	1.2000E+01	1.2000E+01	0.0000E+00	0.0000E+00	0.0000E+00	0.0000E+00	4.0000E+00	-1.4500E+00	0.0000E+00	0.0000E+00	0.0000E+00	
17	1.2000E+01	6.0000E+00	0.0000E+00	0.0000E+00	0.0000E+00	0.0000E+00	4.0000E+00	-1.4500E+00	0.0000E+00	0.0000E+00	0.0000E+00	
18	1.2000E+01	0.0000E+00	0.0000E+00	0.0000E+00	0.0000E+00	0.0000E+00	4.0000E+00	-1.4500E+00	0.0000E+00	0.0000E+00	0.0000E+00	
22	1.8000E+01	1.2000E+01	0.0000E+00	0.0000E+00	0.0000E+00	0.0000E+00	4.0000E+00	-2.1750E+00	0.0000E+00	0.0000E+00	0.0000E+00	
23	1.8000E+01	6.0000E+00	0.0000E+00	0.0000E+00	0.0000E+00	0.0000E+00	4.0000E+00	-2.1750E+00	0.0000E+00	0.0000E+00	0.0000E+00	
24	1.8000E+01	0.0000E+00	0.0000E+00	0.0000E+00	0.0000E+00	0.0000E+00	4.0000E+00	-2.1750E+00	0.0000E+00	0.0000E+00	0.0000E+00	
28	2.4000E+01	1.2000E+01	0.0000E+00	0.0000E+00	0.0000E+00	0.0000E+00	4.0000E+00	-2.9000E+00	0.0000E+00	0.0000E+00	0.0000E+00	
29	2.4000E+01	6.0000E+00	0.0000E+00	0.0000E+00	0.0000E+00	0.0000E+00	4.0000E+00	-2.9000E+00	0.0000E+00	0.0000E+00	0.0000E+00	
30	2.4000E+01	0.0000E+00	0.0000E+00	0.0000E+00	0.0000E+00	0.0000E+00	4.0000E+00	-2.9000E+00	0.0000E+00	0.0000E+00	0.0000E+00	
43	6.0000E+01	1.2000E+01	0.0000E+00	0.0000E+00	0.0000E+00	0.0000E+00	4.0000E+00	-7.2500E+00	0.0000E+00	0.0000E+00	0.0000E+00	
44	6.0000E+01	6.0000E+00	0.0000E+00	0.0000E+00	0.0000E+00	0.0000E+00	4.0000E+00	-7.2500E+00	0.0000E+00	0.0000E+00	0.0000E+00	
45	6.0000E+01	0.0000E+00	0.0000E+00	0.0000E+00	0.0000E+00	0.0000E+00	4.0000E+00	-7.2500E+00	0.0000E+00	0.0000E+00	0.0000E+00	
49	6.6000E+01	1.2000E+01	0.0000E+00	0.0000E+00	0.0000E+00	0.0000E+00	4.0000E+00	-7.9750E+00	0.0000E+00	0.0000E+00	0.0000E+00	
50	6.6000E+01	6.0000E+00	0.0000E+00	0.0000E+00	0.0000E+00	0.0000E+00	4.0000E+00	-7.9750E+00	0.0000E+00	0.0000E+00	0.0000E+00	
51	6.6000E+01	0.0000E+00	0.0000E+00	0.0000E+00	0.0000E+00	0.0000E+00	4.0000E+00	-7.9750E+00	0.0000E+00	0.0000E+00	0.0000E+00	
55	7.2000E+01	1.2000E+01	0.0000E+00	0.0000E+00	0.0000E+00	0.0000E+00	4.0000E+00	-8.7000E+00	0.0000E+00	0.0000E+00	0.0000E+00	
56	7.2000E+01	6.0000E+00	0.0000E+00	0.0000E+00	0.0000E+00	0.0000E+00	4.0000E+00	-8.7000E+00	0.0000E+00	0.0000E+00	0.0000E+00	
57	7.2000E+01	0.0000E+00	0.0000E+00	0.0000E+00	0.0000E+00	0.0000E+00	4.0000E+00	-8.7000E+00	0.0000E+00	0.0000E+00	0.0000E+00	
61	7.8000E+01	1.2000E+01	0.0000E+00	0.0000E+00	0.0000E+00	0.0000E+00	4.0000E+00	-9.4250E+00	0.0000E+00	0.0000E+00	0.0000E+00	
62	7.8000E+01	6.0000E+00	0.0000E+00	0.0000E+00	0.0000E+00	0.0000E+00	4.0000E+00	-9.4250E+00	0.0000E+00	0.0000E+00	0.0000E+00	
63	7.8000E+01	0.0000E+00	0.0000E+00	0.0000E+00	0.0000E+00	0.0000E+00	4.0000E+00	-9.4250E+00	0.0000E+00	0.0000E+00	0.0000E+00	
67	8.4000E+01	1.2000E+01	0.0000E+00	0.0000E+00	0.0000E+00	0.0000E+00	4.0000E+00	-1.0150E+01	0.0000E+00	0.0000E+00	0.0000E+00	
68	8.4000E+01	6.0000E+00	0.0000E+00	0.0000E+00	0.0000E+00	0.0000E+00	4.0000E+00	-1.0150E+01	0.0000E+00	0.0000E+00	0.0000E+00	
69	8.4000E+01	0.0000E+00	0.0000E+00	0.0000E+00	0.0000E+00	0.0000E+00	4.0000E+00	-1.0150E+01	0.0000E+00	0.0000E+00	0.0000E+00	



NODE NO.	COORDINATE			X			Y			Z		
	X	Y	Z	MAGNITUDE	PHASE (DEG)	PHASE (DEG)	MAGNITUDE	PHASE (DEG)	MAGNITUDE	PHASE (DEG)	MAGNITUDE	PHASE (DEG)
24	1.0000E+01	0.0000E+00	0.0000E+00	0.0000E+00	0.0000E+00	4.0000E+00	-6.4767E+00	0.0000E+00	0.0000E+00	0.0000E+00	0.0000E+00	0.0000E+00
28	2.4000E+01	1.2000E+01	0.0000E+00	0.0000E+00	0.0000E+00	4.0000E+00	-8.6355E+00	0.0000E+00	0.0000E+00	0.0000E+00	0.0000E+00	0.0000E+00
29	2.4000E+01	6.0000E+00	0.0000E+00	0.0000E+00	0.0000E+00	4.0000E+00	-8.6355E+00	0.0000E+00	0.0000E+00	0.0000E+00	0.0000E+00	0.0000E+00
30	2.4000E+01	0.0000E+00	0.0000E+00	0.0000E+00	0.0000E+00	4.0000E+00	-8.6355E+00	0.0000E+00	0.0000E+00	0.0000E+00	0.0000E+00	0.0000E+00
43	6.0000E+01	1.2000E+01	0.0000E+00	0.0000E+00	0.0000E+00	4.0000E+00	-2.1569E+01	0.0000E+00	0.0000E+00	0.0000E+00	0.0000E+00	0.0000E+00
44	6.0000E+01	6.0000E+00	0.0000E+00	0.0000E+00	0.0000E+00	4.0000E+00	-2.1569E+01	0.0000E+00	0.0000E+00	0.0000E+00	0.0000E+00	0.0000E+00
45	6.0000E+01	0.0000E+00	0.0000E+00	0.0000E+00	0.0000E+00	4.0000E+00	-2.1569E+01	0.0000E+00	0.0000E+00	0.0000E+00	0.0000E+00	0.0000E+00
49	6.6000E+01	1.2000E+01	0.0000E+00	0.0000E+00	0.0000E+00	4.0000E+00	-2.3748E+01	0.0000E+00	0.0000E+00	0.0000E+00	0.0000E+00	0.0000E+00
50	6.6000E+01	6.0000E+00	0.0000E+00	0.0000E+00	0.0000E+00	4.0000E+00	-2.3748E+01	0.0000E+00	0.0000E+00	0.0000E+00	0.0000E+00	0.0000E+00
51	6.6000E+01	0.0000E+00	0.0000E+00	0.0000E+00	0.0000E+00	4.0000E+00	-2.3748E+01	0.0000E+00	0.0000E+00	0.0000E+00	0.0000E+00	0.0000E+00
55	7.2000E+01	1.2000E+01	0.0000E+00	0.0000E+00	0.0000E+00	4.0000E+00	-2.5907E+01	0.0000E+00	0.0000E+00	0.0000E+00	0.0000E+00	0.0000E+00
56	7.2000E+01	6.0000E+00	0.0000E+00	0.0000E+00	0.0000E+00	4.0000E+00	-2.5907E+01	0.0000E+00	0.0000E+00	0.0000E+00	0.0000E+00	0.0000E+00
57	7.2000E+01	0.0000E+00	0.0000E+00	0.0000E+00	0.0000E+00	4.0000E+00	-2.5907E+01	0.0000E+00	0.0000E+00	0.0000E+00	0.0000E+00	0.0000E+00
61	7.8000E+01	1.2000E+01	0.0000E+00	0.0000E+00	0.0000E+00	4.0000E+00	-2.8065E+01	0.0000E+00	0.0000E+00	0.0000E+00	0.0000E+00	0.0000E+00
62	7.8000E+01	6.0000E+00	0.0000E+00	0.0000E+00	0.0000E+00	4.0000E+00	-2.8065E+01	0.0000E+00	0.0000E+00	0.0000E+00	0.0000E+00	0.0000E+00
63	7.8000E+01	0.0000E+00	0.0000E+00	0.0000E+00	0.0000E+00	4.0000E+00	-2.8065E+01	0.0000E+00	0.0000E+00	0.0000E+00	0.0000E+00	0.0000E+00
67	8.4000E+01	1.2000E+01	0.0000E+00	0.0000E+00	0.0000E+00	4.0000E+00	-3.0224E+01	0.0000E+00	0.0000E+00	0.0000E+00	0.0000E+00	0.0000E+00
68	8.4000E+01	6.0000E+00	0.0000E+00	0.0000E+00	0.0000E+00	4.0000E+00	-3.0224E+01	0.0000E+00	0.0000E+00	0.0000E+00	0.0000E+00	0.0000E+00
69	8.4000E+01	0.0000E+00	0.0000E+00	0.0000E+00	0.0000E+00	4.0000E+00	-3.0224E+01	0.0000E+00	0.0000E+00	0.0000E+00	0.0000E+00	0.0000E+00

FREE-FIELD DISPLACEMENT AT EXCITATION FREQUENCY 0.2849 (HZ)



FREE-FIELD DISPLACEMENT AT EXCITATION FREQUENCY 0.5714 (HZ)

NODE NO.	COORDINATE			X			Y			Z		
	X	Y	Z	MAGNITUDE	PHASE (DEG)	PHASE (DEG)	MAGNITUDE	PHASE (DEG)	MAGNITUDE	PHASE (DEG)	PHASE (DEG)	
18	1.2000E+01	0.0000E+00	0.0000E+00	0.0000E+00	0.0000E+00	4.0000E+00	-6.667E+00	0.0000E+00	0.0000E+00	0.0000E+00	0.0000E+00	
22	1.8000E+01	1.2000E+01	0.0000E+00	0.0000E+00	0.0000E+00	4.0000E+00	-1.5002E+01	0.0000E+00	0.0000E+00	0.0000E+00	0.0000E+00	
23	1.8000E+01	6.0000E+00	0.0000E+00	0.0000E+00	0.0000E+00	4.0000E+00	-1.5002E+01	0.0000E+00	0.0000E+00	0.0000E+00	0.0000E+00	
24	1.8000E+01	0.0000E+00	0.0000E+00	0.0000E+00	0.0000E+00	4.0000E+00	-1.3002E+01	0.0000E+00	0.0000E+00	0.0000E+00	0.0000E+00	
28	2.4000E+01	1.2000E+01	0.0000E+00	0.0000E+00	0.0000E+00	4.0000E+00	-1.7336E+01	0.0000E+00	0.0000E+00	0.0000E+00	0.0000E+00	
29	2.4000E+01	6.0000E+00	0.0000E+00	0.0000E+00	0.0000E+00	4.0000E+00	-1.7336E+01	0.0000E+00	0.0000E+00	0.0000E+00	0.0000E+00	
30	2.4000E+01	0.0000E+00	0.0000E+00	0.0000E+00	0.0000E+00	4.0000E+00	-1.7336E+01	0.0000E+00	0.0000E+00	0.0000E+00	0.0000E+00	
43	6.0000E+01	1.2000E+01	0.0000E+00	0.0000E+00	0.0000E+00	4.0000E+00	-4.3359E+01	0.0000E+00	0.0000E+00	0.0000E+00	0.0000E+00	
44	6.0000E+01	6.0000E+00	0.0000E+00	0.0000E+00	0.0000E+00	4.0000E+00	-4.3359E+01	0.0000E+00	0.0000E+00	0.0000E+00	0.0000E+00	
45	6.0000E+01	0.0000E+00	0.0000E+00	0.0000E+00	0.0000E+00	4.0000E+00	-4.3359E+01	0.0000E+00	0.0000E+00	0.0000E+00	0.0000E+00	
49	6.6000E+01	1.2000E+01	0.0000E+00	0.0000E+00	0.0000E+00	4.0000E+00	-4.7673E+01	0.0000E+00	0.0000E+00	0.0000E+00	0.0000E+00	
50	6.6000E+01	6.0000E+00	0.0000E+00	0.0000E+00	0.0000E+00	4.0000E+00	-4.7673E+01	0.0000E+00	0.0000E+00	0.0000E+00	0.0000E+00	
51	6.6000E+01	0.0000E+00	0.0000E+00	0.0000E+00	0.0000E+00	4.0000E+00	-4.7673E+01	0.0000E+00	0.0000E+00	0.0000E+00	0.0000E+00	
55	7.2000E+01	1.2000E+01	0.0000E+00	0.0000E+00	0.0000E+00	4.0000E+00	-5.2007E+01	0.0000E+00	0.0000E+00	0.0000E+00	0.0000E+00	
56	7.2000E+01	6.0000E+00	0.0000E+00	0.0000E+00	0.0000E+00	4.0000E+00	-5.2007E+01	0.0000E+00	0.0000E+00	0.0000E+00	0.0000E+00	
57	7.2000E+01	0.0000E+00	0.0000E+00	0.0000E+00	0.0000E+00	4.0000E+00	-5.2007E+01	0.0000E+00	0.0000E+00	0.0000E+00	0.0000E+00	
61	7.8000E+01	1.2000E+01	0.0000E+00	0.0000E+00	0.0000E+00	4.0000E+00	-5.6340E+01	0.0000E+00	0.0000E+00	0.0000E+00	0.0000E+00	
62	7.8000E+01	6.0000E+00	0.0000E+00	0.0000E+00	0.0000E+00	4.0000E+00	-5.6340E+01	0.0000E+00	0.0000E+00	0.0000E+00	0.0000E+00	
63	7.8000E+01	0.0000E+00	0.0000E+00	0.0000E+00	0.0000E+00	4.0000E+00	-5.6340E+01	0.0000E+00	0.0000E+00	0.0000E+00	0.0000E+00	
67	8.4000E+01	1.2000E+01	0.0000E+00	0.0000E+00	0.0000E+00	4.0000E+00	-6.0674E+01	0.0000E+00	0.0000E+00	0.0000E+00	0.0000E+00	
68	8.4000E+01	6.0000E+00	0.0000E+00	0.0000E+00	0.0000E+00	4.0000E+00	-6.0674E+01	0.0000E+00	0.0000E+00	0.0000E+00	0.0000E+00	
69	8.4000E+01	0.0000E+00	0.0000E+00	0.0000E+00	0.0000E+00	4.0000E+00	-6.0674E+01	0.0000E+00	0.0000E+00	0.0000E+00	0.0000E+00	



12	6.0000E+00	0.0000E+00	0.0000E+00	0.0000E+00	4.0000E+00	-2.3071E+01	0.0000E+00	0.0000E+00	0.0000E+00
16	1.2000E+01	1.2000E+01	0.0000E+00	0.0000E+00	4.0000E+00	-4.6142E+01	0.0000E+00	0.0000E+00	0.0000E+00
17	1.2000E+01	6.0000E+00	0.0000E+00	0.0000E+00	4.0000E+00	-4.6142E+01	0.0000E+00	0.0000E+00	0.0000E+00
18	1.2000E+01	0.0000E+00	0.0000E+00	0.0000E+00	4.0000E+00	-4.6142E+01	0.0000E+00	0.0000E+00	0.0000E+00
22	1.8000E+01	1.2000E+01	0.0000E+00	0.0000E+00	4.0000E+00	-6.9213E+01	0.0000E+00	0.0000E+00	0.0000E+00
23	1.8000E+01	6.0000E+00	0.0000E+00	0.0000E+00	4.0000E+00	-6.9213E+01	0.0000E+00	0.0000E+00	0.0000E+00
24	1.8000E+01	0.0000E+00	0.0000E+00	0.0000E+00	4.0000E+00	-6.9213E+01	0.0000E+00	0.0000E+00	0.0000E+00
28	2.4000E+01	1.2000E+01	0.0000E+00	0.0000E+00	4.0000E+00	-9.2284E+01	0.0000E+00	0.0000E+00	0.0000E+00
29	2.4000E+01	6.0000E+00	0.0000E+00	0.0000E+00	4.0000E+00	-9.2284E+01	0.0000E+00	0.0000E+00	0.0000E+00
30	2.4000E+01	0.0000E+00	0.0000E+00	0.0000E+00	4.0000E+00	-9.2284E+01	0.0000E+00	0.0000E+00	0.0000E+00
43	6.0000E+01	1.2000E+01	0.0000E+00	0.0000E+00	4.0000E+00	1.2929E+02	0.0000E+00	0.0000E+00	0.0000E+00
44	6.0000E+01	6.0000E+00	0.0000E+00	0.0000E+00	4.0000E+00	1.2929E+02	0.0000E+00	0.0000E+00	0.0000E+00
45	6.0000E+01	0.0000E+00	0.0000E+00	0.0000E+00	4.0000E+00	1.2929E+02	0.0000E+00	0.0000E+00	0.0000E+00
49	6.6000E+01	1.2000E+01	0.0000E+00	0.0000E+00	4.0000E+00	1.0622E+02	0.0000E+00	0.0000E+00	0.0000E+00
50	6.6000E+01	6.0000E+00	0.0000E+00	0.0000E+00	4.0000E+00	1.0622E+02	0.0000E+00	0.0000E+00	0.0000E+00
51	6.6000E+01	0.0000E+00	0.0000E+00	0.0000E+00	4.0000E+00	1.0622E+02	0.0000E+00	0.0000E+00	0.0000E+00
55	7.2000E+01	1.2000E+01	0.0000E+00	0.0000E+00	4.0000E+00	8.3147E+01	0.0000E+00	0.0000E+00	0.0000E+00
56	7.2000E+01	6.0000E+00	0.0000E+00	0.0000E+00	4.0000E+00	8.3147E+01	0.0000E+00	0.0000E+00	0.0000E+00
57	7.2000E+01	0.0000E+00	0.0000E+00	0.0000E+00	4.0000E+00	8.3147E+01	0.0000E+00	0.0000E+00	0.0000E+00
61	7.8000E+01	1.2000E+01	0.0000E+00	0.0000E+00	4.0000E+00	6.0076E+01	0.0000E+00	0.0000E+00	0.0000E+00
62	7.8000E+01	6.0000E+00	0.0000E+00	0.0000E+00	4.0000E+00	6.0076E+01	0.0000E+00	0.0000E+00	0.0000E+00
63	7.8000E+01	0.0000E+00	0.0000E+00	0.0000E+00	4.0000E+00	6.0076E+01	0.0000E+00	0.0000E+00	0.0000E+00
67	8.4000E+01	1.2000E+01	0.0000E+00	0.0000E+00	4.0000E+00	3.7005E+01	0.0000E+00	0.0000E+00	0.0000E+00
68	8.4000E+01	6.0000E+00	0.0000E+00	0.0000E+00	4.0000E+00	3.7005E+01	0.0000E+00	0.0000E+00	0.0000E+00
69	8.4000E+01	0.0000E+00	0.0000E+00	0.0000E+00	4.0000E+00	3.7005E+01	0.0000E+00	0.0000E+00	0.0000E+00



INPUT DATA FOR PROGRAM DASSIN2 ON TAPE = 0  
\*\*\*\*\*

THE TAPE CONTAINS THE FOLLOWING :

DATA OF CONNECTIVITY OF ELEMENTS  
STIFFNESS SUBMATRICES  
MASS VECTORS + LOAD VECTORS  
EIGENMODES AND EIGENVALUES  
COMPLIANCE MATRIX OF SOIL  
FREE FIELD DISPLACEMENT VECTOR  
\*\*\*\*\*

OVERALL LOG  
TOTAL TIME= 5.646

\*\*\*\*\*

PRINT TIME OF DIFFERENT  
COMPUTATIONAL UNITS  
\*\*\*\*\*

INITIALIZATION TIME	0.006
MODAL POINT INPUT	0.032
ELEMENT DATA INPUT	0.024
TIME OF ORIGINAL PLOT	0.000
FORM ELEMENT STIFFNESS	0.532
INPUT MODAL LOADS	0.005
FORM GLOBAL STIFFNESS	0.048
WRITE TAPE	0.051
EXTRACTION OF NATURAL MODES	0.809
SAVE RESULTS ON TAPE	0.169
TIME OF MODAL PLOTS	0.000
COMPUTATION OF SOIL IMPEDANCE	4.026
TIME FOR FREE WAVE MOTION	0.110

\*\*\*\*\*



MODE SHAPE PLOTS FROM BASSIN1





MODE 1

FREQUENCY: 1.041 Hz

DESCRIPTION:

FUNDAMENTAL BENDING MODE  
FOR ROAD DECK IN x-z PLANE  
(z-DISPLACEMENTS SYMMETRIC  
ABOUT MIDSPAN)

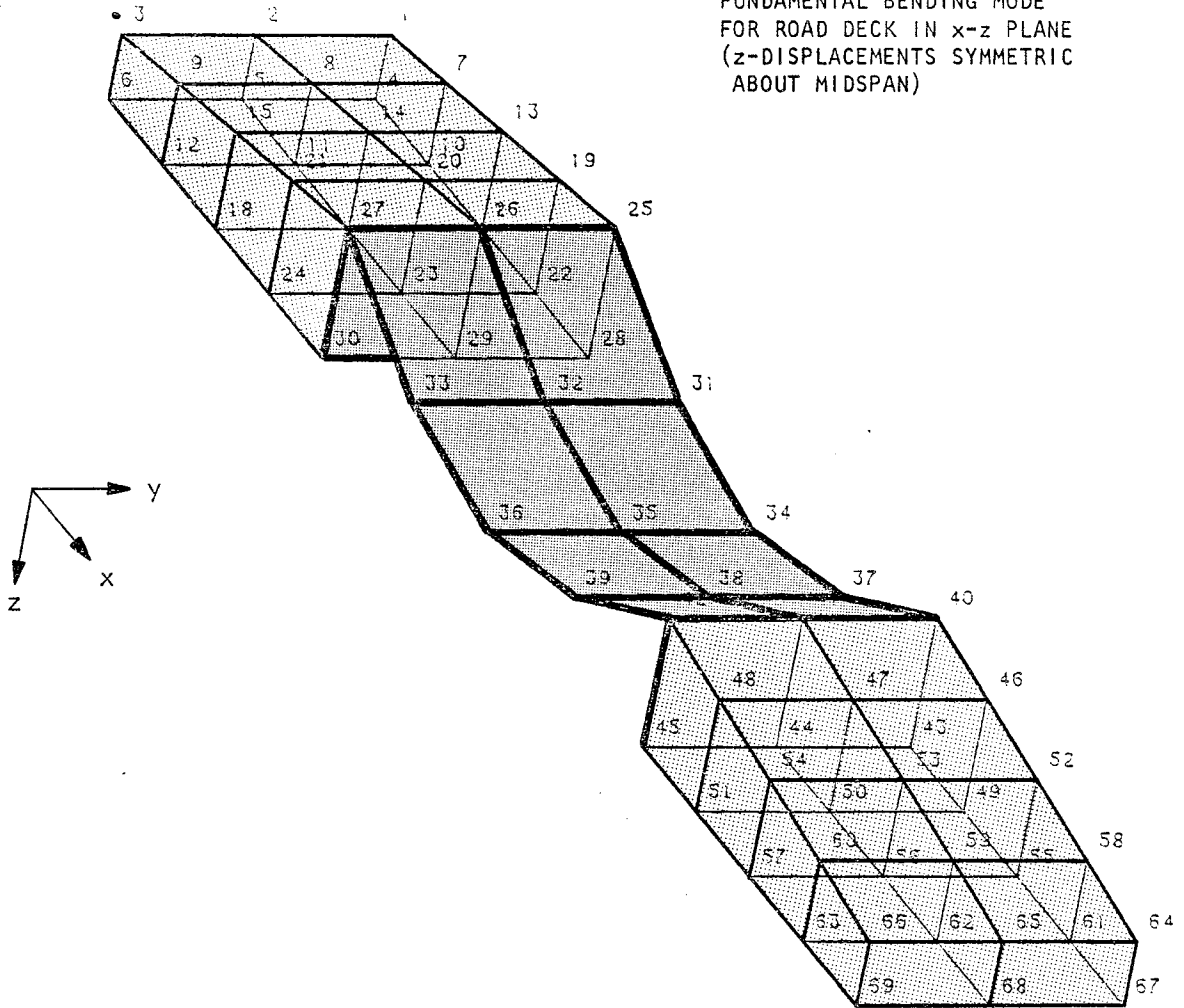


FIGURE C-2. EIGENVECTOR FOR MODE 1



MODE 2

FREQUENCY: 4.249 Hz

DESCRIPTION:

SECOND BENDING MODE FOR  
ROAD DECK IN x-z PLANE  
(z-DISPLACEMENTS ANTI-  
SYMMETRIC ABOUT MIDSPAN)

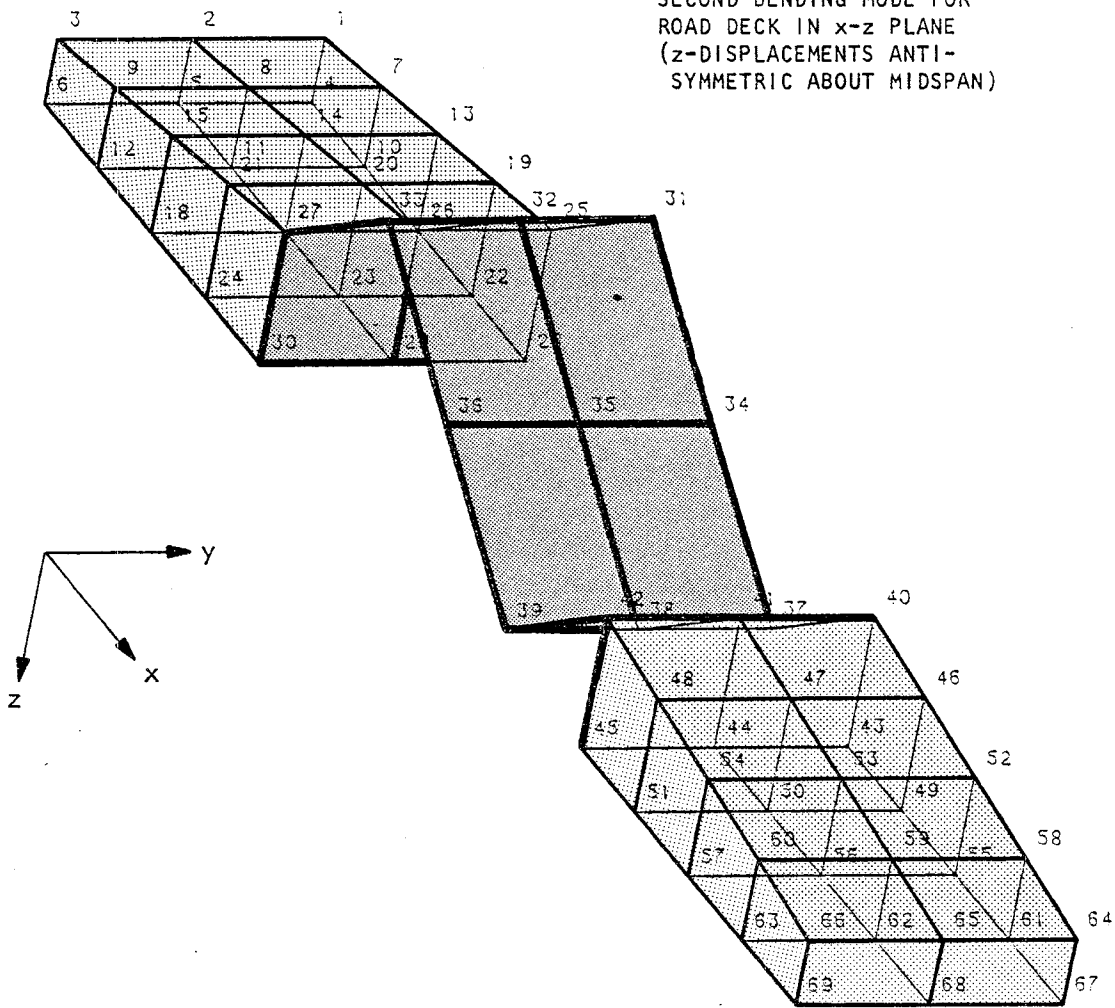


FIGURE C-3. EIGENVECTOR FOR MODE 2



MODE 3

FREQUENCY: 9.618 Hz

DESCRIPTION:

THIRD BENDING MODE FOR  
ROAD DECK IN x-z PLANE  
(z-DISPLACEMENTS SYMMETRIC  
ABOUT MIDSPAN)

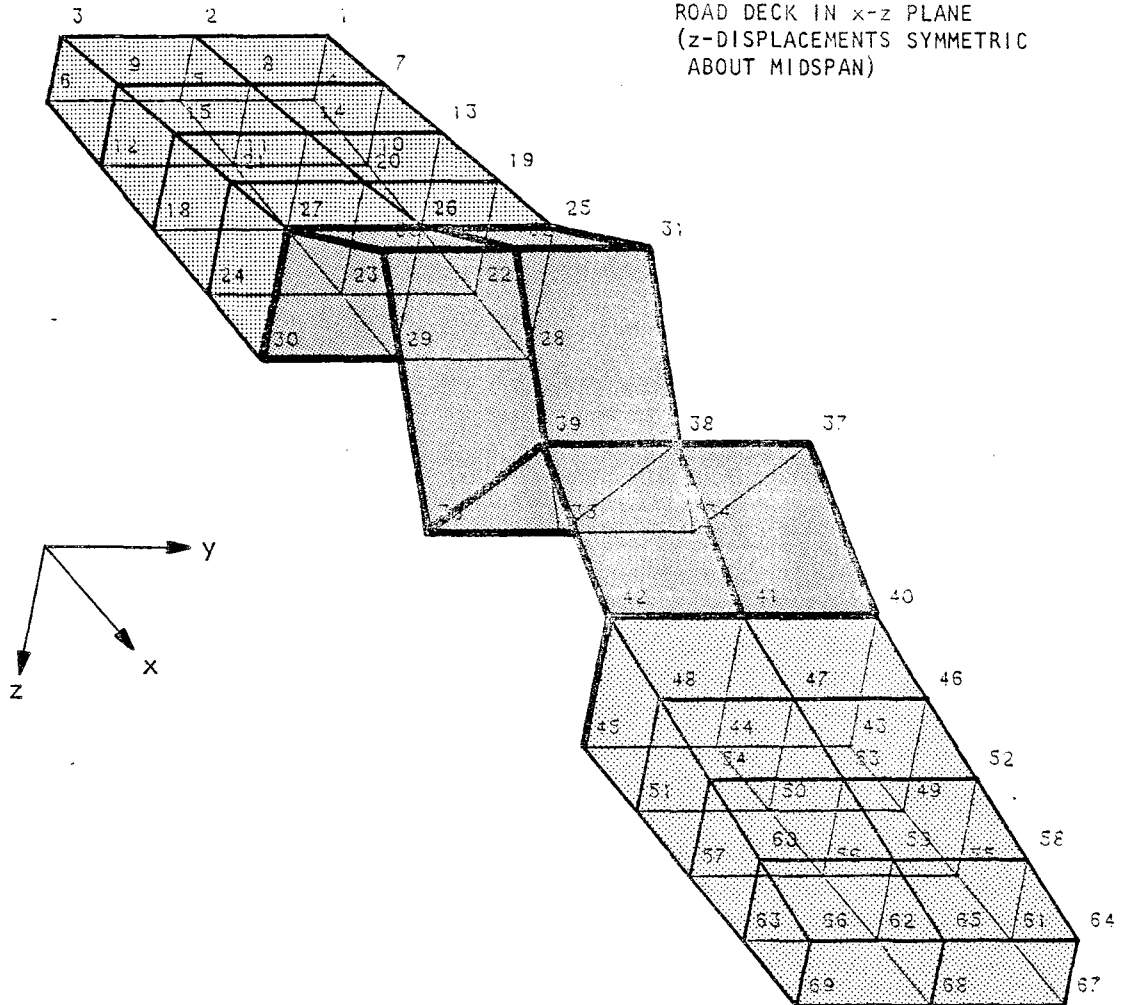


FIGURE C-4. EIGENVECTOR FOR MODE 3



MODE 4

FREQUENCY: 11.274 Hz

DESCRIPTION:

FUNDAMENTAL BENDING MODE FOR  
BRIDGE/END-WALL SYSTEM IN x-y  
PLANE (y-DISPLACEMENTS SYMMETRIC  
ABOUT MIDSPAN)

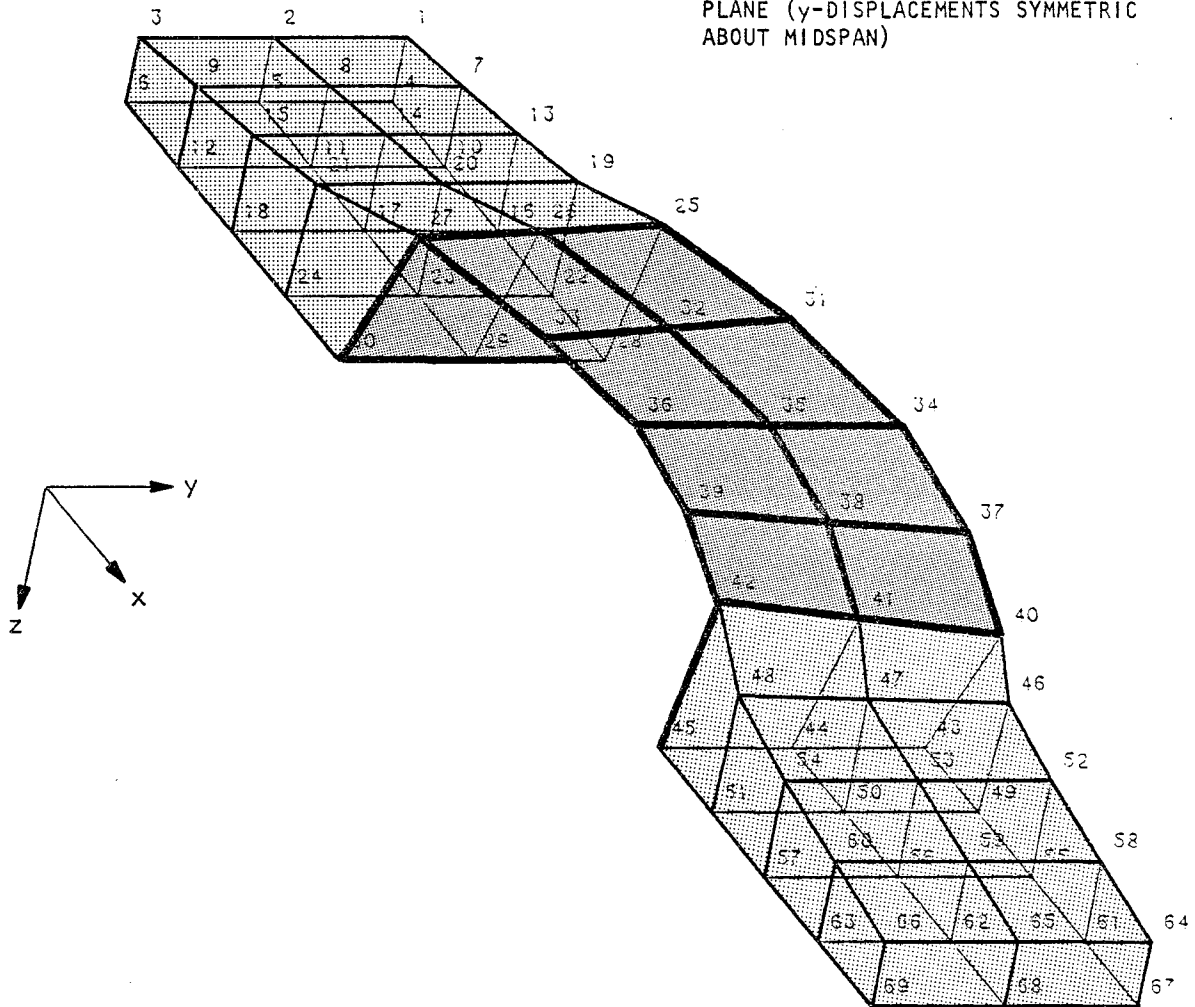


FIGURE C-5. EIGENVECTOR FOR MODE 4





MODE 5

FREQUENCY: 13.207 Hz

DESCRIPTION:

FUNDAMENTAL SIDESWAY MODE  
FOR BRIDGE/END-WALL SYSTEM  
IN x-z PLANE

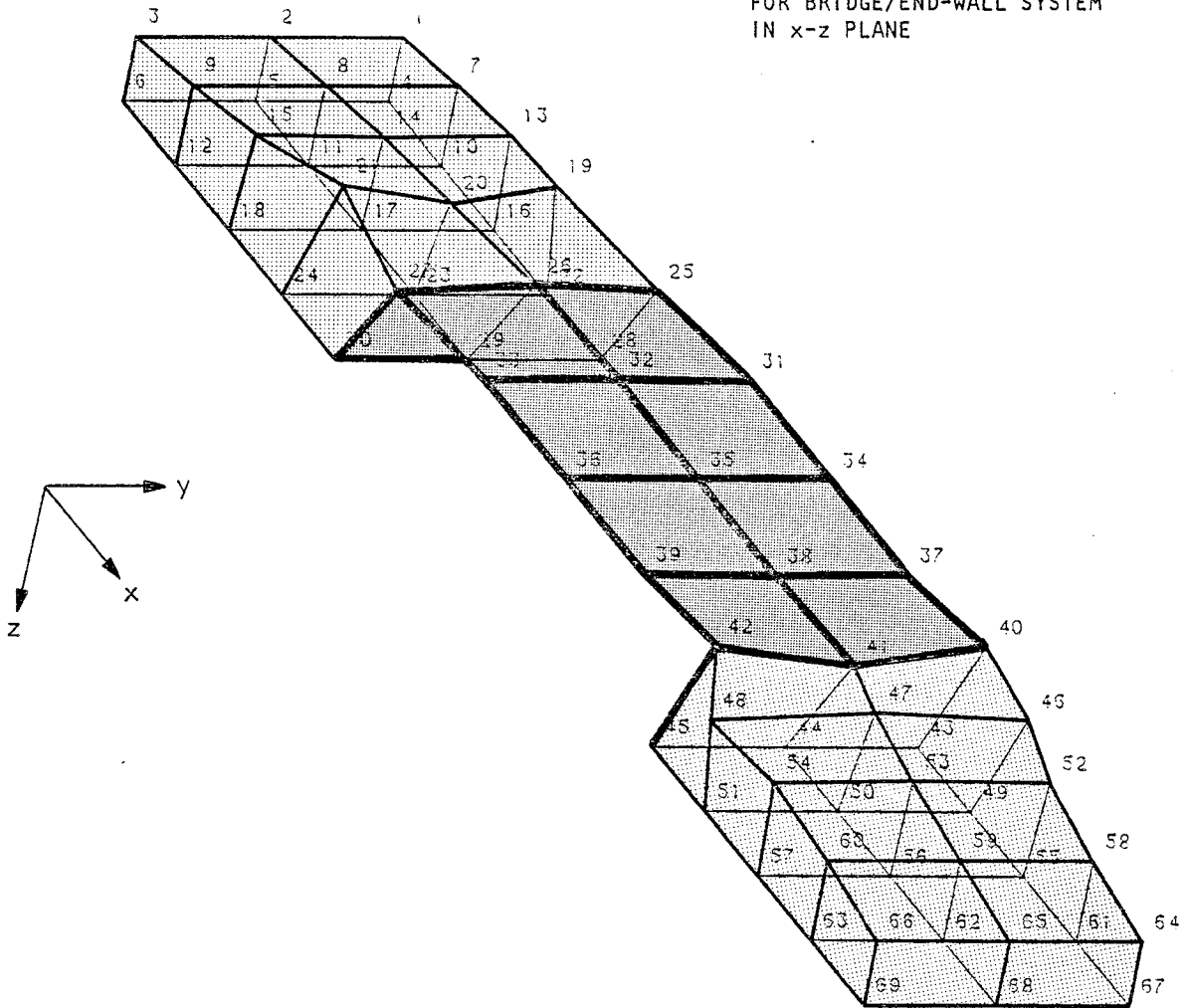


FIGURE C-6. EIGENVECTOR FOR MODE 5



MODE 6

FREQUENCY: 20.889 Hz

DESCRIPTION:

SECOND BENDING MODE FOR  
BRIDGE/END-WALL SYSTEM IN  
x-y PLANE (y-DISPLACEMENTS  
ANTISYMMETRIC ABOUT MID-  
SPAN)

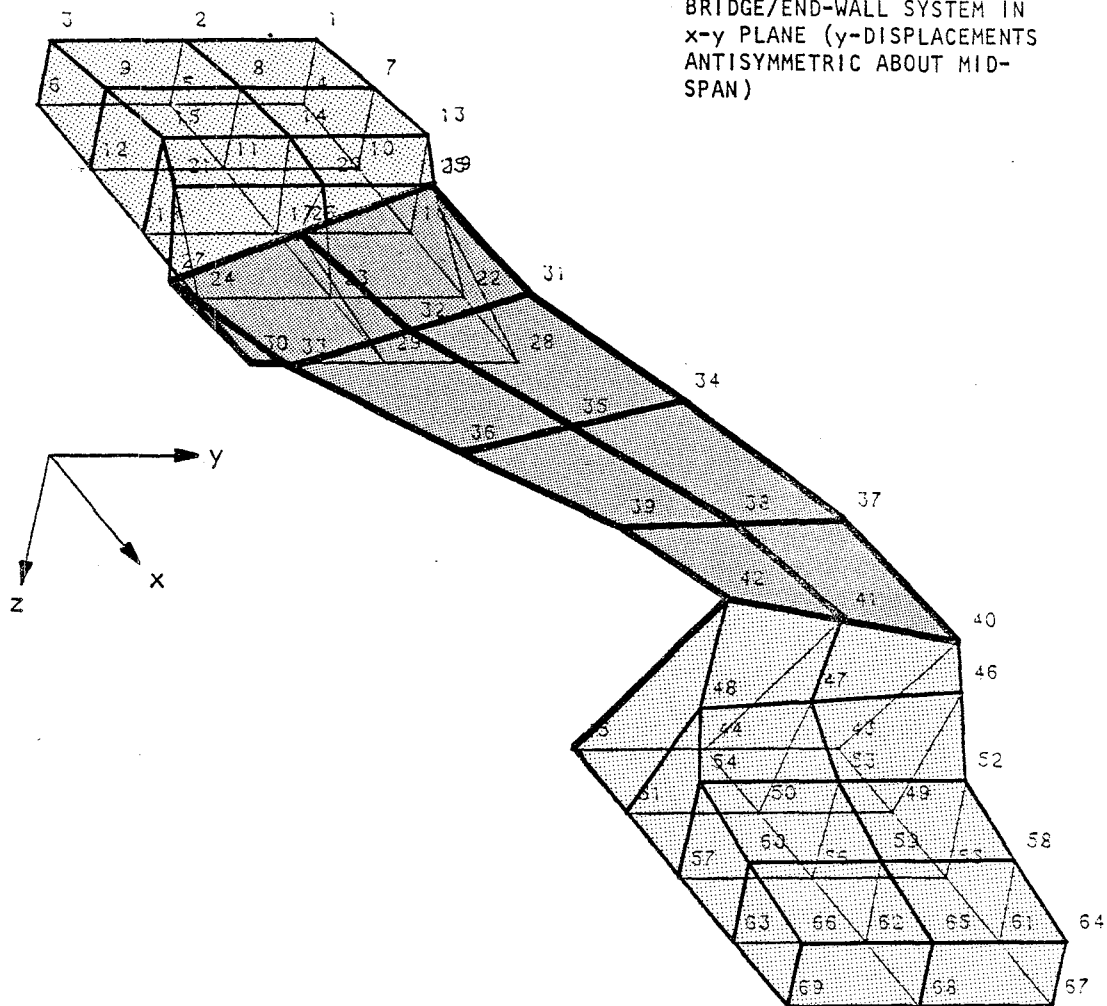


FIGURE C-7. EIGENVECTOR FOR MODE 6



MODE 7

FREQUENCY: 21.109 Hz

DESCRIPTION:

FUNDAMENTAL TORSIONAL MODE  
FOR ROAD DECK (x-ROTATIONS  
SYMMETRICAL ABOUT MIDSPAN)

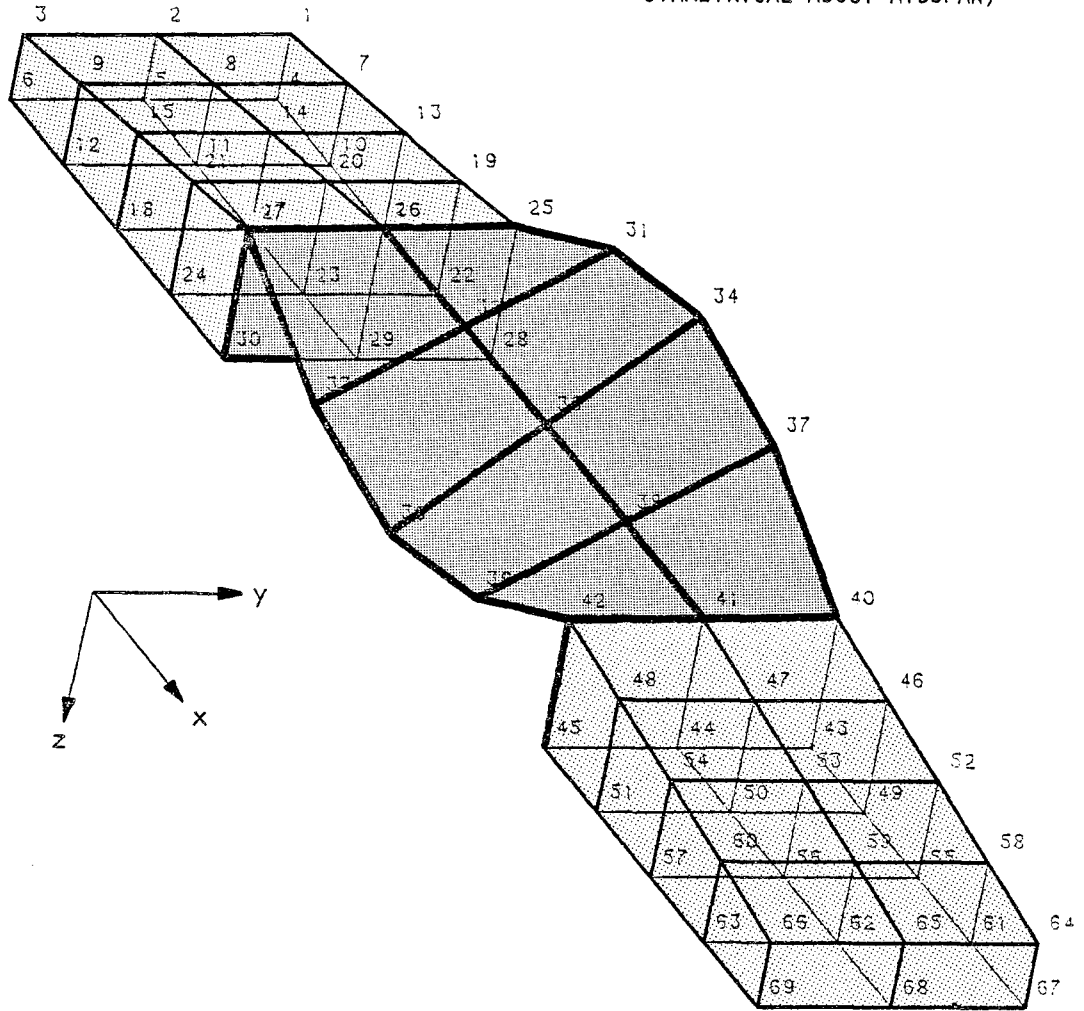


FIGURE C-8. EIGENVECTOR FOR MODE 7



MODE 8

FREQUENCY: 22.852 Hz

DESCRIPTION:

SECOND TORSIONAL MODE FOR  
ROAD DECK (x-ROTATIONS ANTI-  
SYMMETRIC ABOUT MIDSPAN)

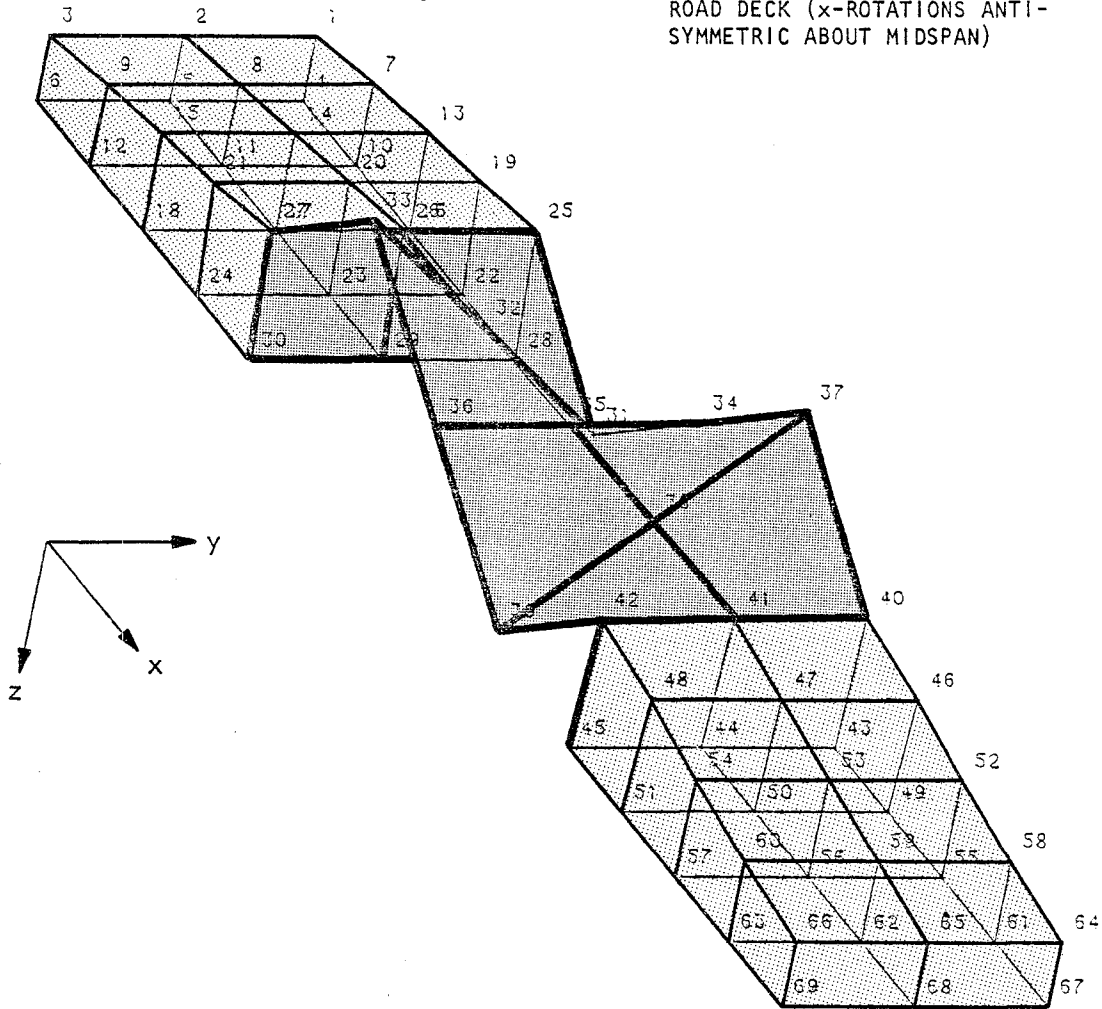


FIGURE C-9. EIGENVECTOR FOR MODE 8



MODE 9

FREQUENCY: 24.580 Hz

DESCRIPTION:

THIRD TORSIONAL MODE FOR  
ROAD DECK (x-ROTATIONS  
SYMMETRIC ABOUT MIDSPAN)

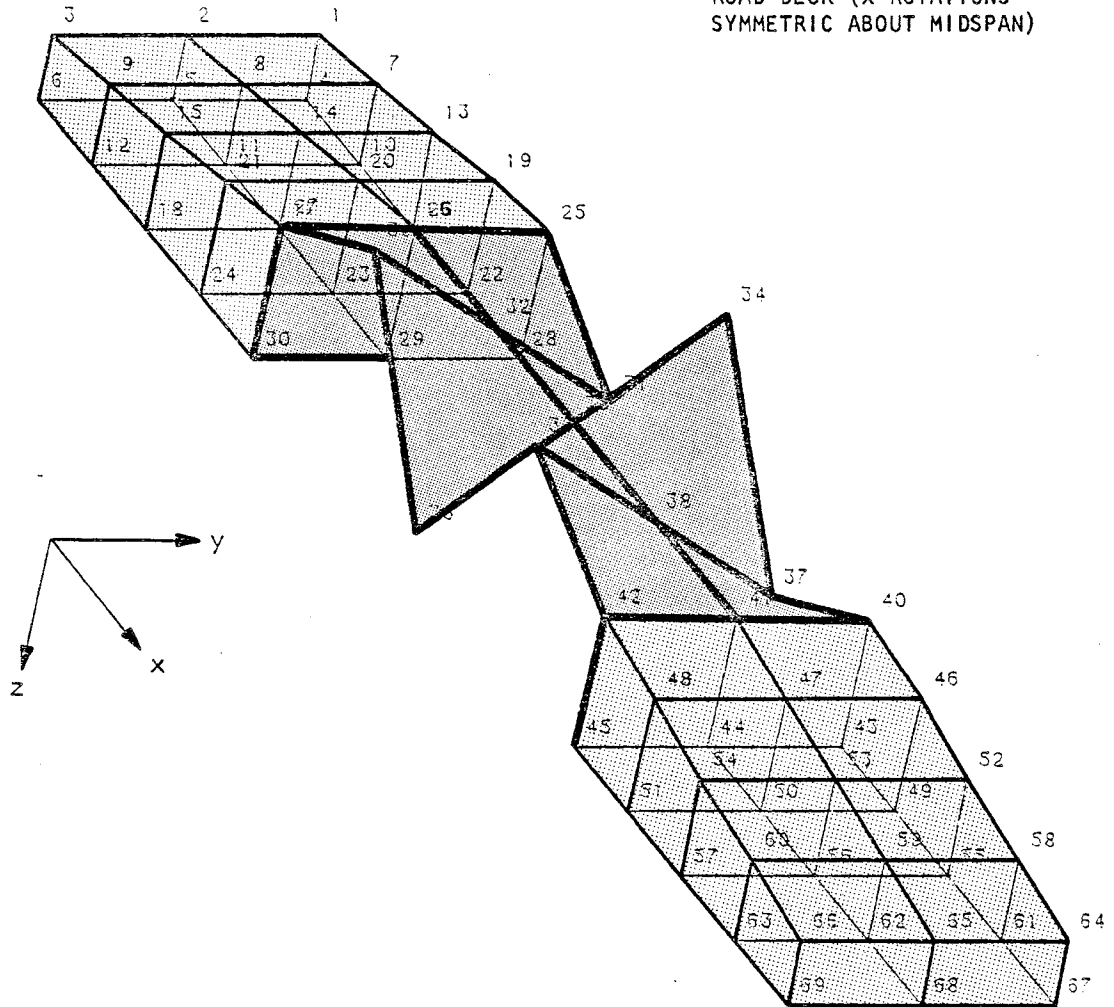


FIGURE C-10. EIGENVECTOR FOR MODE 9



MODE 10

FREQUENCY: 25.983 Hz

DESCRIPTION:

BACKFILL DEFORMATION MODE  
(y-DISPLACEMENTS SYMMETRIC  
ABOUT CENTERLINE AND MID-  
SPAN OF BRIDGE)

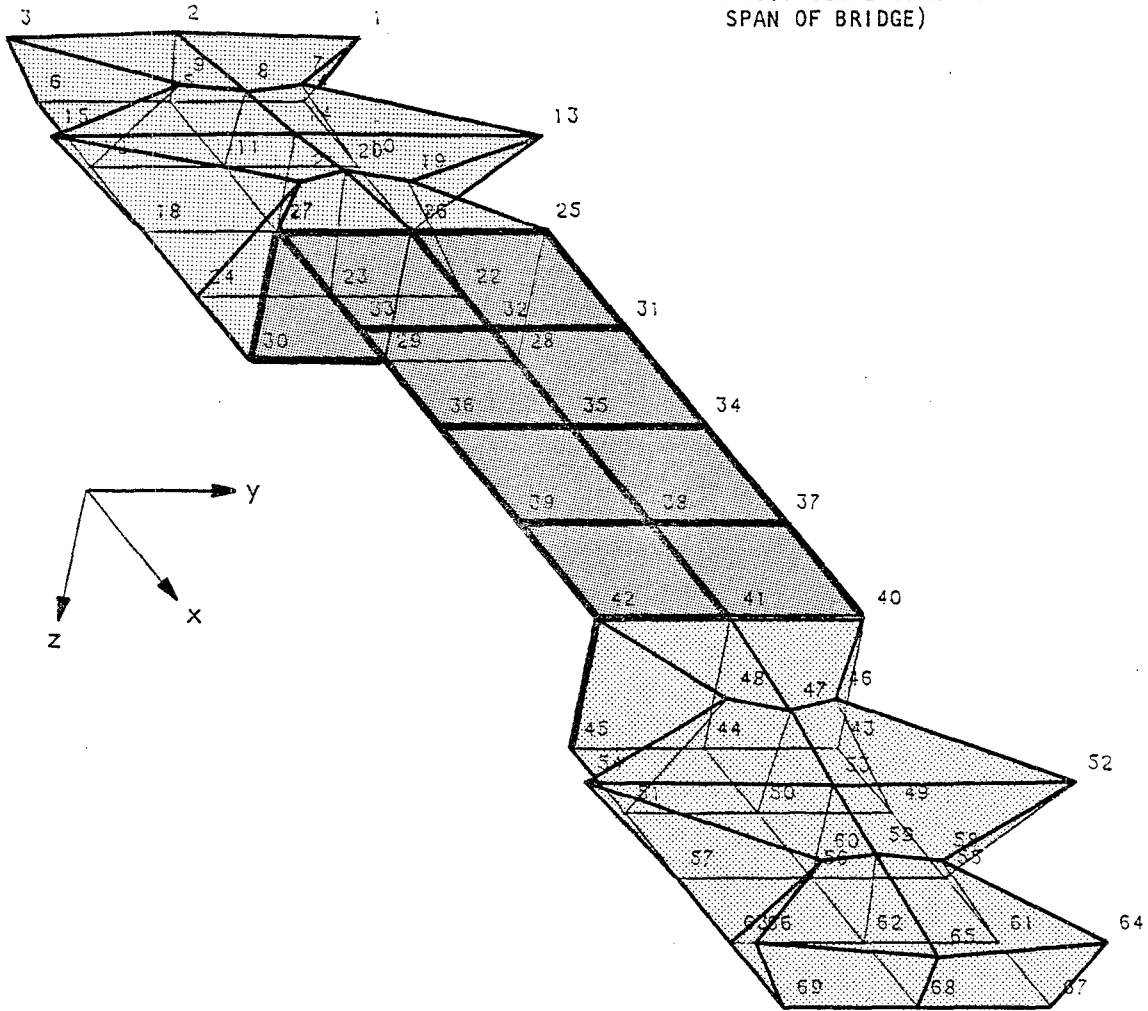


FIGURE C-11. EIGENVECTOR FOR MODE 10



INPUT DATA FOR BASSIN2





```

LOCAPP  CARD  *****1*****2*****3*****4*****5*****6*****7*****8
1 1 * DYNAMIC INTERACTION OF MASSING
2 4
3 5 55 Y A
4 5 55 Y P
5 5 55 Z A
6 5 55 Z P
7 1
8 0.10 0.10 0.10 0.10 0.10 0.10 0.10
9 0.10
10 0.07161972
11 0.14323945
12 0.21526762
13 0.28680755
14 0.35830707
15 0.42812680
16 0.57150625
17 1.15959359
18 2.27909379
    
```





PRINTED OUTPUT FROM BASSIN2





BASSING REV. 100, 01 D03 1201

-----  
\* SUCCESSFUL RELOAD OF K(SS) M(SS)  
-----

-----  
\* SUCCESSFUL RELOAD OF K(FF) K(SF)  
-----

-----  
\* SUCCESSFUL RELOAD OF F(SOIL),DIS  
-----

-----  
SUCCESSFUL COMPUTATION OF INFLUENCE COEFFICIENTS  
-----

MODAL TRUNCATION PROCEDURE IS USED IN THIS APPLICATION

FREQUENCY IN HERTZ = 0.71620E+01  
FREQUENCY IN RPS = 0.45000E+00  
\*\*\*\*\*

DISPLACEMENT FIELD OF BRIDGE  
\*\*\*\*\*

\*\*\*\*\*

\*\*\*\*\*

\*\*\*\*\*

NODE	X	Y	Z
1 SUP	0.394E-01	0.152E+01	0.540E-01
2 SUP	0.520E-02	0.139E+01	0.145E-02
3 SUP	0.458E-01	0.150E+01	0.368E-01
4 INT	0.356E-01	0.152E+01	0.540E-01
5 INT	0.314E-02	0.145E+01	0.142E-02
6 INT	0.418E-01	0.150E+01	0.368E-01
7 SUP	0.401E-01	0.152E+01	0.270E-01
8 SUP	0.328E-02	0.139E+01	0.120E-02
9 SUP	0.466E-01	0.150E+01	0.295E-01
10 INT	0.360E-01	0.152E+01	0.270E-01
11 INT	0.513E-02	0.144E+01	0.120E-02
12 INT	0.422E-01	0.150E+01	0.295E-01
13 SUP	0.412E-01	0.151E+01	0.203E-01
14 SUP	0.343E-02	0.136E+01	0.796E-05
15 SUP	0.481E-01	0.149E+01	0.220E-01
16 INT	0.359E-01	0.152E+01	0.203E-01
17 INT	0.505E-02	0.144E+01	0.795E-03
18 INT	0.420E-01	0.150E+01	0.220E-01
19 SUP	0.428E-01	0.151E+01	0.128E-01
20 SUP	0.365E-02	0.138E+01	0.178E-03
21 SUP	0.500E-01	0.149E+01	0.132E-01
22 INT	0.355E-01	0.152E+01	0.127E-01
23 INT	0.298E-02	0.143E+01	0.192E-03
24 INT	0.414E-01	0.151E+01	0.149E+01
25 SUP	0.451E-01	0.150E+01	0.146E+01
26 SUP	0.592E-02	0.157E+01	0.155E+01
27 SUP	0.528E-01	0.148E+01	0.149E+01
28 INT	0.345E-01	0.152E+01	0.535E-02
29 INT	0.285E-02	0.144E+01	0.766E-03
30 INT	0.402E-01	0.151E+01	0.222E-02
31 SUP	0.452E-01	0.149E+01	0.559E-02
32 SUP	0.393E-02	0.157E+01	0.151E+01
33 SUP	0.530E-01	0.148E+01	0.106E+01
34 SUP	0.452E-01	0.149E+01	0.116E+01
35 SUP	0.594E-02	0.157E+01	0.109E+01
36 SUP	0.530E-01	0.147E+01	0.645E+00
37 SUP	0.499E-01	0.149E+01	0.798E-01
38 SUP	0.596E-02	0.157E+01	0.110E+01
39 SUP	0.528E-01	0.147E+01	0.511E-03
40 SUP	0.495E-01	0.148E+01	0.311E-03
41 SUP	0.597E-02	0.157E+01	0.465E-03
42 SUP	0.524E-01	0.147E+01	0.755E-03
43 INT	0.408E-01	0.146E+01	0.108E+01
44 INT	0.458E-05	0.110E+01	0.149E+01



45 INT	0.417E-01	0.145E+01	0.400E+01	-0.125E+00	0.522E-02	-0.140E+01
46 SUP	0.425F-01	0.147E+01	0.400E+01	-0.137E+00	0.121E-02	-0.135E+01
47 SUP	0.369E-02	0.140E+01	0.400E+01	-0.137E+00	0.250E-02	0.140E+01
48 SUP	0.497E-01	0.146E+01	0.400E+01	-0.138E+00	0.589E-02	0.119E+01
49 INT	0.421E-01	0.147E+01	0.400E+01	-0.138E+00	0.112E-02	-0.119E+01
50 INT	0.595E-03	0.751E+00	0.400E+01	-0.138E+00	0.242E-02	0.157E+01
51 INT	0.427F-01	0.146E+01	0.400E+01	-0.138E+00	0.597E-02	0.121E+01
52 SUP	0.414E-01	0.146E+01	0.400E+01	-0.149E+00	0.220E-02	-0.125E+01
53 SUP	0.296E-02	0.154E+01	0.400E+01	-0.149E+00	0.609E-02	0.142E+01
54 SUP	0.485E-01	0.145E+01	0.400E+01	-0.148E+00	0.115E-01	0.152E+01
55 INT	0.424E-01	0.147E+01	0.400E+01	-0.149E+00	0.223E-02	-0.125E+01
56 INT	0.525E-03	0.152E+01	0.400E+01	-0.150E+00	0.617E-02	0.143E+01
57 INT	0.424E-01	0.146E+01	0.400E+01	-0.160E+00	0.435E-02	-0.124E+01
58 SUP	0.411E-01	0.146E+01	0.400E+01	-0.160E+00	0.880E-02	0.157E+01
59 SUP	0.210E-02	0.128E+01	0.400E+01	-0.159E+00	0.197E-01	0.153E+01
60 SUP	0.474E-01	0.145E+01	0.400E+01	-0.161E+00	0.431E-02	-0.124E+01
61 INT	0.422F-01	0.148E+01	0.400E+01	-0.161E+00	0.873E-02	0.157E+01
62 INT	0.553E-03	-0.124E+01	0.400E+01	-0.161E+00	0.197E-01	0.153E+01
63 INT	0.423E-01	0.146E+01	0.400E+01	-0.171E+00	0.588E-02	-0.112E+01
64 SUP	0.414E-01	0.146E+01	0.400E+01	-0.171E+00	0.121E-01	0.156E+01
65 SUP	0.135E-02	0.116E+01	0.400E+01	-0.171E+00	0.280E-01	0.156E+01
66 SUP	0.464F-01	0.145E+01	0.400E+01	-0.172E+00	0.597E-02	-0.13E+01
67 INT	0.411E-01	0.147E+01	0.400E+01	-0.173E+00	0.117E-01	0.155E+01
68 INT	0.154E-02	-0.145E+01	0.400E+01	-0.173E+00	0.280E-01	0.134E+01
69 INT	0.423E-01	0.146E+01	0.400E+01	-0.173E+00	0.280E-01	0.134E+01

FREQUENCY IN HERTZ = 0.14524E+00  
FREQUENCY IN RPS = 0.90000E+00  
\*\*\*\*\*

DISPLACEMENT FIELD OF BRIDGE  
\*\*\*\*\*

\*\*\*\*\*

\*\*\*\*\*

\*\*\*\*\*

MODE	X	Y	Z
1 SUP	0.788E-01	0.402E+01	-0.193E-01
2 SUP	0.638E-02	0.402E+01	-0.191E-01
3 SUP	0.915E-01	0.402E+01	-0.194E-01
4 INT	0.711E-01	0.402E+01	-0.999E-02
5 INT	0.626E-02	0.403E+01	-0.104E-01
6 INT	0.836E-01	0.402E+01	-0.100E-01
7 SUP	0.803E-01	0.401E+01	-0.415E-01
8 SUP	0.655E-02	0.401E+01	-0.415E-01
9 SUP	0.932E-01	0.401E+01	-0.416E-01
10 INT	0.719E-01	0.402E+01	-0.327E-01
11 INT	0.623E-02	0.402E+01	-0.328E-01
12 INT	0.843E-01	0.402E+01	-0.327E-01
13 SUP	0.825E-01	0.401E+01	-0.637E-01
14 SUP	0.684E-02	0.401E+01	-0.637E-01
15 SUP	0.960E-01	0.401E+01	-0.638E-01
16 INT	0.718E-01	0.401E+01	-0.558E-01
17 INT	0.609E-02	0.401E+01	-0.558E-01
18 INT	0.839E-01	0.401E+01	-0.851E-01
19 SUP	0.855E-01	0.401E+01	-0.851E-01
20 SUP	0.729E-02	0.401E+01	-0.850E-01
21 SUP	0.999E-01	0.401E+01	-0.852E-01
22 INT	0.710E-01	0.401E+01	-0.797E-01
23 INT	0.587E-02	0.401E+01	-0.797E-01
24 INT	0.827E-01	0.401E+01	-0.796E-01
25 SUP	0.901E-01	0.401E+01	-0.106E+00
26 SUP	0.782E-02	0.401E+01	-0.106E+00
27 SUP	0.105E+00	0.401E+01	-0.106E+00
28 INT	0.691E-01	0.401E+01	-0.104E+00
29 INT	0.572E-02	0.401E+01	-0.104E+00
30 INT	0.804E-01	0.401E+01	-0.104E+00
31 SUP	0.903E-01	0.400E+01	-0.143E+00
32 SUP	0.784E-02	0.400E+01	-0.143E+00
33 SUP	0.106E+00	0.400E+01	-0.143E+00
34 SUP	0.903E-01	0.400E+01	-0.179E+00
35 SUP	0.787E-02	0.400E+01	-0.179E+00
36 SUP	0.106E+00	0.400E+01	-0.179E+00
37 SUP	0.898E-01	0.400E+01	-0.216E+00
38 SUP	0.790E-02	0.400E+01	-0.216E+00
39 SUP	0.105E+00	0.400E+01	-0.216E+00
40 SUP	0.699E-01	0.401E+01	-0.253E+00
41 SUP	0.792E-02	0.401E+01	-0.253E+00
42 SUP	0.105E+00	0.401E+01	-0.253E+00
43 INT	0.814E-01	0.400E+01	-0.251E+00
44 INT	0.974E-03	0.400E+01	-0.251E+00

45 INT	0.835E-01	0.154E+01	0.400E+01	-0.251E+00	0.104E-01	-0.151E+01
46 SUP	0.845E-01	0.137E+01	0.401E+01	-0.275E+00	0.251E-02	-0.149E+01
47 SUP	0.757E-02	0.129E+01	0.401E+01	-0.275E+00	0.520E-02	0.151E+01
48 SUP	0.993E-01	0.135E+01	0.401E+01	-0.275E+00	0.769E-02	0.119E+01
49 INT	0.841E-01	0.136E+01	0.401E+01	-0.275E+00	0.231E-02	-0.147E+01
50 INT	0.896E-03	0.512E+00	0.401E+01	-0.275E+00	0.501E-02	0.151E+01
51 INT	0.854E-01	0.135E+01	0.401E+01	-0.275E+00	0.786E-02	0.121E+01
52 SUP	0.826E-01	0.135E+01	0.401E+01	-0.297E+00	0.444E-02	-0.151E+01
53 SUP	0.588E-02	0.123E+01	0.401E+01	-0.297E+00	0.125E-01	0.134E+01
54 SUP	0.968E-01	0.134E+01	0.401E+01	-0.297E+00	0.226E-01	0.127E+01
55 INT	0.847E-01	0.136E+01	0.401E+01	-0.299E+00	0.450E-02	-0.151E+01
56 INT	0.109E-02	0.122E+01	0.401E+01	-0.299E+00	0.125E-01	0.156E+01
57 INT	0.847E-01	0.135E+01	0.401E+01	-0.299E+00	0.225E-01	0.127E+01
58 SUP	0.820E-01	0.134E+01	0.402E+01	-0.320E+00	0.894E-02	-0.159E+01
59 SUP	0.414E-02	0.117E+01	0.402E+01	-0.320E+00	0.176E-01	0.150E+01
60 SUP	0.947E-01	0.134E+01	0.402E+01	-0.319E+00	0.389E-01	0.126E+01
61 INT	0.843E-01	0.137E+01	0.402E+01	-0.322E+00	0.885E-02	-0.159E+01
62 INT	0.115E-02	-0.117E+01	0.402E+01	-0.322E+00	0.174E-01	0.150E+01
63 INT	0.845E-01	0.135E+01	0.402E+01	-0.323E+00	0.390E-01	0.126E+01
64 SUP	0.827E-01	0.135E+01	0.403E+01	-0.342E+00	0.124E-01	-0.121E+01
65 SUP	0.267E-02	0.104E+01	0.403E+01	-0.342E+00	0.240E-01	0.130E+01
66 SUP	0.926E-01	0.134E+01	0.403E+01	-0.341E+00	0.552E-01	0.125E+01
67 INT	0.822E-01	0.137E+01	0.402E+01	-0.345E+00	0.126E-01	-0.122E+01
68 INT	0.504E-02	-0.152E+01	0.402E+01	-0.345E+00	0.232E-01	0.129E+01
69 INT	0.845E-01	0.135E+01	0.402E+01	-0.346E+00	0.552E-01	0.129E+01

FREQUENCY IN HERTZ = 0.21527E+00  
 FREQUENCY IN RPS = 0.15400E+01  
 \*\*\*\*\*

DISPLACEMENT FIELD OF BRIDGE  
 \*\*\*\*\*

\*\*\*\*\*

NODE	X			Y			Z		
	A	P	A	A	P	A	A	P	
1 SUP	0.117E+00	0.140E+01	0.404E+01	-0.302E-01	0.102E+00	0.138E+01			
2 SUP	0.953E-02	0.119E+01	0.404E+01	-0.300E-01	0.646E-02	0.527E+00			
3 SUP	0.136E+00	0.137E+01	0.404E+01	-0.304E-01	0.109E+00	0.129E+01			
4 INT	0.106E+00	0.139E+01	0.405E+01	-0.165E-01	0.102E+00	0.138E+01			
5 INT	0.935E-02	0.132E+01	0.405E+01	-0.175E-01	0.645E-02	0.530E+00			
6 INT	0.124E+00	0.137E+01	0.405E+01	-0.166E-01	0.109E+00	0.129E+01			
7 SUP	0.119E+00	0.140E+01	0.405E+01	-0.631E-01	0.807E-01	0.134E+01			
8 SUP	0.979E-02	0.118E+01	0.405E+01	-0.630E-01	0.459E-02	0.552E+00			
9 SUP	0.136E+00	0.137E+01	0.405E+01	-0.632E-01	0.877E-01	0.127E+01			
10 INT	0.107E+00	0.139E+01	0.404E+01	-0.501E-01	0.807E-01	0.154E+01			
11 INT	0.931E-02	0.130E+01	0.404E+01	-0.502E-01	0.458E-02	0.552E+00			
12 INT	0.125E+00	0.137E+01	0.404E+01	-0.501E-01	0.877E-01	0.127E+01			
13 SUP	0.125E+00	0.139E+01	0.402E+01	-0.959E-01	0.606E-01	0.151E+01			
14 SUP	0.102E-01	0.117E+01	0.402E+01	-0.958E-01	0.279E-02	0.724E+00			
15 SUP	0.143E+00	0.136E+01	0.402E+01	-0.960E-01	0.657E-01	0.126E+01			
16 INT	0.107E+00	0.139E+01	0.405E+01	-0.845E-01	0.607E-01	0.151E+01			
17 INT	0.910E-02	0.129E+01	0.405E+01	-0.843E-01	0.279E-02	0.715E+00			
18 INT	0.125E+00	0.137E+01	0.405E+01	-0.842E-01	0.659E-01	0.126E+01			
19 SUP	0.127E+00	0.137E+01	0.401E+01	-0.128E+00	0.380E-01	0.150E+01			
20 SUP	0.109E-01	0.117E+01	0.401E+01	-0.128E+00	0.617E-03	0.151E+01			
21 SUP	0.148E+00	0.134E+01	0.401E+01	-0.128E+00	0.395E-01	0.151E+01			
22 INT	0.106E+00	0.140E+01	0.402E+01	-0.120E+00	0.379E-01	0.150E+01			
23 INT	0.876E-02	0.127E+01	0.402E+01	-0.120E+00	0.671E-03	0.154E+01			
24 INT	0.123E+00	0.136E+01	0.402E+01	-0.120E+00	0.394E-01	0.150E+01			
25 SUP	0.134E+00	0.134E+01	0.401E+01	-0.156E+00	0.105E-01	-0.144E+01			
26 SUP	0.117E-01	0.116E+01	0.401E+01	-0.158E+00	0.240E-02	0.649E+00			
27 SUP	0.157E+00	0.131E+01	0.401E+01	-0.158E+00	0.887E-02	-0.998E+00			
28 INT	0.103E+00	0.141E+01	0.401E+01	-0.156E+00	0.111E-01	-0.140E+01			
29 INT	0.856E-02	0.129E+01	0.401E+01	-0.156E+00	0.241E-02	0.654E+00			
30 INT	0.119E+00	0.139E+01	0.401E+01	-0.156E+00	0.966E-02	-0.104E+01			
31 SUP	0.130E+00	0.133E+01	0.400E+01	-0.213E+00	0.124E-02	0.775E+00			
32 SUP	0.117E-01	0.116E+01	0.400E+01	-0.213E+00	0.114E-02	0.141E+00			
33 SUP	0.157E+00	0.130E+01	0.400E+01	-0.213E+00	0.147E-02	-0.586E+00			
34 SUP	0.134E+00	0.132E+01	0.400E+01	-0.268E+00	0.101E-02	-0.127E+01			
35 SUP	0.118E-01	0.116E+01	0.400E+01	-0.268E+00	0.115E-02	-0.129E+01			
36 SUP	0.157E+00	0.129E+01	0.400E+01	-0.268E+00	0.128E-02	-0.129E+01			
37 SUP	0.135E+00	0.131E+01	0.400E+01	-0.362E+00	0.150E-02	0.116E+01			
38 SUP	0.118E-01	0.116E+01	0.400E+01	-0.362E+00	0.237E-02	0.137E+01			
39 SUP	0.157E+00	0.128E+01	0.400E+01	-0.362E+00	0.529E-02	0.140E+01			
40 SUP	0.132E+00	0.130E+01	0.402E+01	-0.376E+00	0.875E-02	-0.126E+01			
41 SUP	0.118E-01	0.116E+01	0.402E+01	-0.376E+00	0.572E-02	0.127E+01			
42 SUP	0.156E+00	0.128E+01	0.402E+01	-0.376E+00	0.154E-01	-0.156E+01			
43 INT	0.121E+00	0.124E+01	0.401E+01	-0.374E+00	0.957E-02	-0.129E+01			
44 INT	0.149E-02	0.500E+00	0.401E+01	-0.374E+00	0.371E-02	0.127E+01			

45 INT	0.124E+00	0.122E+01	0.401E+01	-0.574E+00	0.163E-01	-0.157E+01
46 SUP	0.125E+00	0.127E+01	0.402E+01	-0.409E+00	0.362E-02	0.149E+01
47 SUP	0.110E-01	0.118E+01	0.402E+01	-0.409E+00	0.755E-02	0.128E+01
48 SUP	0.147E+00	0.125E+01	0.402E+01	-0.409E+00	0.108E-01	0.119E+01
49 INT	0.125E+00	0.125E+01	0.402E+01	-0.410E+00	0.553E-02	0.141E+01
50 INT	0.149E-02	0.207E+00	0.402E+01	-0.410E+00	0.723E-02	0.126E+01
51 INT	0.127E+00	0.123E+01	0.402E+01	-0.410E+00	0.111E-01	0.122E+01
52 SUP	0.123E+00	0.124E+01	0.403E+01	-0.443E+00	0.670E-02	0.159E+01
53 SUP	0.871E-02	0.111E+01	0.403E+01	-0.442E+00	0.183E-01	0.128E+01
54 SUP	0.144E+00	0.123E+01	0.403E+01	-0.442E+00	0.331E-01	0.123E+01
55 INT	0.126E+00	0.126E+01	0.403E+01	-0.445E+00	0.686E-02	0.139E+01
56 INT	0.166E-02	0.904E+00	0.403E+01	-0.445E+00	0.185E-01	0.129E+01
57 INT	0.126E+00	0.124E+01	0.403E+01	-0.445E+00	0.528E-01	0.123E+01
58 SUP	0.122E+00	0.123E+01	0.404E+01	-0.477E+00	0.138E-01	-0.152E+01
59 SUP	0.609E-02	0.106E+01	0.404E+01	-0.476E+00	0.260E-01	0.124E+01
60 SUP	0.141E+00	0.122E+01	0.404E+01	-0.474E+00	0.568E-01	0.119E+01
61 INT	0.125E+00	0.126E+01	0.404E+01	-0.479E+00	0.137E-01	-0.152E+01
62 INT	0.199E-02	-0.114E+01	0.404E+01	-0.479E+00	0.258E-01	0.124E+01
63 INT	0.126E+00	0.124E+01	0.404E+01	-0.480E+00	0.570E-01	0.119E+01
64 SUP	0.123E+00	0.124E+01	0.406E+01	-0.509E+00	0.198E-01	-0.130E+01
65 SUP	0.390E-02	0.917E+00	0.406E+01	-0.508E+00	0.353E-01	0.124E+01
66 SUP	0.137E+00	0.122E+01	0.405E+01	-0.507E+00	0.808E-01	0.116E+01
67 INT	0.122E+00	0.126E+01	0.405E+01	-0.512E+00	0.200E-01	-0.150E+01
68 INT	0.458E-02	0.155E+01	0.405E+01	-0.512E+00	0.341E-01	0.124E+01
69 INT	0.126E+00	0.124E+01	0.405E+01	-0.514E+00	0.808E-01	0.116E+01

FREQUENCY IN HERTZ = 0.20989E+00  
FREQUENCY IN KPS = 0.17900E+01

DISPLACEMENT FIELD OF BRIDGE

\*\*\*\*\*

NODE	X	Y	Z
1 SUP	0.156E+00	0.407E+01	0.137E+00
2 SUP	0.128E-01	0.407E+01	0.107E-01
3 SUP	0.181E+00	0.408E+01	0.146E+00
4 INT	0.140E+00	0.409E+01	0.157E+00
5 INT	0.125E-01	0.409E+01	0.108E-01
6 INT	0.166E+00	0.409E+01	0.146E+00
7 SUP	0.159E+00	0.405E+01	0.109E+00
8 SUP	0.132E-01	0.405E+01	0.115E-02
9 SUP	0.184E+00	0.405E+01	0.118E+00
10 INT	0.142E+00	0.407E+01	0.109E+00
11 INT	0.125E-01	0.407E+01	0.114E-02
12 INT	0.167E+00	0.406E+01	0.118E+00
13 SUP	0.163E+00	0.405E+01	0.818E-01
14 SUP	0.137E-01	0.405E+01	0.408E-02
15 SUP	0.190E+00	0.405E+01	0.408E-02
16 INT	0.142E+00	0.405E+01	0.886E-01
17 INT	0.122E-01	0.405E+01	0.115E+00
18 INT	0.166E+00	0.405E+01	0.116E+01
19 SUP	0.169E+00	0.402E+01	0.122E+01
20 SUP	0.147E-01	0.402E+01	0.741E-03
21 SUP	0.198E+00	0.402E+01	0.535E-01
22 INT	0.140E+00	0.403E+01	0.512E-01
23 INT	0.117E-01	0.403E+01	0.121E+01
24 INT	0.164E+00	0.403E+01	0.115E+01
25 SUP	0.178E+00	0.402E+01	0.121E+01
26 SUP	0.157E-01	0.402E+01	0.145E-01
27 SUP	0.209E+00	0.402E+01	0.359E-02
28 INT	0.157E+00	0.402E+01	0.137E-01
29 INT	0.115E-01	0.402E+01	0.157E-01
30 INT	0.159E+00	0.402E+01	0.476E+00
31 SUP	0.179E+00	0.400E+01	0.148E-01
32 SUP	0.157E-01	0.400E+01	0.164E-02
33 SUP	0.210E+00	0.400E+01	0.177E-02
34 SUP	0.170E+00	0.400E+01	0.245E-02
35 SUP	0.158E-01	0.399E+01	0.566E+00
36 SUP	0.210E+00	0.399E+01	0.412E-01
37 SUP	0.177E+00	0.400E+01	0.514E+00
38 SUP	0.159E-01	0.400E+01	0.191E+01
39 SUP	0.209E+00	0.400E+01	0.494E+00
40 SUP	0.176E+00	0.405E+01	0.103E+01
41 SUP	0.159E-01	0.403E+01	0.125E-01
42 SUP	0.207E+00	0.403E+01	0.561E-02
43 INT	0.161E+00	0.402E+01	0.109E+01
44 INT	0.254E-02	0.402E+01	0.220E-01
			0.136E-01
			0.559E-02
			0.109E+01

45 INT	0.165E+00	0.110E+01	0.402E+01	-0.250E+00	0.252E-01	0.151E+01
46 SUP	0.167E+00	0.116E+01	0.403E+01	-0.254E+00	0.498E-02	0.122E+01
47 SUP	0.148E-01	0.106E+01	0.403E+01	-0.2547E+00	0.956E-02	0.124E+01
48 SUP	0.196E+00	0.114E+01	0.403E+01	-0.2546E+00	0.131E-01	0.122E+01
49 INT	0.167E+00	0.114E+01	0.403E+01	-0.2547E+00	0.461E-02	0.152E+01
50 INT	0.240E-02	-0.271E-01	0.403E+01	-0.2547E+00	0.909E-02	0.122E+01
51 INT	0.169E+00	0.112E+01	0.403E+01	-0.2547E+00	0.153E-01	0.123E+01
52 SUP	0.165E+00	0.115E+01	0.405E+01	-0.2591E+00	0.976E-02	0.116E+01
53 SUP	0.117E-01	0.998E+00	0.405E+01	-0.2591E+00	0.241E-01	0.121E+01
54 SUP	0.191E+00	0.112E+01	0.405E+01	-0.2590E+00	0.425E-01	0.120E+01
55 INT	0.168E+00	0.115E+01	0.405E+01	-0.2594E+00	0.988E-02	0.117E+01
56 INT	0.244E-02	0.572E+00	0.405E+01	-0.2594E+00	0.244E-01	0.123E+01
57 INT	0.168E+00	0.112E+01	0.405E+01	-0.2594E+00	0.421E-01	0.120E+01
58 SUP	0.162E+00	0.112E+01	0.407E+01	-0.2636E+00	0.197E-01	0.149E+01
59 SUP	0.181E-02	0.944E+00	0.407E+01	-0.2635E+00	0.544E-01	0.119E+01
60 SUP	0.187E+00	0.111E+01	0.406E+01	-0.2633E+00	0.737E-01	0.115E+01
61 INT	0.167E+00	0.115E+01	0.407E+01	-0.2658E+00	0.142E-01	0.149E+01
62 INT	0.305E-02	-0.110E+01	0.407E+01	-0.2659E+00	0.341E-01	0.116E+01
63 INT	0.167E+00	0.113E+01	0.407E+01	-0.2640E+00	0.739E-01	0.113E+01
64 SUP	0.163E+00	0.112E+01	0.410E+01	-0.2679E+00	0.289E-01	-0.130E+01
65 SUP	0.526E-02	0.796E+00	0.410E+01	-0.2678E+00	0.469E-01	0.119E+01
66 SUP	0.183E+00	0.111E+01	0.410E+01	-0.2676E+00	0.105E+00	0.107E+01
67 INT	0.165E+00	0.115E+01	0.409E+01	-0.2683E+00	0.293E-01	-0.159E+01
68 INT	0.610E-02	0.151E+01	0.409E+01	-0.2683E+00	0.452E-01	0.119E+01
69 INT	0.167E+00	0.112E+01	0.409E+01	-0.2685E+00	0.105E+00	0.107E+01





45 INT	0.206E+00	0.979E+01	0.405E+01	-0.626E+00	0.299E-01	0.145E+01
46 SUP	0.297E+00	0.106E+01	0.405E+01	-0.684E+00	0.631E-02	0.974E+00
47 SUP	0.187E-01	0.952E+00	0.405E+01	-0.684E+00	0.116E-01	0.120E+01
48 SUP	0.244E+00	0.104E+01	0.405E+01	-0.684E+00	0.157E-01	0.120E+01
49 INT	0.207E+00	0.105E+01	0.405E+01	-0.685E+00	0.595E-02	0.885E+00
50 INT	0.566E-02	-0.142E+00	0.405E+01	-0.685E+00	0.109E-01	0.118E+01
51 INT	0.211E+00	0.100E+01	0.405E+01	-0.685E+00	0.163E-01	0.129E+01
52 SUP	0.203E+00	0.102E+01	0.407E+01	-0.759E+00	0.125E-01	0.986E+00
53 SUP	0.149E-01	0.883E+00	0.407E+01	-0.759E+00	0.297E-01	0.115E+01
54 SUP	0.238E+00	0.101E+01	0.407E+01	-0.738E+00	0.521E-01	0.117E+01
55 INT	0.209E+00	0.104E+01	0.407E+01	-0.742E+00	0.127E-01	0.947E+00
56 INT	0.569E-02	0.580E+00	0.407E+01	-0.742E+00	0.501E-01	0.117E+01
57 INT	0.209E+00	0.101E+01	0.407E+01	-0.743E+00	0.515E-01	0.118E+01
58 SUP	0.201E+00	0.101E+01	0.410E+01	-0.793E+00	0.250E-01	0.137E+01
59 SUP	0.105E-01	0.847E+00	0.410E+01	-0.793E+00	0.426E-01	0.114E+01
60 SUP	0.253E+00	0.996E+00	0.410E+01	-0.791E+00	0.901E-01	0.107E+01
61 INT	0.208E+00	0.105E+01	0.410E+01	-0.797E+00	0.244E-01	0.157E+01
62 INT	0.438E-02	-0.105E+01	0.410E+01	-0.798E+00	0.422E-01	0.115E+01
63 INT	0.209E+00	0.101E+01	0.411E+01	-0.800E+00	0.904E-01	0.107E+01
64 SUP	0.203E+00	0.101E+01	0.415E+01	-0.847E+00	0.577E-01	-0.146E+01
65 SUP	0.684E-02	0.696E+00	0.415E+01	-0.846E+00	0.562E-01	0.115E+01
66 SUP	0.228E+00	0.995E+00	0.415E+01	-0.843E+00	0.129E+00	0.992E+00
67 INT	0.203E+00	0.105E+01	0.414E+01	-0.852E+00	0.541E-01	-0.146E+01
68 INT	0.716E-02	0.148E+01	0.415E+01	-0.852E+00	0.561E-01	0.115E+01
69 INT	0.209E+00	0.101E+01	0.414E+01	-0.855E+00	0.129E+00	0.991E+00

FREQUENCY IN HERTZ = 0.42813E+00  
FREQUENCY IN PPS = 0.26900E+01  
\*\*\*\*\*

DISPLACEMENT FIELD OF BRIDGE  
\*\*\*\*\*

\*\*\*\*\*

\*\*\*\*\*

\*\*\*\*\*

\*\*\*\*\*

NODE	X	Y	Z	A	P	A	P	A	P
1 SUP	0.231E+00	0.122E+00	0.415E+01	-0.758E-01	0.205E+00	0.122E+01	0.252E-01	0.167E+00	0.122E+01
2 SUP	0.197E-01	0.482E+00	0.414E+01	-0.752E-01	0.252E-01	-0.167E+00	0.218E+00	0.104E+01	0.104E+01
3 SUP	0.269E+00	0.118E+01	0.415E+01	-0.763E-01	0.218E+00	0.104E+01	0.209E+00	0.122E+01	0.122E+01
4 INT	0.209E+00	0.119E+01	0.417E+01	-0.497E-01	0.259E-01	-0.181E+00	0.259E-01	0.104E+01	0.104E+01
5 INT	0.148E-01	0.116E+01	0.418E+01	-0.517E-01	0.216E+00	0.104E+01	0.163E+00	0.110E+01	0.110E+01
6 INT	0.247E+00	0.117E+01	0.417E+01	-0.498E-01	0.163E+00	0.110E+01	0.143E-01	-0.544E-01	-0.544E-01
7 SUP	0.236E+00	0.122E+00	0.409E+01	-0.138E+00	0.177E+00	0.999E+00	0.177E+00	0.999E+00	0.999E+00
8 SUP	0.202E-01	0.865E+00	0.409E+01	-0.159E+00	0.163E+00	0.114E+01	0.143E-01	-0.544E-01	-0.544E-01
9 SUP	0.274E+00	0.117E+01	0.409E+01	-0.159E+00	0.177E+00	0.999E+00	0.177E+00	0.999E+00	0.999E+00
10 INT	0.211E+00	0.119E+01	0.413E+01	-0.114E+00	0.143E-01	-0.544E-01	0.143E-01	-0.544E-01	-0.544E-01
11 INT	0.189E-01	0.110E+01	0.413E+01	-0.114E+00	0.177E+00	0.999E+00	0.177E+00	0.999E+00	0.999E+00
12 INT	0.248E+00	0.117E+01	0.413E+01	-0.114E+00	0.124E+00	0.105E+01	0.124E+00	0.105E+01	0.105E+01
13 SUP	0.202E+00	0.120E+01	0.405E+01	-0.203E+00	0.750E-02	0.124E+00	0.750E-02	0.124E+00	0.124E+00
14 SUP	0.211E-01	0.851E+00	0.405E+01	-0.202E+00	0.134E+00	0.970E+00	0.134E+00	0.970E+00	0.970E+00
15 SUP	0.282E+00	0.115E+01	0.405E+01	-0.203E+00	0.124E+00	0.105E+01	0.124E+00	0.105E+01	0.105E+01
16 INT	0.210E+00	0.120E+01	0.409E+01	-0.180E+00	0.750E-02	0.134E+00	0.750E-02	0.134E+00	0.134E+00
17 INT	0.185E-01	0.107E+01	0.409E+01	-0.180E+00	0.135E+00	0.970E+00	0.135E+00	0.970E+00	0.970E+00
18 INT	0.247E+00	0.118E+01	0.409E+01	-0.180E+00	0.786E-01	0.104E+01	0.786E-01	0.104E+01	0.104E+01
19 SUP	0.251E+00	0.116E+01	0.404E+01	-0.265E+00	0.920E-05	0.722E+00	0.920E-05	0.722E+00	0.722E+00
20 SUP	0.226E-01	0.841E+00	0.404E+01	-0.265E+00	0.811E-01	0.103E+01	0.811E-01	0.103E+01	0.103E+01
21 SUP	0.294E+00	0.111E+01	0.404E+01	-0.266E+00	0.784E-01	0.103E+01	0.784E-01	0.103E+01	0.103E+01
22 INT	0.208E+00	0.121E+01	0.405E+01	-0.249E+00	0.105E-02	0.775E+00	0.105E-02	0.775E+00	0.775E+00
23 INT	0.178E-01	0.105E+01	0.405E+01	-0.249E+00	0.608E-01	0.103E+01	0.608E-01	0.103E+01	0.103E+01
24 INT	0.203E+00	0.119E+01	0.405E+01	-0.249E+00	0.244E-01	0.151E+01	0.244E-01	0.151E+01	0.151E+01
25 SUP	0.265E+00	0.110E+01	0.404E+01	-0.326E+00	0.670E-02	0.177E+00	0.670E-02	0.177E+00	0.177E+00
26 SUP	0.242E-01	0.829E+00	0.404E+01	-0.327E+00	0.265E-01	0.986E+00	0.265E-01	0.986E+00	0.986E+00
27 SUP	0.511E+00	0.106E+01	0.404E+01	-0.327E+00	0.261E-01	0.152E+01	0.261E-01	0.152E+01	0.152E+01
28 INT	0.203E+00	0.125E+01	0.402E+01	-0.521E+00	0.671E-02	0.181E+00	0.671E-02	0.181E+00	0.181E+00
29 INT	0.176E-01	0.106E+01	0.402E+01	-0.521E+00	0.280E-01	0.103E+01	0.280E-01	0.103E+01	0.103E+01
30 INT	0.237E+00	0.122E+01	0.402E+01	-0.521E+00	0.280E-01	0.103E+01	0.280E-01	0.103E+01	0.103E+01
31 SUP	0.265E+00	0.108E+01	0.599E+01	-0.434E+00	0.280E-02	0.189E+00	0.280E-02	0.189E+00	0.189E+00
32 SUP	0.242E-01	0.829E+00	0.599E+01	-0.434E+00	0.367E-02	0.573E+00	0.367E-02	0.573E+00	0.573E+00
33 SUP	0.312E+00	0.104E+01	0.599E+01	-0.434E+00	0.519E-02	0.668E+00	0.519E-02	0.668E+00	0.668E+00
34 SUP	0.265E+00	0.106E+01	0.597E+01	-0.543E+00	0.329E-02	0.154E+01	0.329E-02	0.154E+01	0.154E+01
35 SUP	0.243E-01	0.850E+00	0.597E+01	-0.543E+00	0.557E-02	0.152E+01	0.557E-02	0.152E+01	0.152E+01
36 SUP	0.312E+00	0.102E+01	0.597E+01	-0.543E+00	0.590E-02	0.151E+01	0.590E-02	0.151E+01	0.151E+01
37 SUP	0.265E+00	0.104E+01	0.400E+01	-0.651E+00	0.441E-02	0.794E+00	0.441E-02	0.794E+00	0.794E+00
38 SUP	0.244E-01	0.851E+00	0.400E+01	-0.651E+00	0.617E-02	0.106E+01	0.617E-02	0.106E+01	0.106E+01
39 SUP	0.311E+00	0.101E+01	0.400E+01	-0.651E+00	0.619E-02	0.120E+01	0.619E-02	0.120E+01	0.120E+01
40 SUP	0.260E+00	0.102L+01	0.406E+01	-0.757E+00	0.219E-01	0.120E+01	0.219E-01	0.120E+01	0.120E+01
41 SUP	0.244E-01	0.852E+00	0.406E+01	-0.757E+00	0.916E-02	0.659E+00	0.916E-02	0.659E+00	0.659E+00
42 SUP	0.309E+00	0.989E+00	0.406E+01	-0.757E+00	0.553E-01	0.140E+01	0.553E-01	0.140E+01	0.140E+01
43 INT	0.240E+00	0.891E+00	0.404E+01	-0.752E+00	0.254E-01	0.152E+01	0.254E-01	0.152E+01	0.152E+01
44 INT	0.541E-02	0.576E-01	0.400E+01	-0.752E+00	0.916E-02	0.657E+00	0.916E-02	0.657E+00	0.657E+00

45 INT	0.247E+00	0.858E+00	0.407E+01	-0.752E+00	0.571E-01	0.139E+01
46 SUP	0.247E+00	0.955E+00	0.407E+01	-0.822E+00	0.779E-02	0.735E+00
47 SUP	0.229E-01	0.840E+00	0.407E+01	-0.822E+00	0.135E-01	0.117E+01
48 SUP	0.292E+00	0.955E+00	0.407E+01	-0.822E+00	0.186E-01	0.132E+01
49 INT	0.247E+00	0.917E+00	0.407E+01	-0.822E+00	0.751E-02	0.651E+00
50 INT	0.525E-02	-0.204E+00	0.407E+01	-0.822E+00	0.127E-01	0.116E+01
51 INT	0.253E+00	0.883E+00	0.407E+01	-0.822E+00	0.194E-01	0.135E+01
52 SUP	0.241E+00	0.915E+00	0.410E+01	-0.887E+00	0.157E-01	0.748E+00
53 SUP	0.182E-01	0.770E+00	0.410E+01	-0.887E+00	0.350E-01	0.110E+01
54 SUP	0.285E+00	0.899E+00	0.410E+01	-0.886E+00	0.616E-01	0.113E+01
55 INT	0.249E+00	0.932E+00	0.410E+01	-0.891E+00	0.159E-01	0.738E+00
56 INT	0.555E-02	0.188E+00	0.411E+01	-0.891E+00	0.355E-01	0.111E+01
57 INT	0.251E+00	0.893E+00	0.410E+01	-0.891E+00	0.609E-01	0.116E+01
58 SUP	0.240E+00	0.894E+00	0.415E+01	-0.953E+00	0.307E-01	0.126E+01
59 SUP	0.131E-01	0.750E+00	0.414E+01	-0.951E+00	0.506E-01	0.169E+01
60 SUP	0.279E+00	0.881E+00	0.414E+01	-0.948E+00	0.106E+00	0.101E+01
61 INT	0.247E+00	0.959E+00	0.415E+01	-0.956E+00	0.304E-01	0.125E+01
62 INT	0.595E-02	-0.105E+01	0.415E+01	-0.956E+00	0.500E-01	0.163E+01
63 INT	0.250E+00	0.899E+00	0.415E+01	-0.958E+00	0.106E+00	0.101E+01
64 SUP	0.242E+00	0.896E+00	0.421E+01	-0.101E+01	0.475E-01	-0.154E+01
65 SUP	0.866E-02	0.601E+00	0.421E+01	-0.101E+01	0.696E-01	0.111E+01
66 SUP	0.273E+00	0.879E+00	0.421E+01	-0.101E+01	0.151E+00	0.915E+00
67 INT	0.241E+00	0.940E+00	0.419E+01	-0.102E+01	0.479E-01	-0.154E+01
68 INT	0.608E-02	0.149E+01	0.421E+01	-0.102E+01	0.672E-01	0.112E+01
69 INT	0.250E+00	0.897E+00	0.420E+01	-0.102E+01	0.151E+00	0.915E+00

FREQUENCY IN HERTZ = 0.57137E+00  
 \* FREQUENCY IN RPS = 0.35900E+01  
 \*\*\*\*\*

DISPLACEMENT FIELD OF BRIDGE  
 \*\*\*\*\*

\*\*\*\*\*

NODE	X	Y	Z	A	P	A	P
1 SUP	0.304E+00	0.111E+01	0.422E+01	0.417E+00	0.269E+00	0.111E+01	0.111E+01
2 SUP	0.277E-01	0.672E+00	0.421E+01	-0.116E+00	0.421E-01	-0.116E+00	-0.563E+00
3 SUP	0.354E+00	0.104E+01	0.423E+01	0.118E+00	0.289E+00	0.870E+00	0.870E+00
4 INT	0.275E+00	0.106E+01	0.426E+01	-0.839E-01	0.269E+00	0.111E+01	0.111E+01
5 INT	0.255E-01	0.107E+01	0.428E+01	-0.869E-01	0.429E-01	-0.375E+00	-0.375E+00
6 INT	0.326E+00	0.104E+01	0.426E+01	-0.832E-01	0.289E+00	0.870E+00	0.870E+00
7 SUP	0.310E+00	0.111E+01	0.412E+01	-0.197E+00	0.216E+00	0.100E+01	0.100E+01
8 SUP	0.284E-01	0.654E+00	0.412E+01	-0.197E+00	0.216E-01	-0.268E+00	-0.268E+00
9 SUP	0.361E+00	0.104E+01	0.412E+01	-0.198E+00	0.257E+00	0.820E+00	0.820E+00
10 INT	0.277E+00	0.106E+01	0.419E+01	-0.166E+00	0.216E+00	0.999E+00	0.999E+00
11 INT	0.257E-01	0.975E+00	0.419E+01	-0.167E+00	0.248E-01	-0.270E+00	-0.270E+00
12 INT	0.328E+00	0.104E+01	0.418E+01	-0.166E+00	0.237E+00	0.819E+00	0.819E+00
13 SUP	0.318E+00	0.108E+01	0.406E+01	-0.281E+00	0.166E+00	0.888E+00	0.888E+00
14 SUP	0.297E-01	0.640E+00	0.407E+01	-0.281E+00	0.125E-01	-0.152E+00	-0.152E+00
15 SUP	0.372E+00	0.101E+01	0.406E+01	-0.281E+00	0.161E+00	0.781E+00	0.781E+00
16 INT	0.276E+00	0.107E+01	0.412E+01	-0.252E+00	0.166E+00	0.886E+00	0.886E+00
17 INT	0.253E-01	0.916E+00	0.412E+01	-0.253E+00	0.125E-01	-0.162E+00	-0.162E+00
18 INT	0.326E+00	0.104E+01	0.412E+01	-0.252E+00	0.181E+00	0.779E+00	0.779E+00
19 SUP	0.329E+00	0.102E+01	0.404E+01	-0.364E+00	0.106E+00	0.862E+00	0.862E+00
20 SUP	0.318E-01	0.625E+00	0.404E+01	-0.364E+00	0.805E-03	0.152E+00	0.152E+00
21 SUP	0.388E+00	0.961E+00	0.404E+01	-0.365E+00	0.109E+00	0.860E+00	0.860E+00
22 INT	0.275E+00	0.109E+01	0.406E+01	-0.343E+00	0.106E+00	0.850E+00	0.850E+00
23 INT	0.245E-01	0.896E+00	0.406E+01	-0.343E+00	0.960E-03	0.236E+00	0.236E+00
24 INT	0.321E+00	0.106E+01	0.406E+01	-0.342E+00	0.109E+00	0.848E+00	0.848E+00
25 SUP	0.347E+00	0.940E+00	0.404E+01	-0.446E+00	0.565E-01	0.156E+01	0.156E+01
26 SUP	0.340E-01	0.613E+00	0.404E+01	-0.446E+00	0.115E-01	-0.322E-01	-0.322E-01
27 SUP	0.412E+00	0.887E+00	0.404E+01	-0.446E+00	0.434E-01	-0.104E+01	-0.104E+01
28 INT	0.267E+00	0.113E+01	0.402E+01	-0.437E+00	0.590E-01	0.155E+01	0.155E+01
29 INT	0.242E-01	0.886E+00	0.402E+01	-0.437E+00	0.115E-01	-0.284E-01	-0.284E-01
30 INT	0.313E+00	0.110E+01	0.402E+01	-0.437E+00	0.455E-01	-0.108E+01	-0.108E+01
31 SUP	0.348E+00	0.916E+00	0.595E+01	-0.587E+00	0.595E+00	0.143E+00	0.143E+00
32 SUP	0.341E-01	0.614E+00	0.595E+01	-0.587E+00	0.666E-02	-0.582E+00	-0.582E+00
33 SUP	0.413E+00	0.867E+00	0.595E+01	-0.587E+00	0.927E-02	-0.805E+00	-0.805E+00
34 SUP	0.547E+00	0.887E+00	0.594E+01	-0.572E+00	0.564E-02	0.153E+01	0.153E+01
35 SUP	0.342E-01	0.616E+00	0.594E+01	-0.572E+00	0.612E-02	0.154E+01	0.154E+01
36 SUP	0.413E+00	0.843E+00	0.594E+01	-0.572E+00	0.661E-02	0.154E+01	0.154E+01
37 SUP	0.345E+00	0.858E+00	0.596E+01	-0.875E+00	0.694E-02	0.638E+00	0.638E+00
38 SUP	0.433E-01	0.617E+00	0.596E+01	-0.875E+00	0.959E-02	0.905E+00	0.905E+00
39 SUP	0.412E+00	0.818E+00	0.596E+01	-0.875E+00	0.122E-01	0.105E+01	0.105E+01
40 SUP	0.340E+00	0.854E+00	0.409E+01	-0.101E+01	0.555E-01	-0.145E+01	-0.145E+01
41 SUP	0.344E-01	0.618E+00	0.409E+01	-0.101E+01	0.134E-01	0.607E+00	0.607E+00
42 SUP	0.408E+00	0.798E+00	0.409E+01	-0.101E+01	0.503E-01	0.127E+01	0.127E+01
43 INT	0.314E+00	0.662E+00	0.406E+01	-0.101E+01	0.552E-01	-0.159E+01	-0.159E+01
44 INT	0.102E-01	-0.209E+00	0.406E+01	-0.101E+01	0.154E-01	0.608E+00	0.608E+00

45 INT	0.5228E+00	0.6171E+00	0.406E+01	-0.101E+01	0.525E-01	0.126E+01
46 SUP	0.5228E+00	0.749E+00	0.411E+01	-0.110E+01	0.110E-01	0.209E+00
47 SUP	0.319E-01	0.611E+00	0.411E+01	-0.110E+01	0.175E-01	0.115E+01
48 SUP	0.506E+00	0.725E+00	0.411E+01	-0.110E+01	0.267E-01	0.102E+01
49 INT	0.523E+00	0.696E+00	0.412E+01	-0.110E+01	0.111E-01	0.144E+00
50 INT	0.991E-02	-0.274E+00	0.411E+01	-0.110E+01	0.165E-01	0.115E+01
51 INT	0.535E+00	0.648E+00	0.412E+01	-0.110E+01	0.279E-01	0.140E+01
52 SUP	0.314E+00	0.692E+00	0.416E+01	-0.110E+01	0.220E-01	0.363E+00
53 SUP	0.259E-01	0.562E+00	0.416E+01	-0.110E+01	0.450E-01	0.101E+01
54 SUP	0.376E+00	0.671E+00	0.416E+01	-0.110E+01	0.822E-01	0.112E+01
55 INT	0.526E+00	0.715E+00	0.410E+01	-0.110E+01	0.250E-01	0.551E+00
56 INT	0.103E-01	-0.140E+00	0.418E+01	-0.119E+01	0.457E-01	0.101E+01
57 INT	0.532E+00	0.662E+00	0.410E+01	-0.119E+01	0.816E-01	0.115E+01
58 SUP	0.515E+00	0.667E+00	0.424E+01	-0.127E+01	0.428E-01	0.105E+01
59 SUP	0.194E-01	0.548E+00	0.424E+01	-0.126E+01	0.668E-01	0.102E+01
60 SUP	0.369E+00	0.652E+00	0.423E+01	-0.126E+01	0.136E+00	0.915E+00
61 INT	0.523E+00	0.725E+00	0.425E+01	-0.127E+01	0.425E-01	0.105E+01
62 INT	0.984E-02	-0.998E+00	0.425E+01	-0.127E+01	0.657E-01	0.101E+01
63 INT	0.332E+00	0.669E+00	0.426E+01	-0.127E+01	0.136E+00	0.916E+00
64 SUP	0.316E+00	0.669E+00	0.436E+01	-0.134E+01	0.704E-01	0.145E+01
65 SUP	0.134E-01	0.412E+00	0.435E+01	-0.134E+01	0.934E-01	0.105E+01
66 SUP	0.361E+00	0.648E+00	0.435E+01	-0.134E+01	0.191E+00	0.774E+00
67 INT	0.316E+00	0.726E+00	0.434E+01	-0.135E+01	0.709E-01	0.144E+01
68 INT	0.101E-01	0.157E+01	0.456E+01	-0.135E+01	0.906E-01	0.106E+01
69 INT	0.332E+00	0.668E+00	0.434E+01	-0.135E+01	0.191E+00	0.774E+00

FREQUENCY IN HERTZ = 0.11395E+01  
FREQUENCY IN RPS = 0.71600E+01  
\*\*\*\*\*

\*\*\*\*\*  
DISPLACEMENT FIELD OF BRIDGE  
\*\*\*\*\*

\*\*\*\*\*

NODE	X			Y			Z		
	A	P	A	A	P	A	A	P	
1 SUP	0.560E+00	0.649E+00	0.436E+01	-0.516E+00	0.450E+00	0.658E+00			
2 SUP	0.778E-01	-0.526E+00	0.435E+01	-0.511E+00	0.137E+00	-0.871E+00			
3 SUP	0.658E+00	0.457E+00	0.437E+01	-0.518E+00	0.527E+00	0.172E+00			
4 INT	0.512E+00	0.566E+00	0.448E+01	-0.264E+00	0.450E+00	0.650E+00			
5 INT	0.522E-01	-0.984E-03	0.453E+01	-0.278E+00	0.138E+00	-0.875E+00			
6 INT	0.606E+00	0.443E+00	0.447E+01	-0.265E+00	0.527E+00	0.172E+00			
7 SUP	0.569E+00	0.650E+00	0.405E+01	-0.447E+00	0.367E+00	0.406E+00			
8 SUP	0.810E-01	-0.338E+00	0.405E+01	-0.445E+00	0.813E-01	-0.884E+00			
9 SUP	0.671E+00	0.449E+00	0.405E+01	0.448E+00	0.441E+00	0.692E-01			
10 INT	0.516E+00	0.561E+00	0.423E+01	-0.407E+00	0.367E+00	0.405E+00			
11 INT	0.572E-01	-0.913E-01	0.423E+01	-0.409E+00	0.814E-01	-0.886E+00			
12 INT	0.611E+00	0.435E+00	0.422E+01	-0.406E+00	0.441E+00	0.684E-01			
13 SUP	0.579E+00	0.602E+00	0.381E+01	-0.604E+00	0.302E+00	0.182E+00			
14 SUP	0.854E-01	-0.545E+00	0.382E+01	-0.604E+00	0.391E-01	-0.979E+00			
15 SUP	0.692E+00	0.400E+00	0.381E+01	-0.605E+00	0.344E+00	0.175E-01			
16 INT	0.516E+00	0.579E+00	0.399E+01	-0.562E+00	0.305E+00	0.19E+00			
17 INT	0.587E-01	-0.141E+00	0.399E+01	-0.564E+00	0.391E-01	-0.966E+00			
18 INT	0.608E+00	0.447E+00	0.399E+01	-0.562E+00	0.545E+00	-0.172E-01			
19 SUP	0.590E+00	0.498E+00	0.369E+01	-0.776E+00	0.216E+00	0.156E+00			
20 SUP	0.923E-01	-0.351E+00	0.371E+01	-0.777E+00	0.112E-01	0.568E+00			
21 SUP	0.725E+00	0.307E+00	0.369E+01	-0.777E+00	0.199E+00	0.298E-01			
22 INT	0.514E+00	0.619E+00	0.380E+01	-0.736E+00	0.216E+00	0.117E+00			
23 INT	0.576E-01	-0.161E+00	0.379E+01	-0.757E+00	0.111E-01	0.598E+00			
24 INT	0.600E+00	0.482E+00	0.380E+01	-0.736E+00	0.199E+00	0.778E-01			
25 SUP	0.634E+00	0.334E+00	0.371E+01	-0.952E+00	0.111E+00	0.294E+00			
26 SUP	0.994E-01	-0.549E+00	0.371E+01	-0.952E+00	0.483E-01	-0.405E+00			
27 SUP	0.778E+00	0.173E+00	0.371E+01	-0.952E+00	0.130E+00	-0.140E+01			
28 INT	0.514E+00	0.697E+00	0.365E+01	-0.926E+00	0.117E+00	0.556E+00			
29 INT	0.574E-01	-0.185E+00	0.365E+01	-0.926E+00	0.484E-01	-0.404E+00			
30 INT	0.590E+00	0.551E+00	0.345E+01	-0.824E+01	0.134E+00	0.194E+01			
31 SUP	0.615E+00	0.288E+00	0.345E+01	-0.824E+01	0.242E-01	0.174E+00			
32 SUP	0.995E-01	-0.348E+00	0.345E+01	-0.824E+01	0.272E-01	-0.141E+00			
33 SUP	0.784E+00	0.137E+00	0.345E+01	-0.824E+01	0.281E-01	-0.469E+00			
34 SUP	0.609E+00	0.255E+00	0.345E+01	-0.824E+01	0.111E-01	0.119E+01			
35 SUP	0.997E-01	-0.347E+00	0.345E+01	-0.824E+01	0.979E-02	0.119E+01			
36 SUP	0.784E+00	0.933E-01	0.345E+01	-0.824E+01	0.652E-02	0.119E+01			
37 SUP	0.599E+00	0.178E+00	0.370E+01	0.132E+01	0.501E-01	-0.867E+00			
38 SUP	0.998E-01	-0.345E+00	0.370E+01	0.132E+01	0.284E-01	-0.619E+00			
39 SUP	0.779E+00	0.494E-01	0.370E+01	0.132E+01	0.289E-01	-0.559E+00			
40 SUP	0.586E+00	0.131E+00	0.415E+01	0.108E+01	0.102E+00	0.155E+01			
41 SUP	0.999E-01	-0.344E+00	0.415E+01	0.108E+01	0.519E-01	-0.558E+00			
42 SUP	0.769E+00	0.123E+00	0.415E+01	0.108E+01	0.121E+00	0.568E+00			
43 INT	0.525E+00	-0.236E+00	0.405E+01	0.109E+01	0.103E+00	0.150E+01			
44 INT	0.492E-01	-0.968E+00	0.405E+01	0.109E+01	0.519E-01	-0.557E+00			

45 INT	0.4604E+00	-0.542E+00	0.405E+01	0.108E+01	0.124E+00	0.567E+00
46 SUP	0.537E+00	-0.549E-01	0.423E+01	0.531E+00	0.540E-01	0.846E+00
47 SUP	0.934E-01	-0.565E+00	0.425E+01	0.931E+00	0.327E-01	0.947E+00
48 SUP	0.717E+00	-0.123E+00	0.423E+01	0.951E+00	0.959E-01	0.924E+00
49 INT	0.541E+00	-0.168E+00	0.428E+01	0.524E+00	0.582E-01	0.881E+00
50 INT	0.483E-01	-0.996E+00	0.427E+01	0.928E+00	0.517E-01	0.940E+00
51 INT	0.612E+00	-0.284E+00	0.428E+01	0.790E+00	0.100E+00	0.953E+00
52 SUP	0.518E+00	-0.159E+00	0.442E+01	0.791E+00	0.517E-01	-0.155E+01
53 SUP	0.813E-01	-0.408E+00	0.442E+01	0.791E+00	0.921E-01	0.418E+00
54 SUP	0.694E+00	-0.216E+00	0.441E+01	0.792E+00	0.219E+00	0.589E+00
55 INT	0.546E+00	-0.129E+00	0.450E+01	0.787E+00	0.529E-01	-0.155E+01
56 INT	0.509E-01	-0.964E+00	0.450E+01	0.788E+00	0.933E-01	0.415E+00
57 INT	0.606E+00	-0.255E+00	0.450E+01	0.786E+00	0.249E+00	0.595E+00
58 SUP	0.514E+00	-0.215E+00	0.468E+01	0.663E+00	0.587E-01	0.202E-01
59 SUP	0.692E-01	-0.427E+00	0.466E+01	0.664E+00	0.151E+00	0.585E+00
60 SUP	0.671E+00	-0.265E+00	0.466E+01	0.670E+00	0.308E+00	0.509E+00
61 INT	0.545E+00	-0.110E+00	0.474E+01	0.659E+00	0.580E-01	0.114E-01
62 INT	0.448E-01	-0.125E+01	0.474E+01	0.660E+00	0.149E+00	0.382E+00
63 INT	0.606E+00	-0.242E+00	0.475E+01	0.655E+00	0.309E+00	0.510E+00
64 SUP	0.520E+00	-0.214E+00	0.502E+01	0.561E+00	0.154E+00	0.685E+00
65 SUP	0.585E-01	-0.527E+00	0.499E+01	0.559E+00	0.222E+00	0.577E+00
66 SUP	0.661E+00	-0.276E+00	0.500E+01	0.567E+00	0.394E+00	0.760E-01
67 INT	0.533E+00	-0.107E+00	0.496E+01	0.540E+00	0.155E+00	0.682E+00
68 INT	0.550E-01	-0.138E+01	0.504E+01	0.550E+00	0.218E+00	0.595E+00
69 INT	0.606E+00	-0.243E+00	0.499E+01	0.535E+00	0.393E+00	0.746E-01

FREQUENCY IN HERTZ = 0.22791E+01  
FREQUENCY IN RPS = 0.14520E+02

\*\*\*\*\*  
DISPLACEMENT FIELD OF RWIUGE  
\*\*\*\*\*

\*\*\*\*\*

MODE X Y Z  
\*\*\*\*\*

	A	P	A	P	A	P
1 SUP	0.430E+00	-0.690E+00	0.408E+01	-0.976E+00	0.420E+00	-0.271E+00
2 SUP	0.102E+00	-0.108E+01	0.405E+01	-0.962E+00	0.283E+00	0.714E+00
3 SUP	0.243E+00	-0.355E+00	0.412E+01	-0.981E+00	0.593E+00	0.151E+01
4 INT	0.422E+00	-0.967E+00	0.406E+01	-0.923E+00	0.419E+00	-0.209E+00
5 INT	0.135E+00	-0.155E+01	0.420E+01	-0.964E+00	0.286E+00	0.752E+00
6 INT	0.259E+00	-0.470E+00	0.405E+01	-0.921E+00	0.592E+00	0.151E+01
7 SUP	0.452E+00	-0.667E+00	0.390E+01	-0.104E+01	0.257E+00	-0.693E+00
8 SUP	0.122E+00	-0.964E+00	0.390E+01	-0.104E+01	0.167E+00	0.772E+00
9 SUP	0.240E+00	-0.395E+00	0.592E+01	-0.104E+01	0.465E+00	0.155E+01
10 INT	0.427E+00	-0.992E+00	0.414E+01	-0.105E+01	0.538E+00	-0.804E+00
11 INT	0.119E+00	0.157E+01	0.413E+01	-0.105E+01	0.167E+00	0.768E+00
12 INT	0.265E+00	-0.525E+00	0.413E+01	-0.105E+01	0.467E+00	0.155E+01
13 SUP	0.514E+00	-0.772E+00	0.579E+01	-0.113E+01	0.521E+00	-0.150E+01
14 SUP	0.126E+00	-0.848E+00	0.562E+01	-0.113E+01	0.841E+01	0.144E+01
15 SUP	0.263E+00	-0.697E+00	0.580E+01	-0.113E+01	0.475E+00	-0.157E+01
16 INT	0.409E+00	-0.966E+00	0.407E+01	-0.115E+01	0.524E+00	-0.150E+01
17 INT	0.112E+00	0.153E+01	0.406E+01	-0.115E+01	0.845E+01	0.144E+01
18 INT	0.266E+00	-0.462E+00	0.406E+01	-0.115E+01	0.478E+00	-0.157E+01
19 SUP	0.635E+00	-0.964E+00	0.570E+01	-0.122E+01	0.231E+00	0.910E+00
20 SUP	0.145E+00	-0.745E+00	0.573E+01	-0.123E+01	0.130E+00	-0.534E+00
21 SUP	0.360E+00	-0.113E+01	0.570E+01	-0.122E+01	0.520E+00	-0.132E+01
22 INT	0.370E+00	-0.873E+00	0.588E+01	-0.125E+01	0.239E+00	0.928E+00
23 INT	0.107E+00	0.150E+01	0.586E+01	-0.124E+01	0.129E+00	-0.555E+00
24 INT	0.264E+00	-0.276E+00	0.588E+01	-0.125E+01	0.528E+00	-0.153E+01
25 SUP	0.842E+00	-0.117E+01	0.565E+01	-0.131E+01	0.537E+00	-0.712E+00
26 SUP	0.160E+00	-0.679E+00	0.565E+01	-0.132E+01	0.250E+00	-0.235E+00
27 SUP	0.579E+00	-0.143E+01	0.565E+01	-0.131E+01	0.253E+00	0.426E+00
28 INT	0.317E+00	-0.630E+00	0.549E+01	-0.131E+01	0.540E+00	-0.717E+00
29 INT	0.106E+00	0.150E+01	0.549E+01	-0.131E+01	0.251E+00	-0.255E+00
30 INT	0.280E+00	0.714E+01	0.549E+01	-0.131E+01	0.253E+00	0.441E+00
31 SUP	0.891E+00	-0.121E+01	0.255E+01	-0.132E+01	0.973E+01	-0.070E+00
32 SUP	0.161E+00	-0.680E+00	0.255E+01	-0.132E+01	0.912E+01	-0.347E+00
33 SUP	0.635E+00	-0.147E+01	0.255E+01	-0.132E+01	0.865E+01	-0.209E+00
34 SUP	0.933E+00	-0.127E+01	0.157E+01	-0.131E+01	0.602E+01	0.225E+01
35 SUP	0.160E+00	-0.680E+00	0.157E+01	-0.131E+01	0.604E+01	-0.157E+03
36 SUP	0.633E+00	-0.150E+01	0.157E+01	-0.131E+01	0.607E+01	-0.226E+01
37 SUP	0.953E+00	-0.128E+01	0.153E+00	-0.131E+01	0.103E+00	-0.366E+01
38 SUP	0.160E+00	-0.680E+00	0.153E+00	-0.131E+01	0.110E+00	-0.851E+01
39 SUP	0.710E+00	-0.153E+01	0.153E+00	-0.131E+01	0.110E+00	-0.129E+00
40 SUP	0.945E+00	-0.150E+01	0.112E+01	-0.147E+01	0.677E+01	0.155E+01
41 SUP	0.160E+00	-0.681E+00	0.112E+01	-0.147E+01	0.557E+01	0.559E+00
42 SUP	0.711E+00	-0.157E+01	0.112E+01	-0.147E+01	0.789E+01	-0.581E+00
43 INT	0.827E+00	0.153E+01	0.112E+01	-0.145E+01	0.719E+01	-0.151E+01
44 INT	0.218E+00	-0.968E+00	0.121E+01	-0.144E+01	0.549E+01	0.362E+00



45 INT	0.554E+00	0.108E+01	0.121E+01	-0.143E+01	0.860E+01	-0.507E+00
46 SUP	0.460E+00	-0.140E+01	0.189E+01	0.151E+01	0.215E+00	-0.512E+00
47 SUP	0.162E+00	-0.128E+00	0.192E+01	0.153E+01	0.693E+01	-0.112E+01
48 SUP	0.655E+00	0.138E+01	0.189E+01	0.151E+01	0.332E+00	-0.747E+00
49 INT	0.855E+00	-0.155E+01	0.209E+01	-0.153E+01	0.216E+00	-0.508E+00
50 INT	0.209E+00	-0.980E+00	0.205E+01	-0.154E+01	0.663E+01	-0.112E+01
51 INT	0.555E+00	0.117E+01	0.209E+01	-0.152E+01	0.335E+00	-0.743E+00
52 SUP	0.807E+00	-0.154E+01	0.265E+01	0.144E+01	0.226E+00	-0.226E+00
53 SUP	0.160E+00	-0.796E+00	0.267E+01	0.145E+01	0.101E+00	-0.150E+01
54 SUP	0.626E+00	0.124E+01	0.264E+01	0.144E+01	0.484E+00	-0.687E+00
55 INT	0.875E+00	-0.152E+01	0.281E+01	0.151E+01	0.228E+00	-0.251E+00
56 INT	0.213E+00	-0.972E+00	0.279E+01	0.151E+01	0.141E+00	-0.155E+01
57 INT	0.550E+00	0.122E+01	0.282E+01	0.151E+01	0.446E+00	-0.880E+00
58 SUP	0.791E+00	0.156E+01	0.354E+01	0.139E+01	0.164E+00	0.533E+00
59 SUP	0.161E+00	-0.847E+00	0.354E+01	0.139E+01	0.228E+00	-0.155E+01
60 SUP	0.603E+00	0.116E+01	0.351E+01	0.140E+01	0.466E+00	-0.110E+01
61 INT	0.886E+00	-0.150E+01	0.344E+01	0.142E+01	0.164E+00	0.525E+00
62 INT	0.222E+00	-0.103E+01	0.342E+01	0.143E+01	0.224E+00	-0.155E+01
63 INT	0.552E+00	0.125E+01	0.346E+01	0.142E+01	0.488E+00	-0.110E+01
64 SUP	0.791E+00	0.156E+01	0.399E+01	0.157E+01	0.250E+00	0.155E+01
65 SUP	0.171E+00	-0.903E+00	0.396E+01	0.156E+01	0.331E+00	-0.130E+01
66 SUP	0.587E+00	0.115E+01	0.397E+01	0.158E+01	0.457E+00	-0.137E+01
67 INT	0.876E+00	-0.150E+01	0.390E+01	0.134E+01	0.259E+00	0.155E+01
68 INT	0.211E+00	-0.107E+01	0.400E+01	0.137E+01	0.330E+00	-0.137E+01
69 INT	0.553E+00	0.125E+01	0.393E+01	0.134E+01	0.456E+00	-0.157E+01



FREQUENCY DEPENDENT RESPONSE PLOTS FROM BASSIN2



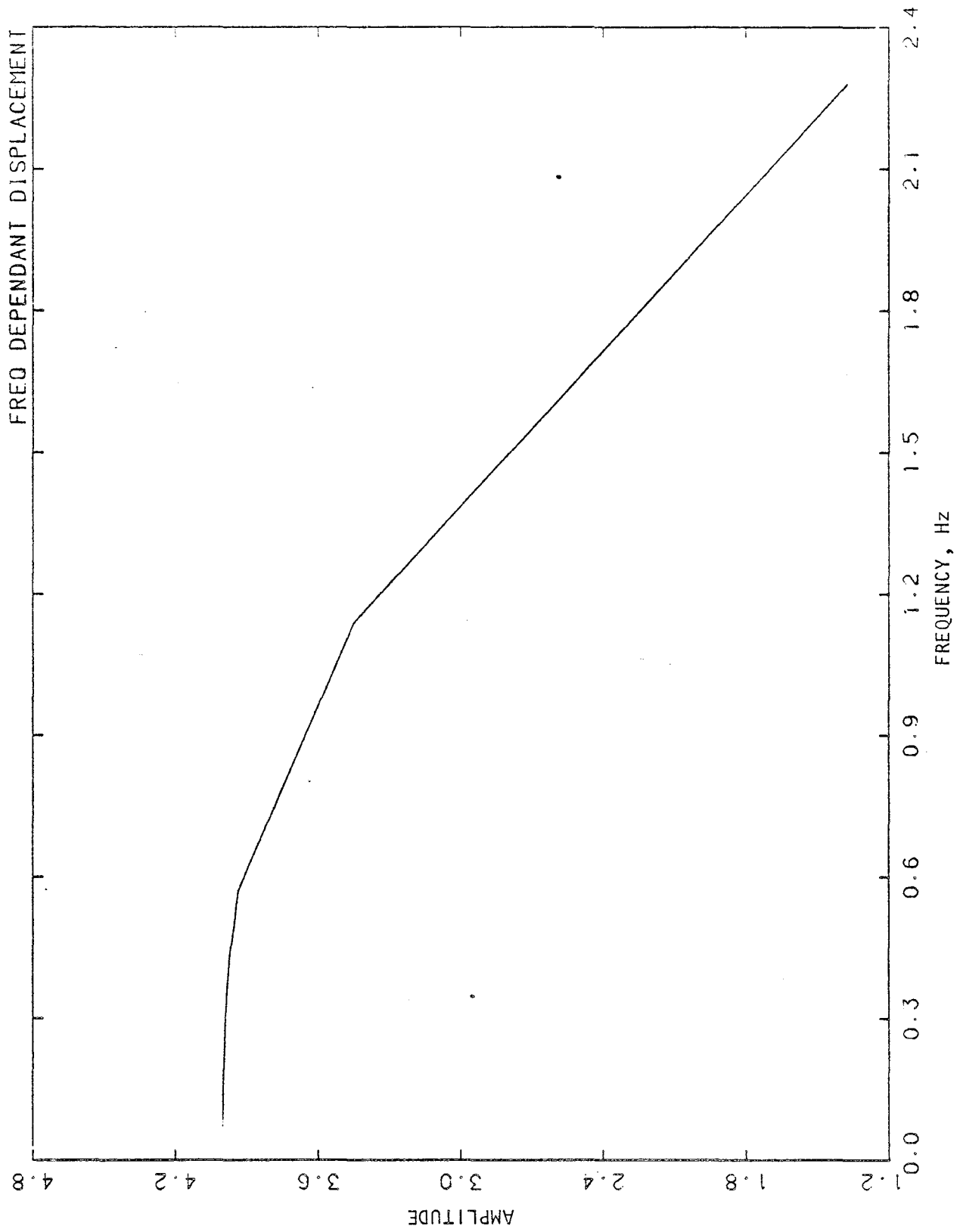


FIGURE C-12. FREQUENCY-DEPENDENT AMPLITUDE: Y-DISPLACEMENT OF NODE 35

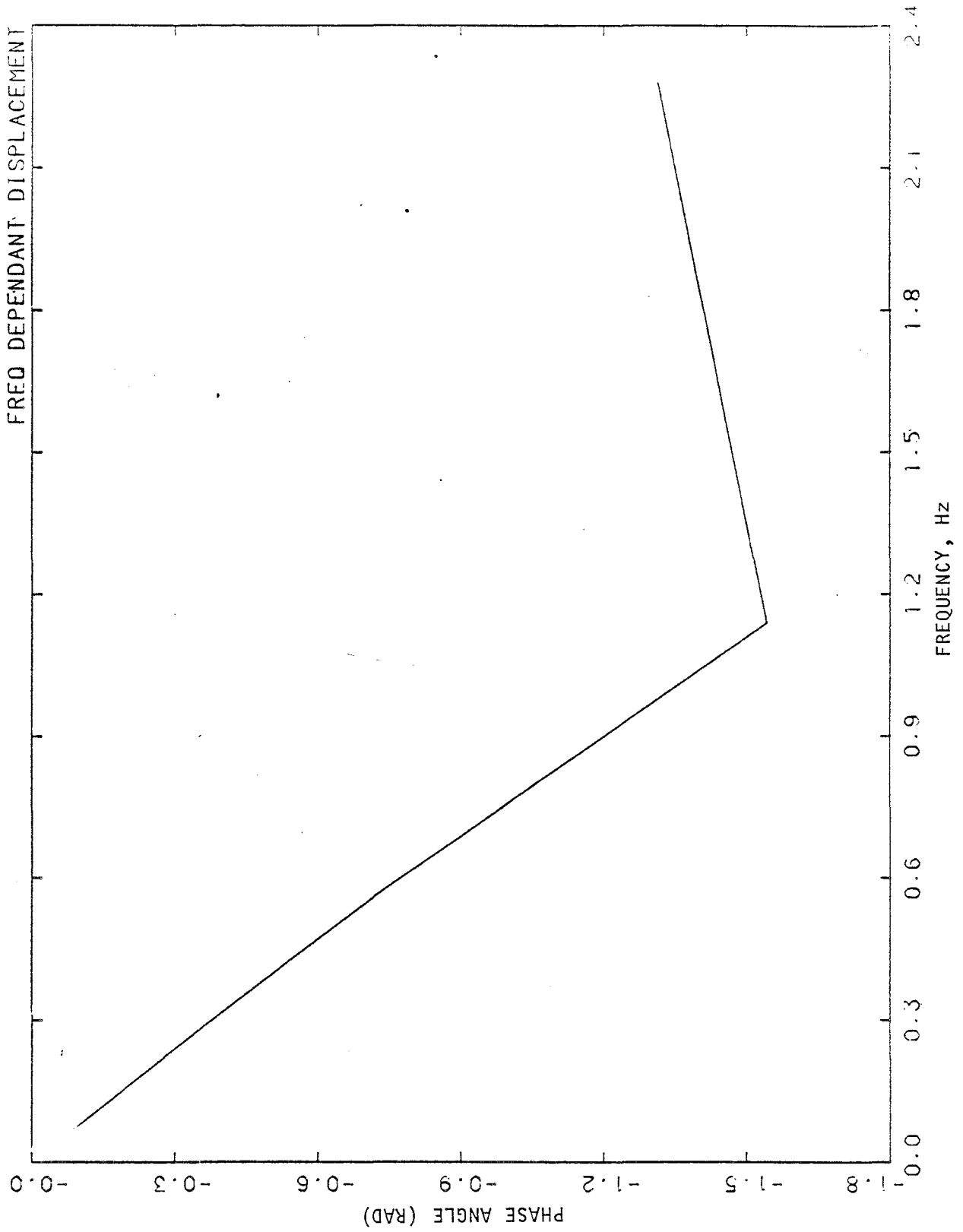


FIGURE C-13. FREQUENCY-DEPENDENT PHASE ANGLE: Y-DISPLACEMENT OF NODE 35

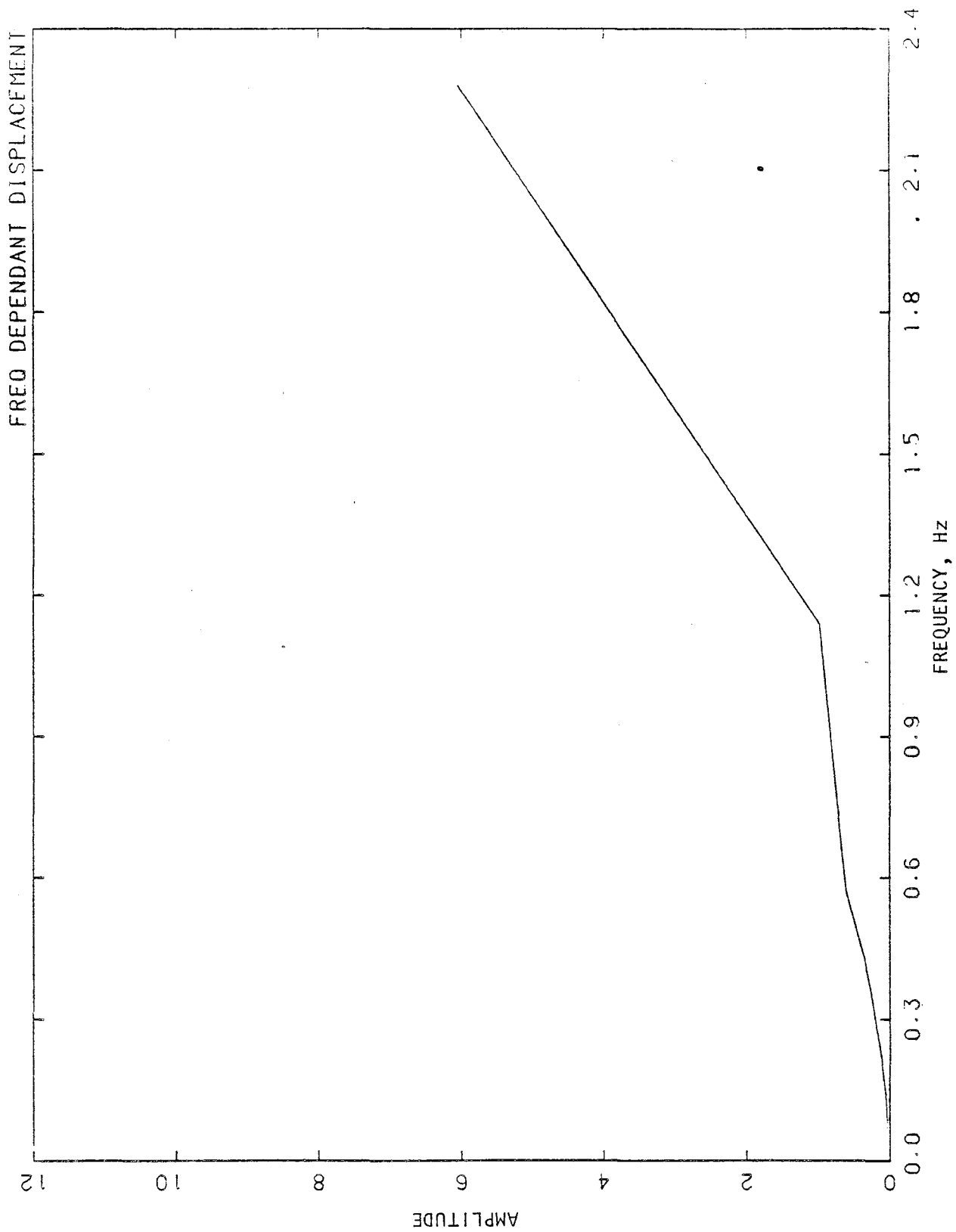


FIGURE C-14. FREQUENCY-DEPENDENT AMPLITUDE: z-DISPLACEMENT OF NODE 35

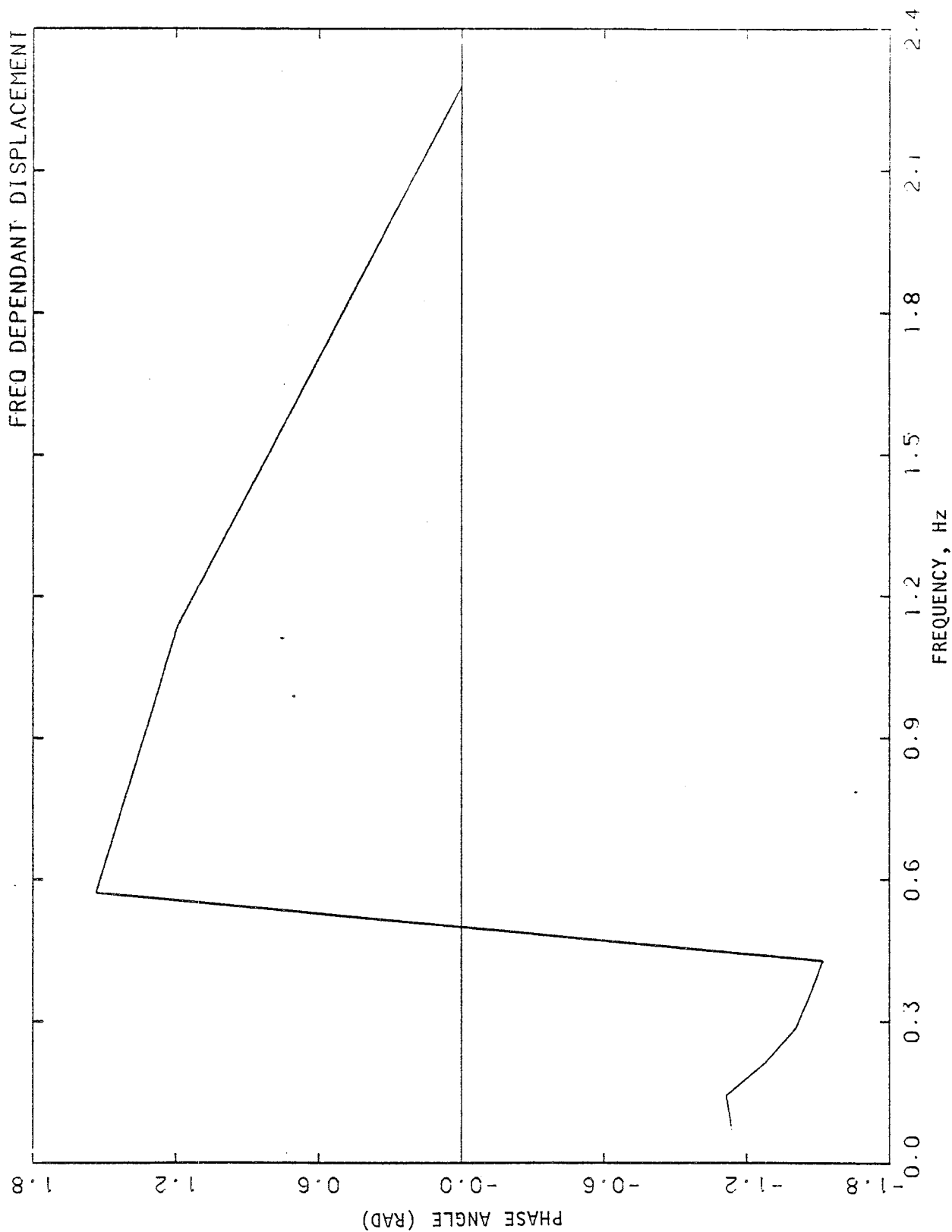


FIGURE C-15. FREQUENCY-DEPENDENT PHASE ANGLE: z-DISPLACEMENT OF NODE 35



<b>REPORT DOCUMENTATION PAGE</b>	1. REPORT NO. R-8113-5470	2.	3. Recipient's Accession No.
4. Title and Subtitle  Bridge Response to Traveling Seismic Waves		5. Report Date  6.	
7. Author(s) Dendrou, B.D., et al.		3. Performing Organization Rept. No.	
9. Performing Organization Name and Address Agbabian Associates 250 North Nash Street P.O. Box 956 El Segundo, CA 90245-0956		10. Project/Task/Work Unit No.  11. Contract(C) or Grant(G) No. (C) (G) CEE-8007518	
12. Sponsoring Organization Name and Address National Science Foundation Washington D.C. 20550		13. Type of Report & Period Covered Final Report 9/15/80 - 3/31/83  14.	
15. Supplementary Notes			
16. Abstract (Limit: 200 words)  This report describes an advanced methodology (BASSIN), for analyzing traveling seismic wave effects on the dynamic response of an arbitrarily-configured, elastic bridge system (comprised of a road deck, piers, abutments, backfill, etc.). A substructuring approach has been used to formulate BASSIN; in this, the bridge system is represented using a three-dimensional finite element model, and the underlying soil is depicted using a boundary element approach based on elastic half-space theory. Seismic excitations are induced by plane body waves or Raleigh waves with arbitrary direction of incidence, wavelength, and amplitude. BASSIN allows for a fully deformable interface between the bridge system and the underlying soil, and incorporates a special modal truncation procedure to account for higher mode response characteristics.			
17. Document Analysis a. Descriptors Bridges (Structures)      Earthquakes Dynamic Response      Seismic Waves Dynamics      Vibration  b. Identifiers/Open-Ended Terms BASSIN  c. COSATI Field/Group			
18. Availability Statement: Release Unlimited		19. Security Class (This Report) Unclassified	21. No. of Pages 251
		20. Security Class (This Page) Unclassified	22. Price

